The development of a humanised mouse model of ANCA associated vasculitis

Coughlan, Alice

Awarding institution:
King's College London

The development of a humanised mouse model of ANCA associated vasculitis

Alice Coughlan

A dissertation submitted to the University of London in candidature of Doctor of Philosophy

MRC Centre for Transplantation
Division of Transplantation, Immunology and Mucosal Biology
King's College London School of Medicine at Guy's, King's and St. Thomas' Hospitals

Abstract

Anti-neutrophil cytoplasmic autoantibodies (ANCA), targeting the neutrophil protein granules myeloperoxidase (MPO) and proteinase 3 (PR3), activate neutrophils *in vitro*, and are associated with a systemic autoimmune vasculitis, in which a pauci-immune crescentic glomerulonephritis is common. The *in vivo* study of ANCA pathogenesis is severely limited, both by the lack of a robust anti-PR3 IgG induced disease model, and by the differences found between human and mouse biology. Therefore the development of a disease model based on humanised mice, defined as mice possessing human immune cells, has the potential to overcome these limitations, while also allowing the direct study of human ANCA *in vivo.* The aims of this thesis were 1) to establish *in vitro* assays of ANCA induced neutrophil activation, and thus allow the study of ANCA:neutrophil interactions and 2) to establish a humanised mouse model of ANCA vasculitis. ANCA were purified from patient plasma, and two human neutrophil respiratory burst assays were developed. Subsequently, it was shown that Granulocyte Colony Stimulating Factor (GCSF) primes neutrophils for an anti-MPO induced respiratory burst, and the inhibition of phosphoinositol 3-kinase β/δ abrogates the ANCA induced release of superoxide. Humanised mice were produced by the engraftment of human haematopoietic stem cells into irradiated, adult NOD-scid IL2r$\gamma^{-/-}$ mice. At least 8 weeks later a population of human neutrophils were identified by flow cytometry, and this population was expanded by treatment with GCSF. It was shown that these cells could respond to inflammatory stimuli *in vivo*, by modulating their expression of activation markers, and *in vitro*, by undergoing respiratory burst and degranulation. Patient derived ANCA was passively transferred into humanised mice that had been primed with GCSF and lipopolysaccharide. Mice were culled 7 days later, but there was no histological or biochemical evidence of disease. Thus, this work has identified GCSF and phosphoinositol-3-kinase β/δ as molecules of potential importance in ANCA vasculitis. Furthermore, the passive transfer of patient ANCA into humanised mice did not prove pathogenic in this study, and possible reasons for this are discussed. The demonstration of functional responses in human neutrophils does, however, suggest that this humanised mouse model has the potential be useful for the study of human neutrophils *in vivo*.

Acknowledgments

I would like to thank my supervisor, Dr. Michael Robson, for the opportunity to carry out this PhD in his laboratory. I am sincerely grateful for his continued support, guidance and enthusiam. I would also like to thank my secondary supervisor, Dr. Stipo Jurcevic, for providing support during the course of this PhD.

Others who contributed significantly towards this project include Simon Freeley, who carried out much of the histology presented here, and Dr. Reena Popat, who assisted with the GCSF priming experiments. I would especially like to thank Simon Freeley for always being willing to provide both help and encouragement. Special thanks goes to Prof. Terry Cook and Dr. Catherine Horsfield, who kindly reviewed the histology presented here. I would also like to thank Dr. Susanne Heck in the BRC flow cytometry facility and Dr. Roseanna Greenlaw for their expert advice. I am also grateful to everyone at Kent and Canterbury, Royal Sussex County, King's College, St Helier and Guy's and St Thomas' hospitals that helped obtain patient samples. My thanks also go to Dr. Neil Doulton and Dr. Charles Turner in the Department of Paediatic Biochemistry, St. Thomas' Hospital, London, who assisted with the serum creatinine measurements. Finally, I would like to thank everyone who kindly donated time, and blood, to me during the course of this PhD.

Guy's & St. Thomas 'Hospital Kidney Patients' Association, Genzyme Renal Innovations Program, The Sir Jules Thorn Charitable Trust and a KRUK project grant funded these PhD studies, and work performed in the laboratory during this time.

Publications arising from work presented here

Coughlan, A.M., Freeley, S.J., Robson, M.G. (2012). Humanised mice have functional human neutrophils. J. Immunol. Methods. *385(1-2):96-104*

Coughlan, A.M., Freeley, S.J., Robson, M.G. (2012). Animal models of anti-neutrophil cytoplasmic antibody-associated vasculitis. Clin Exp Immunol. *169 (3):229-37*

Acknowledgments

Freeley, S.J., Coughlan, A.M., Popat, R.J., Dunn-Walters, D.K., Robson, M.G. (2013). Granulocyte colony stimulating factor exacerbates anti-neutrophil cytoplasmic antibody vasculitis. Ann Rheum Dis. 72(6):1053-8

Alice Coughlan - 2013

ERRATA CORRIGE

Page	Line	Note	ERRATA	CORRIGE
111		Table 3.2		V41 and V57 were from plasma exchange fluid. V54 was from the residual plasma fraction after diluted blood was used for a ficoll separation to obtain cells. Blood was diluted 1 in 2 before the ficoll. The plasma fraction (diluted) was stored. Most purifications were from this diluted plasma (which would be about 1 in 3 diluted, depending on the haematocrit). The low yields for V54 are probably due to a technical issue (this is the same data as in table 3.5).
112		Table 3.3		For the healthy donors, nearly all of these were taken from the residual plasma fraction after diluted blood was used for a ficoll separation as above.
113-4		Table 3.4-3.5		The majority of these were taken from diluted blood used for a ficoll separation to obtain cells. Of the remainder, most are plasma exchange fluid, with a few neat serums (eg V43, V44, V45, V46, V48). V54 is from residual plasma fraction after diluted blood was used for a ficoll separation to obtain cells. The low yields for two of the three purifications were due to a technical issue on that day (same data as in table 3.2).

These corrections relate to the IgG yields for controls, PR3 positive patients, and MPO-ANCA positive patients.

The indication that these are all purified from neat plasma with the yield stated is not correct.

The text above should be inserted into the indicated table legend.

None of the above has any bearing on the rest of the data in the thesis. It simply explains why many stated IgG yields may be lower than what might be expected from neat plasma.

Date 3 June 2021

Signed by 

Table of contents

List of figures

List of figures

List of tables

Abbreviations

A1AT	Alpha 1-Antitrypsin
ANCA	Anti-neutrophil cytoplasmic autoantibodies
APC	Allophycocyanin
BLT mouse	Bone Marrow Liver Thymic mouse
BSA	Bovine Serum Albumin
CD	Cluster of Differentiation
CXCL	Chemokine (C-X-C motif) Ligand
DAG	Diacylglycerol
DC	Dendritic Cell
DHR123	Dihydrorhodamine 123
EBV	Epstein–Barr Virus
EDTA	Ethylenediaminetetraacetic Acid
ELISA	Enzyme-Linked Immunosorbent Assay
FCS	Foetal Calf Serum
FITC	Fluorescein isothiocyanate
fMLP	N-formyl-methionine-leucine-phenylalanine
GCSF	Granulocyte Colony-Stimulating Factor
GM-CSF	Granulocyte-Macrophage Colony-Stimulating Factor
GN	Glomerulonephritis
GPA	Granulomatosis with Polyangiitis
HBH	HBSS + 1M HEPES
HBSS	Hank's Balanced Salt Solution
HEPES	4-(2-hydroxyethyl)-1-piperazineethanesulfonic acid
HIV	Human Immunodeficiency Virus
HLA	Human Leukocyte Antigen
HSC	Haematopoietic Stem Cells
Ig	Immunoglobulin
IL	Interleukin
IFNγ	Interferon γ
IP_3	Inositol trisphosphate
LAMP-2	Lysosomal-Associated Membrane Protein-2
LFA-1	Lymphocyte Function-associated Antigen-1
LPS	Lipopolysaccharides
MAPK	Mitogen-Activated Protein Kinase

MFI	Median Fluorescence Intensity
MHC	Major Histocompatibility Complex
MPA	Microscopic Polyangiitis
MPO	Myeloperoxidase
NADPH	Nicotinamide Adenine Dinucleotide Phosphate
NB1	Human neutrophil antigen B1
NCGN	Necrotising Crescentic Glomerulonephritis
NK	Natural Killer
NOD	Non-Obese Diabetic
O.D.	Optical Density
PA	Phosphatidic Acid
PAS	Periodic Acid-Schiff stain
PBL	Peripheral Blood Leukocytes
PBMCs	Peripheral Blood Mononuclear Cells
PBS	Phosphate Buffered Saline
PE	Phycoerythrin
PI3K	Phosphoinositide 3-kinase
PIP_2	Phosphatidylinositol 4,5-bisphosphate
PIP_3	Phosphatidylinositol (3,4,5)-trisphosphate
PIPKinIγ	Phosphoinositol (4) phosphate-5-kinase Iγ
PKC	Protein Kinase C
PLC	Phospholipase c
PLP	Phosphate-Lysine-Periodate
PMA	Phorbol-12-Myristate-13-Acetate
PR3	Proteinase 3
RAG	Recombinase Activating Gene
ROS	Reactive oxygen species
SCID	Severe Combined Immunodeficiency
SOD	Superoxide Dismutase
TGFβ	Transforming Growth Factor β
TNF	Tumour Necrosis Factor
TLR	Toll-like Receptor
UCB	Umbilical Cord Blood

WKY rat	Wistar Kyoto rat

1.1 Overview

The primary focus of this thesis is the development of a humanised mouse model of anti-neutrophil cytoplasmic autoantibody (ANCA) associated vasculitis. However, in the course of this study, the ability of ANCA to activate human neutrophils was also examined. Therefore, this introductory chapter comprises detailed reviews of ANCA associated vasculitis, with a focus on results obtained from both *in vivo* and *in vitro* studies, the current available animals models of this disease, and finally, the current state, and emerging potential, of humanised mouse models.

The second chapter describes general methods, and this is followed by five results chapters, each divided into four sections: introduction, specific methods, results and discussion. Chapter 3 details the establishment of a supply of patient derived ANCA, for use in both *in vitro* and *in vivo* experiments, together with the development and optimisation of *in vitro* ANCA induced neutrophil activation assays. Chapter 4 begins with data from a series of *in vitro* experiments looking at the expression of antigens for ANCAs, and is followed by data showing a potential role for granulocyte colony stimulating factor in the priming of neutrophils for ANCA induced responses. The chapter is closed with an investigation of the potential role of phosphoinositol-3-kinase β/δ in signalling pathways downstream of ANCA ligation. Chapter 5 details the development of a humanised mouse model, while chapter 6 contains data confirming these humanised mice possess functional human neutrophils. Chapter 7 describes attempts to induce ANCA associated vasculitis in these mice. Finally, chapter 8 is a discussion of the implications, limitations and future directions of the work presented in this thesis.

1.2 Anti-neutrophil cytoplasmic autoantibody (ANCA) associated vasculitis

1.2.1 Pathology of ANCA associated vasculitis

Anti-neutrophil cytoplasmic autoantibody (ANCA) associated vasculitis is a pauci immune, necrotising, small vessel vasculitis that predominantly affects microscopic vessels, such as capillaries and venules, within organs and tissues. Thus it is a severe, systemic autoimmune disease frequently affecting areas rich in small blood vessels such as the kidneys and lungs. It is a leading cause of progressive glomerulonephritis with approximately 28% of patients experiencing end stage renal failure within 5 years of diagnosis [1]. Indeed, while disease is systemic, with joints, skin, lungs, kidneys and other tissues frequently being affected, necrotising crescentic glomerulonephritis (NCGN) and inflammation of the respiratory system are particularly associated with high morbidity and mortality. If left untreated mortality is approximately 80% [2]. In contrast, if treated with currently available therapies, patients with renal involvement have an 85% chance of survival 1-year post diagnosis, with this decreasing to 75% after 5 years [1]. Current therapy generally involves the induction of remission with high dose glucocorticoids and cyclophosphamide. Once achieved, remission is maintained with azathioprine or methotrexate [3].

The two most common forms of ANCA associated vasculitis are microscopic polyangiitis (MPA) and granulomatosis with polyangiitis (formally Wegener's granulomatosis) (GPA). MPA can affect any organ or tissue, however, dermal venulitis, pulmonary alveolar capillaritis, NCGN and epineural arteritis are particularly common [4]. Although disease is described as pauci immune, most patients have some evidence of focal IgG and complement deposition at the sites of vascular inflammation [4]. The acute vascular lesions found in affected vessels are characteristed by a neutrophilic infiltrate and significant leukocytoclasia, an accumulation of nuclear remnants from unscavenged neutrophils, together with vessel wall necrosis and, frequently, with the accumulation of fibrin. Within approximately one week, acute lesions progress to lesions rich in monocytes, macrophages and T cells, before progressing to

fibrotic lesions shortly thereafter [4]. Multiple vascular lesions of varying ages can be observed in any given affected tissue, and this is particularly evident in renal biopsy specimens in which glomerular lesions range from acute lesions with segmental fibrinoid necrosis, to chronic lesions with segmental sclerosis [4].

GPA and MPA are almost pathologically identical, with only the presence of necrotising granulomatous inflammation found in GPA patients fully distinguishing the two diseases [4]. In GPA, necrotising granulomatous inflammation can be found within affected vessels or in extravascular tissue [4]. Although it can occur anywhere in the body, including the skin, nervous system and eye, granulomatous inflammation is most common in the upper and lower respiratory tract of patients [4]. Indeed, approximately 90% of patients have upper or lower airway involvement [5]. Importantly, and in contrast to the monocyte and T cell rich acute lesions typically associated with granulomatous inflammation in sarcoidosis, mycobacterial infection, and fungal infection, acute lesions found in GPA are predominantly composed of a neutrophilic infiltrate [4]. In addition, and although necrotic vessels are not generally identifiable in the acute lesions, focal accumulations of fibrinoid material can be observed. This is likely due to substantial vascular exudation or vascular disruption. Importantly, the resulting acute injury leads to the recruitment of monocytes, which transform into macrophages and multinucleated giant cells, as well as lymphocytes. Thus acute lesions eventually transform into more classic granulomas with palisading macrophages and giant cells present at the margins of areas of necrosis [4].

1.2.2 ANCA, neutrophils and infection: Three key mediators of disease

In 1982, Davies et al. first observed anti-neutrophil cytoplasmic autoantibodies (ANCA) in patients with focal and segmental glomerulonephritis, identifying, in the blood of patients, an IgG of unknown specificity that was capable of staining the cytoplasm of neutrophils [6]. This finding was later confirmed, and expanded, in a study which showed that antibodies against neutrophils and monocytes were not only present in patients, but also that the levels of these

antibodies were related to disease activity [7]. Since then ANCA have become established diagnostic markers of disease. Furthermore, there is now strong evidence that they are in fact pathogenic and, indeed, levels of ANCA often correlate with disease severity, although this is not the case in all patients [8-10].

Myeloperoxidase (MPO) and Proteinase 3 (PR3) were eventually identified as the primary antigenic targets of ANCA, and both can be found in the azurophilic granules of neutrophils and the peroxidase positive lysosomes of monocytes [11, 12]. The most common forms of small vessel vasculitis, granulomatosis with polyangiitis (formally Wegener's granulomatosis) (GPA) and microscopic polyangiitis (MPA), are often associated with ANCA directed against just one of these antigens, GPA with anti-PR3 antibodies and MPA with antibodies against MPO. However, it is important to also note that antibodies associated with GPA may be present in MPA patients and vice versa. In addition antibodies against both are occasionally present [13]. Importantly, both MPO and PR3 have also been shown to be present on the surface of cytokine-primed neutrophils isolated from whole blood [14, 15]. It is therefore likely that ANCA can bind to their antigens on the surface of neutrophils and through this, and Fc receptor interactions (Discussed in the following sections), recruit transmembrane molecules leading to intracellular signalling cascades culminating in neutrophil activation and the subsequent tissue damage associated with disease. Supporting this is *in vitro* data demonstrating that ANCA are capable of activating cytokine-primed neutrophils resulting in respiratory burst and degranulation [14, 16], inflammatory cytokine release [17], neutrophil extracellular trap formation (NETosis) [18] and damage to endothelial cell walls [19, 20]. Finally *in vivo* evidence of the importance of neutrophils in ANCA associated vasculitis includes reports that the number of activated PMN cells present in the renal biopsies of patients with GPA corresponds with renal tissue damage as assessed by serum creatinine levels [21]. In addition, using a mouse model of disease, Xiao et al. demonstrated that neutrophil depleted mice were completely protected from necrotising crescentic NCGN induced by the passive transfer of anti-MPO antibodies [22]. Notably, under the conditions of

this model ANCA:monocyte interactions were unable to induce disease. Thus, it is thought that ANCA-neutrophil interactions are key to disease pathogenesis (Fig 1.1).

While it has been shown that neutrophils are key effecter cells, their presence together with that of ANCA may not be sufficient to cause disease. Huugen et al. demonstrated that, in a passive transfer model of NCGN, the administration of lipopolysaccharide (LPS) together with the anti-MPO antibodies significantly increased the severity of the disease compared with mice treated with anti-MPO antibodies alone [23]. The effect of LPS was shown to be related to increased levels of circulating tumour necrosis factor (TNF)α and MPO. The importance of TNFα was confirmed by the use of TN3, an anti-TNFα antibody that completely attenuated the effect of LPS on disease severity. These data, together with clinical observations that infection frequently precedes ANCA associated vasculitis diagnosis and/or relapse [24], and *in vitro* data showing that TNFα priming is required for ANCA induced neutrophil activation [14, 16], suggests that ANCA associated vasculitis is not induced by ANCA alone, but by a combination of ANCA and proinflammatory stimuli (Fig 1.1).

The effect of LPS in ANCA associated vasculitis was further examined in two recent studies. In the first study, it was shown, using intravital microscopy of exposed glomeruli, that LPS treatment promoted anti-MPO induced glomerular leukocyte adhesion in a lymphocyte function-associated antigen (LFA)-1 dependent manner [25]. Furthermore, it was shown that LPS promoted the binding of anti-MPO IgG to neutrophils. These findings, together with the evidence that the effect of LPS is mediated through TNFα, are consistent with the hypothesis that TNFα induces MPO translocation to the surface of neutrophils *in vivo* [14, 15, 26]. In the second study, the role of Toll-like receptor (TLR) 4, the main receptor for LPS, was examined [27]. It was first demonstrated that LPS together with anti-MPO IgG increased TLR4 and chemokine (C-X-C motif) ligand (CXCL)-1 and -2 expression by glomerular endothelial cells, and that this in turn increase neutrophil recruitment to the

glomerulus. Both bone marrow and tissue cell TLR4 was found to be necessary for full expression of CXCL1 and CXCL2, and thus for maximal neutrophil recruitment. Furthemore, TLR4$^{-/-}$ mice had significantly less albuminuria, haematuria, glomerular hypercellularity and focal and segmental lesions after LPS and anti-MPO treatment than wildtype controls. Finally anti-MPO IgG induced NCGN in LPS treated mice was attenuated in mice pretreated with anti-CXCL1 and anti-CXCL2 antibodies. Together these studies suggests that LPS, and thus infection, has several roles in the induction of ANCA associated vasculitis including in 1) the translocation of ANCA antigens to the surface of neutrophils, 2) the recruitment of neutrophils to the glomerulus and 3) the upregulation of β_2 intergrins, and thus the adhesion of neutrophils to glomerular endothelial cells.

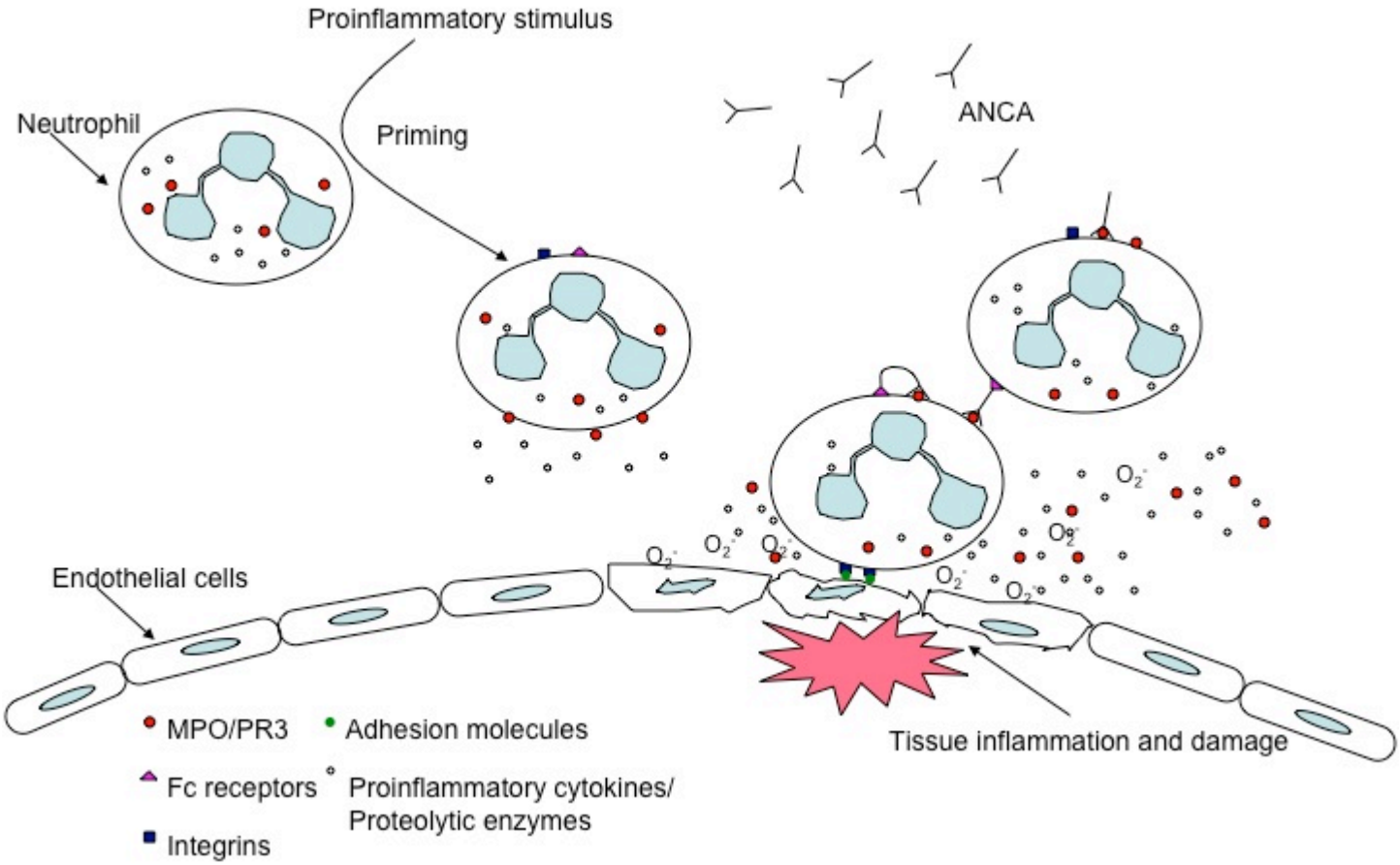

Figure 1.1 Pathogenesis of ANCA associated vasculitis.
Neutrophils become primed by proinflammatory stimuli *in vivo*, most likely as a result of infection. This leads to the upregulation of integrins and the translocation of ANCA antigens, PR3 and MPO, from their position in the granules to the surface of the neutrophils. In addition, the presence of proinflammatory stimuli leads to the upregulation of endothelial cell adhesion molecules. Thus, neutrophil adhesion and transmigration is increased. With PR3 and MPO now present on the cell membrane, circulating ANCA can bind their antigen and, in an Fc dependent manner, activate neutrophils leading to the release of reactive oxygen species (O_2^-), proteolytic enzymes and further proinflammatory cytokines. The subsequent inflammation and tissue damage results in disease.

1.2.3 ANCA antigens

1.2.2.1 PR3 and MPO

PR3, human leukocyte elastase (HLE), cathepsin G and azurocidin, are homologous neutral serine proteases found in the azurophilic granules of neutrophils [28, 29]. The primary function of these enzymes is thought to be the degradation of extracellular proteins, such as elastin, fibronectin, type IV collegen and lamin, at sites of inflammation [30]. However, other roles in the immune system have been suggested. For example, separate to its enzymatic activity, PR3 has been shown to effectively kill bacteria, particularly gram-negative strains, and fungi [29, 31]. This microbicidal role is associated with the ability of PR3 to inhibit macromolecule synthesis, energy dependent transport and oxygen metabolism, and probably occurs as a result of charge interactions with the pathogen plasma membrane [32]. In addition, PR3 can interact with cytokines, and thus potentially modify the immune response. PR3 can inactivate interleukin (IL)6 by degradation [33] and, interestingly, activate latent transforming growth factor (TGF)β [34], suggesting an anti-inflammatory role. The ability of PR3 to inhibit the activation of the nicotinamide adenine dinucleotide phosphate (NADPH) oxidase [35] also suggests that under some conditions PR3 may be able to down regulate the immune response. In contrast, PR3 has also been shown to increase the activity of IL8, a pivotal chemokine that preferentially induces neutrophil recruitment [36]. Therefore, PR3 may play a role in increasing neutrophil accumulation at the site of its release. Finally, PR3 can cleave membrane bound TNFα [37, 38], IL-1β [38] and the IL2 and IL6 receptors [39], although the functionality of resulting products is yet to be determined. Interestingly, PR3 is also capable of inhibiting thrombin through its cleavage, and subsequent inactivation, of protease activated receptors (PAR) on platelets and endothelial cells [40, 41]. It is also worth noting that PR3 is not only found in the azurophilic granules of neutrophils, but also in the specific and secretory granules [42], as well as in the cytoplasmic granules of monocytes [43].

MPO is a member of the heme peroxidase enzyme family and a major constituent of the azurophilic granules of neutrophils. It is an important component of the phagocyte oxygen dependent intracellular microbicidal system, where it primarily catalyses the H_20_2 mediated oxidation of halide ions, notably chloride, to hypohalous acids [44]. Separate to its enzymatic activity, MPO has also been implicated in leukocyte recruitment [45]. In *in vitro* chemotaxis experiments, MPO was shown to induce neutrophil movement via electrostatic interactions with the leukocyte plasma membrane. In addition, and in the same study, $MPO^{-/-}$ mice exhibited reduced neutrophil infiltration at sites of inflammation. Finally, and perhaps most importantly, the deposition of MPO in the vasculature of these mice led to neutrophil adhesion in otherwise uninflamed blood vessels. Although primarily associated with neutrophils, MPO is also present in the cytoplasmic granules of monocytes and a subpopulation of macrophages [46].

Neutrophil activation by ANCA is entirely dependent on the ability of these autoantibodies to bind to their target antigens. Therefore, ANCA must be internalised by neutrophils, or PR3 and MPO must be present on the cell surface. It is also possible that both may occur, with some ANCAs being internalised while others bind to membrane bound antigen. Further to this, PR3 is present on the surface of resting, isolated neutrophils and monocytes [47], and, in the case of neutrophils, is upregulated following stimulation with fMLP and cytokines such as TNFα [14, 15, 42]. Interestingly, PR3 expression on isolated neutrophils has a bimodal pattern [48], with those cells possessing high membrane PR3 expression ($mPR3^{high}$) generating more extracellular superoxide, and undergoing increased degranulation, in response to anti-PR3 antibodies [49]. In contrast, the level of expression of mPR3 had no effect on the production of intracellular reactive oxygen species in response to anti-PR3 IgG stimulation [50]. Notably, a high population of $mPR3^{high}$ neutrophils is a risk factor for GPA and rheumatoid arthritis [51]. Studies suggest that PR3 is anchored to the neutrophil membrane in one of two ways. In the first, PR3 is inserted into the plasma membrane via interactions involving basic amino acid residues [52]. In the second, PR3 is bound to the GPI-linked membrane receptor human neutrophil antigen B1 (NB1) (also known as CD177). Indeed

both NB1 and mPR3 are expressed on the same subset of neutrophils, and these molecules co-localise and co-immunoprecipitate together [53, 54]. Furthermore, it has been shown that a hydrophobic patch on the PR3 molecule mediates binding to NB1 [55]. Interestingly, it has been shown that only neutrophils that co-express NB1 and PR3 exhibit high levels of mPR3 expression [56]. In addition, and unsurprisingly given earlier data regarding the effect of PR3 expression levels on anti-PR3 induced neutrophil activation [49], neutrophils that present PR3 via NB1 produced greater levels of extracellular, but not intracellular reactive oxygen species, and underwent more robust degranulation, than their NB1 negative counterparts [56]. As NB1 is a GPI-linked membrane receptor lacking an intracellular signalling domain, questions remain as to how anti-PR3 binding to mPR3 induces neutrophil activation. While it is possible that ANCA binding to PR3 on the surface of the cell leads to the internalisation of the resulting antibody:antigen:receptor complex, this seems unlikely given the current available data. Indeed, the PR3:NB1 complex has been shown to exist in lipid rafts on the surface of neutrophils as part of a larger signalling complex that also includes CD11b/CD18 (Mac-1), FcγRIIIb and p22phox, an important component of the NADPH oxidase complex [56-58] (Fig 1.2). Therefore, it is likely that the ANCA signal is transduced across the plasma membrane by the transmembrane chains of CD11b and CD18. Further to this, blocking either of these β_2 integrins greatly reduces the ANCA induced respiratory burst and degranulation response in anti-PR3 IgG stimulated neutrophils [56].

In contrast to PR3, MPO is not found on the surface of isolated, resting neutrophils and the increase in surface expression after neutrophil activation is relatively small [49]. While there is little data on how MPO is anchored at the cell surface, it is possible that it is due to this highly cationic protein binding to negatively charged residues on the plasma membrane. Indeed, the ability of positively charged MPO to induce neutrophil chemotaxis via electrostatic interactions [45], suggests that MPO is indeed capable of interacting in such a manner with the neutrophil plasma membrane. Similarly to mPR3, it has been it has been shown that MPO on the surface of

neutrophils associates with membrane bound CD11b/CD18 (Fig 1.2). Furthermore, data suggests that this interaction plays an important role in anti-MPO induced degranulation, expression of integrins, and activation of NADPH oxidase [59].

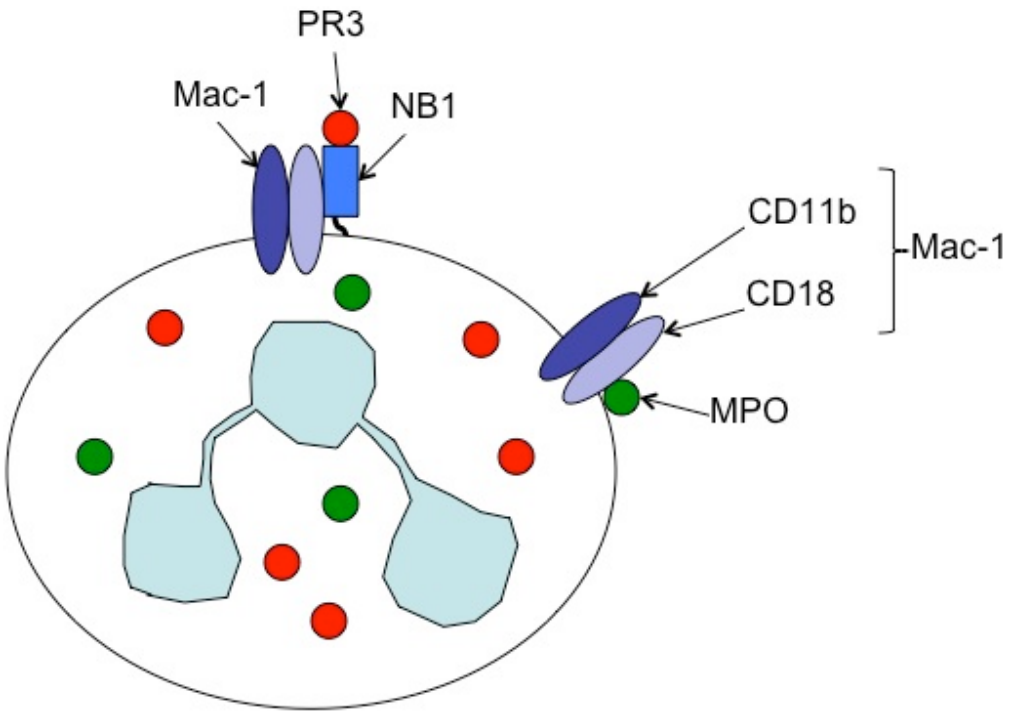

Figure 1.2 Surface expression of PR3 and MPO
PR3 on the surface of neutrophils is likely to be bound to the GPI-linked membrane receptor NB1. It has been shown that this complex also interacts with Mac-1 and thus is likely to signal through the transmembrane domains of CD11b and CD18. There is little data on how MPO is anchored to the cell membrane. However, it has been shown that it associates with Mac-1, and through this interaction modulates neutrophil signalling pathways.

1.2.2.2 LAMP-2: An additional target for ANCA?

In 1995 Kain et al. showed, having carried out a systematic search for ANCA antigens, that in addition to possessing autoantibodies against either PR3 or MPO, 14 out of 16 patients with pauci-immune NCGN also had antibodies to lysosomal membrane protein (LAMP)-2 [60]. LAMP-2 is a heavily glycosylated type I membrane protein expressed by both neutrophils and endothelial cells. It is a major component of the lysosomes, and is also present in the membranes of intracellular vesicles and, most notably, on the plasma membrane [60, 61]. Thus, due to this expression pattern, LAMP-2 on both neutrophils and endothelial cells is directly accessible to circulating antibodies.

In 2008, Kain et al. confirmed their initial study by showing that 78 out of 84 patients with active NCGN possessed antibodies against LAMP-2 and that this correlated with disease activity [62]. Furthermore, they showed that, *in vitro*, a monoclonal anti-LAMP-2 antibody could induce MPO release from neutrophils and apoptosis of human microvascular endothelial cells. *In vivo*, they showed that Wistar Kyoto (WKY) rats injected with polyclonal rabbit antibody against LAMP-2 developed severe pauci-immune NCGN. Notably, the potential for molecular mimicry to be involved in breaking tolerance by initiating anti–LAMP-2 autoantibody formation was suggested. First, it was shown that anti-LAMP-2 autoantibodies from individuals with pauci-immune NCGN bind an epitope that shares 100% sequence homology with the gram negative bacterial adhesin Fimbriae (Fim) H. Consequently, it was shown that patient antibodies cross reacted with FimH and, furthermore, that rats immunised with FimH developed antibodies that cross reacted with human and rat LAMP-2. Importantly, these rats subsequently developed pauci-immune NCGN. Finally, it was shown that infection with FimH-expressing bacteria is common in patients before the development of NCGN. This then provided evidence that FimH may indeed be responsible for triggering anti-LAMP-2 autoimmunity.

These finding, however, have been challenged by a North American study in which Roth et al. showed that only 21% of sera from 329 ANCA positive NCGN patients possessed anti-LAMP-2 autoantibodies, and that these did not correlate with disease [63]. Furthermore, they showed that anti-PR3 and anti-MPO titres were 10,000 and 1,500-fold higher that LAMP-2 titres, respectively. Finally, they did not observe any signs of disease in WKY rats immunised with anti-LAMP-2 antibodies. In contrast, and in a side-by-side publication, Kain et al. reconfirmed their findings in an additional European cohort showing that, overall, 81% of ANCA associated vasculitis patients in this study had circulating autoantibodies against LAMP-2 [64]. The reasons for this discrepancy are not entirely clear but it may be related to methodological differences, the most obvious being with regards to the patient populations tested. Kain et al showed that the highest anti-LAMP-2 titres were consistently found in newly presented, untreated patients with active NCGN. Furthermore, they found that anti-LAMP-2 antibody titres were highly sensitive to disease activity and immunosuppression. Indeed, in their most recent study, anti-LAMP-2 antibodies were found to be undetectable in 36 out of 37 patients as little as one month post treatment. In contrast, Roth et al. tested patients, the majority of which had received some form of treatment, with a range of disease activities. In addition to variation in the patient cohorts tested, the ELISAs used by Kain et al. and Roth et al. to measure anti-LAMP-2 antibody titres differed in the antigen substrate used, and thus this represents another potential point of divergence. Whatever the reasons for this conflicting data, further work will be required to determine whether anti-LAMP-2 antibodies have a role, either alone or in conjuction with anti-PR3/anti-MPO antibodies, in the pathogenesis of ANCA associated vasculitis.

1.2.4 Both the antigen binding region and the Fc portion of the ANCA molecule play a critical roles in neutrophil activation

The binding of ANCA to its antigen begins a signalling cascade that culminates in neutrophil activation. The region of the ANCA molecule responsible for this has been the subject of intense investigation with conflicting data emerging. While some studies have shown that signalling via

the cross linking of antigen by the antibody-binding region ($F(ab')_2$) is sufficient to induce full neutrophil activation [65, 66], others have demonstrated a need for concurrent Fc receptor (FcR) signalling [67-69]. Despite this conflicting evidence, the emerging picture is that both the antigen-binding region and the Fc portion of the ANCA molecule play critical roles in neutrophil activation. Using microarray gene chip analysis Yang et al. demonstated that ANCA IgG and ANCA-$F(ab')_2$ fragments induce the transcription of leukocyte genes [70]. Importantly, some of the transcribed genes were found to be unique to either the whole IgG or the $F(ab')_2$ region, while others were found to be common to both fragments. Further to this, signalling via both the antigen-binding region and the Fc portion of the ANCA molecule was shown to be necessary for full neutrophil activation, with ANCA $F(ab')_2$ fragments stimulating G protein coupled pathways and FcγR signalling activating tyrosine kinases [71] (Fig 1.3). Interestingly, both FcγRIIa and FcγRIIIb were shown to be involved, with the inhibition of either significantly reducing superoxide production in response to ANCA. This was not the first study to show a potential role for both FcγRIIa and FcγRIIIb in ANCA associated vasculitis and, indeed, ANCA has been shown to bind to both receptors. In addition, it has been established that FcγRIIa inhibition abrogates ANCA induced neutrophil activation. The data regarding FcγRIIIb blockade is, however, less clear [65-69]. Perhaps the most compelling evidence with regards the role of Fcγ receptors in ANCA induced neutrophil activation comes from *in vivo* data showing that anti-MPO IgG failed to induce leukocyte adhesion or transmigration in Fc receptor γ chain$^{-/-}$ mice [72]. This suggests that, whatever the role of FcγRIIa and/or FcγRIIIb ligation in the ANCA induced respiratory burst, it is likely that the FcγRs are necessary for neutrophil adhesion to endothelial cells, and thus disease pathogenesis.

Interestingly a recent study investigated the consequences of differences in the FcγRIIIb genotype on ANCA associated vasculitis [73]. Two common genetic varients exist, NA1 and NA2, with the NA1 allele producing stronger neutrophil response including phagocytosis, respiratory burst, and degranulation. Although no difference was found in the frequency of these

alleles among patients with GPA compared with healthy controls, the presence of the NA1 allele was associated with more severe renal disease. Similarly the allelic phenotype of FcγRIIa was shown to strongly influence the ability of anti-PR3 and anti-MPO to induce the production of neutrophil reactive oxygen species *in vitro* [67]. The presence of either a histidine or an arginine at position 131 of the receptor determines whether a high or low responding version of the receptor is expressed, with neutrophils possessing the high-responder variant showing a stronger ANCA response [67]. These data taken together suggest that the FcR genotype influences the phenotype of ANCA associated vasculitis.

While the majority of studies have focused on the role of IgG ANCA, and thus FcγRs, in ANCA associated vasculitis, there is some evidence that IgA ANCA, and thus FcαRs, are also important. In a recent study by Kelley et al. IgA ANCA was found to account for 27% of the ANCA present in GPA patients [73]. Interestingly, IgA ANCA was found to be less frequent in patients with severe renal disease, while it appeared to be more frequent in patients with upper airway involvement. In addition, this study also examined the genotype of the FcαR found in GPA patients. Two allelic variants of the FcαR have been identified, the result of a single-nucleotide polymorphism (SNP) that changes a serine (A) residue to a glycine (G). Importantly, the presence of the A allele is associated with a decreased immune responses, such as proinflammatory cytokine release, while the G allele is associated with increased cellular activation and phagocytosis. Kelley et al. demonstrated that the G allele was less common in patients with severe renal disease and more common in patients with upper airway involvement. Furthermore, neutrophils with the G allele were shown to undergo a stronger activation in response to IgA ANCA *in vitro*, perhaps unsurprising given the generally proinflammatory phenotype associated with this variant.

1.2.5 ANCA binding activates intracellular signalling leading to neutrophil activation

Various intracellular signalling molecules (Summarised in Fig 1.3) have been reported to have important roles in ANCA stimulated neutrophil activation. In 1999, Radford et al. showed that tyrosine kinases and protein kinase C (PKC), probably the β_{II} isoform, were required for ANCA induced superoxide release [74]. Using a similar approach, that is introducing specific inhibitors into neutrophil activation assays *in vitro*, Kettritz et al. showed that the mitogen activated protein kinase (MAPK) pathway had a crucial role in ANCA induced neutrophil activation [26]. In this study the inhibition of both extracellular signal-regulated kinase (ERK) and p38 MAPK significantly reduced the TNFα dependent, ANCA stimulated release of superoxide. Interestingly, it was shown that the inhibition of p38 MAPK, but not ERK, prevented the TNFα induced translocation of PR3 and MPO to the surface of neutrophils, thus suggesting that p38 MAPK activation is responsible for making these antigens available to circulating ANCA. ERK, in contrast, was thought to inhibit the TNFα mediated priming of neutrophils, required for the maximal generation of reactive oxygen species.

The role of phosphoinositol 3-kinase (PI3K) in ANCA associated vasculitis was investigated in a number of studies. Ben-Smith et al. first demonstrated that the PI3K inhibitors LY294002 and wortmannin were capable of suppressing the ANCA stimulated release of superoxide, thus suggesting that PI3Ks play an important role in ANCA signalling [75]. Furthermore, they showed that ANCA induced neutrophil activation results in the generation of the PI3K product phosphatidylinositol 3,4,5-triphosphate (PIP_3). Importantly, it was also shown that ANCA stimulation did not lead to the recruitment of the p85/p110 isoform of PI3K. Instead, the ability of Pertussis toxin to inhibited ANCA induced superoxide release, via the inhibition of G protein coupled receptors, indirectly suggested that ANCAs were likely to activate the p101/p110γ isoform. Kettritz et al. later confirmed that PI3K inhibition abrogates ANCA stimulated superoxide generation [76]. Furthermore, they

demonstrated that ANCA induced PI3K and p38 MAPK, but not ERK, activation leads to the phosphorylation and subsequent activation of Akt, an important serine/threonine-specific protein kinase that plays a role in mediating the neutrophil respiratory burst [77]. Importantly, Williams et al. showed that a combination of tyrosine kinase activation, requiring intact IgG ANCA signalling, and the recruitment of heterotrimeric G proteins, including Ras, by IgG ANCA $F(ab')_2$ fragments, is necessary for ANCA induced PI3K activation and subsequent superoxide generation [71].

Syk is a cytosolic protein and a member of the Src family of tyrosine kinases. It is essential for FcγIIa mediated leukocyte functions and is activated upstream by a receptor associated Src kinase. Targets of Syk include phospholipase C (PLC)γ and p85-PI3K. Importantly, it was found that the inhibition of Syk abrogated ANCA stimulated superoxide release [78]. In addition, Syk was shown to be phosphorylated, and thus activated, by the incubation of human neutrophils with intact IgG ANCA, but not with ANCA $F(ab')_2$ fragments, suggesting that its activation is linked to FcγR ligation. Indeed, anti-FcγRIIa and anti-FcγRIIIb antibodies partially inhibited Syk phosphorylation and subsequent superoxide release. Interestingly, antibodies to CD18 also reduced Syk phosphorylation in response to ANCA. The ability of Syk to activate PLCγ suggests a potential role for diacylglycerol (DAG) and inositol triphosphate (IP_3), products of the PLCγ mediated cleavage of phosphatidylinositol 4,5-bisphosphate (PIP_2), in ANCA induced neutrophil activation. Indeed, DAG is required for PKC activation, which, as mentioned previously, has a role in the ANCA induced generation of superoxide [74]. Further to this, Williams et al. showed that ANCA stimulation led to the DAG kinase catalysed formation of phosphatidic acid (PA) from DAG, and that this had an important role in Mac-1 mediated, ANCA induced, neutrophil adhesion [79]. The subsequent generation of PIP_2 from PA by the action of phosphoinositol (4) phosphate-5-kinase Iγ (PIPKIγ) was suggested as the mechanism of this PA dependent adhesion, with PIP_2 going on to activate Mac-1 through interactions with talin, a cytoskeletal protein known to be involved in intergrin activation.

In vitro data does not always reflect the *in vivo* situation and thus animal studies are an important step in the elucidation of signalling pathways in disease pathogenesis. Despite convincing *in vitro* results combined with data showing that activated p38 MAPK was identified in the glomerular lesions of patients with ANCA associated vasculitis [80], *in vivo* inhibition of p38 MAPK, using a daily oral treatment protocol on mice that had received a passive transfer of anti-MPO IgG, had only modest protective results [81]. While both treatment and pre-treatment with the p38 MAPK inhibitor slightly decreased the number of glomerular crescents and the influx of macrophages, there was no effect evident on albuminuria or haematuria. These results show that although p38 MAPK has a pivotal role in ANCA induced neutrophil activation *in vitro*, there are likely to be other more important molecules at work *in vivo*. Once such molecule may be PI3Kγ. As previously discussed, *in vitro* data using PI3K inhibitors [75, 76], together with data showing the importance of signalling molecules downstream of PI3K [71, 75, 76], have identified it as a possible key signalling molecule in ANCA associated vasculitis. Importantly, Schreiber et al. recently examined this *in vivo* using their bone marrow transplantation model of disease [82]. In this study, PI3Kγ deficiency completely protected mice from disease induced by anti-MPO antibodies. Furthermore, mice expressing normal levels of PI3Kγ, when treated with the PI3Kγ inhibitor AS605240, were also protected from anti-MPO induced NCGN. Although the results from this study are promising, the authors failed to address issues regarding the role played by PI3Kγ in neutrophil chemotaxis. Several studies have shown that PI3Kγ deficient neutrophils exhibit impaired migration in response to fMLP [83-85], IL8 [84] and C5a [84, 85]. Thus, it is possible that the protective effect of PI3Kγ loss is due, not to an effect on ANCA signalling, but is instead the result of insufficient neutrophil trafficking to the kidneys of mice. Despite this, the combination of *in vitro* data using human cells and data derived from *in vivo* mouse work, though incomplete, suggests that PI3Kγ may be an important potential therapeutic target for the treatment of ANCA associated vasculitis.

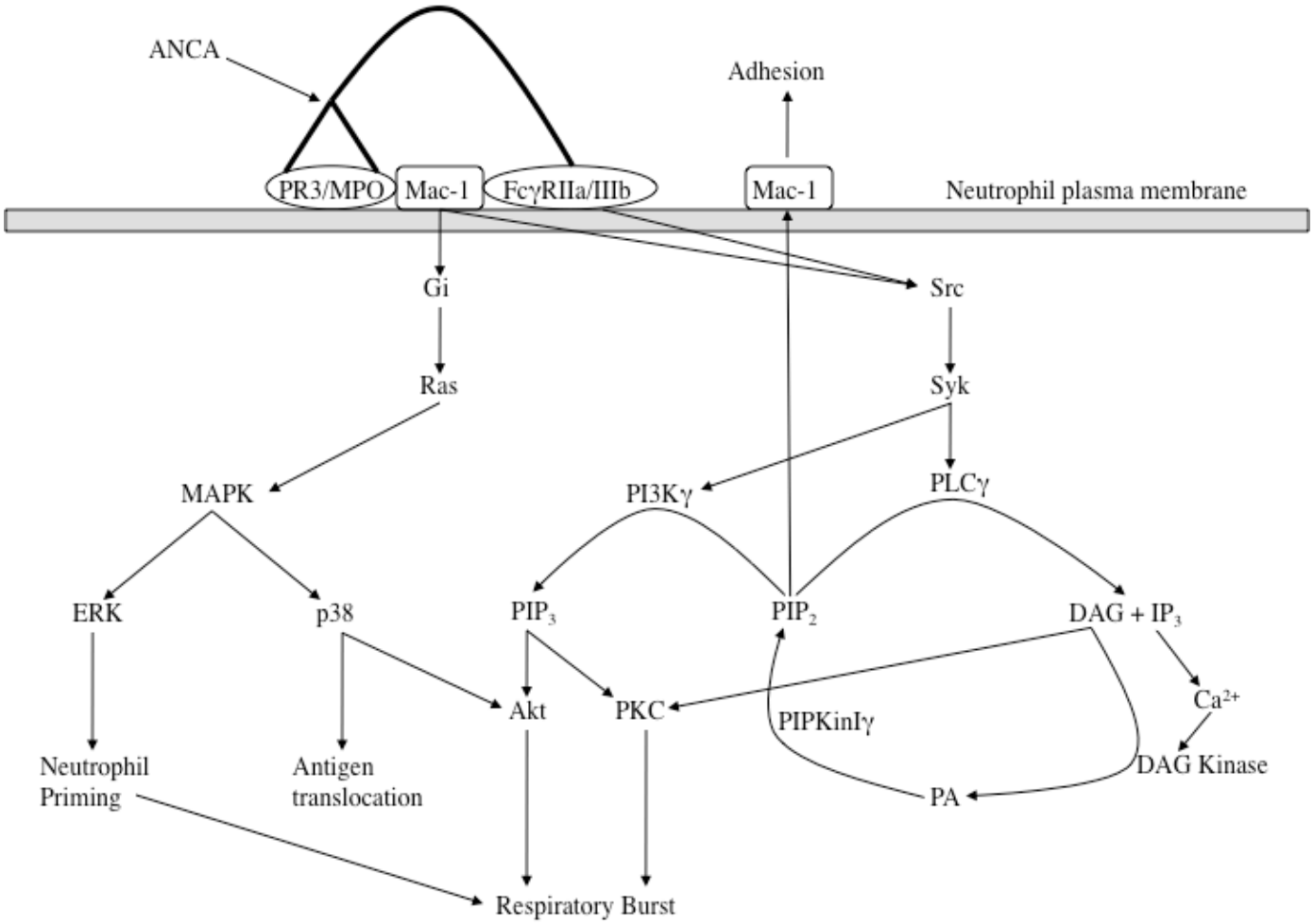

Figure 1.3 ANCA signalling.

This figure shows the potential key signalling molecules involved in the IgG ANCA induced neutrophil respiratory burst. PR3 exists in lipid rafts on the surface of neutrophils as part of a larger signalling complex that also includes Mac-1 and FcgRIIIb. In addition, MPO has also been shown to be associated with Mac-1 on the surface of neutrophils. The binding of ANCA to PR3/MPO stimulates G coupled protein pathways, likely via these antigens interacting with Mac-1. This leads to the activation of the MAPK pathway, as well as to signalling via PI3K, culminating in the activation of the neutrophil respiratory burst. Meanwhile, FcgR ligation by the Fc portion of the ANCA molecule leads to the activation of Src family tyrosine kinases, and thus to an increase in neutrophil adhesion, via generation of PIP_2 , and reactive oxygen species production, primarily via pathways downstream of PI3K.

1.2.6 A role for Complement in ANCA associated vasculitis?

The observation that mice treated with cobra venom factor (CVF), and thus depleted of complement, were protected from anti-MPO antibody induced disease was the first evidence that the complement system plays an important role in ANCA associated vasculitis. Indeed, it was shown that it is most likely the alternative pathway, and not the classical or lectin pathways of compliment activation, that is important in disease pathogenesis [86]. While C4 deficient mice developed disease comparable to wildtypes when treated with anti-MPO antibodies, factor B deficient mice appeared to be resistant to anti-MPO IgG induced NCGN. Furthermore, mice lacking the complement component C5, an important protein involved in neutrophil chemotaxis and activation, were completely protected from disease induced by the passive transfer of anti-MPO antibodies. In addition to this, the importance of C5 was confirmed in a separate study in which mice treated with an anti-C5 monoclonal antibody were protected from NCGN induced by the passive transfer of anti-MPO antibodies [87]. *In vitro* experiments showed a specific role for C5a with the observation that the supernatant from TNFα primed, ANCA stimulated neutrophils was sufficient to cause the generation of C3a and C5a in normal serum but not in serum lacking C5 [88]. Furthermore, the blockade of the C5a receptor was shown to inhibit the ANCA induced respiratory burst. The importance of the C5a receptor was then confirmed *in vivo* using a bone marrow transplant model of disease, with mice receiving C5aR deficient bone marrow developing relatively mild GN in response to anti-MPO IgG when compared mice receiving wildtype bone marrow. These data suggest that the alternative pathway, and particularly C5a, may represent an important therapeutic target in ANCA associated vasculitis treatment.

1.3 Animal models of ANCA associated vasculitis

1.3.1 Anti-MPO antibody induced models of disease

1.3.1.1 Spontaneous disease (Table 1.1 Model 1)

The spontaneous crescentic glomerulonephritis/Kinjoh (SCG/Kinjoh) strain of mice spontaneously produces anti-MPO antibodies while simultaneously developing necrotizing vasculitis and crescentic GN [89]. Consequently this strain has been suggested to represent a possible model of ANCA associated vasculitis. However, as these mice are the result of selective breeding, for a high percentage of glomerular crescent formation, among the offspring of mated siblings of (BXSB/Mp x MRL/Mp-lpr/lpr) F1 hybrid mice, they also possess anti-nuclear autoantibodies [90] that may contribute to kidney pathology. Furthermore, disease is associated with significant immune complex deposition, and thus does not mirror the pauci-immune NCGN typically observed in patients. Therefore, while these mice may provide useful data on the spontaneous generation of anti-MPO autoantibodies, the study of monoclonal anti-MPO from these mice has already provided insight into their structure [91], they are not suited to the study anti-MPO induced tissue damage.

1.3.1.2 Passive transfer model (Fig 1.4 A, Table 1.1 Model 2)

Xiao et al. were the first to show, using a mouse model, that anti-MPO antibodies were pathogenic [92]. This was achieved using a passive transfer model. Anti-MPO antibodies were raised by the immunisation of $MPO^{-/-}$ mice with murine MPO, and these antibodies were found to induce a pauci-immune NCGN when subsequently transferred to either wild type or recombinase activating gene (RAG) $2^{-/-}$ mice, a strain lacking functional T and B cells. Although disease was mild, with less than 5% of glomeruli affected in wild type mice, this represented a major breakthrough in the study of ANCA induced disease. Not only did it provide evidence that anti-MPO antibodies alone were sufficient to induce pathological changes, but it also presented a

model of disease that could be used to both explored the pathogenic mechanisms of ANCA associated vasculitis, and to test potential therapeutic interventions. In the same study, the transfer of whole splenocytes from MPO immunised $MPO^{-/-}$ mice into either wild type or $RAG2^{-/-}$ mice induced a far more severe NCGN. However, this was associated with significant immune complex deposition, and thus did not represent the pauci-immune vasculitis seen in man. The presence of these immune complexes, not seen in the IgG transfer model, is likely due to the proliferation of transferred lymphocytes.

The relatively mild manifestation of disease is a major drawback of the passive transfer model. However, in a subsequent study Huugen et al. demonstrated that the administration of LPS together with the anti-MPO antibodies could exacerbate disease, although not to extent seen in patients [23]. This was shown to be the result of an increase in circulating TNFα and MPO. As TNFα has been shown to induce the translocation of MPO to the surface of human neutrophils *in vitro*, and thus to be important for *in vitro* ANCA assays [14, 16, 26], it is likely that LPS serves, at least partially, to prime mouse neutrophils for anti-MPO IgG induced activation. In addition, LPS has been shown to be important in other models of GN due to its ability to stimulate renal cells via the activation of TLR4 [93, 94]. Therefore, effect of LPS on disease severity may be the result of the activation of numerous signalling pathways.

1.3.1.3 Bone marrow transplant model (Fig 1.4 B, Table 1.1 Model 3)

Using a similar approach, that is immunising $MPO^{-/-}$ mice with murine MPO, Schreiber et al. developed an alternative model of anti-MPO induced NCGN [95]. In this model $MPO^{-/-}$ mice that have been primed with MPO, and thus have developed anti-MPO antibodies, are irradiated and then reconstituted with wildtype bone marrow derived cells. As antibody-producing plasma cells are generally able to survive irradiation, anti-MPO titres are kept relatively constant, and, with the transplanted bone marrow providing neutrophils possessing MPO, a mild NCGN is induced.

A minor drawback of this approach, however, especially when compared with the passive transfer model, is that the reconstitution of these bone marrow chimeras takes time and consequently disease can take approximately 8 weeks to develop. Despite this the bone marrow transfer model provides (1) further evidence that ANCA are directly pathogenic, (2) evidence that bone marrow derived cells are sufficient targets for ANCA to induce disease, (3) another model of ANCA associated vasculitis that may be used to both examine mechanisms of disease, particularly through the use of bone marrow derived from genetically modified strains of mice, and to test possible therapies.

1.3.1.4 Mouse model of autoimmune vasculitis (Fig 1.4 C, Table 1.1 Model 4)

Another recently described model involves the immunisation of wild type mice with MPO, thus allowing both cellular and humoral immune responses to be raised against the native mouse protein [96]. Despite this, and perhaps due to the relatively low levels of anti-MPO antibodies generated, immunisation with MPO is not sufficient to induce renal damage. This issue can, however, be overcome by the administration of an anti-glomerular basement membrane antibody. The glomerular binding antibody used is a polyclonal sheep antibody raised against a crude glomerular preparation and serves to attract neutrophils to the glomeruli leading to the deposition of MPO, which then acts as a planted autoantigen for anti-MPO antibodies and, importantly, specific $CD4^+$ T cells, resulting in significant NCGN.

The main disadvantage of this model is the need for a glomerular binding antibody to trigger disease induction. As there is no equivalent to this seen in ANCA induced disease in patients, this complicates the model leading to questions regarding its relevance to the human condition. Despite this, and in contrast to the other models described, this approach allows the study of cellular anti-MPO immune response and their role in NGCN associated with anti-MPO autoimmunity. Indeed, this model has been used to demonstrate the importance of anti-MPO $CD4^+$ T cell responses, with their depletion prior

to disease induction found to be protective in a manner independent of the anti-MPO antibody titre [96]. Furthermore, this model has been used to implicate Th17 cells, a highly proinflammatory subset of $CD4^+$ T cell, in the pathogenesis of anti-MPO induced disease [97]. Following on from this, the same group showed that TLR2 and TLR9 are likely to have roles in the pathogenesis of ANCA associated vasculitis [27]. Interestingly, TLR2 activation was shown to enhance disease via the stimulation of Th17 responses, including IL17 production, while TLR9 ligation induced Th1 responses, primarily interferon (IFN)γ production, and a through this an increase in disease severity.

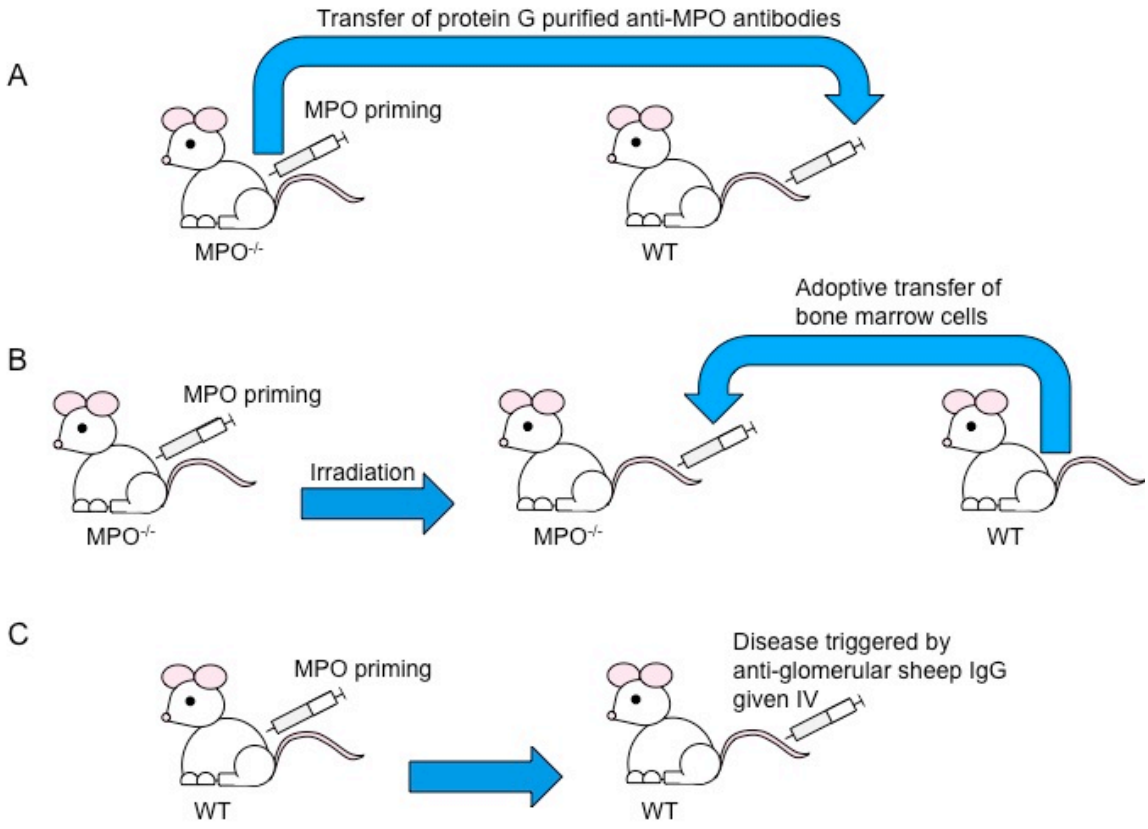

Figure 1.4 Mouse models of ANCA associated vasculitis.
Summary of the three most commonly used mouse models of ANCA associated vasculitis. (A) The passive transfer model, (B) the bone marrow transplantation model and (C) the mouse model of autoimmune vasculitis. $MPO^{-/-}$- myeloperoxidase deficient mouse, WT-wildtype (C57BL/6) mouse

1.3.1.5 Rat model of autoimmune vasculitis (Table 1.1 Model 5)

In addition to mouse models of disease an experimental autoimmune model of vasculitis has also been developed in rats [98]. In the initial study, the immunisation of WKY rats with human MPO in Complete Freund's Adjuvant (CFA) led to the generation of high levels of cross-reactive anti-MPO antibodies in all rats tested. Between 6 and 8 weeks post immunisation approximately 60% of the immunised animals had developed a mild form of NCGN. Interestingly, approximately 40% of the immunised rats showed signs of pulmonary haemorrhage. A subsequent study by the same group confirmed that human MPO administration could induce anti-MPO antibody generation and associated GN, and pulmonary damage, in WKY rats [99]. Furthermore, this study showed that the disease severity depended on the dose of MPO administered and, interestingly, that the addition of pertussis toxin to the CFA during the immunisation stage allowed disease to be induced in all immunised rats. As pertussis toxin has been shown to not only activate naïve $CD4^+$ T cells but to also stimulate TLR2/4 activation, and thus skew for Th1/Th17 responses [100], this result reiterates the potential role of these factors, shown to be critical in the mouse model of autoimmune vasculitis, in disease induction [27, 97].

In should be noted that to date disease has only been induced in the WKY rats, an inbred strain already known to be susceptible to GN. Interestingly, the Lewis, Wistar Furth and Brown Norway strains of rats appeared resistant to disease, despite generating similar levels of anti-MPO antibodies upon immunisation [99]. This suggests that there are also other complex, and likely multi-genetic, components involved in susceptibility to disease.

1.3.2 Anti-PR3 antibody induced models of disease

Various attempts have been made to develop an *in vivo* model of PR3-ANCA induced vasculitis, and thus provide evidence of a pathogenic role for anti-PR3 antibodies. Unfortunately, and despite the development of anti-PR3 antibodies in both mice and rats, there has been limited success in inducing

disease in rodents. An early study showed that mouse specific PR3 antibodies could be generated by immunising PR3/neutrophil elastase double deficient mice with recombinant mouse PR3 [101]. However, these PR3 antibodies failed to induce disease when transferred into LPS primed wildtype recipients, although, interestingly they did significantly increase inflammation in TNFα primed skin. This suggests that while anti-PR3 antibodies have an effect, they are insufficient to induce histological and subsequent functional changes in the kidneys of mice in and of themselves. In another study, van der Geld et al. immunised mice and rats with chimeric human/mouse PR3 leading to the development of circulating anti-PR3 antibodies [102]. However, while both mice and rats had high anti-PR3 antibody titres, they did not develop any signs of disease. More recently, it was observed that non-obese diabetic (NOD) mice, immunised with recombinant mouse PR3, developed anti-PR3 antibodies but, as with previous studies, displayed no signs of disease [103]. Importantly, however, it was found that the transfer of splenocytes from these mice into highly immunodeficient NOD/SCID mice resulted in vasculitis with a severe segmental and necrotising glomerulonephritis, ultimately leading to acute kidney failure and death (Table 1.1 Model 6). Therefore, and taking account the lack of disease in controls, this study provides some of the first evidence that anti-PR3 immune responses are capable of inducing disease *in vivo*. In contrast to this, and in the same study, a similar transfer of splenocytes into immunodeficient C57BL/6-RAG$^{-/-}$ recipients did not result in disease. This then suggests that there are not only factors present in NOD mice that protect against disease but that there are also other multi-genetic factors involved in pathogenesis.

The lack of success in developing a mouse model of anti-PR3 associated disease is mostly likely due to the differences between mouse and human PR3 [104] perhaps most importantly with regards to their expression patterns. While the expression of human PR3 on the surface of circulating neutrophils has been confirmed, and shown to be induced by treatment with TNFα among other cytokines, to date PR3 has not been found to be present on the plasma membrane of circulating mouse cells [101]. Thus mouse PR3 is likely to

remain unavailable to any anti-PR3 antibodies that are generated. However, that there do exist data showing a limited affect of anti-PR3 antibodies *in vivo* [101, 103] suggests that under certain conditions anti-PR3 antibodies are capable of interacting with mouse PR3. It is unknown whether this is due to membrane expression of mouse PR3, or some degree of ANCA internalisation which makes surface PR3 expression unnecessary.

1.3.3 Limitations of the current models of ANCA associated vasculitis: A summary

Each of the models of ANCA associated vasculitis described above comes with its own set of advantages and disadvantages and, as a result, the best model to use depends heavily on the question being asked. Table 1.4 shows a brief summary of the important points that may need to be considered when choosing a suitable animal model of ANCA induced disease.

Of the six models described, four (Model 1 and Model 4-6) can be considered autoimmune. Of these only one is due to the spontaneous generation of anti-MPO immunity (Model 1), however, this model is neither pauci-immune nor is pathology necessarily due to anti-MPO responses alone. Indeed both autoantibodies to ssDNA and dsDNA are present in these mice, thus making pathogenesis studies complicated. Furthermore, genetically modified strains of mice cannot easily be employed. Of the models of induced by anti-MPO immunity, Model 4 (the autoimmune mouse model) requires additional antibodies, against the glomerular basement membrane, to recruit neutrophils and thus trigger disease, while Model 5 (the autoimmune rat model) has only relatively mild disease. It should be noted however that new technology, allowing the genetic manipulation of embryos, has made the generation of knockout rats possible [105], thus making the use of this autoimmune model in the study of ANCA induced vasculitis slightly more attractive. The sole PR3-ANCA induced disease model described requires the use of a specific strain of mice, and while disease is robust it is unknown whether it is pauci-immune. However, based on similar experiments using splenocyte transfer from mice immunised against MPO (Model 2a) it is likely that there is significant immune

complex deposition as a result of homeostatic proliferation of transferred lymphocytes.

In contrast to the autoimmune models, disease in both the passive transfer models (Model 2a and 2b) and the bone marrow transplantion model (Model 3) is the result of the generation of an immume response to a foreign antigen and therefore may differ to the disease induced following a break in tolerance. Furthermore, in the case of the Model 2a (the passive transfer model) and Model 3 (the bone marrow transplantation model) disease is both mild, and induced in the absence of cellular immune responses and indeed this may be why the disease observed is not as severe as that seen in patients. In contrast the transfer of splenocytes (Model 2b) induces a much more severe disease but it is not pauci-immune, and thus does not reflect the GN seen in humans.

Model	Autoimmune?	Pauci-immune?	Cellular immunity involvement?	Disease severity?	Allows for the use of genetically modified rodents?
1. Spontaneous disease	Yes	No	Yes	Robust	No
2a. Passive transfer of antibody	No	Yes	No	Mild	Yes
2b. Passive transfer of splenocytes	No	No	Yes	Robust	Yes
3. Bone marrow transplant	No	Yes	No	Mild	Yes
4. Autoimmune disease of mice	Yes	Yes*	Yes	Robust	Yes
5. Autoimmune disease of rats	Yes	Yes	Yes	Mild	Yes
6. Transfer of splenocytes from PR3 primed NOD mice into NOD/SCID mice	Yes	Not reported	Yes	Robust	No

Table 1.1 Summary of the recently used rodent models of anti-MPO (Models 1-5) and anti-PR3 (Model 6) antibody induced GN.

* Disease is pauci-immune, however, anti-glomerular basement membrane antibody administration is required to attract neutrophils to the kidneys were they deposit MPO which acts as a planted autoantigen thus allowing disease induction.

1.4 Humanised mice

1.4.1 A brief history

Due to moral and ethical constraints, studies on human physiology and pathology are largely dependent on the use of surrogate *in vitro* assays and *in vivo* experiments carried out on small vertabrates, and to a lesser extent invertebrates. Sharing many basic characteristics with humans, mice in particular, due to their small size and reproductive characteristics (short gestation period, large litters, rapid sexual maturity), have become the main animals used for *in vivo* biomedical research. However, millions of years of evolution have led to fundamental differences in mouse and human biology, and thus discoveries made in mice do not always translate to humans, a fact that has led to a search for alternative methods to study human biological processes *in vivo*.

The idea of creating more human like animals is not new. In an 1896 novel, The Island of Dr. Moreau by H.G. Wells, the eponymous scientist creates sentient human like creatures from animals and, using this device, the narrative explores both the distinction between man and animal and the potential limits of natural science. Outside the realms of science fiction, an early study showed that foetal sheep could be successfully engrafted with human haematopoietic stem cells (HSC) and could therefore express cellular components of the human immune system [106]. In this model, the transplanted human cells colonised the bone marrow where they persisted for many years. Importantly, these cells retained the ability to undergo multilineage differentiation and, furthermore, were capable of responding to human cytokines, with regular granulocyte-macrophage colony-stimulating factor (GM-CSF) and IL3 administration leading to an increase (from approximately 5-15%) in the percentage of human cells found in the bone marrow [106, 107]. Despite this, low levels of engraftment combined with both financial and time constraints, made the use of this model undesirable. Initial studies in mice, on the other hand, were less successful. Genetically athymic, and thus T cell deficient, nude mice failed to support the growth of human

HSCs [108]. Fortunately, three years later the first of three major breakthroughs that would allow for the successful engraftment of human HSCs into mice occurred. The discovery of a severe combined immunodeficient (SCID) mouse, the result of a $Prkdc^{scid}$ (protein kinase, DNA activated, catalytic polypeptide; severe combined immunodefiency) mutation in CB17 mice, provided a model lacking in both T and B cell activity, and thus unable to effectively reject transplanted human cells or tissues [109]. Following on from this, in 1988 Mosier et al. carried out the first successful xenogeneic graft of human immune cells into SCID mice using peripheral blood mononuclear cells (PBMCs) [110]. Shortly after, the engraftment of these mice with foetal haematopoietic liver and thymus [111], and human HSCs [112] was also shown to be possible. Despite these early successes human engraftment levels remained low, human cells represented approximately 0.5-5% of the mouse bone marrow, and no functional immune responses were observed. Reasons for this include an abundance of natural killer (NK) cells and other innate immune cells, which act to limit engraftment, and the age related “leakiness” of this model, which results in the spontaneous generation of functional mouse T and B cells and thus induces further graft rejection [113].

The second major breakthrough was the crossing of the scid mutation onto mice with a nonobese diabetic (NOD) background. The resulting NOD-scid mice not only lacked functional T and B cells but also had defects in their NK cell, macrophage and complement activity [114], thus allowing for greater levels of human cell engraftment post transfer of human PBMCs and HSCs [115-117]. Although an improvement over previous models, showing approximately 5- to 10-fold greater human chimerism compared to SCID mice, the use of humanised NOD-scid mice remained limited by residual NK cell activity, leading to low engraftment, and the short lifespan of the mice, due in part to the tendency of this strain to develop lethal thymomas [118, 119].

The third and final breakthrough was the development of mice with mutations in their IL2 receptor common gamma chain (IL2rγ chain). As the IL2rγ chain is

required for high-affinity signalling through multiple cytokine receptors, including IL2, IL4, IL7, IL9, IL15 and IL.21 [120], its impairment leads not only to the absence of T and B cells but, crucially, the loss of NK cells as well [121, 122]. This in turn leads to an environment in which transplanted human cells can survive and engraft. Consequently, mice bearing mutations in their IL2rγ chain, whether it results in an absent [123] or truncated γ chain [121, 122, 124], have thus far provided the best models for engraftment of human immune cells, with several early studies showing high levels of human leukocytes present in the circulation of these mice several months post adoptive transfer of human HSCs [125-127]. Importantly, IL2rγ$^{-/-}$ mice have similar life spans to their wild type counterparts [119].

1.4.2 Immune models

IL2rγ$^{-/-}$ mice are available on a number of backgrounds with commonly used strains including NOD/LtSz-scid IL2rγ$^{-/-}$, NOD/Shi-scid IL2rγ$^{-/-}$ (both referred to as NOD-scid IL2γ$^{-/-}$ mice), NOD-Rag1$^{-/-}$IL2rγ$^{-/-}$ and BALB/c-Rag2$^{-/-}$ IL2rγ$^{-/-}$ [119, 128]. In addition, a number human cell and tissue types from a number of different sources can be used to generate these human-mouse chimeras or "humanised mice". Furthermore, several injection routes can be used in order to introduce the human cells into the mouse host, depending at least partially on the whether mice are engrafted as neonates or adults [129]. Consequently, a number of techniques to generate humanised mice have been developed over the last few years. Notably, for the majority of models developed, the mouse host must first be conditioned to allow optimal human engraftment. This usually takes the form of sublethal γ irradiation. The dose of radiation required is both age and strain specific, with neonatal mice requiring smaller doses than adults. Furthermore, mice with the scid mutation are more radiosensitive, due to defects in DNA repair, than mice with the Rag1$^{-/-}$ or Rag2$^{-/-}$ mutations, and thus also require smaller doses of radiation [119]. The humanised mouse models used most frequently in the *in vivo* study of the human immune system will be summarised in the following subsections while

the main advantages and disadvantages of each model is further detailed in Table 1.2.

1.4.2.1 The Hu-PBL model (Fig 1.5 A)

Peripheral blood leukocyte (PBL) engraftment of both NOD-scid IL2$\gamma^{-/-}$ [119] and BALB/c-Rag2$^{-/-}$ IL2r$\gamma^{-/-}$ mice has been observed, although BALB/c-Rag2$^{-/-}$ IL2r$\gamma^{-/-}$ mice require significant conditioning, including both irradiation and treatment with macrophage depleting clondronate-containing liposomes, before the transplanted human cells are accepted [130]. In contrast, NOD-scid IL2$\gamma^{-/-}$ mice do not require conditioning before engraftment and thus are the preferred strain used to generate these mice [119]. T cells are the main human cell type observed in this model post PBL transfer, and thus this system has the potential to be used to study mature effector T cell responses, although the inability of these human leukocyte antigen (HLA) restricted T cells to interact with mouse major histocompatibitily complex (MHC) molecules is a significant limitation that must first be overcome [131]. In addition, this model has been used to study xenogeneic graft vs host disease [132], and with the transplantation of human skin grafts onto mice, has proved a useful tool for the *in vivo* study of human transplant rejection [133].

1.4.2.2 The Hu-HSC model (Fig 1.5 B)

HSCs have the potential to develop into cells of either the lymphoid or myeloid lineage. They are self-renewing, and once they colonise the host mouse, capable of providing a long-term source of human cells [134]. They can be derived from peripheral blood, bone marrow, foetal liver and umbilical cord blood (UCB). CD34, an early stage stem cell marker, is frequently used to identify and isolate HSCs for subsequent transfer into conditioned immunodeficient mice. Thus humanised mice, with high levels of engraftment, can be generated by the transfer of human CD34^{+} stem cells into a) irradiated adult NOD-scid IL2$\gamma^{-/-}$ mice by intravenous or, less commonly, intrafemoral injection or b) irradiated neonatal NOD-scid IL2$\gamma^{-/-}$ or BALB/c-Rag2$^{-/-}$ IL2r$\gamma^{-/-}$

mice by intrahepatic or intravenous (via the facial vein or the heart) injection [129]. To date mice engrafted in this way have been shown to reconstitute human T cells, B cells, NK cells, myeloid and plasmacytoid dendritic cells (mDCs and pDCs, respectively), monocytes/macrophages and granulocytes (Discussed in detail in Section 1.4.3). Importantly, neonatal mice have been shown to not only have higher overall levels of engraftment, but also significantly greater T cell reconstitution when compared with adult mice, a fact likely related to thymic atrophy in older mice [128]. Importantly, this is perhaps the most commonly used humanised mouse model for the *in vivo* study of human immunity.

1.4.2.3 The BLT model (Fig 1.5 C)

This model was first described in NOD-scid mice [135], although NOD-scid IL2$\gamma^{-/-}$ mice are now more commonly used. It involves the implantation of foetal human liver and thymus under the renal capsule of adult mice. Once the mice have recovered from surgery, they are then irradiated and reconstituted with human foetal liver $CD34^{+}$ stem cells. The result is a mouse with a relatively robust human immune system comprising human B cells, DCs, monocytes/macrophages and, importantly, a high percentage of HLA Class I and Class II restricted T cells, the result of the formation of a thymus like organoid of human origin [136]. In addition, these mice develop human mucosal immune responses and thus are have become important tools for the *in vivo* study of HIV [137].

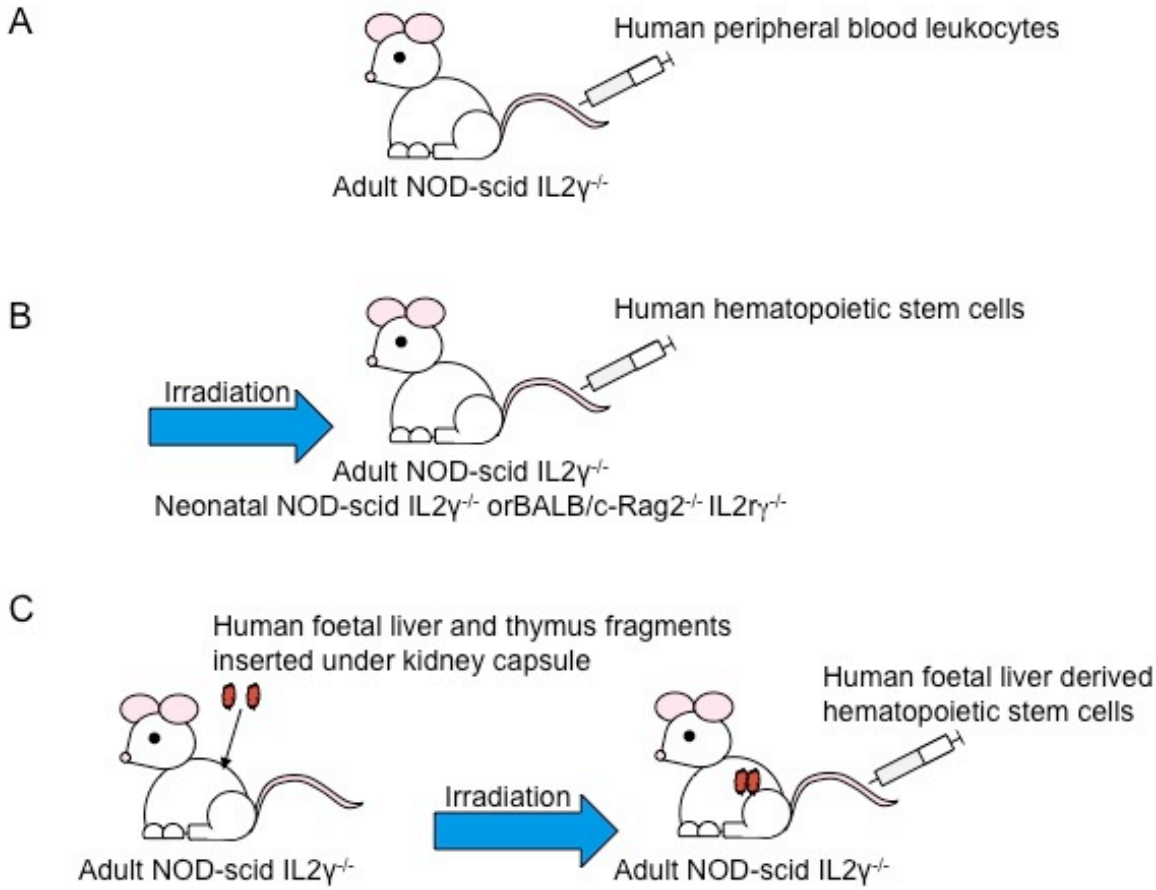

Figure 1.5 Humanised mouse models.

The three most commonly used humanised mouse models (A) The Hu-PBL model (B) the Hu-HSC model and (C) the BLT model

Model	Human engraftment	Advantages	Disadvantages
Hu-PBL	T cells, B cells, NK cells, monocytes/macrophages	Easy to generate, allows the in vivo study of human host vs graft disease	Human HLA restricted T cells do not interact well with mouse MHC molecules, poor myeloid cell engraftment
Hu-HSC	T cells, B cells, NK cells, myeloid and plasmacytoid DCs monocytes/macrophages and granulocytes	Most complete human cell reconstitution, easy to generate compared to the BLT model	Poor human T cell engraftment, poor myeloid cell engraftment
BLT	T cells, B cells, DCs, NK cells, monocytes/macrophages	Mice develop a human thymic organoid allowing for a strong HLA-restricted T cell response to be achieved	Difficult to generate, poor myeloid cell engraftment, lack of HLA APCs

Table 1.2 Summary of the most commonly used humanised mouse models

1.4.3 Engraftment: Current perspectives and steps towards a better model

The following section will provide an overview of the human cells reconstituted by humanised mice. The main focus will be on the characterisation of human cells in these mice, however, some of the limitations associated with humanised mice models, together with current and potential stratagies for overcoming them, will also be discussed.

1.4.3.1 Lymphoid lineage cells

1.4.3.1.1 Natural Killer cells

Human NK cells have been reported in the bone marrow, spleen, thymus, lymph nodes, liver, lung and peripheral blood of humanised mice engrafted with human HSCs [138-141]. Furthermore, both cytolytic $CD56^{hi}CD16^{+}$ and cytokine producing $CD56^{lo}CD16^{+}$ NK cell subsets have been identified [138, 142]. However, the overall percentage of NK cells seen in each of these compartments was very low. This is likely due to the lack of cross reactivity between human and mouse CD15, an important regulator of NK cell proliferation and activation. Indeed, several studies have confirmed that engrafted mice treated with exogenous human IL15 develop significantly higher levels of human NK cells [140, 141, 143]. Furthermore, following the hydrodynamic tail vein delivery of plasmid DNA, containing expression vectors for human IL15 and Flt-3/Flk-2 ligand, humanised mice developed significantly more NK cells [139]. Interestingly, while human cytokine expression persisted for 2-3 weeks, the mice maintained elevated NK cell levels for over a month. Furthermore, these cells were shown to express both inhibitory (NKG2A and KIR) and activating receptors (NKG2D), as well as the cytotoxicity receptor NKp46. Importantly, these human NK cells were shown to lyse MHC class I deficient target cells and to produce IFNγ in response to poly I:C challenge both *in vitro* and *in vivo*. In addition, they appeared to be capable of mounting a robust response against adenovirus infection, as measured by liver damage

(mediated by NK cells) and serum levels of IFNγ. The functionality of humanised mouse human NK cells was further confirmed both *in vitro* and *in vivo* [138, 144]. The co-culture of spleen and mesenteric lymph node derived NK cells with K562 cells, a human erythroleukemic cell line, led to NK cell activation as measured by IFNγ production, CD107a expression (indicating cell degranulation) and K562 cell inhibition and death [144]. In addition, humanised mice injected with K562 cells had a greater survival rate than non-engrafted controls, and this effect was lost in human $CD56^{+}$ cell depleted humanised mice. Interestingly, these mice had not received exogenous human IL15, although cells were incubated with human IL15 for the *in vitro* studies. In contrast, a study on NK cells generated by humanised NOD-scid $IL2\gamma^{-/-}$ mice engrafted with human PBLs (the previously described study used BALB/c-$Rag2^{-/-}$ $IL2r\gamma^{-/-}$ mice engrafted with UCB derived HSCs), and lacking human IL15, failed to respond to either K596 cells or a combination of PMA and ionomycin [142] *in vivo*. This discrepancy suggests that the function of humanised mouse human cells may be dependent the strain of mice used and the source of human cells used to engraft them.

1.4.3.1.2 B cells

B cells are the most abundant human cell type reconstituted by humanised mice. Post engraftment both the spleen and the bone marrow were reported to house large populations of immature human $CD24^{int/hi}$ and $CD38^{hi}$ expressing B cells, with the majority of splenic B cells also expressing IgM, and, in some cases, IgD. In addition, human B cells were identified in the lymph nodes and in the peripheral blood, where they were found to express IgM and/or IgD [126, 127, 145]. Notably, few $CD27^{+}$ memory B cells were detected, indicating that these humanised mouse human B cells were naïve [145]. Importantly, human B cell responses to both immunisation and viral infection have been reported. However, IgM has been found to be the main antibody produced in response to B cell challenge [126, 127, 146, 147]. Indeed, the relative paucity of IgG generated by humanised mouse human B cells suggested that these cells had difficulty undergoing class switching.

However, a recent study revealed that poor IgG production is most likely the result of a lack of T cell help rather than any intrinsic fault in the reconstituted human B cells [145]. While *in vivo* IgG production in response to immunisation was confirmed to be rare in this study, splenic human B cells cultured in the presence of human IL2, IL21 and an anti-CD40 antibody were found to produce IgM and IgG at levels comparable to that of normal B cells isolated from healthy volunteers. Furthermore, activation-induced cytidine deaminase (AID) induction and $IgD^{-}CD38^{+}$ and $IgD^{-}CD27^{+}$ expression were also observed under these conditions, confirming B cell differentiation into antibody secreting cells and memory B cells, respectively. In addition, it was demonstrated that IgG responses could be induced *in vivo* upon adoptive transfer of normal human T cells. Indeed, the introduction of volunteer PBMC derived T cells bearing a HLA matching that of the human progenitor cells, together with a HA peptide ($HA_{307-319}$) specific T cell receptor, led to the *in vivo* generation of HA-specific IgG. Together these data suggest that humanised mouse human B cells have all the molecular machinery required to undergo class switching, and that, it is the lack of T cell-B cell cooperation, due to human T cell restriction by murine MHC, that is likely to be the cause of the suboptimal human antibody responses observed in humanised mice [148].

1.4.3.1.3 T cells

Human T cells have been reported in the bone marrow, spleen, thymus, lymph nodes and peripheral blood of humanised mice engrafted with human HSCs [126, 127]. Unlike human B cells, which first appear approximately 1 month post engraftment, human T cells first appear at about 3 months, and peak at 5-6 months, post transfer of HSCs [149-151]. Subsets identified to date include $CD4^{+}$ and $CD8^{+}$ $\alpha\beta$ T cells, $CD4^{+}Foxp3^{+}$ T regulatory cells, NKT cells and $\gamma\delta$ T cells [126]. Interestingly, human T cell reconstitution was found to be greater in mice engrafted as neonates. While the exact reason for this is unclear it has been speculated that it is due to thymic organogenesis, with adult mice undergoing thymic hyperplasia before treatment with HSCs, and thus being unable to support significant T cell development [128]. Regardless,

the number of human T cells present in the periphery of these mice remains very low. It was initially thought that this might be due in part to the poor cross reactivity between human and mouse IL7, an important cytokine with roles in both T cell development and survival. However, while treatment with exogenous human IL7 led to an increase in the number of thymocytes, this did not translate to an increase in the number of peripheral human T cells [152]. In contrast, mice treated with human IL15, which has roles in both NK cell and T cell proliferation and activation, showed elevated levels of both $CD4^+$ and $CD8^+$ T cells [140]. However, these cells were of an activated/memory phenotype [142, 147, 152, 153]. Furthermore, NOD-scid $IL2\gamma^{-/-}$ mice made triply transgenic for human stem cell factor, GM-CSF and IL-3, were unexpectedly shown to have increased numbers of $CD4^+Foxp3^+$ T regulatory cells in their spleens but not their thymuses [154]. As the receptors for these cytokines were shown to be absent from the $CD4^+Foxp3^+$ T regulatory cells, it is likely that this was due to an indirect mechanism resulting in either the expansion of thymically derived T regulatory cells in the periphery, or the conversion of effector T cells to an induced-regulatory phenotype.

Data regarding the ability of humanised mouse human T cells to respond appropriately to immune challenge has been inconsistent. Early studies reported the induction of human T cell responses to inflammatory stimuli, including proliferation in response to Epstein–Barr virus (EBV) infection [126] and phytohemagglutinin, as well as cytotoxicity against cell lines [155]. However, data from later studies indicates that reconstituted human T cells have several functional defects. While human splenic T cells were capable of proliferating and producing cytokines in response to phytohemagglutinin, anti-CD3 antibodies and a mixure of PMA and ionomycin *in vitro*, the response observed was approximately 10-fold lower than that of normal human T cells [142, 145]. Interestingly, the ability of $CD4^+CD8^-$ single positive thymocytes to produce IL2 *in vitro* suggested that the functional impairment might occur after cells have migrated to the periphery [145]. Importantly, humanised mouse human $CD4^+$ T cells appear to respond poorly to immunisation with keyhole

limpet hemocyanin (KLH), with little IFNγ or IL4 production being induced following specific re-stimulation of these cells *in vitro* [145]. Indeed, this is consistent with the lack of B cell class switching, as measure by IgG secretion, observed *in vivo* in the same study. In contrast, human $CD8^+$ T cells were shown to aid the survival of humanised mice infected with EBV. When these mice were treated with either anti-CD3 or anti-CD8 antibodies their life span was reduced [156]. Furthermore, $CD4^+$ and $CD8^+$ T cells from EBV and HIV infected mice were reported to produce low levels of IFNγ and display some cytotoxicity in response to re-stimulation *in vitro* [126, 150, 157]. However, it must be noted that despite these positive results other studies have reported cellular responses to be absent in virally infected humanised mice [147].

The lack of HLA restriction affects both the number and functionality of human T cells reconstituted by humanised mice. Inefficient positive selection in the thymus likely results in low T cell production, while the lack of HLA interactions leads to poor T cell responses., and consequently B cell functional impairment [148]. Indeed, the generation of human HLA-transgenic mice has confirmed the importance of HLA restriction for T cell functional responses, with mice expressing HLA-A2 and HLA-DR4, and engrafted with HLA-matching HSCs, developing appropriate HLA-restricted T cell responses, and thus exhibiting increased cytokine and IgG production in response to viral challenge [158-161]. However, as these mice still express murine MHC class I and II molecules, some unwanted MHC restriction may still occur, leading to a degree of human T cell functional impairment. However, whether the replacement of mouse MHC molecules with their human counterparts will produce a model with more robust human T, B and NK cell (HLA-NK cell receptor interactions promote NK cell development and functionality) responses remains to be seen.

1.4.3.2 Myeloid lineage cells

To date the majority of research into the generation of humanised mice has focused on the development and study of lymphoid lineage cells. Consequently, there is relatively little known about the reconstitution or functional responses of human cells of myeloid origin, although this is beginning to change. The lack of focus on human myeloid reconstitution in humanised mice is perhaps due in large part to the suboptimal engraftment of human cells of this lineage in the current models. While human monocytes/macrophages, granulocytes and both mDCS and pDCs have been identified in humanised mice, they represent only a small percentage of the total human leukocytes reconstituted [119, 145]. The likely explanation for this is that the mouse environment in which these human cells develop does not provide the correct factors to allow the differentiation of human myeloid cells. Notably, while many human cytokines have been shown to cross-react with mouse receptors, many mouse haematopoietic cytokines appear to have no cross-reactivity with human cells [118, 162]. Therefore, in order to overcome this limitation, a number of groups have introduced human factors with important roles in myeloid differentiation/function into these mice, with varying degrees of success.

The hydrodynamic injection of plasmid DNA encoding human macrophage colony stimulating factor (M-CSF/CSF-1) into the tail vein of HSC engrafted mice enhanced the reconstitution of human $CD14^+$ monocytes [139]. In the same study, the injection of plasmid DNA encoding GM-CSF and IL4 led to an increase in the percentage of human $CD11c^+CD209^+$ DCs in the blood, spleen, bone marrow, lung and liver of all mice tested. Similarly, human CSF-1 knockin BALB/c-$Rag1^{-/-}\gamma c^{-/-}$mice engrafted with human foetal liver HSCs demonstrated enhanced reconstitution of human monocytes/macrophages [163]. Further to this, the human monocytes/macrophages taken from these mice were shown to have improved functional properties *in vitro*, including migration, phagocytosis, and activation. In addition, the human monocytes/macrophages in these mice were shown to respond more efficiently to LPS *in vivo*. This was demonstrated by the significant increase

the number of these cells present in the spleen, combined with the enhanced levels of human IL6 and TNFα found in the serum, of the human CSF-1 knockin mice 48 hours post LPS treatment. Around the same time, myeloid cell reconstitution in the lung was shown to be improved through the generation of humanised mice in which the murine IL3 and GM-CSF genes were replaced with human homologues [164]. The loss of murine GM-CSF results in pulmonary alveolar proteinosis syndrome; however, the generation of human alveolar macrophages by the human IL3/GM-CSF knockin humanised mice partially rescued them from this disorder. Furthermore, human alveolar macrophages correlated with improved human immune responses in mice challenged with influenza virus. Interestingly, NOD-scid IL2$\gamma^{-/-}$ mice made triply transgenic for human stem cell factor, GM-CSF and IL-3, were found to have only modest increases in myeloid engraftment while having significantly higher levels of human regulatory T cells in their periphery [154].

A recent study on the development of human myeloid subsets in humanised mice identified both granulocytes and myeloid lineage antigen presenting cells (APCs) in the bone and spleen of NOD-scid IL2$\gamma^{-/-}$ mice engrafted, as neonates, with human CD34$^+$ HSCs [165]. Granulocytes identified included CD15$^+$CD33^{low}HLA-DR$^-$ neutrophils, CD117$^-$CD123$^+$CD203c$^+$ basophils and CD117$^+$ CD123$^+$CD203c$^+$HLA-DR$^-$ mast cells, while the APC subsets comprised CD14$^+$CD33$^+$HLA-DR$^+$BDCA-1$^-$BDCA-3$^-$ monocytes, CD14$^-$ CD33$^+$HLA-DR$^+$BDCA-1$^+$BDCA-3$^+$ cDCs and CD123$^+$BDCA-2$^+$HLA-DR$^+$ pDCs. Furthermore, it was demonstrated that these cells responded appropriately to inflammatory stimuli *in vivo* and *in vitro*. Having first shown that human CD45$^+$CD33$^+$ cells expressed the appropriate cytokine receptors, it was shown that recombinant human (rh) GM-CSF, rhIFNγ and rhGCSF induced STAT phosphorylation in bone marrow derived neutrophils and monocytes, with *in vivo* GCSF treatment leading to an increase in myeloid lineage cells in the peripheral blood of 3 out of 3 mice tested. In addition, human monocytes and BDCA-1$^+$ DCs were shown to express TLR2, while human monocytes, neutrophils and DCs were shown to express TLR4.

Importantly, *in vivo* stimulation with the TLR4 ligand LPS induced the production of human TNFα, IL6 and IL8. Furthermore, lung derived human $CD45^+CD33^+$ cells were shown to be capable of phagocytosis *in vitro*, while BM derived human monocytes/macrophages could be induced to phagocytise and kill *Salmonella typhimurium in vitro* by treatment with IFNγ.

Although there have been significant advances made in our knowledge of human myeloid engraftment in humanised mice over the last few years, there are still numerous myeloid cell subsets yet to be evaluated. In addition, if we wish to establish the most accurate *in vivo* model of the human immune system, in which myeloid cells typically comprised approximately 50-70% of the human immune cells found, possible then models with significantly increased human myeloid cell engraftment are required.

1.4.4 Discoveries made using humanised mouse models: An overview

Humanised mice represent an important advancement in our ability to study the human immune system *in vivo*. Indeed, these models have already been shown to support infection with a number of human pathogens including HIV, EBV, dengue virus, *Plasmodium falciparum* and *Salmonella typhi*. In addition, it has been shown that humanised mice have the potential to model type I diabetes and various forms of cancer, including both solid tumours and haematological malignancies [131]. As humanised mouse models represent a broad and ever-expanding field, the following section will discuss a small selection of findings made through their use.

1.4.4.1 Human Immunodeficiency Virus (HIV)

Humanised mice provide a useful tool for the *in vivo* study of the human immune response to pathogens, particularly those of a viral nature that do not infect small laboratory animals. Thus, HIV was one of the first human diseases to be studied using humanised mice [166]. Subsequent studies have shown that the Hu-HSC and the BLT models support robust infection,

exhibiting both viremia in the bloodstream and dissemination of the virus to various organs [167]. Furthermore, the BLT model was shown to allow infection via the mucosal route [168]. Importantly, the infection of humanised mice with HIV was found to lead to the depletion of $CD4^+$ T cells [169], including T regulatory cells [170], and the proliferation of $CD8^+$ T cells [168, 171]. Interestingly, humoural immune responses have also been reported, with specific IgG production observed in infected BLT mice, a response likely made possible by improved T cell help provided by the HLA restricted human T cells generated by these mice [172].

To date humanised mice have been used to study the pathogenesis of HIV infection *in vivo* as well as to test potential HIV therapies. For example, BALB/c-Rag2$^{-/-}$ IL2r$\gamma^{-/-}$ mice engrafted with HSCs have been used to study the evolution of the HIV viral envelope gene, which encodes the viral surface glycoprotein (Env), a key mediator of viral entry to into cells [173]. Furthermore, a study using human HSC engrafted NOD-scid IL2$\gamma^{-/-}$ mice provided evidence that host APOBEC3s, cellular cytidine deaminases, are involved in inducing G-to-A mutations in the cDNA of the HIV virus *in vivo*, and thus may play a role in negatively regulating HIV infection [174]. With regards therapeutic trials, a mixture of Hu-HSC and BLT mice have been used to show that HIV infection can be suppressed by treatment with anti-retrovirals [175] and by the use of targeted siRNA therapy [176]. In addition, it has been shown that vaginal, rectal and intravenous transmission of HIV can be prevented by pre-treatment with anti-retrovirals [177, 178].

1.4.4.2 Epstein–Barr virus (EBV)

To date humans are the only known natural hosts of EBV, a herpesvirus thought to infect approximately 90% of the adult population. While infection is generally asymptomatic, EBV, particularly in immunocompromised hosts, is associated with a number of B cell and epithelial-cell malignancies, including Burkitt lymphoma, Hodgkin lymphoma, lymphoproliferative diseases and nasopharyngeal carcinoma. The study of EBV is complicated by its inability to

infect non-human cells. In fact humanised mice present the only animal model of infection currently available [179]. Indeed, humanised mice have been shown to support EBV infection with high viral doses leading to the formation of lymphoproliferative diseases that resemble, by their expression of latent EBV proteins, tumours found in patients [180]. Furthermore, EBV infection of humanised mice is associated with T cell proliferation, $CD4^+/CD8^+$ T cell ratio inversion [126, 135, 181] and the generation of activated memory T cells [135, 158]. In addition, the generation of protective T cell response have been shown to be dose-dependent [135, 158]. However, as previously discussed, T cell responses in humanised mice are suboptimal, with human T cell education in the mouse thymus leading to a lack of HLA restriction, and thus low numbers of weakly responding human T cells. Importantly then, NOD-scid $IL2\gamma^{-/-}$ HLA-A2 transgenic mice engrafted with HLA-matching HSCs developed appropriate HLA-restricted T cells responses, including cytotoxicity, in response to EBV epitopes [159].

Notably, the use of humanised mouse models of EBV has led to the discovery that the absence of the EBNA3B gene, a virus encoded tumour suppressor, leads increased viral evasion of the host immune response as well as virus driven lymphomagenesis [182]. In addition, humanised mice have been used to provide evidence that lytic EBV infection, EBV can infect cells in latent or lytic forms, plays an important role in the development of B cells lymphomas [183, 184].

1.4.4.3 Dengue Virus

Dengue virus is small, enveloped RNA flavivirus, of which there are four serotypes, transmitted by mosquito bite. Infection can result in either a flu-like, self-limiting illness called dengue fever (DF), or, particularly after secondary infection with a different serotype, a severe and often fatal disease called dengue hemorrhagic fever (DHF). There is no specific treatment or vaccination available, which may be due, at least in part, to the lack of appropriate animal models. While non-human primates can support dengue virus infection, neither DF nor DHF are observed in these models.

Furthermore, while some mouse models do exist they require either unphysiologically high levels of virus to induce disease, or the use of immunocompromised mouse strains [179]. Humanised mice support infection with dengue virus, with infected mice developing an elevated body temperature, rash and thrombocytopenia [185]. In addition, B cell responses, with the production of dengue virus specific antibodies, have been reported in infected humanised mice [186, 187]. Furthermore, T cells from HLA-A2 transgenic humanised mice have been shown to respond to specific restimulation by producing IFNγ, IL2 and TNFα [160], thus showing their responsiveness to dengue virus infection. Importantly, TNFα production by human DCs in humanised mice infected with dengue virus has been shown to be suppressed by siRNA directed against TNFα [188]. As TNFα is thought to play a major role in pathology, this then represents a possibly future therapy.

1.4.4.4 Autoimmunity and Cancer

In addition to providing tools for the *in vivo* study of human pathogens, humanised mice have also been used in translational biomedical research to study diseases including type I diabetes and various forms of cancer. For example, in the case of type I diabetes, HLA-A2 transgenic humanised mice were used to identify autoantigens that are potentially involved in disease pathogenesis [189]. In addition, humanised mice have been used to evaluate various potential cancer treatments including cell-based therapies, with transplanted activated NK cells being shown to be cytotoxic against leukemic cells [190], humanised antibodies, showing the efficacy of rituximab in treating B cell lymphomas [191], and tumour-growth inhibitors, showing that NFκB inhibition suppresses tumour growth [192, 193].

1.5 Conclusions

ANCA associated vasculitis is a complex human disease, the study of which is limited by inadequate animal models, and the lack of an anti-PR3 antibody induced model in particular. Indeed, the ability of anti-PR3 antibodies to induce NCGN, or pulmonary inflammation, often associated with disease, remains unconfirmed. Consequently, the development of a new model in which the ability of anti-PR3 antibodies to activate neutrophils, and thus induce renal and/or pulmonary disease, would represent a major advancement in the field of ANCA associated vasculitis research.

As discussed, the fundamental differences in human and mouse PR3 may well be responsible for the difficulties encountered in establishing a suitable model of anti-PR3 induce disease. Furthermore, the differences in rodent and human biology make results derived from animal studies difficult to interpret from the perspective of attempting to understand the pathogenesis of human disease. For example, and with regards ANCA associated vasculitis, it is noteworthy that while inhibition of the MAPK pathway prevented ANCA induced neutrophil activation in human neutrophils *in vitro*, it appeared to have only a mild protective effect with regards the induction of disease in mice. This discrepancy may be due to a number of reasons, however, the most obvious is species differences.

Importantly, a humanised mouse model of ANCA associated vasculitis would have the potential to overcome these limitations, providing a model in which human neutrophils, expressing both human PR3 and human signaling molecules, could be used to test the ability of human anti-PR3 antibodies to induce disease *in vivo* and ultimately serve as an alternative method to study disease *in vivo*.

1.6 Aims of thesis

The aims of the present study are summarised below:

- To optimise the purification of ANCA from patient plasma, so that it may be used for both *in vitro* and *in vivo* studies

- To establish *in vitro* ANCA assays and use them to examine novel processes with potential roles in ANCA associated vasculitis pathogenesis

- To establish a humanised mouse model

- To determine if human neutrophils can be reconstited by humanised mice and if so whether they are functional

- To determine if a humanised mouse model with functional human neutrophils can be used to study human ANCA induced pathology *in vivo*

The following chapters detail the methods used in the course of this study and the results obtained as a consequence of the pursuit of these aims.

General procedures used are described in this chapter, with further methods specific to each set of experiments given in the relevant results chapters.

2.1 Reagents

All chemicals were purchased from Sigma unless otherwise stated.

Saturated Ammonium Sulphate

Prepared by dissolving 300g NH_4SO_4 in 500ml tissue culture H_2O. This required heating at ~56-60˚, with frequent shaking. The solution was then cooled overnight, with crystal formation indicating saturation.

0.1M Glycine, pH 2.7

Prepared by dissolving 3.75g Glycine in 500ml tissue culture H_2O. The pH was the adjusted with HCl.

1M Tris, pH 9

Prepared by dissolving 24.23g Tris in 200ml tissue culture H_2O. The pH was the adjusted with HCl.

Red Cell Lysis Buffer, pH 7.3

Prepared by dissolving 4.17g NH_4Cl, 0.0185g EDTA and 0.5g $NaHCO_3$ in 500 ml tissue culture H_2O.

Bouin's Solution

Prepared by adding 3 volumes of picric acid 1.2% saturated solution to 1 volume formaldehyde 40%. Just before use acetic acid was added to the stock solution at a dilution of 1:20.

Phosphate-lysine-periodate (PLP)

A paraformaldehyde solution was made up by dissolving 4g paraformaldehyde in 100ml of distilled H_2O. This was stored at -20°C.
A lysine stock solution was made up by combining 3.65g/100ml lysine monohydrochloride to an equal volume of 3.58g/100ml disodium hydrogen

orthophosphate. The pH was adjusted to 7.4, and this solution was also stored at -20°C. Immediately before use, 1 volume paraformaldehyde was mixed with 3 volumes of lysine solution, to which sodium metaperiodate was added (0.124g/100ml).

Flow cytometry antibodies

Target	Isotype	Clone	Fluorophore	Supplier
CD3	Mouse IgG1, κ	UCHT1	APC	BD
CD3	Mouse IgG2a, κ	BW264/56	APC	Miltenyi
CD11b	Mouse IgG1, κ	CBRM1/5	APC	Biolegend
CD11b	Mouse IgG1, κ	ICRF44	APC	BD
CD14	Mouse IgG2a, κ	M5E2	PE	BD
CD14	Mouse IgG2a, κ	M5E2	APC	BD
CD16	Mouse IgG1, κ	3G8	APC	BD
CD16	Mouse IgG1, κ	3G8	PerCP-Cy5.5	BD
CD19	Mouse IgG1,κ	HIB19	FITC	BD
CD34	Mouse IgG2a, κ	AC136	PE	Miltenyi
CD45	Mouse IgG1, κ	HI30	V450	BD
CD45	Mouse IgG1, κ	HI30	PE-Cy7	BD
CD62L	Mouse IgG1, κ	DREG-56	PerCP-Cy5.5	Biolegend
CD63	Mouse IgG1, κ	H5C6	PE	BD
CD66b	Mouse IgM, κ	G10F5	FITC	BD
CD66b	Mouse IgM, κ	G10F5	PE	Biolegend
CD66b	Mouse IgM, κ	G10F5	PerCP-Cy5.5	Biolegend
PR3	Mouse IgG1, κ	PR3G-2	FITC	Hycult
Isotype control	Mouse IgG1, κ	MOPC-21	FITC	Biolegend
MPO	Mouse IgG1, κ	MPO-7	APC	Dako
Isotype control	Mouse IgG1, κ	MOPC-21	APC	Biolegend

Table 2.1 Anti-human antibodies used for flow cytometry. All antibodies were obtained from commercial sources. Antibodies were titrated to give optimal concentration for use. BD-Becton Dickinson, Oxford, UK. Milenyi-Miltenyi Biotech, Germany. Biolegend-San Diego, CA, USA. Hycult-Hycult Biotech, The Netherlands. Dako-DakoCytomation, Denmark.

Target	Isotype	Clone	Fluorophore	Supplier
CD45	Rat (LOU) IgG2b, κ	30-F11	FITC	BD
CD45	Rat (LOU) IgG2b, κ	30-F11	PE	BD
CD45	Rat (LOU) IgG2b, κ	30-F11	PerCP-Cy5.5	BD
Ly-6G	Rat (LEW) IgG2b, κ	IA8	AlexaFluor 700	BD
CD11b	Rat (LEW) IgG2b, κ	M1/70	FITC	BD
CD11c	Armenian Hamster IgG	N418	PE	Biolegend
CD62L	Rat IgG2a, κ	MEL-14	Pacific Blue	Biolegend

Table 2.2 Anti-mouse antibodies used for flow cytometry. All antibodies were obtained from commercial sources. Antibodies were titrated to give optimal concentration for use. BD-Becton Dickinson, Oxford, UK. Biolegend-San Diego, CA, USA.

Monoclonal neutrophil activating antibodies

Target	Isotype	Clone	Supplier
Human Proteinase 3	Mouse IgG_1	PR3-G2	Hycult Biotech
Human Myeloperoxidase	Mouse IgG_1	266.6K2	IQ Products
NA/LE Isotype Control	Mouse IgG_1	107.3	BD

Table 2.3 Monoclonal anti-human anti-PR3 and anti-MPO IgG used in neutrophil activation assays. Both antibodies were obtained from commercial sources as indicated. Hycult Biotech, Uden, The Netherlands. IQ Products, Groningen, The Netherlands, BD-Becton Dickinson.

2.2 Methods

2.2.1 Flow cytometry

Whole blood from humanised mice was blocked by incubation with 10% AB serum (Sigma, Poole, UK) and 1μg/ml mouse BD Fc Block (Becton Dickinson, Oxford, UK) for 20 minutes at room temperature. Isolated human cells, resuspened at $1x10^7$ cells/ml, were blocked with 10% AB serum. Isolated humanised mouse cells, at the same concentration, were blocked with 10% AB serum and 1μg/ml mouse BD Fc Block. The appropriate antibodies were added and the whole blood or cell suspension was kept in the dark for 20 minutes at room temperature. Red cells were lysed using BD FACS Lysing Solution (Becton Dickinson, Oxford, UK) according to manufacturers instructions. Briefly, 2ml of a 1:10 dilution of BD FacsLyse was added to approximately 100μl whole blood and incubated for 10 minutes at room temperature and in the dark. This was then spun at 280g for 5 minutes. Cells were washed with 2ml phosphate buffered saline (PBS) (Sigma, Poole, UK) containing 0.1% sodium azide, spinning at 280g for 5 minutes. Finally the cells were resuspended in 300μl PBS containing 0.1% sodium azide and stored in the fridge until flow cytometric analysis could be carried out.

Flow cytometry was performed on either a FACS Canto flow cytometer (Becton Dickinson, Oxford, UK) or a LSR II flow cytometer (Becton Dickinson, Oxford, UK) using FACSDiva software (Becton Dickinson, Oxford, UK). At least 10,000 events were collected per sample, and data was analysed using FlowJo software (Treestar, Ashland, OR, USA).

2.2.2 Cells counts

An Olympus BX51 microscope (Olympus Microscopy, Southend-on-sea, UK) set to phase contrast and a counting chamber (Improved Neubauer haemocytometer) was used for calculating cells numbers. To determine cell viability, cells were with diluted 1:1 using Trypan blue dye (Sigma, Poole, UK).

Non-viable cells stained blue and were excluded from the cell count. To perform white blood counts, whole blood was diluted 1:10 in Turk's solution (Sigma, Poole, UK). Turk's solution is a mixture of acetic acid and gentian violet that haemolises red blood cells and stains the nuclei of white cells purple. The total number of cells within the 25 grid square was counted. This was multiplied by the dilution factor and 10^4 to obtain the number of cells/ml of medium i.e. cell concentration. The cell concentration was multiplied by the volume of the cell suspension to obtain the total cell yield.

2.2.3 IgG Purification

All blood and plasma samples, from both patients or healthy controls, were taken with informed consent and ethical approval (NRES committee London—London Bridge 09/H084/72). Plasma exchange samples were obtained from patients with active ANCA associated vasculitis in the renal units of Kent and Canterbury, Royal Sussex County, King's College, St Helier and Guy's and St. Thomas' hospitals. All patients had evidence of active renal involvement with some also exhibiting other clinical manifestations of disease. For further information on the patient samples used throughout this project please see Table 3.6 and Table 3.7.

2.2.3.1 Ammonium sulphate precipitation

Plasma stored at -80ºC was defrosted in a water bath at 37ºC. In order to precipitate out the antibody, and thus to remove fibrin that may block a Protein G column, saturated ammonium sulphate was used. A 25% saturated ammonium sulphate solution of the plasma was first obtained by adding saturated ammonium sulphate at a third of the volume of the plasma slowly at room temperature. Only proteins with a high molecular weight such as fibrin precipitate out at this stage. The plasma was left to precipitate for 6 hours at 4ºC. The sample was spun at 1000g for 30 minutes and the supernatant was removed. A 50% saturated ammonium sulphate solution of the supernatant was obtained by adding a volume (x) of saturated ammonium sulphate slowly

at room temperature. The following calculation was used to determine the volume (x) required

$$\frac{(\%\ \text{saturation of sample})\ (\text{volume}) + (\%\ \text{saturation of stock})\ (\text{volume (x)})}{\text{volume} + \text{volume (x)}} = 50\%$$

The plasma was left to precipitate overnight at 4ºC. The sample was spun at 1000g for 30 minutes. The supernatant was removed and the pellet was resuspended in a minimum volume of PBS. This was then transferred to dialysis tubing and dialysed in a large volume (~5 litres) of PBS at 4°C. The dialysis was completed the following day after at least 2 changes of PBS. The contents of the dialysis tubing were emptied into a 50ml falcon, spun at 1000g for 30 minutes, and the supernatant was passed through a 0.2μm filter before purification using a HiTrap HP Protein G column (GE Healthcare Life Sciences, Buckinghamshire, UK). 5ml Protein G columns were first washed with 50ml 0.2μm filtered PBS. A syringe pump set at 60ml/hr was used to pass the PBS through the column. The filtered sample was run through the column at 20ml/hr. The column was washed with 20ml sterile filtered PBS, and the bound IgG was eluted by passing 0.2μm filtered 0.1M glycine, pH 2.7, through the column at 60ml/hr. The eluate was collected in 1.5 ml fractions into eppendorfs containing 150μl 1M Tris, pH 9. The wavelength of each fraction of the eluted antibody was measured at 280nm using a spectrophotometer, and samples with an OD greater that 0.5 were pooled. They were then transferred to dialysis tubing and dialysed in a large volume (~5 litres) of PBS at 4°C. The dialysis was completed the following day after at least 2 changes of PBS. The final concentration of antibody was determined using a quartz cuvette and spectrophotometer at 280nm. The following equation was used to calculate the final concentration:

$$\text{Absorbance}^{280} / 1.4 = \text{concentration},$$

were $1.4 = \text{Absorbance}^{280}$ of 1mg/ml IgG

The antibody was concentrated to a working stock concentration of between 5 and 50mg/ml and stored in small aliquots at -20ºC.
For some samples a 1ml Protein G column was used as described below.

2.2.3.2 Sodium chloride precipitation

Plasma stored at -80ºC was defrosted in a water bath at 37ºC. Solid sodium chloride was added at 18g/100ml of plasma to remove fibrin. The plasma was left to precipitate overnight at 4ºC. The sample was spun at 1000g for 30 minutes and the supernatant was removed and diluted 1 in 5 in endotoxin free, tissue culture water before being passed through a 0.2μm filter for purification using a Protein G column. 1ml Protein G columns were first washed with 10ml 0.2μm filtered PBS using a syringe pump set at 20ml/hr before the filtered sample was run through the column at 10ml/hr. The column was washed with 5ml sterile filtered PBS and the bound IgG was eluted by passing 0.2μm filtered 0.1M glycine, pH 2.7, through the column at 20ml/hr. The eluate was collected in 1.5 ml fractions into eppendorfs containing 150μl 1M Tris, pH 9. The wavelength of each fraction of the eluted antibody was measured at 280nm using a spectrophotometer and samples with an OD greater than 1.5 were pooled and buffer exchanged into PBS using a PD10 Desalting column (GE Healthcare Life Sciences, Buckinghamshire, UK). The final concentration of antibody was calculated and the antibody was aliquoted and stored at -20ºC.

2.2.4 SDS Polyacrylamide Gel Electrophoresis (SDS-PAGE)

Patient IgG samples were diluted to 250μg/ml in PBS and 26μl of this was added to 10μl NuPAGE® Sample Buffer (Invitrogen, Paisley, UK) and 4μl NuPAGE® Reducing Agent (Invitrogen, Paisley, UK). The mixture was incubated at 95ºC for 5 minutes and then immediately transferred to ice. Approximately 12μl of SeeBlue® Prestained Standard (Invitrogen, Paisley, UK) was loaded into the first well of a NuPAGE® 4-12% Bis-Tris Gel (Invitrogen, Paisley, UK) and 15μl of sample was loaded per well after that.

Gels were run for 35 minutes at 200V, 120mA and 25W using the NuPAGE® SDS-PAGE Gel System (Invitrogen, Paisley, UK). Gels were washed three times each for 5 minutes in distilled water before being stained with SimplyBlue® Safe Stain (Invitrogen, Paisley, UK) for 1 hour. Gels were then left in distilled water for at least 24 hours before being washed in fresh distilled water for 1 hour and dried using Gel Drying Kit (Invitrogen, Paisley, UK).

2.2.5 PR3 and MPO ANCA binding ELISA

ELISAs for antibodies against PR3 and MPO were carried out using the Weislab Capture PR3 and MPO ELISA Kits (Euro Diagnostica, Malmö, Sweden). Patient IgG samples were diluted to give a final concentration of either 20μg/ml or 50μg/ml in PBS. 100μl per well in duplicate of Calibrator 1-6, positive control, negative control and diluted patient IgG was pipetted into pre-coated 96 well plates. This was incubated at room temperature for 1 hour. The plate was washed three times with 300μl washing solution per well. The plate was then gently tapped dried using absorbent tissue and 100μl conjugate was added per well. This was incubated for 30 minutes at room temperature. The plate was washed as before and 100μl substrate pNPP was added to each well. This was incubated for 30 minutes at room temperature and in the dark. 100μl stop solution was added to each well and the absorbance at 405nm was read on a SpectraMax Plus384 Microplate Reader (Molecular Devices, California, USA).

2.2.6 Neutrophil isolation

2.2.6.1 Polymorphprep

Sodium Citrate, ethylenediaminetetraacetic acid (EDTA) or heparin anti-coagulated blood from healthy controls was gently layered over an equal volume of Polymorphprep (Axis-Shield, Oslo, Norway) and spun for 45 minutes at 380g, 20ºC and with the brake off. The lower band was harvested and washed with an equal volume of 1:1 H_20:PBS, spinning at 280g and 20ºC

for 10 minutes. The supernatant was discarded and the pellet washed with PBS, spinning at 280g and 20ºC for 10 minutes. To remove contaminating red cells the pellet was then either resuspended in 36ml water for 10-20 seconds before 4ml 10 x PBS was added or resuspended in 1ml red blood cell lysis buffer for 5 minutes before the volume was made up to 50ml with PBS. In both case this was spun at 280g and 20ºC for 10 minutes. The red cell lysis was repeated if necessary. Finally the cells were resuspended in Hanks Balanced Salt Soltion (HBSS) (Sigma, Poole, UK) with 1M HEPES (Sigma, Poole, UK) or PBS with calcium chloride and magnesium chloride (Sigma, Poole, UK) depending on the assay. The cells were counted using a 1:10 dilution of Turk's Solution to exclude any contaminating red cells. Figure 2.1 (A) show the typical purity of neutrophils isolated in this manner.

2.2.6.2 Ficoll

Heparinised blood from healthy controls was diluted 1:1 with HBSS. In 15ml tubes, 8ml of the blood/HBSS mixture was carefully layered on top of 4ml Ficoll-Paque™ PLUS (GE Healthcare Life Sciences, Buckinghamshire, UK). This was spun for 20 minutes at 380g, 20ºC and with the brake off. The upper layer including the lymphoctyes was aspirated with circular movement. Gentle tapping loosened the pellet and 10 ml RBC lysis buffer was added to remove the erythrocytes. The tube was inverted several times and incubated on ice for 5 minutes, with occasional mixing. This was spun at 380g and 20ºC for 5 minutes. The supernatant was aspirated, being careful not to disturb the cell pellet which was then resuspend in 10 ml RBC lysis buffer and incubated on ice for 5 minutes. This was spun at 280g and 20ºC for 5 minutes. The supernatant was removed and the pellet was washed with ice-cold HBSS, spinning at 200g for 5 minutes. The cells were resuspend in HBH (500ml Hanks Balanced Salt soln + 5ml 1M HEPES) and counted using a 1:10 dilution of Turk's Solution. Figure 2.1 (B) show the typical purity of neutrophils isolated in this manner.

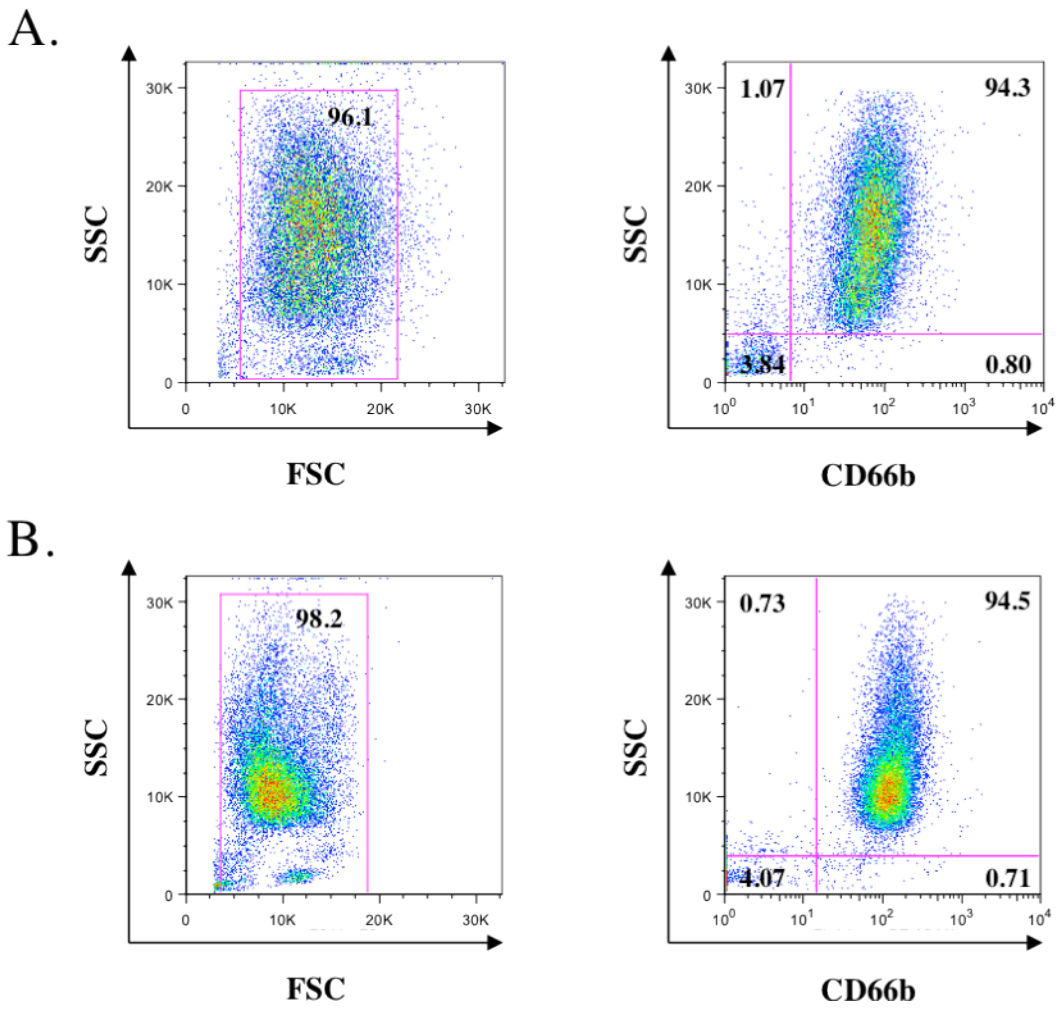

Figure 2.1 Representative plots showing the purity of neutrophils following (A) isolation using Polymorphprep and (B) isolation using Ficoll followed by red cell lysis. The plots on the left show the typical forward and side scatter of the neutrophil preparations while the plots on the right show the typical purity as determined here by high side scatter combined with expression of CD66b.

2.2.7 Respiratory Burst Assays

2.2.7.1 Superoxide dismutase inhibitable ferricytochrome C reduction assay

Neutrophils were resuspended at $2x10^6$ cells/ml in HBH and primed by incubation with 2ng/ml TNFα (Peprotech, London, UK) together with 5μg/ml cytochalasin B (Sigma, Poole, UK) for 15 min at 37˚C with gentle mixing at 5 minute intervals. For the GCSF experiments cells were primed with 50ng/ml GCSF (Peprotech, London, UK) under the same conditions as TNFα.
Each well in a flat-bottomed 96 well plate had the following:

Cytochrome C	10μl
Stimulus	10μl
SOD+/-	5μl
Neutrophils	50μl
HBH	To give final volume of 250μl

Cytochrome C (from horse heart)(Sigma, Poole, UK) was made fresh on the day to give a stock of 23.25mg/ml in HBH and kept in the dark until use. Superoxide dismutase (SOD) (Sigma, Poole, UK) was used at a stock of 30,000U/ml. Neutrophils were stimulated with either 250μg/ml patient IgG or 2.5-10μg/ml monoclonal anti-PR3/anti-MPO antibodies (Table 2.3). Before being added to the wells IgG was spun at 16,000g in a tabletop microcentrifuge at 4˚C for 15 minutes to remove aggregates. 5μg/ml of N-formyl-methionine-leucine-phenylalanine (fMLP)(Sigma, Poole, UK) was used as a positive control for neutrophil activation. All tests were done in triplicate. Neutrophils were added to each well last and the absorbance at 550nm was read on a SpectraMax Plus384 Microplate Reader (Molecular Devices, California, USA) at intervals of 5 minutes over 2 hours. The absorbances were then converted to nmol/10^5 neutrophils of O_2^- using the difference in $O.D._{550}$ between the supernatants of comparable cells incubated with or without SOD, and the molar extinction coefficient for cytochrome c (21×10^3/mol/cm).

2.2.7.2 Dihydrorhodamine (DHR) 123 assay using isolated human neutrophils

DHR123 is a non-reduced non-fluorescent molecule that in the presence of H_2O_2 is converted to rhodamine 123, which fluoresces at a wavelength of approximately 534nm, and can therefore be seen in the FITC (FL-1)-light channel. This allows neutrophils that have undergone a respiratory burst to be detected using flow cytometry.

Neutrophils were resuspended at $2.5x10^6$ cells/ml in HBH and loaded with 17μg/ml DHR123 (Calbiochem, Nottingham, UK) together with 5μg/ml cytochalasin B and 2 mM sodium azide (Sigma, Poole, UK). This was incubated in the dark for 10 minutes at 37ºC. Cells were primed by incubation with 2ng/ml TNFα for 15 min at 37˚C with gentle mixing at 5 minute intervals. For the GCSF experiments cells were primed with 50ng/ml GCSF under the same conditions as TNFα. 200 μl of the cell suspension was added to each FACS tube (500,000 cells/tube) and stimulated with either 250μg/ml patient IgG or 2.5-10μg/ml monoclonal anti-PR3/anti-MPO antibodies (Table 2.3) for 1 hour at 37˚C. Before being added to the cells IgG was spun at 16,000g in a tabletop microcentrifuge at 4˚C for 15 minutes to remove aggregates. 5μg/ml of fMLP or 0.1μg/ml phorbol myristate acetate (PMA) was used as a positive control for neutrophil activation. The reaction was stopped by the addition of a 30-fold volume of cold HBSS containing 1% bovine serum albumin (BSA) (Sigma, Poole, UK). This was spun at 280g and 4˚C for 5 minutes. The cells were finally resuspended in a small volume of HBSS (~300μl) and kept on ice and in the dark until measurement.

Flow cytometry was performed on a FACS Canto flow cytometer (Becton Dickinson, Oxford, UK) using FACSDiva software (Becton Dickinson, Oxford, UK). At least 10,000 events were collected per sample and data was analysed using FlowJo software (Treestar, Ashland, OR, USA).

2.2.7.3 Dihydrorhodamine (DHR) 123 assay using whole blood from humanised mice

Respiratory burst assays were carried out using heparinised whole blood from mice pre-treated (5 days before the assay was performed) with human pegylated GCSF (Neupogen® Filgrastim, Amgen, UK). For the fMLP response whole blood was first incubated with 2mM sodium azide, 1μg/ml cytochalasin B and 2ng/ml human TNFα for 15 minutes at 37°C. This was then stimulated with 5μg/ml fMLP for 10 minutes at 37°C. For the *Escherichia coli (E.coli)* response the whole blood was incubated with 2mM sodium azide together with opsonized *E. coli* (taken from the Phagoburst kit from Glycotope biotechnology GmBH, Heidelberg, Germany) for 10 minutes at 37°C. The stimulated blood was incubated with 17μg/ml DHR123 at 37°C in the dark for 10 minutes. The reaction was stopped on ice and the whole blood was blocked and stained for flow cytometry as previously described.

Flow cytometry was performed on a FACS Canto flow cytometer (Becton Dickinson, Oxford, UK) using FACSDiva software (Becton Dickinson, Oxford, UK). At least 20,000 events were collected per sample and data was analysed using FlowJo software (Treestar, Ashland, OR, USA).

2.2.8 Degranulation

Degranulation assays were carried out using heparinised whole blood from mice pre-treated (5 days before the assay was performed) with human pegylated GCSF. For the fMLP response whole blood was first incubated with 1μg/ml cytochalasin B and 2ng/ml human TNFa for 15 minutes at 37˚C with gentle mixing at 5 minute intervals. This was then stimulated with 5μg/ml fMLP for 10 minutes at 37˚C. For the *E.coli* response the whole blood was incubated with the *E.coli* for 10 minutes at 37˚C. The reaction was stopped on ice and the whole blood was blocked with 10% AB serum for 10 minutes on ice and then stained for flow cytometry for 20 minutes at room temperature. The red cells were lysed using BD FacsLyse.

Flow cytometry was performed on a FACS Canto flow cytometer (Becton Dickinson, Oxford, UK) using FACSDiva software (Becton Dickinson, Oxford, UK). At least 20,000 events were collected per sample and data was analysed using FlowJo software (Treestar, Ashland, OR, USA).

2.2.9 Passive transfer of human neutrophils into mice

Neutrophils were purified from healthy controls using Polymorphprep as described in Section 2.2.6.1. Approximately $1x10^7$ neutrophils in 200μl PBS were injected into NOD.Cg-*Prkdc*^{scid} *Il2rg*^{tm1Wjl}/SzJ mice (referred to as NOD-scid IL2$\gamma^{-/-}$) obtained from Jaxmice (Bar Harbor, Maine, USA) via the lateral tail vein. Mice were bled from the saphenous vein 10, 30 and 60 minutes post transfer and whole blood was stained for the presence of human neutrophils using human CD45 and human CD66b antibodies. A small volume of blood was used to perform whole blood counts using Turk's solution. Flow cytometry was performed as previously described. Absolute numbers of neutrophils were calculated from flow cytometry data and total leukocyte numbers.

2.2.10 CD34$^+$ cell purification

2.2.10.1 Defrosting frozen cord blood

Cryopreserved human cord blood was purchased from The Anthony Nolan Trust. It was defrosted in a water bath at 37˚C and diluted 1:1 in thawing solution (47ml Dextran, 2.5ml AB serum, 960μl sodium citrate (39%w/v), 500μl MgCl (0.5M) and 50μl DNAse-1 (10^6U/ml)). The sample was then diluted with culture media (RPMI-1640 + 5nM glutamine + 2.5% AB serum) and spun at 450g and 4˚C in order to remove the DMSO. The pellet was treated with 2 volumes of neat DNAse stock solution for approximately 5 minutes. This was diluted with 10ml culture media and spun at 400g for 5 minutes at room temperature. The resulting cell pellet was resuspended in MACS buffer (PBS with 0.5% BSA and 2mM EDTA) for CD34$^+$ cell purification using the Miltenyi MACS separation system (Miltenyi Biotec Ltd., Surrey, UK).

2.2.10.2 $CD3^+$ cell depletion of fresh cord blood

Fresh human cord blood was purchased from the National Blood Service and stored overnight at room temperature. The next morning the $CD3^+$ cells were depleted using the RosetteSep system (Stemcell Technologies, Grenoble, France). 1.25ml RosetteSep Human CD3 Depletion cocktail was added for every 25ml of cord blood. This was mixed and incubated for 20 minutes at room temperature. The cord blood was then diluted 1:4 in PBS containing PBS with 2% foetal calf serum (FCS) and 1mM EDTA. This was carefully layered over Ficoll, with 35ml of blood for 15ml of Ficoll, and spun at 400g for 45 minutes at 20˚C and with the brake off. The enriched cells were transferred to a clean Falcon tube and diluted in an equal volume of PBS with 2% FCS and 1mM EDTA and spun at 200g for 10 minutes. $CD3^+$ cell depleted cord blood cells were then either resuspended in PBS and injected into mice, resuspened in 90% FCS and 10% DMSO and cryopreserved, or resuspended in MACS buffer or PBS with 2% FCS and 1mM EDTA for further processing using the Miltenyi MACS separation (described in Section 2.2.10.2) or EasySep separation (described in Section 2.2.10.4) systems.

2.2.10.3 $CD34^+$ cell purification using the Miltenyi MACS separation system

Cord blood cells in MACS buffer (PBS with 0.5% BSA and 2mM EDTA) were passed through a 40μm filter and counted in trypan blue. The cell suspension was spun at 130g for 10 minutes and resuspended in 300μl MACS buffer for up to 10^8 total cells. Keeping the cell suspension at 6˚C, 100μl FcR blocking agent together with 100μl of CD34 MicroBeads were added for up to 10^8 cells. This was mixed and incubated for 30 minutes at 6˚C. The cells were washed with 5-10ml buffer for 10^8 cells and spun at 130g for 10mins. The supernatant was discarded and the cells resuspended in 500μl MACS buffer for up to 10^8 cells.

A MS magnetic separation column was placed in the magnetic field of a VarioMACS separator and washed three times with 500μl of buffer. The cell suspension was then passed through the column. Unlabelled cells that passed through the column were collected and the column was washed three times with 500μl MACS buffer. The column was removed from the separator and placed over a collection tube. 1-5ml of MACS buffer was applied to the column and the magnetically labelled cells were immediately flushed out by firmly pushing a plunger into the column. The yield and purity of the labelled fraction was determined using flow cytometry and staining for both $CD34^+$ cells and contaminating $CD3^+$ cells.

2.2.10.4 $CD34^+$ cell purification using Easysep

EasySep (Stemcell Technologies, Grenoble, France) was added to cord blood cells in PBS containing 2% FCS and 1mM EDTA at 100μl/ml of cells (up to $2x10^7$ cells were suspended in 100μl, $2x10^7$-$2x10^8$ cells were suspended at $2x10^8$ cells/ml and 2-$5x10^8$ cells were suspended in 1ml) and this was incubated at room temperature for 15 minutes. The EasySep magnetic nanoparticles were mixed, but not vortexed, to give a uniform suspension and then added to the cell suspension at 50μl/ml of cells. This was mixed and incubated at room temperature for 10 minutes. The cell suspension was brought to a total volume of 2.5ml with PBS containing 2% FCS and 1mM EDTA. The cells were mixed by gentle pipetting and the tube containing the cell suspension was placed, without a lid, into the magnet and set aside for 5 minutes. In one continuous movement the magnet containing the tube with the cell suspension was inverted thus pouring off the supernatant. Once upright the tube was removed from the magnet and remaining cells were resuspended in 2.5ml PBS containing 2% FCS and 1mM EDTA. The cells were once again mixed by gentle pipetting and the tube containing the cell suspension was placed, without a lid, into the magnet and set aside for 5 minutes. In one continuous movement the magnet containing the tube with the cell suspension was inverted thus pouring off the supernatant. This was repeated 3 times total and finally the yield and purity of the labelled fraction

was determined using flow cytometry before the cells were either injected into mice or cryopreserved in 90% FCS and 10% DMSO.

2.2.11 Generating humanised mice

NOD.Cg-*Prkdc*^{scid} *Il2rg*^{tm1Wjl}/SzJ mice (referred to has NOD-scid IL2$\gamma^{-/-}$) were obtained from Jaxmice (Bar Harbor, Maine, USA) and bred in house, with some animals from Charles River (Margate, Kent, UK). All animals were housed in specific pathogen free conditions in filtered top cages and Scantainer ventilated cabinets. All animal procedures were performed according to UK Home Office regulations. Humanised mice were generated by injecting 1x10^5 human cord blood CD34$^+$ stem cells (either purified as described in Section 2.2.10 or purchased from Lonza, Slough, Berkshire, UK) into 6-12 week old NOD-scid IL2$\gamma^{-/-}$ mice approximately 4 hours post irradiation at 2.4Gy with a Cs-source irradiator. As NOD-scid IL2$\gamma^{-/-}$ mice are particularly radiosensitive, due to defects in DNA repair, this dose, while low, is enough to allow engraftment without leading to unacceptable losses [119]. Engraftment of human cells in the peripheral blood was assessed using flow cytometry at least 8 weeks post engraftment.

2.2.12 Anaesthetising mice

Mice were anaesthetised using 0.15ml/kg of metomidine hydrochloride 1mg/ml domitor (Pfizer Ltd, Kent. U.K.) and ketamine hydrochloride 100mg/ml vetalar (Pharmacia Animal Health Ltd, Northamptonshire, U.K.) This was made up to a working dilution by adding 4.16ml normal saline to 0.34ml vetalar and 0.5ml domitor and was administered via intraperitoneal injection

2.2.13 Sample collection

2.2.13.1 Blood

Peripheral blood was taken from the saphenous vein of mice and collected into either EDTA for flow cytometry or lithium heparin for neutrophil activation assays. Terminal bleeds were from the axillary vessels of mice under terminal anaesthesia.

2.2.13.2 Spleen

Whole spleens were collected into PBS. They were forced through a 40μm strainer using the plunger of a 5ml syringe and into approximately 10ml PBS. They were spun at 200g for 10 minutes at room temperature and resuspended in 1-5ml of red blood cell lysis buffer. This was incubated at room temperature for 5 minutes and then diluted to 50ml with PBS before being spun at 200g for 10 minutes. The cells were counted in Turk's solution, washed once in PBS and finally resuspended at $1x10^7$ cell/ml in PBS for flow cytometry.

2.2.13.3 Bone marrow

Bone marrow was flushed, with PBS, from the femurs and tibiae of mice using a 27G needle. Large aggregates were broken apart using a 19G needle. The cells suspension was transferred to a 50ml falcon and centrifuged for 10 minutes at 200g and at room temperature. The cells were resuspended in PBS and passed through a 40μm filtered before being counted using Turk's solution. Cells were resuspended at $1x10^7$ cells/ml for flow cytometry.

2.2.13.2 Lungs

Lungs were collected into PBS and then transferred into 1-3ml DMEM (Invitrogen, Paisley, UK) with 10% FCS. They were cut into small sections

and collagenase, type IV-S from *Clostridium histolyticum* (Sigma, Poole, UK), was added to give a final concentration of 500μg/ml. This was mixed and incubated for 45 minutes at 37˚C and 5% CO_2. Each sample was pipetted vigorously to release the cells and then washed with PBS containing 1% FCS, spinning at 200g and room temperature for 10 minutes. The cells were passed through a 40μm strainer and counted in Turk's solution. Finally the cells were resuspended at $1x10^7$ cells/ml in PBS for flow cytometry.

2.2.14 Immunostaining for PR3 and MPO

Bone marrow cells were resuspended at $2x10^5$ cells/ml. The slides were pre-labelled and mounted with the paper pad and the cuvette in the metal holder and then placed in the cytospin. 100μl of cells were loaded and this was spun at 100g for 5 minutes. The slides were allowed to dry at room temperature for at least 30 minutes. A circle was drawn loosely around the cells using a wax pen. 100μl of primary anti-PR3 or anti-MPO (See Table 2.1) at a concentration of 500μg/ml was added to the cells. This was incubated for 20 minutes in a humidity box. The slides were washed with PBS three times for 5 minutes each and 100μl of secondary anti-mouse IgG (Jackson ImmunoResearch, Suffolk, UK), FITC at a 1:200 dilution for MPO and Dylight488 at at a 1:400 dilution for for PR3, was added. This was incubated for 30 minutes in a humidity box. The slides were washed with PBS three times for 5 minutes each and mounted in PermaFluor mountant (Thermo Scientific, Loughborough, UK) together with 0.3μg/ml Hoechst 3342 dye (Sigma, Poole, UK) to visualise the nuclei. Cells were examined using an Olympus BX51 fluorescent microscope (Olympus, Southend-on-sea, UK).

2.2.15 Inducing disease

Mice at least 8 weeks post engraftment were given either 4mg human anti-PR3 or MPO IgG or 10mg anti-PR3 IgG, this was day 0. Mice receiving 4mg antibody also received 10μg LPS subcutaneously (s.c.) and 6μg GCSF (Neupogen® Filgrastim, Amgen, UK) intraperitoneally (i.p.) on day 0. The

GCSF was given daily for the next 7 days and the LPS given again on day 4. Mice receiving 10mg anti-PR3 IgG were given one 50μg dose of long lasting pegylated GCSF (Neupogen® Filgrastim, Amgen, UK) on day 0 together with LPS on day 0 and again on day 4. On day 6 the mice were placed in metabolic cages for urine collection. On day 7 the mice were terminally bled and their lungs were examined for signs of punctate haemorrhage. Finally their lungs and kidneys were harvested for histological analysis as described in Section 2.2.16.

2.2.16 Histological sample processing

Kidney sections were collected in Bouin's solution and transferred into formalin after 4 hours. Lungs were inflated with formalin and stored in formalin until processing. The samples were processed using an automatic tissue processor and then embedded in paraffin wax. Tissue sections were cut to 1μm thickness and incubated in an oven for at least 30 minutes before being stained with periodic acid-Schiff stain (PAS) and haematoxylin. To stain sections they first were placed directly into xylene for 10 minute and then into 100%, 90% and 70% alcohol for 20 seconds each. They were then placed into running water for 2 minutes, and incubated with 1% periodic acid for 10 minutes. Following a further wash in water for 3 minutes, kidney sections were incubated with Schiff reagent for 20 minutes and lung sections for 5 minutes. Both were then washed in water for 3 minutes and incubated with haematoxylin for 10 minutes for kidney sections and 15 minutes for lung sections. Slides were then taken back through graded alcohols for 20 seconds each and then into xylene before being mounted in DPX. The sections were left to dry and analysed for evidence of injury.

For immunofluorescent staining lungs were inflated with phosphate-lysine-periodate (PLP) and fixed in PLP overnight at 4˚C. The following day they were transferred to 13% sucrose, again incubated overnight at 4˚C and finally frozen in isopentane and stored at -80˚C. Kidneys were either frozen in isopentane upon harvest or fixed in PLP for 4 hours at 4˚C and transferred to

13% sucrose overnight at 4˚C. They were then frozen in isopentane the next morning and stored at -80˚C

2.2.17 Immunofluorescent staining

Frozen sections of lung were cut to 5μm thickness. The sections were then incubated with the primary mouse anti-human CD66b (Serotec, Oxford, UK) antibody then with the secondary Dylight 488 goat anti-mouse IgG antibody (Jackson ImmunoResearch, Suffolk, UK) and mounted in PermaFluor mountant (Thermo Scientific, Loughborough, UK). Neutrophil numbers were taken from the average counts of 5 high-powered fields using the x40 objective and a BX51 fluorescent microscope (Olympus, Southend-on-sea, UK). Counts were performed by two investigators and an average was taken to give the final numbers.

2.2.18 Albuminuria measurement

Mice were housed in metabolic cages for 24 hours for urine collections. The urine albumin concentration was measured by ELISA using a mouse albumin ELISA quantitation set from Bethyl Laboratories (Montgomery, Texas, USA). Flat-bottomed 96 well plates were coated with a 100μl/well of affinity purified mouse albumin coating antibody, diluted 1:100 in 500mM bicarbonate buffer, pH 9.5, for 1 hour at room temperature. The plate was washed 5 times with PBS containing 0.05% Tween 20 and blotted dry on clean tissue paper. 200μl of blocking solution (PBS with 1% BSA) was added to each well and this was incubated for 30 minutes at room temperature. The plate was washed as before. Mouse albumin (Sigma, Poole, UK) was diluted to the following concentrations: 250ng/ml, 125ng/ml, 62.5ng/ml, 31.25ng/ml, 15.625ng/ml, 7.7ng/ml and 3.9ng/ml. For each well, 100μl of the appropriate concentration was added as a standard. Urine samples were diluted 1:1000 in PBS with 1% BSA, and 100μl was added to the appropriate well. The plate was incubated for 1 hour at room temperature and then washed as before. The horseradish peroxidase (HRP) detection antibody was diluted 1:30,000 in PBS with 1%

BSA, and 100μl was added to each well. This was incubated for 1 hour at room temperature. The 3,3',5,5'-Tetramethylbenzidine (TMB) substrate (Sigma, Poole, UK) was made up as follows: 1 TMB tablet was added to a 1:10 dilution in H_2O of 10x TMB buffer (51.4ml 1M Na_2HPO_4 solution and 46.8ml 0.5M citric acid, pH 5), 2μl hydrogen peroxide was then added. 100μl of substrate was then added per well and the plate was incubated in the dark and at room temperature. After approximately 15 minutes the reaction was stopped using 100μl of a 1:5 dilution of H_2SO_4 in H_20. The plate was read at 450nm on a SpectraMax Plus384 Microplate Reader (Molecular Devices, California, USA)

2.2.19 Urine creatinine measurement

Urine creatinine was measured with the help of Dr N Dalton and Dr C Turner in the Department of Paediatric Biochemistry at St. Thomas' Hospital by mass spectrometry. The urine was diluted 1:10 in PBS and 5μl of this was diluted into 250μl D3 creatinine isotope and 250μl acetonitrile containing 0.5% formic acid. The creatinine level of each sample was then measured using Applied Biosystems MDS Sciex API 4000 (Applied Biosystems, Warrington, UK) and the software Applied Biosystems Analysis Version 1.4.

2.2.20 Statistics

Statistics were performed using Graphpad Prism software (Graphpad Software Inc, La Jolla, CA, USA). Specific statistical tests used will be discussed in the Methods section of each chapter.

3.1 Introduction

ANCA associated vasculitis is a systemic autoimmune disease that primarily affects the elderly, with a peak age of onset of between 65 and 74 years old [194]. There is substantial evidence that ANCA are key mediators of disease, which they induce by aberrantly activating neutrophils leading to tissue damage and subsequent pathology (reviewed in Chapter 1). *In vitro*, cytokine-primed neutrophils isolated from healthy controls have been shown to be activated by incubation with IgG derived from patients positive for anti-PR3 and anti-MPO antibodies, but not by incubation with IgG taken from ANCA negative controls. In addition, monoclonal anti-PR3 and anti-MPO antibodies have been shown to similarly activate neutrophils. Once activated, neutrophils carry out a number of effector functions that can be easily measured *in vitro*. These include, but are not limited to, phagocytosis, respiratory burst, degranulation and inflammatory cytokine release. To date the majority of studies investigating the role of ANCA in neutrophil activation have focussed on the ability of these autoantibodies to induce the neutrophil respiratory burst, and to a lesser degree, degranulation responses.

Superoxide (O_2^-) is a highly reactive oxygen species produced during the neutrophil respiratory burst by the one electron reduction of oxygen by NADPH oxidase [195, 196]:

$$O_2 + NADPH \rightarrow O_2^- + NADP^+ + H^+$$

The majority of this superoxide reacts with itself to produce oxygen and hydrogen peroxide (H_2O_2) in a reaction catalysed by the enzyme superoxide dismutase [195, 197, 198]:

$$2O_2^- + 2H^+ \rightarrow H_2O_2 \text{ and } O_2$$

Both superoxide and hydrogen peroxide are important starting materials for the production of microbicidal substances, and thus play pivotal roles in the innate immune response. Cytochrome C is a small heme protein and an

important component of the electron transport chain in mitochondria [195, 197]. It can accept electrons from superoxide, and thus the reduction of cytochrome C can be used as a measure of superoxide production [195]. In 1990 Falk et al. first used the superoxide dismutase inhibitable reduction of ferricytochrome C to measure ANCA induced superoxide release, thus demonstrating that ANCA activates neutrophils [14].

Dihyrorhodamine (DHR)123 is a non-fluorescent molecule that is taken up by phagocytes and converted to the green fluorescent molecule rhodamine 123 upon oxidation by reactive oxygen intermediates, primarily H_2O_2, produced during the respiratory burst response. Consequently, rhodamine 123 production as measured by flow cytometry has been widely used to study the neutrophil respiratory burst [199, 200]. Together with the ferricytochrome C reduction assay, which measures extracellular superoxide production, the DHR123 assay, which primarily measures intracellular ROS production, has become a standard tool in the study of ANCA induced neutrophil responses.

Precipitation of immunoglobulins using ammonium sulphate has been in practice for many years [201]. It works on the principle that each protein in the solution will aggregate at a characteristic salt concentration, allowing it to be easily removed using centrifugation. At a 25% ammonium sulphate solution contaminants such as fibrin will begin to precipitate out of solution. Once these have been removed, a 50% ammonium sulphate solution can be used to precipitate out immunoglobulins [202]. Ammonium sulphate fractionation alone does not provide sufficient purity for *in vitro* ANCA analysis, however, when followed by Protein G affinity chromatography, a highly pure IgG preparation can be achieved. Protein G is a protein isolated from the bacterial cell wall of a human group G streptococcal strain (G148). It binds the Fc receptor of all human IgG subclasses as well as rabbit, mouse and goat IgG [203].

In this chapter monoclonal anti-PR3 and anti-MPO, together with IgG purified from the plasma of PR3- and MPO-ANCA positive patients, was used to

develop neutrophil respiratory burst assays to allow the study of ANCA induced neutrophil activation *in vitro*.

3.2 Aims

- To set up ANCA induced neutrophil respiratory burst assays
- To optimise the purification of patient IgG

3.3 Methods

All blood and plasma samples, from both patients or healthy controls, were taken with informed consent and ethical approval (NRES committee London—London Bridge 09/H084/72)

3.3.1 Superoxide dismutase inhibitable ferricytochrome C reduction assay

Neutrophils were isolated from either EDTA, sodium citrate or lithium heparin anti-coagulated blood using Polymorphprep as described in Section 2.2.6.1 or Ficoll as described in Section 2.2.6.2. The assay was performed as described in Section 2.2.7.1.

3.3.2 DHR123 assay

In the initial experiments neutrophils were isolated from EDTA coagulated blood using Polymorphprep as described in Section 2.2.6.1 unless otherwise stated. These cells were then loaded with 1μg/ml DHR123. The assay was otherwise carried out as described in Section 2.2.7.2. In later experiments neutrophils were isolated from heparinised blood using Ficoll as described in Section 2.2.6.2, with assays being performed as described in Section 2.2.7.2. To remove aggregates from purified IgG, samples were either spun at 16,000g in a tabletop microcentrifuge at 4°C or passed through a 300,000 MWCO PES Vivaspin 500 centrifugal concentrator (Sartorius Stedim Biotech).

3.3.3 IgG Purifications

IgG was purified from plasma or serum taken from either healthy controls or PR3 and/or MPO-ANCA positive patients. Ammonium sulphate or sodium chloride precipitation, as described in Sections 2.2.3.1 and 2.2.3.2 respectively, was used to remove fibrin before HiTrap HP Protein G columns were employed as described. Purity and ANCA binding potential of patient IgG was determined using SDS-PAGE as described in Section 2.2.4 and anti-PR3/MPO antibody capture ELISAs as described in Section 2.2.5.

3.3.4 Acknowledgements

I would like to thank Dr. Reena Popat for contributing the anti-PR3 and anti-MPO titration data presented in Figure 3.6.

3.4 Results: ANCA activates human neutrophils *in vitro*

3.4.1 ANCA induces superoxide release

The ANCA induced release of superoxide from neutrophils is shown in Figure 3.1. Neutrophils were isolated using Polymorphprep, primed with TNFα and then stimulated with either a commercial monoclonal anti-PR3 or anti-MPO antibody. An IgG isotype control was included to discount non-specific superoxide production. fMLP was used as a positive control for neutrophil activation. Both the anti-PR3 and anti-MPO antibodies induced similar levels of superoxide release and this was comparable to the fMLP induced response. (Fig 3.1. A). To confirm that the ANCA induced response was not restricted to the specific monoclonal antibodies used, IgG purifed, using ammonium sulphate and protein G purification, from PR3- and MPO-ANCA positive patients was also included in the assay. IgG from healthy donors served as a negative control in this case (Fig 3.1. B). The MPO positive patient IgG induced response was comparable to that of the monoclonal anti-MPO IgG induced response. However, the response to PR3 positive patient IgG was less potent than that induced by the equivalent monoclonal antibody.

Finally, in all cases the response was superoxide dismutase (SOD) inhibitable. As SOD catalyses the conversion of superoxide to hydrogen peroxide, thus removing superoxide from the reaction, this demonstrates that the reduction of cytochrome C was the result of superoxide release.

3.4.2 ANCA induces the release of reactive oxygen species as measured by the conversion of dihydrorhodamine (DHR)-123 into fluorescent rhodamine 123

Neutrophils were isolated from EDTA coagulated blood using Polymorphprep, primed with TNFα, and then stimulated with a commercial monoclonal anti-PR3 antibody. An IgG isotype control was included to discount non-specific rhodamine 123 production. PMA was used as a positive control for neutrophil activation. Rhodamine 123 production in response to the anti-PR3 monoclonal antibody was comparable to that of the PMA positive control, however, a subpopulation of the neutrophils treated with the isoytpe control IgG also activated to the same extent as the anti-PR3 IgG stimulated cells (Fig 3.2 A). To determine if this was a problem associated with the monoclonal antibodies used, the assay was repeated using IgG purifed, using ammonium sulphate and protein G purification, from a PR3-ANCA positive patient. IgG from a healthy donor served as a negative control in this experiment (Fig 3.2.B). Both the PR3 positive patient IgG and the healthy control IgG induced rhodamine 123 production to a level comparable to that induced by the PMA positive control. This raised the question as to whether aggregates in the antibody preparations could be activating the neutrophils. To address this concern the assay was repeated using antibody preparations that were either untreated or, in order to remove aggregates, centrifuged at high speed or forced through a high molecular weight Vivaspin centrifugal concentrator. Initially it appeared that forcing the antibody preparations through the concentrator would allow a marginal difference between the isotype control and ANCA induced responses to be identified. However, this could not be repeated (Fig 3.3, representative of 3 experiments).

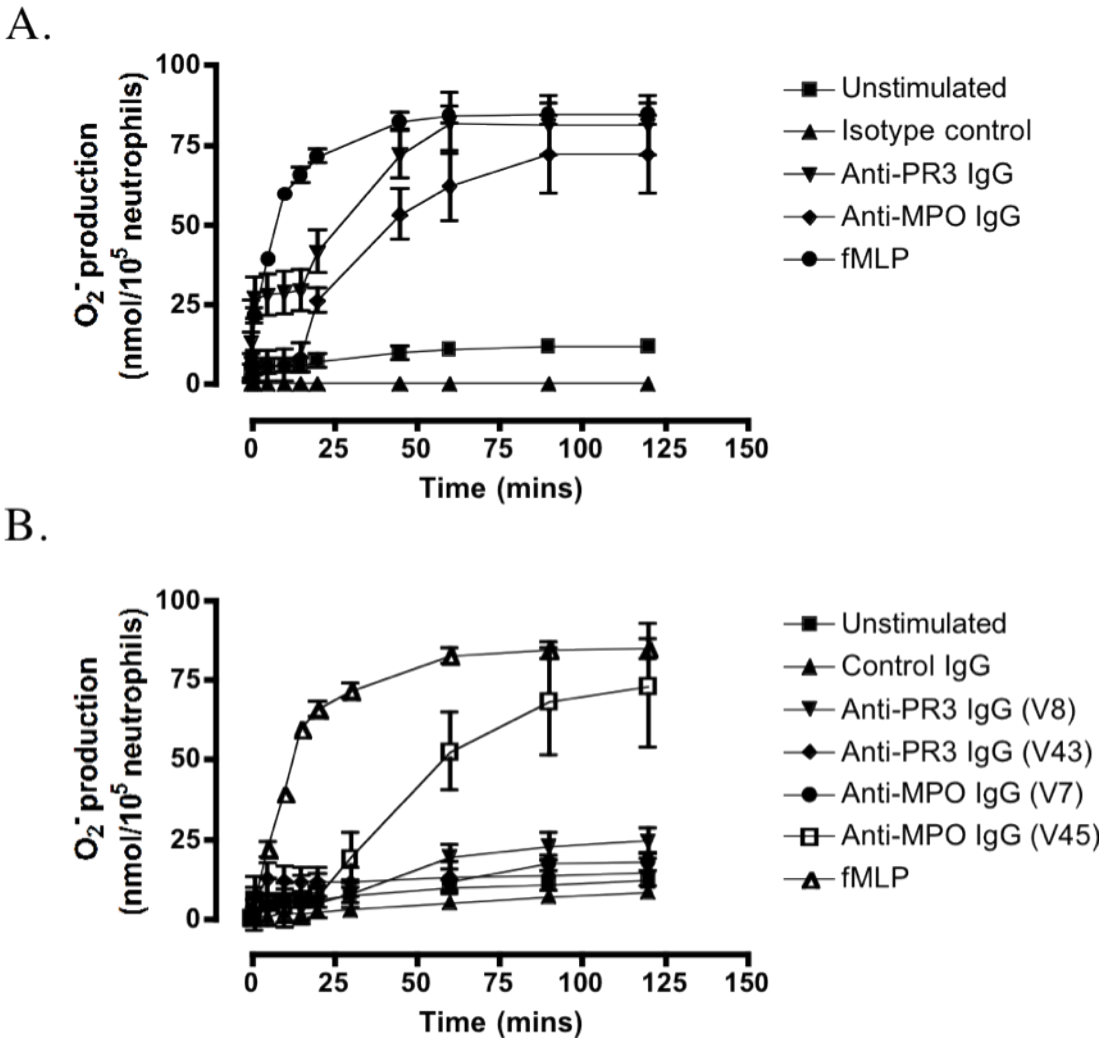

Figure 3.1 ANCA induced superoxide release as measured by the superoxide dismutase (SOD) inhibitable reduction of ferricytochrome C. TNFα primed neutrophils were isolated from a healthy volunteer using Polymorphprep as described. (A) Neutrophils stimulated with either 10μg/ml monoclonal human anti-MPO IgG (n=1), 5μg/ml monoclonal human anti-PR3 IgG (n=1) or a relevant isotype control (n=1). (B) Neutrophils stimulated with 200μg/ml polyclonal anti-MPO IgG (n=2) or anti-PR3 IgG (n=2) purified from patient plasma. IgG purified from a healthy volunteer (n=1) was used as a negative control. fMLP was used a positive control for neutrophil activation. Data are presented as mean values ± SEM of triplicate wells.

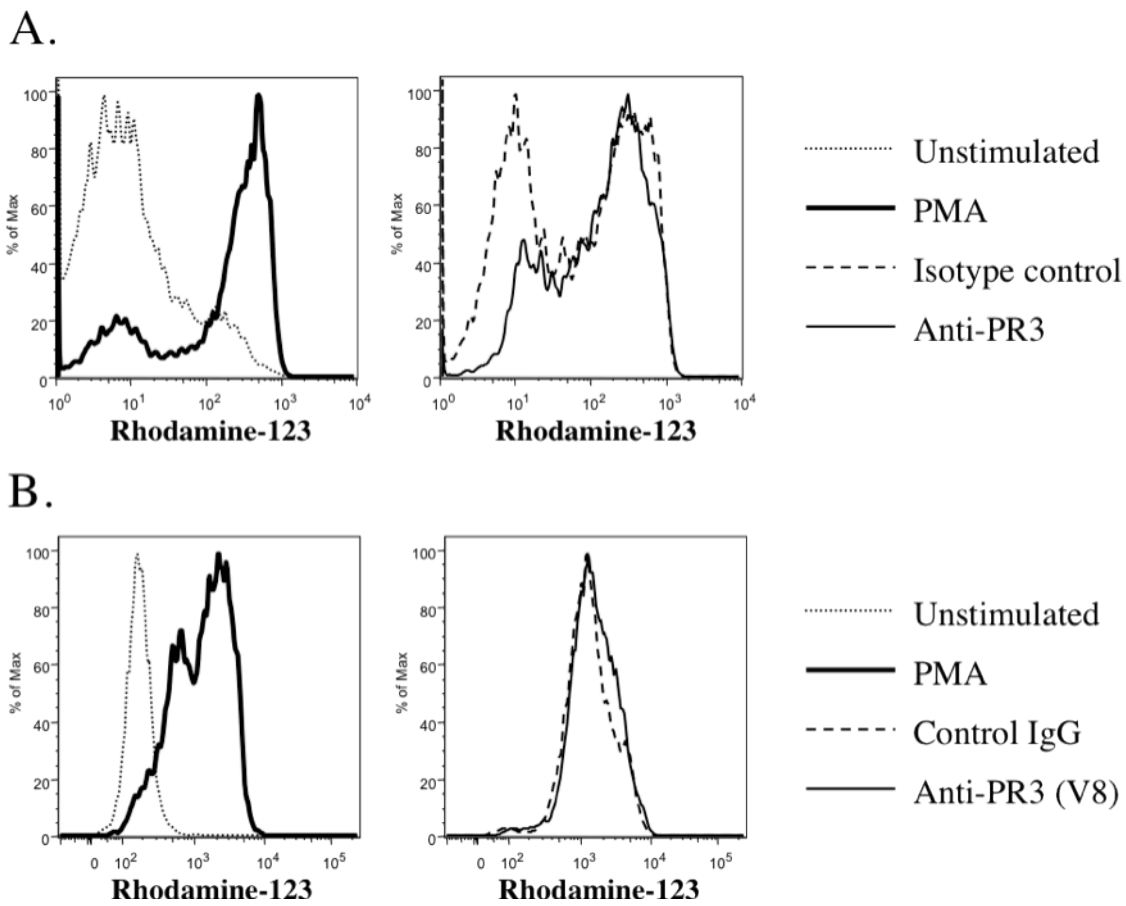

Figure 3.2 ANCA induced respiratory burst as measured by the conversion of DHR123 into fluorescent rhodamine-123. TNFα primed neutrophils were isolated from a healthy volunteer using Polymorphprep as described and stimulated with (A) 5μg/ml monoclonal human anti-PR3 IgG (n=1) or a relevant isotype control or (B) 200μg/ml polyclonal human anti-PR3 IgG (n=1) purified from patient plasma. IgG purified from a healthy control was used as a negative control. PMA was used as a positive control.

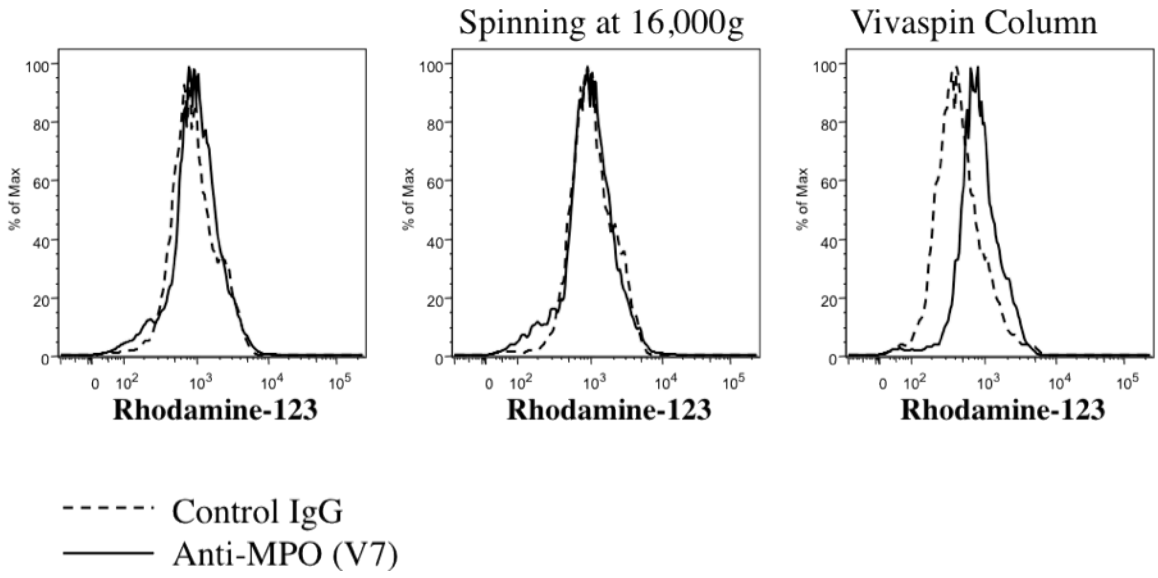

Figure 3.3 Filtering IgG through a vivaspin column removes aggregates but has minimal effect on the ANCA induced respiratory burst as measured by the conversion of DHR123 into fluorescent rhodamine-123. TNFα primed neutrophils were isolated from a healthy volunteer using Polymorphprep as described and stimulated with 200μg/ml polyclonal human anti-MPO IgG (n=1) purified from patient plasma. IgG purified from a healthy volunteer was used as a negative control. IgG was either untreated, spun at 16,000g for 15 minutes in a temperature controlled table top microcentrifuged, or passed through a vivaspin column in order to remove aggregates that may be inducing a respiratory burst in the response to control IgG. Data is representative of 3 separate experiments.

In a recent report, Freitas et al. examined the effect of the anticoagulant used in blood collection during neutrophil isolation, by a gradient density centrifugation method using Histopaque solutions, on the PMA induced respiratory burst [204]. They showed that while EDTA provided the highest yield of isolated neutrophils compared with citrate and heparin, it also resulted in the lowest degree of PMA induced neutrophil respiratory burst as measured by chemiluminescence. To determine if this was also true for the ANCA induced release of reactive oxygen species, and thus responsible for the lack of difference seen between the ANCA and control IgG induced production of rhodamine 123, blood was collect using EDTA, sodium citrate or lithium heparin, and a DHR123 assay using a commercial monoclonal anti-PR3 antibody was carried out (Fig 3.4). The difference between the three anticoagulants was marginal, however, it was decided to use lithium heparin in blood collection for neutrophil isolation from this point onwards. It should be noted that while there was a small response to anti-PR3 antibodies seen in this experiment, this was not typical.

It has been established that isolation of neutrophils can lead to phenotypic and functional changes that may affect neutrophil activation [205]. With the view of setting up a reliable ANCA induced DHR123 assay, neutrophil isolation using Polymorphprep was abandoned and the more widely used method of isolating neutrophils using density gradient sedimentation to remove the PBMCs, the neutrophils pellet with the red cells, followed by red cell lysis was adopted. Figure 3.5 shows ANCA induced rhodamine 123 production by neutrophils isolated using the Ficoll method described in Section 2.2.6.1. Neutrophils were primed with TNFα and then stimulated with either a commercial monoclonal anti-PR3 or anti-MPO antibody. An IgG isotype control was included to discount non-specific rhodamine-123 production. fMLP was used as a positive control for neutrophil activation. Both the anti-PR3 and anti-MPO antibodies induced similar levels rhodamine-123, with the anti-PR3 IgG induced response being marginally stronger (Fig 3.5 A). To confirm that the ANCA induced response was not restricted to the specific monoclonal antibodies used, IgG purifed from PR3- and MPO-ANCA positive patients was also tested. IgG from healthy donors served as a negative

control in this case (Fig 3.5 B). The PR3- and MPO-ANCA positive patient IgG induced rhodamine 123 production to a strong degree, comparable to that induced by the fMLP positive control. Although never formally compared side-by-side with Polymorphprep, using this method of neutrophil isolation a reliable assay was established.

To further optimise the DHR123 assay for future use in the investigation of ANCA induced neutrophil activation, titrations of the anti-PR3 and anti-MPO monoclonal antibodies were performed (Fig 3.6). For the monoclonal anti-PR3 antibody, 5μg/ml was found to give optimal activation with lower concentrations inducing less neutrophil activation (Fig 3.6 A). In contrast, the anti-MPO antibody was found to induced similar levels of activation when used at 5, 2.5 and 1.25μg/ml of IgG (Fig 3.6 B).

3.5 Results: Purification of human IgG from anti-PR3 and anti-MPO ANCA positive patients

3.5.1 IgG Purifications

Using SDS PAGE under reducing conditions, Figure 3.7 shows the various stages of human IgG purification from plasma using ammonium sulphate precipitation followed by Protein G purification. The IgG heavy and light chains can be seen at approximately 55kDa and 25kDa, respectively, in all samples with the exception of the flow through. Post ammonium sulphate precipitations, one at 25% to remove fibrin and one at 50% to precipitate out the antibody, a number of impurities remain. These impurities are largely absent after protein G purification.

3.5.2 Optimisation of IgG purification protocol

Ammonium sulphate precipitation has a number of disadvantages. Firstly, a large volume of saturated ammonium sulphate solution must be added to the plasma to achieve 50% saturation. Secondly, the ammonium sulphate must

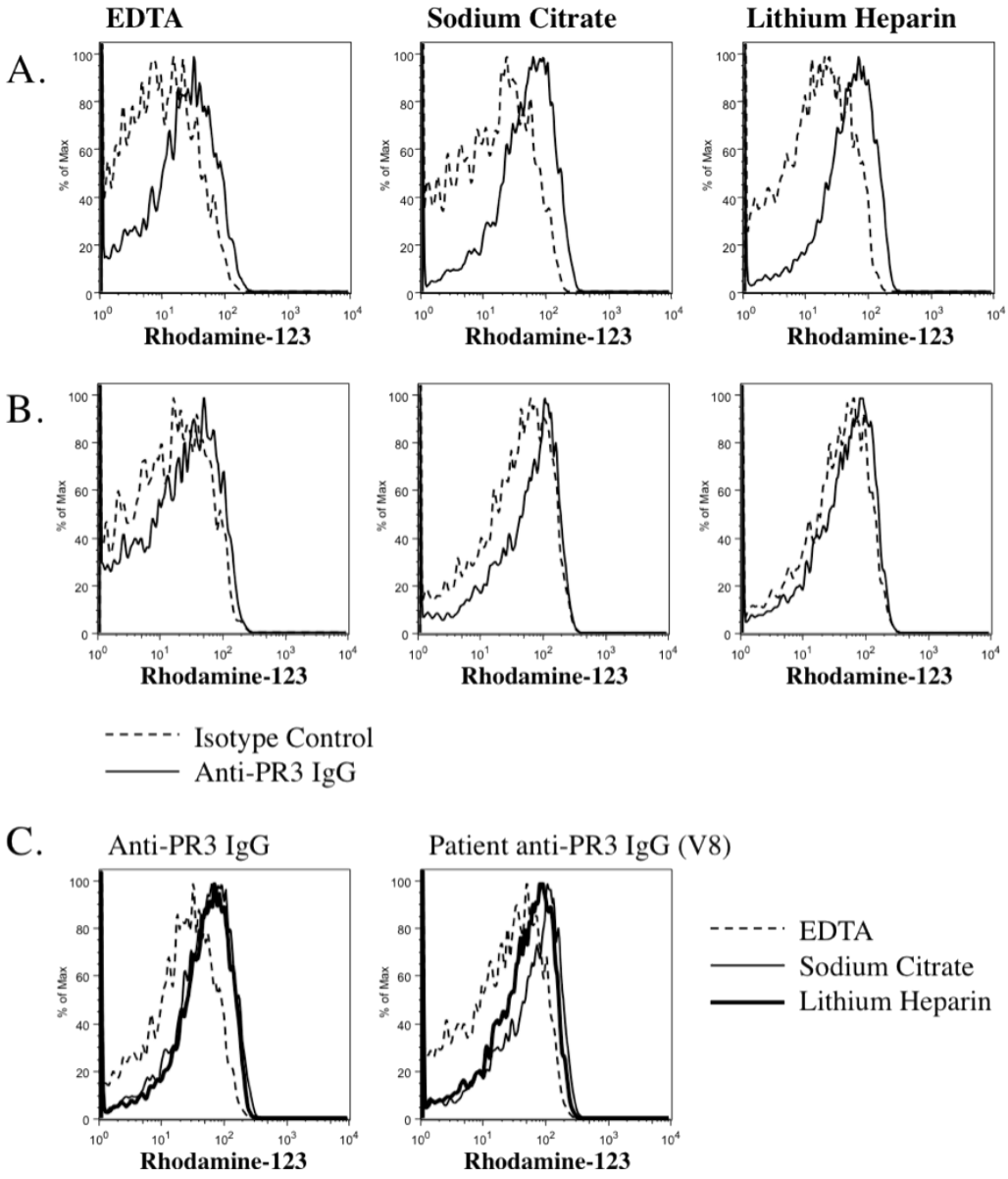

Figure 3.4 The effect of the anticoagulant used during blood collection on the ANCA induced respiratory burst as measured by the conversion of DHR123 into fluorescent Rhodamine-123. TNFα primed neutrophils were isolated, using Polymorphprep, from blood taken from a healthy volunteer and collected into one of the following anticoagulants: EDTA, sodium citrate or lithium heparin. Neutrophils were then stimulated with (A) 5μg/ml monoclonal human anti-PR3 IgG (n=1) or a relevant isotype control or (B) 200μg/ml patient derived anti-PR3 IgG (V8, n=1). IgG purified from a healthy volunteer was used as a negative control. (C) Shows the data from (A) and (B) with a direct comparison of the effect of the anticoagulant used on the level of rhodamiine-123 production.

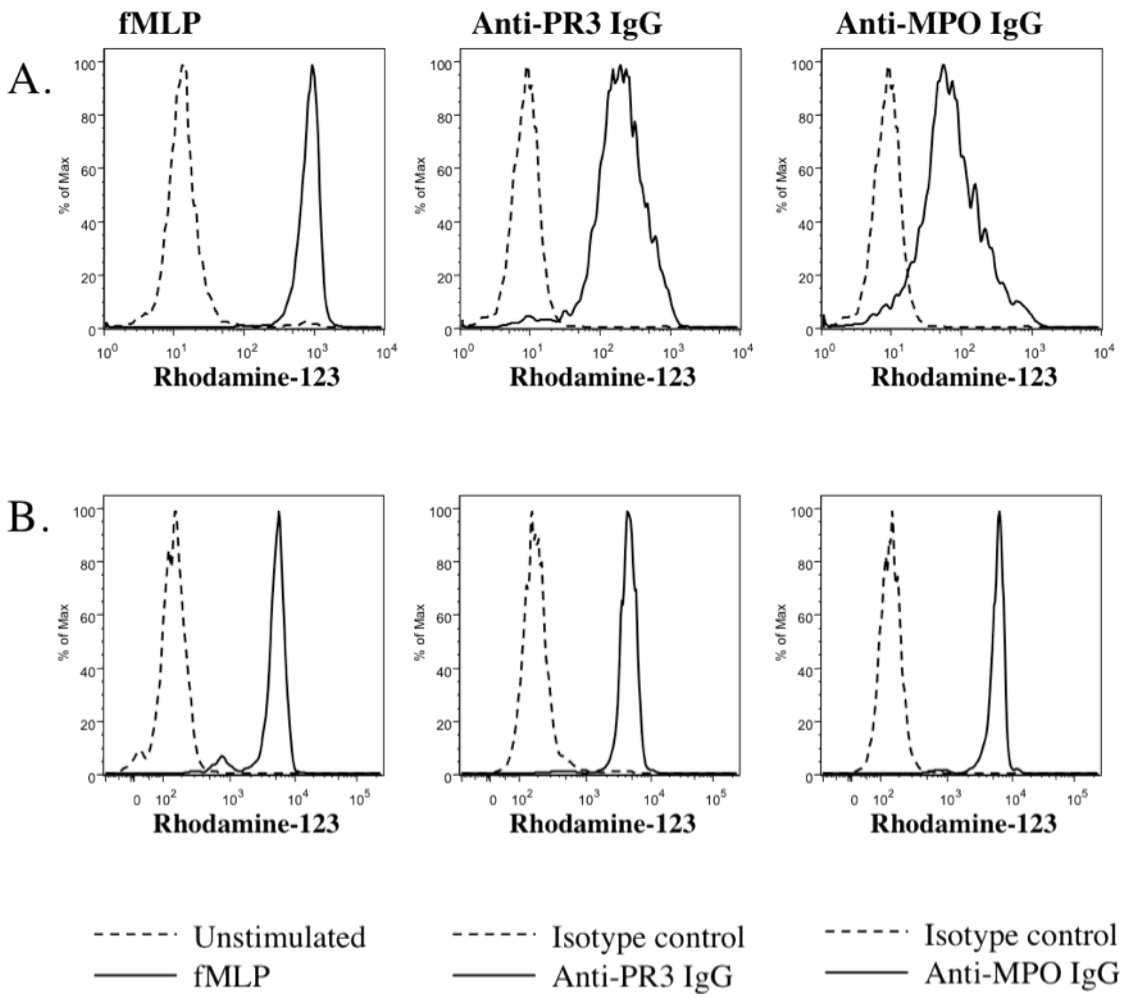

Figure 3.5 ANCA induced respiratory burst as measured by the conversion of DHR123 into fluorescent rhodamine-123. TNFα primed neutrophils isolated from heparinised blood, using Ficoll and red cell lysis as described, were stimulated with (A) either 5μg/ml monoclonal human anti-PR3 IgG (n=1), 10μg/ml monoclonal human anti-MPO IgG (n=1) or a relevant isotype control (B) either 200μg/ml polyclonal human anti-PR3 IgG (V16) (n=1), polyclonal human anti-MPO IgG (V30) (n=1) purified or a relevant control (L1) (n=1). fMLP was used as a positive control.

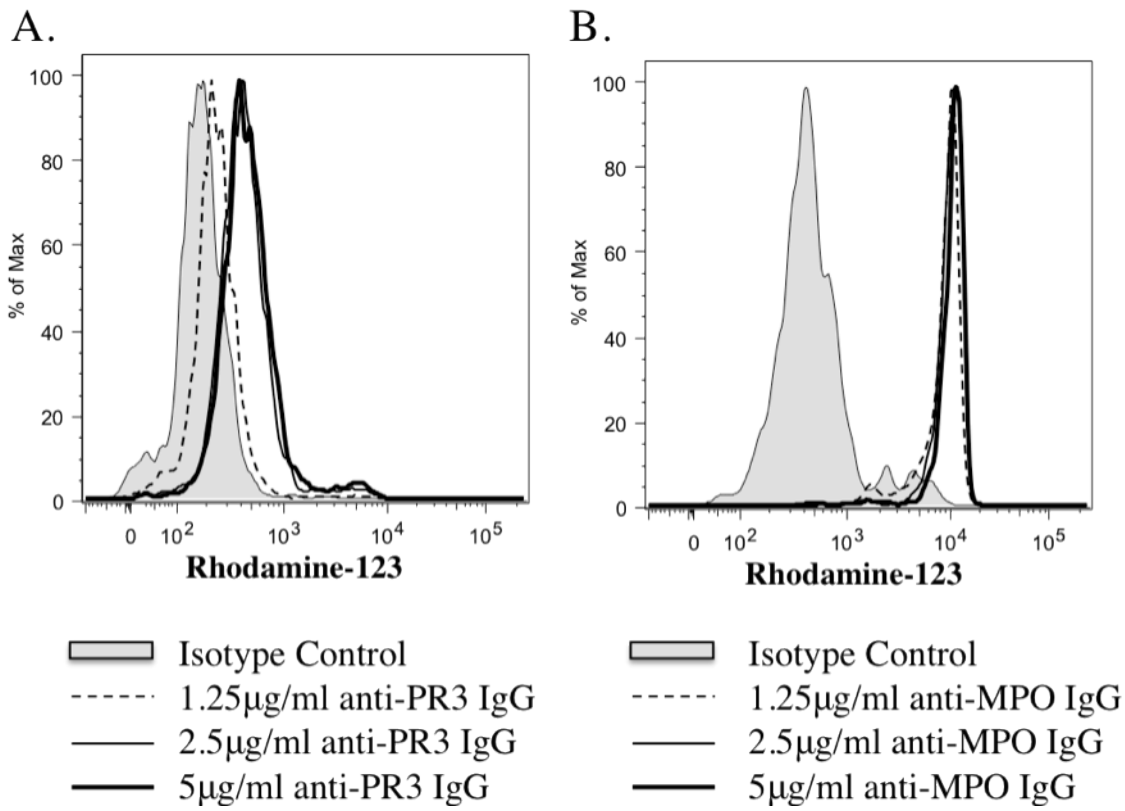

Figure 3.6 Monoclonal anti-neutrophil antibody titration. TNFα primed neutrophils isolated from heparinised blood, using Ficoll and red cell lysis as described, were loaded with DHR123 and stimulated with (A) 5, 2.5 or 1.25µg/ml monoclonal human anti-PR3 IgG (n=1) or (B) 5, 2.5 or 1.25µg/ml monoclonal human anti-MPO IgG (n=1). An irrelevant isotype control was used at 5µg/ml as a negative control for neutrophil activation.

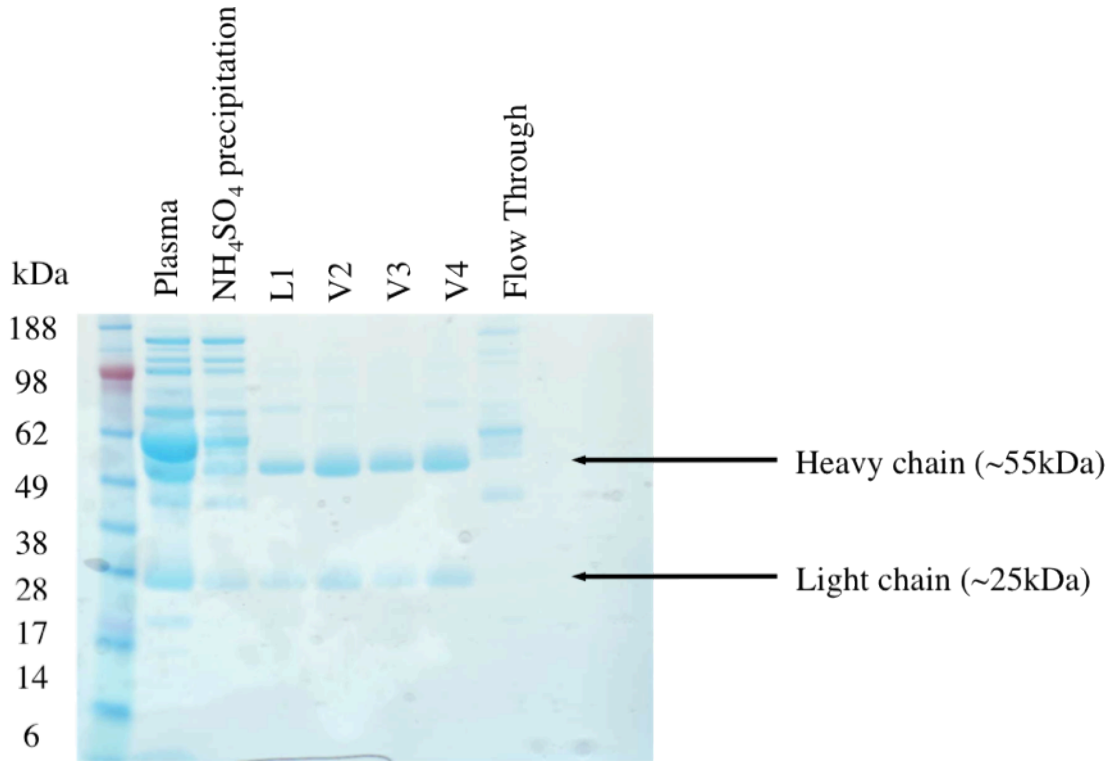

Figure 3.7 Testing the purity of the IgG preparation from both patient and control plasma after the various stages of purification using SDS PAGE under reducing conditions. L1=healthy volunteer IgG, V2=patient anti-PR3 IgG, V3= patient anti-PR3 IgG, V4= patient anti-PR3 IgG. V-Vasculitis patient, L-Lab volunteer

be exchanged for PBS using dialysis before the antibody preparation can be Protein G purified, thus lengthening the time required to isolated the antibody. However, in order to avoid blocking the Protein G column fibrin must be removed from plasma, and therefore some form of precipitation to remove contaminants must be carried out. One alternative to ammonium sulphate precipitation that was examined was precipitation using sodium chloride. Sodium chloride works in a similar manner to ammonium sulphate, however, as solid sodium chloride was used only a small amount was required (18g/100ml). The contaminants were removed by centrifugation after a single precipitation step and once the supernatant containing the antibody was diluted 1:5 with water, the sample was ready to be put through the Protein G column. There was no distinguishable difference found between antibodies purified using these two methods (Fig 3.8 A). To examine the effect of sodium chloride precipitation relative to ammonium sulphate precipitation, antibody preparations purified side-by-side using both methods were compared.

Table 3.1 shows, using a MPO antibody binding ELISA, that the binding ability of individual patient anti-MPO IgG was similar regardless of the precipitation method used. Table 3.2 compares the yield and ability to induce neutrophil respiratory burst of antibodies purified using both methods. For 2 of the 3 patient samples tested the yield was unaffected by precipitation method used. For the third sample the yield was higher when ammonium sulphate precipitation was used. With regards functionality of the antibody, anti-MPO antibodies isolated from patient samples using sodium chloride induced a greater respiratory burst, as measured by rhodamine 123 production, than that isolated using ammonium sulphate, in 2 out of 3 patient samples tested (Fig 3.8 B). However, this was not great enough to be statistically significant.

3.5.2 Summary of IgG preparations

Table 3.3, 3.4 and 3.5 list the control IgG, patient anti-PR3 ANCA positive IgG and patient anti-MPO ANCA positive IgG isolated, respectively, together with the volume of plasma and the precipitation method used as well the concentration and volume of the final product after purification. Table 3.6 lists

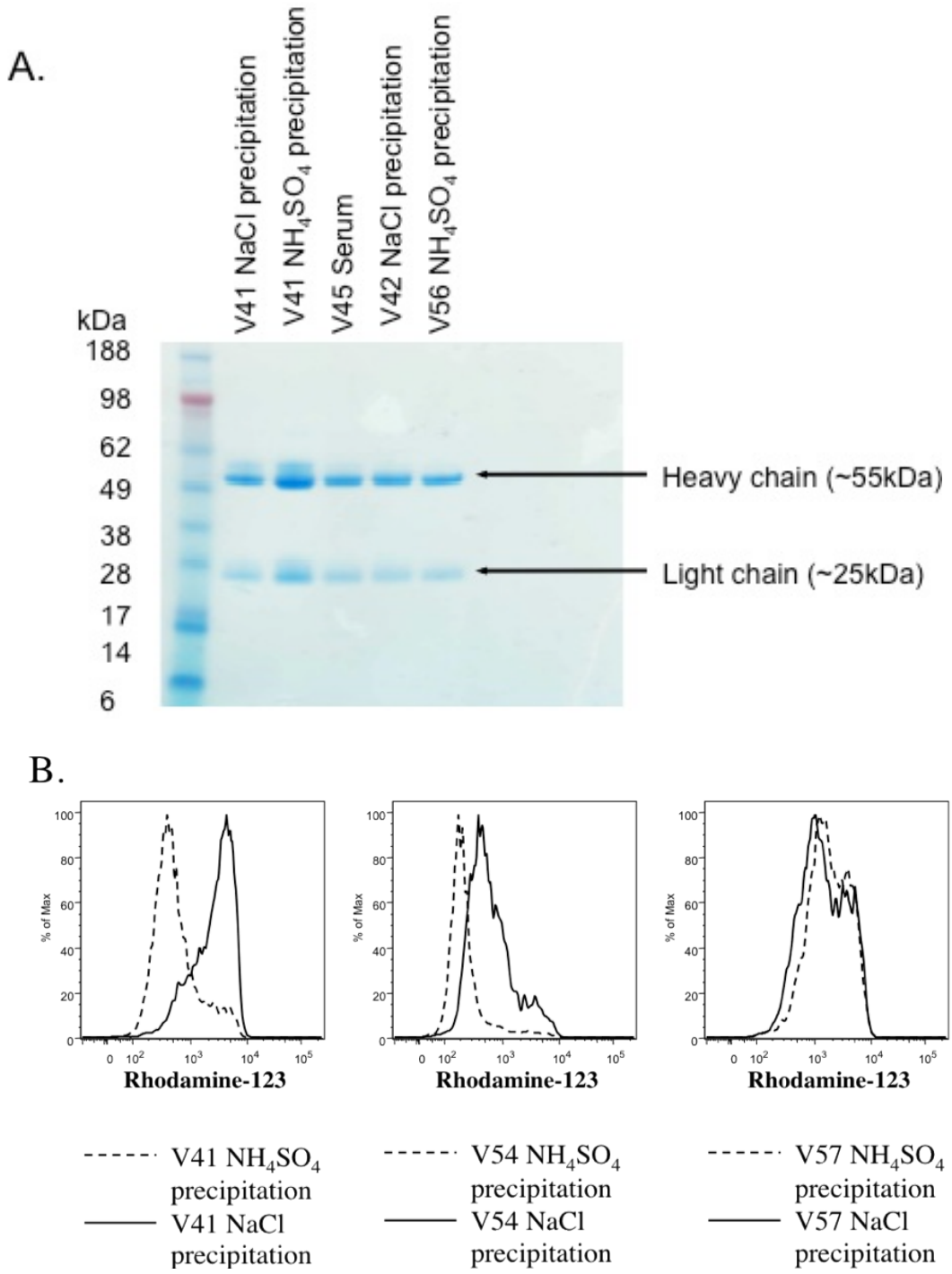

Figure 3.8 Comparing ammonium sulphate (NH_4SO_4) and sodium chloride (NaCl) precipitation with regards to (A) the purity of the IgG preparation (n=2), and, (B) the ability of 200μg/ml of the resulting purified ANCA to induced a respiratory burst in TNFα primed neutrophils isolated from heparinised blood using Ficoll and red cell lysis (n=3). V41, V45, V54 and V57 are patient anti-MPO IgG preparations. V-Vasculitis patient

Sample ID	Preparation	MPO Binding ELISA (U/ml)
V41	NH_4SO_4 precipitation	17.6
V41	NaCl precipitation	17.8
V7	NH_4SO_4 precipitation	174.3
V7	NaCl precipitation	147.2

Table 3.1 MPO Capture ELISA results comparing the binding of antibody purified on the same day using either a NH_4SO_4 precipitation or NaCl precipitation. Antibody was used at a concentration of 20μg/ml. V7 and V41 are patient anti-MPO IgG preparations. V-Vasculitis patient

Sample ID	Preparation	Yield	Respiratory Burst (MFI)
V41	NH_4SO_4 precipitation	23mg	465
V41	NaCl precipitation	24mg	3051
V54	NH_4SO_4 precipitation	5.7mg	202
V54	NaCl precipitation	3mg	526
V57	NH_4SO_4 precipitation	9mg	1698
V57	NaCl precipitation	8.4mg	1321

Table 3.2 Comparing the yield (from 5ml of plasma) of, and respiratory burst induced by, antibody purified on the same day using either a NH_4SO_4 precipitation or NaCl precipitation. V41, V45, V54 and V57 are patient anti-MPO IgG preparations. V-Vasculitis patient

Sample ID	Preparation	Concentration	Volume
L1	25ml Plasma, NH_4SO_4 Precipitation	4.56mg/ml	10ml
L1	5ml Plasma, NaCl Precipitation	1.77mg/ml	3ml
L2	50ml Plasma, NH_4SO_4 Precipitation	4.61mg/ml	20ml
L2	5ml Plasma, NaCl Precipitation	7mg/ml	3ml
L2	5ml Serum	4.4mg/ml	3ml
L1, L2	90ml Plasma, NH_4SO_4 Precipitation	50mg/ml	1.2ml
L13	5ml Plasma, NaCl Precipitation	1mg/ml	3ml
L17	5ml Plasma, NaCl Precipitation	2mg/ml	3ml
L18	5ml Plasma, NaCl Precipitation	2mg/ml	3ml
L18	5ml Plasma, NaCl Precipitation	3.4mg/ml	3ml
L27	5ml Plasma, NaCl Precipitation	3.89mg/ml	3ml

Table 3.3 List of purified IgG from healthy controls. V-Vasculitis patient.

Sample ID	Preparation	Concentration	Volume
V2	45ml Plasma, NH_4SO_4 Precipitation	4.97mg/ml	20ml
V3	40ml Plasma, NH_4SO_4 Precipitation	4.36mg/ml	20ml
V4	45ml Plasma, NH_4SO_4 Precipitation	5.97mg/ml	12ml
V5	50ml Plasma, NH_4SO_4 Precipitation	4.5mg/ml	12ml
V8	50ml Plasma, NH_4SO_4 Precipitation	6mg/ml	10ml
V8	5ml Plasma, NaCl Precipitation	2mg/ml	3ml
V12	90ml Plasma, NH_4SO_4 Precipitation	4.78mg/ml	20ml
V13	45ml Plasma, NH_4SO_4 Precipitation	4.87mg/ml	5ml
V14	45ml Plasma, NH_4SO_4 Precipitation	5.34mg/ml	15ml
V14	45ml Plasma, NH_4SO_4 Precipitation	20.72mg/ml	2.6ml
V14	45ml Plasma, NH_4SO_4 Precipitation	50mg/ml	1.6ml
V14	5ml Plasma, NaCl Precipitation	4.68mg/ml	3ml
V16	5ml Plasma, NaCl Precipitation	4.23mg/ml	3ml
V18	5ml Plasma, NaCl Precipitation	4.36mg/ml	3ml
V20	5ml Plasma, NaCl Precipitation	3.7mg/ml	3ml
V21	5ml Plasma, NaCl Precipitation	4.25mg/ml	3ml
V42	5ml Plasma, NH_4SO_4 Precipitation	4.68mg/ml	3ml
V43	5ml Plasma, NaCl Precipitation	8.63mg/ml	3ml
V44	5ml Plasma, NH_4SO_4 Precipitation	7.69mg/ml	3ml
V49	5ml Plasma, NaCl Precipitation	7.36mg/ml	3ml
V51	5ml Plasma, NH_4SO_4 Precipitation	3.9mg/ml	3ml
V52	5ml Plasma, NaCl Precipitation	8.2mg/ml	3ml
V56	5ml Plasma, NaCl Precipitation	6.6mg/ml	3ml

Table 3.4 List of purified IgG from patients with PR3 positive granulomatosis with polyangiitis (formally Wegener's granulomatosis). V-Vasculitis patient.

Sample ID	Preparation	Concentration	Volume
V7	50ml Plasma, NH_4SO_4 Precipitation	5.7mg/ml	10ml
V7	5ml Plasma, NaCl Precipitation	2mg/ml	3ml
V26	45ml Plasma, NH_4SO_4 Precipitation	4.98mg/ml	16ml
V30	45ml Plasma, NH_4SO_4 Precipitation	20mg/ml	1ml
V30	5ml Plasma, NaCl Precipitation	3.75mg/ml	3ml
V31	90ml Plasma, NH_4SO_4 Precipitation	50mg/ml	1.4ml
V32	5ml Plasma, NaCl Precipitation	8mg/ml	3ml
V33	5ml Plasma, NaCl Precipitation	4mg/ml	3ml
V35	5ml Plasma, NaCl Precipitation	5mg/ml	3ml
V38	5ml Plasma, NaCl Precipitation	8.47mg/ml	3ml
V41	5ml Plasma, NH_4SO_4 Precipitation	7.7mg/ml	3ml
V41	5ml Plasma, NaCl Precipitation	8mg/ml	3ml
V45	5ml Serum	8.47mg/ml	3ml
V46	5ml Plasma, NaCl Precipitation	7.5mg/ml	3ml
V48	5ml Plasma	8.25mg/ml	3ml
V50	5ml Plasma, NaCl Precipitation	3.7mg/ml	3ml
V54	5ml Plasma, NaCl Precipitation	4.48mg/ml	3ml
V54	5ml Plasma, NH_4SO_4 Precipitation	1.9 mg/ml	3ml
V54	5ml Plasma, NaCl Precipitation	1mg/ml	3ml
V57	5ml Plasma, NaCl Precipitation	6.79mg/ml	3ml
V57	5ml Plasma, NH_4SO_4 Precipitation	3.19mg/ml	3ml
V57	5ml Plasma, NaCl Precipitation	2.81 mg/ml	3ml
V59	5ml Plasma, NH_4SO_4 Precipitation	3.4mg/ml	3ml

Table 3.5 List of purified IgG from patients with MPO positive microscopic polyangiitis. V-Vasculitis patient.

Sample ID	Renal BVAS	Total BVAS	Renal Biopsy	Non-renal Features	O_2^- Production (nmol/10^5 cells above control)	Rhodamine-123 production (MFI above control)
V2	12	35	Yes	Eyes/ent/chest/ns	1±1	0
V3	12	31	No	Chest/ns/ent/skin	1±1	56
V4	12	19	Yes	Skin/eyes/ns	3±1	103
V5	12	32	Yes	Eyes/ns/abdo	1±1	195
V8	12	14	Yes	No	5±2	32
V12	12	27	Yes	Ent/chest/eyes	3±2	232
V13	12	33	Yes	Ent/chest/eyes/ns	2±2	114
V14	12	21	Yes	Ent	0	2719
V16	12	15	Yes	No	6±2	4407
V18	12	19	Yes	Skin	471±5	6725
V20	12	23	Yes	Ent/chest	No data	395
V21	12	23	Yes	Eyes/chest	0	1433
V31	12	15	Yes	No	No data	No data
V43	12	21	Yes	Ent	No data	13
V44	12	27	Yes	Ent/chest	8±7	34
V49	10	14	Yes	Ent/eyes	No data	69
V51	12	24	Yes	Ns	15±6	93
V56	12	30	Yes	Eyes/ent/chest	7±6	200

Table 3.6 List of purified IgG from anti-PR3 ANCA positive patients including relevant clinical information and ability to induce a respiratory burst as measured by O_2^- (presented as mean values ± SEM of triplicate wells of triplicate wells) and rhodamine-123 production. All patients had evidence of active renal involvement, which was confirmed by renal biopsy in most cases. Clinical evidence of other tissue involvement (ent-ear, nose or throat, ns-nervous system, abdo-abdomen) is also indicated. V-Vasculitis patient. BVAS-Birmingham Vasculitis Activity Score.

the IgG isolated anti-PR3 ANCA positive patients including relevant clinical information. Data on the ability of these patient derived ANCA to induce a respiratory burst as measured by both a ferricytochrome C reduction assay (Fig 3.9) (O_2^- production with data presented as mean values ± SEM of triplicate wells of triplicate wells) and a DHR123 assay (Fig 3.10) (rhodamine 123 production) is also included. Table 3.7 lists the same information for IgG purified anti-MPO ANCA positive patients.

Sample ID	Renal BVAS	Total BVAS	Renal Biopsy	Non-renal Features	O_2^- Production (nmol/10^5 cells above control)	Rhodamine-123 production (MFI above control)
V7	12	20	No	Chest/ent	15±3	9
V26*	12	22	Yes	Ent/chest	9±1	0
V30	12	18	No	Chest	18±1	6020
V32	12	15	Yes	No	No data	56
V33	12	18	Yes	Ent/chest	6±1	2632
V35	6	10	Yes	Eyes/skin	No data	13
V38	12	18	No	Chest	8±2	21
V41	12	15	Yes	No	0	2998
V42	12	25	No	Skin/eyes/ent	14±2	208
V45	12	15	Yes	No	40±2	158
V48	12	12	Yes	No	12±5	10
V50	12	12	Yes	No	5±0	139
V54	12	12	Yes	No	16±2	310
V57	12	15	Yes	No	3±0	127
V59	12	12	Yes	No	6±1	108

Table 3.7 List of purified IgG from anti-MPO ANCA positive patients including relevant clinical information and ability to induce a respiratory burst as measured by O_2^- (presented as mean values ± SEM of triplicate wells of triplicate wells) and rhodamine-123 production. All patients had evidence of active renal involvement, which was confirmed by renal biopsy in most cases. Clinical evidence of other tissue involvement (ent-ear, nose or throat) is also indicated. V-Vasculitis patient. BVAS-Birmingham Vasculitis Activity Score. *Patient positive for both anti-MPO and anti-PR3 antibodies.

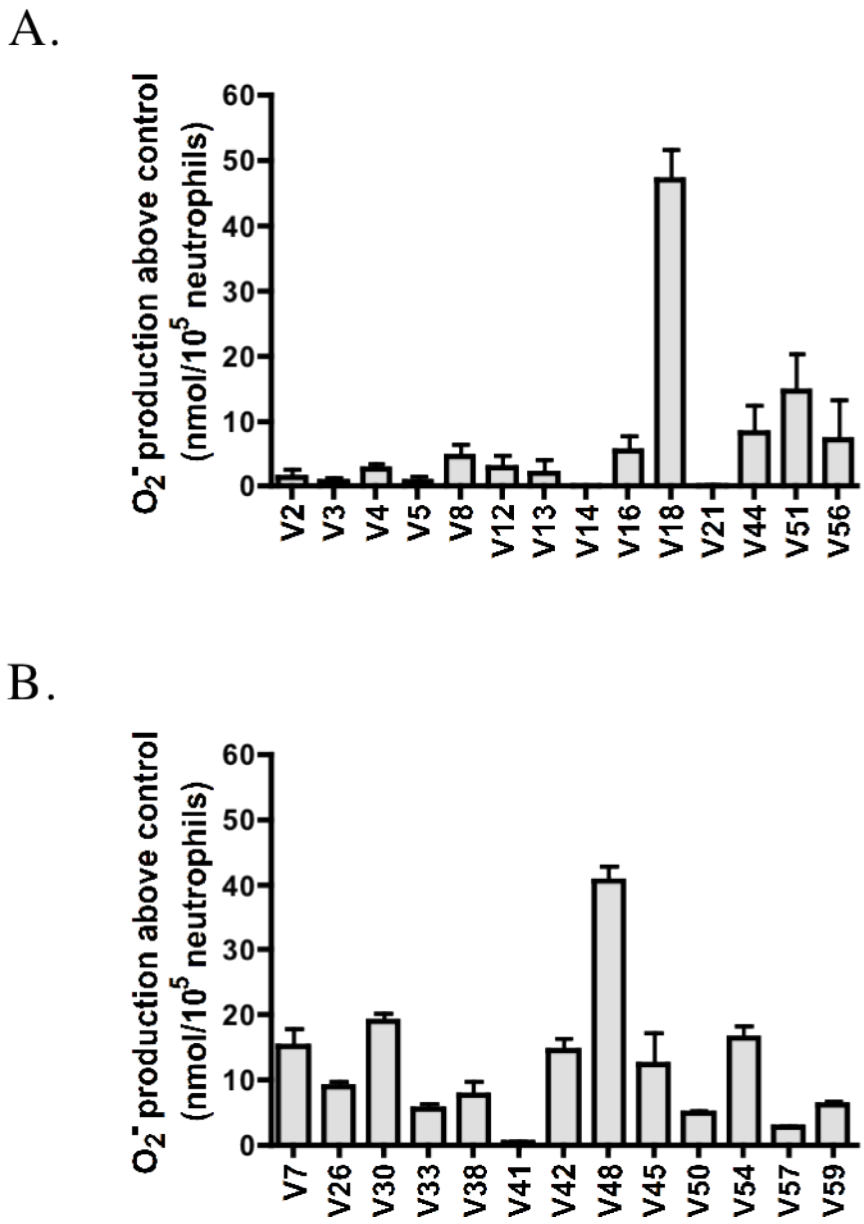

Figure 3.9 ANCA induced superoxide release as measured by the superoxide dismutase inhibitable reduction of ferricytochrome C. TNFα primed neutrophils isolated from heparinised blood using Ficoll and red cell lysis as described were stimulated with 200μg/ml of polyclonal human (A) anti-PR3 (n=14) or (B) anti-MPO IgG (n=13) purified from patient plasma. O_2^- production above control was obtained from the O_2^- production of the ANCA stimulated cells minus the average O_2^- production of the isotype control (n=3) stimulated cells. Data are presented as mean values ± SEM of triplicate wells. V-Vasculitis patient

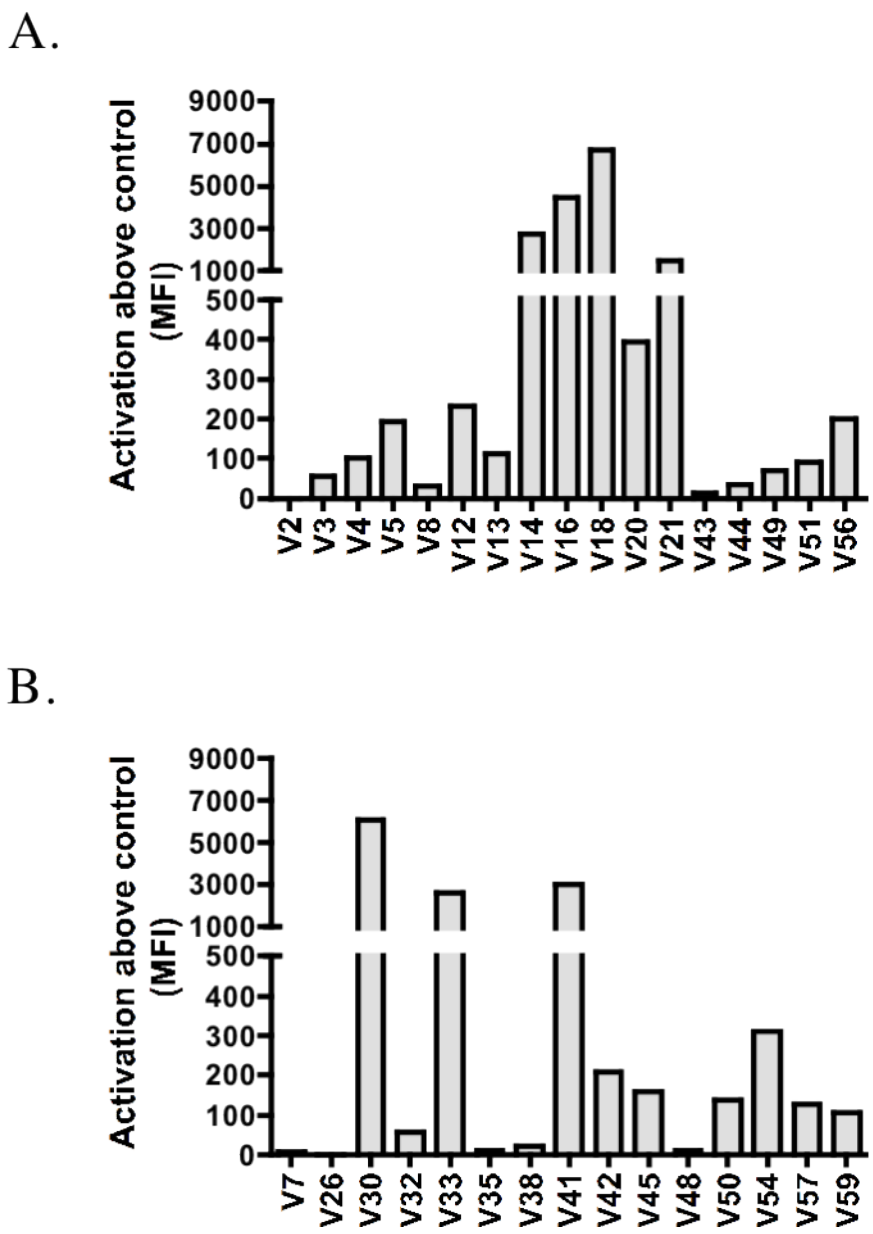

Figure 3.10 ANCA induced respiratory burst as measured by the conversion of DHR123 into fluorescent rhodamine-123. TNFα primed neutrophils isolated from heparinised blood, using Ficoll and red cell lysis as described, were stimulated with 200μg/ml of polyclonal human (A) anti-PR3 (n=17) or (B) anti-MPO IgG (n=15) purified from patient plasma. Activation above control was obtained from the median fluorescence intensities (MFI) of the ANCA stimulated cells minus the average MFI of the isotype control (n=3) stimulated cells. V-Vasculitis patient

3.6 Discussion

ANCA induced respiratory burst assays

Using both monoclonal, and patient purified polyclonal, anti-PR3 and anti-MPO antibodies, two respiratory burst assays to measure the ANCA-induced activation of neutrophils were developed. The superoxide dismutase inhibitible ferricytochrome C reduction assay measures extracellular superoxide release. In this assay both monoclonal anti-PR3 and anti-MPO antibodies were capable of inducing high levels of superoxide release (Fig 3.1).

In the DHR123 assay, DHR123 is taken up by phagocytes and converted into the fluorescent dye rhodamine-123 in the presence of reactive oxygen species. As the positively charged rhodamine-123 accumulates specifically in the mitochondria [206], and any DHR123 converted to rhodamine-123 by extracellular reactive oxygen species (ROS) should be removed during the various wash steps, the DHR123 assay primarily measures intracellular ROS production. In this assay, the method of neutrophil isolation appears to be very important. This may be due to the sensitivity of this assay combined with the differing basal activation levels of neutrophils purified using different isolation methods [205]. Using a version of the Ficoll method of PBMC isolation, modified to purify the PMN cells, a reliable DHR123 assay for use in ANCA studies was established (Fig 3.5). In this assay both monoclonal and patient polyclonal ANCA antibodies induced high levels of ROS production as measured by rhodamine 123 generation.

Both assays have their advantages and disadvantages. Fewer patient samples gave reliable responses in the ferricytochrome C assay (Tables 3.6 and 3.7). As assays were done on different days, and with different donors, the two responses could not be formally correlated and this is simply an observation. Conversely, it does allow ROS production to be examined over time, which is not possible using the DHR123 assay. Furthermore, as extracellular ROS production may be involved in endothelial cell damage during disease progression, the ferricytochrome C reduction assay may

provide a more relevant readout than the DHR123 assay. Finally, both assays suffer from the variability of neutrophil responses between donors. However, despite their limitations both assays provide a useful measure of neutrophil activation in response to ANCA.

Monoclonal antibodies

Commercially available monoclonal anti-PR3 and anti-MPO antibodies were used to set up ANCA assays and to provide preliminary data. As will be discussed, there were two major drawbacks to this approach. However, given the limited availability of consistently activating patient antibodies (discussed in the following section), and the time required to recruit patients, these monoclonal antibodies provided a useful tool to allow preliminary studies of the ANCA induced neutrophil respiratory burst.

The first major drawback associated with the monoclonal antibodies used in this and the following chapter is that the Fc portions of the antibodies in question are mouse and not human. As discuss in chapter 1, data suggests that both the antigen binding region and the Fc portion of the ANCA molecule are important in ANCA signaling. Indeed, both FcγRIIa and FcγRIIIb have been shown to have a potential role in ANCA induced neutrophil activation *in vitro*. Consequently, it is important to note that while human FcγRIIa binds both human and mouse IgG_1, human FcγRIIIb only binds human IgG [207]. Therefore it must be taken into account that Fc receptor signaling resulting from mouse IgG_1 ligation likely differs from that induced by human IgG_1 ligation and, as a consequence, results gained by using monoclonal antibodies raised in mice may not accurately reflect what is happening with human antibodies.

The second major disadvantage associated with the monoclonal antibodies used in this, and the following chapter, is with regards the antigenic targets of the antibodies. Firstly, the exact antigenic targets of the antibodies are unknown, and secondly, as only one anti-PR3 and one anti-MPO antibody was used, the results only hold true for these particular antibodies and not for

anti-PR3 and anti-MPO antibodies in general. What is known about these monoclonal antibodies will be discussed below.

The monoclonal antibody to PR3 used, PR3G-2, was generated as part of a study designed to determine the antigenic targets of a number of established and newly developed monoclonal antibodies to PR3 [208]. It was produced from a hybridoma derived from mice immunised with a crude neutrophil granule extract. The antigen specificity of the antibody was established by four different methods including indirect immunofluorescence on ethanol-fixed neutrophils, Western blotting on a crude granule extract, flow cytometric analysis on isolated primed neutrophils, and antigen-specific direct and capture ELISA. In addition, and using a subclass antigen specific ELISA, the antibody isotype was confirmed to be IgG_1. Further to this, biosensor technology was used to show that eight established and four newly generated monoclonal antibodies against PR3, including PR3G-2, recognised four separate epitopes on PR3. The antibodies tested in this study and their epitopes, designated Epitope 1-4, are shown in Table 3.8 (second column). In this study PR3G-2 was found to belong to the first epitope group. In a subsequent study, aimed at identifying the specific conformational surface epitopes recognised by a variety of monoclonal anti-PR3 monoclonal antibodies, this was taken a step further with PR3G-2 being shown to recognise a region of PR3 said to be “South East” of the substrate binding pocket of the molecule [209]. The antibodies tested in this study and their epitopes, designated Epitope 1, 3, 4 and 5 (the existance of the previously described Epitope 2 was not confirmed in this study while a new epitope, Epitope 5, was identified) are shown in the third and fourth columns of Table 3.8. With regards patient derived PR3-ANCA, seven epitopes commonly bound by antibody from the sera of GPA patients have been identified [210]. Interestingly several of these epitopes were located in the catalytic region of the PR3 molecule. However, how these epitopes overlap with the antigenic target of PR3G-2 monoclonal antibody is unknown. Although there is no detailed comparison of this monoclonal antibody with patient derived anti-PR3 IgG, it should be noted that published data has shown that PR3G-2 is capable

of activating isolated neutrophils to undergo respiratory burst in a manner similar to patient derived PR3-ANCA [81].

With regards the anti-MPO monoclonal antibody, the exact MPO binding site has unfortunately never been elucidated. The clone (266.6K2) used was developed in the nineties by IQ Products in collaboration with the University of Groningen, The Netherlands, with antibodies against the whole human MPO molecule being raised in mice. The isotype of this monoclonal antibody is IgG_1. Although no information about the binding site is available, previous published data has shown that the antibody in question is capable of activating isolated neutrophils to undergo respiratory burst in a manner similar to patient derived MPO-ANCA [81].

IgG purification

Antibody purification can be split into two main groups: precipitation methods and chromatographic methods. Used together these two groups can be effective in providing highly pure antibody solutions. Traditionally ammonium sulphate has been used to precipitate immunoglobulins out of plasma and thus produce an antibody preparation that can be further purified, using Protein G columns, to give a reasonably pure IgG solutions (Fig 3.6). This method of IgG purification is quite long, taking up to four days, and involves multiple precipitation and dialysis steps that may lead to loss of antibody. To overcome these limitations precipitation of fibrin from plasma using sodium chloride followed by Protein G purification was examined. This method resulted in antibody solutions similar in a) purity (Fig 3.7 A), b) ability to bind their antigen (Table 3.1), and, c) yield (Table 3.2), to those produced using the ammonium sulphate method. Furthermore, and for indeterminate reasons, 2 of the 3 anti-MPO IgG solutions obtained using the sodium chloride precipitation method activated neutrophils to a greater extent than those obtained, in a side-by-side purification, using the ammonium sulphate precipitation method. In the case of 1 of these patient purified IgG samples the effect was striking. Although the sodium chloride precipitation method did not lead to greater antibody yields, it did halve the time required to produce a

Epitope Number	Monoclonal antibody clones binding to epitope [208]	Monoclonal antibody clones binding to epitope [209]	Approximate location of epitope [209]
1	**PR3G-2**, 6A6, 12.8, Hz1F12	**PR3G-2**, 6A6, 12.8	**"South East" of the substrate binding pocket of PR3**
2	PR3G-4, PR3G-6, WGM3	Unconfirmed as separate epitope in this study	Not available
3	4A5, WGM2, PR3G-3	4A5, WGM2, 2E1, 1B10, MCPR3-3	At the back of the PR3 molecule, adjacent to epitope 4
4	4A3, MCPR3-2	4A3, MCPR3-2, 2E1, WGM2	"North East" of the substrate binding pocket of PR3, adjacent to epitope 3
5	Not identified in this study	MCPR3–7, MCPR3–11, PR3G-4	At the binding site of PR3 to neutrophil membrane

Table 3.8 Monoclonal anti-PR3 antibodies and their antigenic targets as elucidated in two separate studies . Clone PR3G-2, the monoclonal antibody used in this thesis, is bolded.

pure IgG solution, while seemingly having no negative effects on the final antibody preparation. What is more, it may provide more effective antibody solutions, although overall the difference was not statistically significant in these experiments. Thus further work would be required to fully confirm, and possibly explain, if real, the reason for the difference in neutrophil respiratory burst activation potential of the same ANCA antibody purified using the two different precipitation methods. Interestingly, it is thought that neutrophil activation by ANCA occurs in an Fc dependent manner [71]. Therefore, and taking into account that there was no apparent precipitation method dependent difference seen in the antibodies ability to bind to its antigen (Table 3.1), it can be speculated that a change may occur in the Fc receptor portion of the antibody as a result of the purification processes in question.

Regardless of purification method, and as seen in Table 3.6 and 3.7, not all patient samples induce neutrophil respiratory burst and, of those that do, there is no discernible correlation between neutrophil activation potential and the severity of the patient's disease. While donor variability accounts for inconsistencies in the ability of a single ANCA antibody solution to activate neutrophils day to day, this does not explain the fact that, of the ANCA antibodies tested, only 14% of anti-PR3 IgG solutions and 46% of anti-MPO IgG solutions induced notable levels of superoxide release (>10 nmol $0_2^-/10^5$ neutrophils produced above control) as measured by the ferricytochrome C reduction assay. The DHR123 assay gave slightly better results with approximately 60% of both anti-PR3 and anti-MPO IgG solutions inducing notable levels of rhodamine 123 production (increase, over control IgG, in MFI of over 100). It should be noted that what constitutes notable reactive oxygen species production is arbitrary and is used only as a rough guide to individual ANCAs ability to activate neutrophils. Although few ANCA antibody solutions consistently failed to induce some ROS production relative to control IgG, a large proportion induced only very weak responses. There are many possible reasons for the varying ability of ANCA in activating neutrophils to undergo respiratory burst *in vitro*:

a) *In vitro* assays do not always accurately reflect what is happening *in vivo*. This is true for any cell-based assay; however, it may be a particular issue with regards neutrophil assays as these cells are thought to be particularly sensitive. It has been established that different methods of neutrophil isolatation lead to different expression of various neutrophil activation markers including CD11b, CD16 and CD32 [205]. Thus it is probable that isolated neutrophils behave differently to neutrophils *in vivo*. The development of a whole blood assay may help to overcome this issue and this will be further discussed in Chapter 4.

b) It is possible that the use of whole IgG solutions leads to a number of problems resulting in decreased ANCA induced responses. Firstly, the percentage of IgG that is anti-PR3 or anti-MPO specific in any given sample is unknown. Therefore, it is possible that patient purified ANCA samples that induce strong neutrophil responses do so simply because they are composed of a higher proportion of anti-PR3 or anti-MPO IgG. Secondly, irrelevant IgG in the solutions may bind to Fc receptors required for ANCA activation; thereby blocking them, and thus inhibiting ANCA induce responses. Both of these issues could be overcome by affinity purifying the anti-PR3 and anti-MPO antibodies. Finally, the IgG purified from patients may differ in regards to its subclass, epitope specificity and affinity; thereby leading to differences in its ability to interact with neutrophils. Of the four IgG subclasses found in humans, three are commonly associated with ANCA. These are IgG_1, IgG_3 and IgG_4. IgG_3 is considered the most pathogenic [211], with levels shown to correlate with disease activity [212]. Furthermore, IgG_3 has been suggested to be the predominate IgG subclass found in renal limited ANCA associated vasculitis [213] and in PR3-ANCA induced disease [214, 215]. However, other studies have suggested that it is IgG_1 and IgG_4 that predominate in PR3-ANCA associated vasculitis [216] and ANCA associated vasculitis as whole [213, 214]. Although patient studies have not provided a clear answer, *in vitro* studies, using monoclonal mouse/human IgG_1, IgG_3 and IgG_4 anti-PR3 antibodies, have shown that these different IgG subclasses affect neutrophils in difference ways [217-219]. Indeed, while anti-PR3 antibodies of all three subclass were able to induce neutrophil adhesion, superoxide release and

degranulation [217-219], only IgG_1 and IgG_3 could induce IL-8 release [217, 218]. Futhermore, IgG_1 was shown to induce higher levels of degranulation [217], while IgG_3 appeared to induce greater adhesion and IL-8 release [217, 219]. With regards epitope specificity, it is interesting to note that there are currently no studies detailing the exact pathogenic potential of the antigenic target of anti-PR3 or anti-MPO antibodies. However, current data does suggest that different patients with GPA have PR3-ANCA that recognised different antigenic targets on PR3 [210]. Importantly, it is likely that this also holds true for MPA, with different patients having MPO-ANCA that recognises different MPO epitopes. Indeed, it has been suggested that this may contribute to the differences in disease, with regards severity and affected organs, seen among patients [210].

Thus it is possible that although a number of the patient antibodies tested were unable to induce significant reactive oxygen species production, they may be capable of inducing other neutrophil response, dependent on the the predominant IgG subclass present and their exact antigenic target.

c) It is possible that the role of ANCA in disease pathogenesis is not related to its ability to activate the neutrophil respiratory burst. ANCA has also been shown to induce neutrophil degranulation [14, 16] as well as the release of proinflammatory cytokines [17] and it is possible that it is through these effects that ANCA mediates endothelial cell damage and thus disease. This is supported by a recent abstract [220] suggesting that respiratory burst deficient mice are not, as one would expect, protected from disease but in fact develop a more severe form of disease when compared with wildtype controls. If this is the case it may simply be coincidence that some ANCA are capable of inducing ROS production.

d) There is ample *in vivo* evidence to suggest that ANCA are pathogenic. For the majority of patients ANCA levels correlate with disease activity, with the risk of relapse for patients persistently negative for ANCA being extremely low [8]. Furthermore, there was a recent report that the transplacental transfer of MPO-ANCA from a mother to a 33-week gestational age neonate resulted in

neonatal pulmonary haemorrhage and renal involvement, thus suggesting that anti-MPO antibodies are indeed pathogenic [221]. Finally, anti-MPO antibodies in mice result in a focal necrotising cresentic glomerulonephritis [92, 95]. While the *in vivo* evidence for ANCA pathogenicity is compelling, it is possible that this is not the whole story. *In vitro*, the ANCA induced neutrophil respiratory burst response requires the neutrophils to be primed with TNFα, and in the case of the ferricytochrome C reduction assay, cytochalasin B. While the need for TNFα can be explained by the hypothesis that proinflammatory stimulus *in vivo* is necessary for the translocation of ANCA antigens to the surface of neutrophils [14, 16], cytochalasin B is a cell-permeable mycotoxin and therefore not native to humans. This, together with the fact that the majority of patient purified ANCA induces only weak neutrophil responses, suggests that there are other as yet unidentified factors involved in neutrophil activation *in vivo* and this may be an important avenue for future work. One such factor that has been suggested is the patient neutrophils themselves, with patients with active disease being shown to have higher neutrophil membrane ANCA antigen expression [16, 222, 223].

Despite these concerns, and taking into account the large body of published data showing that ANCA are pathogenic, the isolated ANCA capable of activating neutrophils to undergo respiratory burst were used to further study mechanisms of ANCA induced neutrophil activation. This will be discussed in the following chapter.

IgG purification: Endotoxin contamination

Endotoxin contamination is an important issue when purifying IgG solutions for use in both *in vitro* and *in vivo* experiments, as endotoxin has the potential to activate cells and thus lead to erroneous results. Therefore, throughout the purification process, every effort was made to ensure that all IgG preparations remained endotoxin free. Further to this, and where possible, only endotoxin free reagents, including endotoxin free 10 x PBS, tissue culture grade endotoxin free water and endotoxin free salts, were purchased, and every

effort was made to ensure that these remained endotoxin free, primarily through limited use and aseptic technique. Where large volumes of water were required, for example to make up 5 litres of PBS for dialysis, Millipore Ultrapure filtered water was used. In addition, all glassware was baked, over night, in a dry heat oven, and spinbar magnetic stirring fleas and dialysis membrane clips were stored in sodium hydroxide, in order to denature any contaminating endotoxin. Once purified, IgG preparations were immediately aliquoted and stored at -20ºC to prevent the possibly of endotoxin contamination in the time between purification and use.

Despite these efforts, and as endotoxin was not tested for, it is impossible to state that all IgG preparations were in fact endotoxin free. However, control IgG, treated in the same manner as patient derived IgG, failed, once the assays were properly established, to activate neutrophils above unstimulated controls. Thus control IgG acted not only as a control for irrelevant IgG induced activation of neutrophils, but also as a control for neutrophil activation induced by endotoxin present in IgG preparations.

4.1 Introduction

Neutrophil activation by ANCAs is dependent on their ability to bind to their target antigens. For this to occur ANCA must be internalised by the neutrophils, or as evidence suggests (reviewed in Chapter 1), PR3 and MPO must be present on the cell surface. It is also possible that both may occur. In addition to this, the ability of ANCA to activate neutrophils *in vitro* is dependent on neutrophil priming, a process through which exposure to a priming agent, frequently a cytokine, increases the response of neutrophils to an activating stimulus. In the case of ANCA activation, priming is primarily thought to induce antigen translocation to the surface of the neutrophils, thus making it available to interact with the ANCA. However, it may also activate various molecules, such as NADPH oxidase, thus preparing the way for ANCA induced neutrophil activation [224]. TNFα is the most commonly used priming agent in *in vitro* ANCA assays, however, IL1, IL6, IL18, fMLP and C5a have also been used to prime for an ANCA induced neutrophil response [14, 16, 88, 225].

Granulocyte colony stimulating factor (GCSF) is a cytokine produced by a variety of cells types including neutrophils, monocytes, platelets and endothelial cells. It is a potent haematopoietic factor that stimulates granulopoiesis, as well as mobilising mature neutrophils from the bone marrow storage pool into the circulation [226]. The GCSF receptor is formed by a homodimer of the CD114 protein [227], and, like the other members of the haematopoietin superfamily, lacks intrinsic tyrosine kinase activity. Thus, the GCSF receptor, upon the binding of its ligand, recruits cytoplasmic tyrosine kinases, including members of the Janus kinase and Src families, and through these activates intracellular pathways such as the Janus kinase/signal transducer and activator of transcription (JAK/STAT) pathway, the phosphatidylinositol-3 kinase pathway and the mitogen-activated protein kinase (MAPK) pathway [228]. The GCSF receptor is highly expressed by neutrophils, and is also found on monocytes, eosinophils, some T- and B-cells lines and several non-haematopoietic cells including endothelial, placental and trophoblastic cells [227]. Interestingly, GCSF receptor expression has

been shown to be decreased in neutrophils during infection [228]. Furthermore, patients with chronic myelogenous leukaemia have been shown to express relatively low levels of the GCSF receptor when compared to healthy controls [229].

There is evidence suggesting that, in addition to regulating neutrophil production, GCSF also induces functional changes [230]. Neutrophils treated with GCSF *in vitro* have been shown to have increased levels of adhesion molecules, enhanced chemotactic responses and greater phagocytic activity [231-235]. Furthermore, GCSF has been shown to increase neutrophil microbicidal activities [235] and antibody-mediated cellular cytotoxicity [236]. Finally, GCSF has been show to prime for a respiratory burst due to fMLP in some [231] but not all [237] studies. In addition to priming neutrophils *in vitro*, the administration of GCSF to both patients and healthy controls *in vivo* has been shown to enhance neutrophil phagocytosis, superoxide generation and bacterial killing [238]. Therefore, a possible role for GCSF in ANCA associated vasculitis was examined. The serum levels of GCSF in patients with active ANCA vasculitis were significantly higher that those of aged matched healthy controls (mean 38.9 vs 16.5 pg/ml, $p<0.001$) [239], while in an anti-MPO antibody transfer model of vasculitis, mice given GCSF had significantly greater disease compared to controls [239]. These data suggest that GCSF may play a role in exacerbating disease in ANCA vasculitis and in this chapter it is considered whether GCSF may prime neutrophils for a response to ANCA.

Phosphoinositol 3-kinases (PI3Ks) are members of a conserved family of intracellular lipid kinases that play a key role in many signal transduction pathways. There are three classes of PI3Ks defined, each of which has a distinct role [240]. It is the Class I PI3Ks that are thought to be key components of the neutrophil signal transduction network [241]. Class I PI3Ks are further divided into two subfamilies based on the receptors to which they are coupled. Class IA PI3Ks are primarily activated through protein tyrosine kinase receptors [242], however there is evidence that they may also be activated by G protein coupled receptors (GPCR) [243]. Class IB PI3Ks are

activated by GPCRs [244]. Both classes produce phosphatidylinositol 3,4-bisphosphate (PI[3,4]P_2) and phosphatidylinositol (3,4,5)-triphosphate (PIP_3), which are recognised by a variety of effector proteins and thus begin signalling cascades that culminate in various neutrophil responses including chemotaxis [83-85], phagocytosis [245], cells spreading [246] and the production of reactive oxygen species [247]. Class IA PI3Ks are composed of a homologous p85 family catalytic subunit and a p110α (PI3Kα), p110β (PI3Kβ) or p110δ (PI3Kδ) regulatory subunit [248], while class IB PI3Ks are heterodimers of a p110γ (PI3Kγ) catalytic subunit and a p101 or p84 regulatory subunit [249]. The specific role of PI3Kα and PI3Kβ in neutrophils is just beginning to be elucidated. A recent study has shown that PI3Kα inhibition significantly reduced reactive oxygen species production by neutrophils in response to both fMLP and TNFα [250]. Furthermore, a reduction in PI3Kα RNA and protein expression in healthy humans placed on a fish oil and borage oil supplemented diet, correlated with decreased ex vivo leukotriene B_4 and IL1β production by neutrophils, thus suggesting a potential role for PI3Kα in proinflammatory cytokine production [251]. With regards PI3Kβ, a recent report indicates that in mouse neutrophils, PI3Kβ and PI3Kδ are necessary for neutrophil spreading and oxidase activation in response to *Aspergillus fumigatus* hyphae [252]. In addition, PI3Kβ has been shown to be essential for the FcγR-dependent activation of mouse neutrophils by immune complexes [253]. Furthermore, PI3Kβ-deficient mice were protected in an FcγR-dependent model of autoantibody-induced skin blistering and partially protected in an FcγR-dependent model of inflammatory arthritis [253]. The role of PI3Kδ in neutrophils is better understood with this isoform being shown to have roles in the generation of reactive oxygen species [250, 254, 255], the release of elastase from neutrophil granules [255] and in neutrophil chemotaxis [256-258]. Similarly, the role of PI3Kγ in neutrophil chemotaxis [83-85, 259, 260], cells spreading [246] and the production of reactive oxygen species [247, 254, 261, 262] has been well established.

In vitro data using PI3K inhibitors [75, 76], together with data showing the importance of signalling molecules downstream of the PI3Ks [75, 76, 79],

have identified them as a possible key signalling molecules in ANCA associated vasculitis pathogenesis. The majority of research to date has been focused on the role of PI3Kγ. However, given the emerging roles of Class IA PI3Ks in neutrophil activation, a potential role for PI3Kβ/δ in ANCA induced neutrophil activation was examined in this chapter.

In this chapter the expression of both PR3 and MPO on the surface of whole blood neutrophils and monocytes was examined. The development of a whole blood ANCA induced respiratory burst assay was briefly considered. A possible role for GCSF in priming neutrophils for an ANCA induced respiratory burst was demonstrated and, finally, PI3Kβ/δ was implicated in ANCA induced neutrophil activation.

4.2 Aims

- To examine ANCA antigen expression on the surface of whole blood neutrophils and monocytes
- To determine if GCSF plays a role in priming neutrophils for ANCA induced respiratory burst
- To determine if PI3Kβ/δ may play a role in the ANCA induced respiratory burst

4.3 Methods

All blood and plasma samples, from both patients or healthy controls, were taken with informed consent and ethical approval (NRES committee London—London Bridge 09/H084/72)

4.3.1 Flow cytometry

Flow cytometry was performed as described in Section 2.2.1 with some modifications. Briefly, human whole blood was not blocked as the presence of native antibody in the plasma made this step unnecessary. Whole blood was

stained immediately or incubated at 37°C in the presence of 2ng/ml TNFα or incubated at 37°C without further priming. Whole blood incubated at 37°C was cooled on ice for 5-10 minutes before being stained at room temperature. Red cells were lysed using BD FacsLyse as previously described.
The antibodies used are shown in Table 4.1. Anti-PR3 FITC and the FITC isotype control were used at 2μg/ml. Anti-MPO APC and the APC isotype control where used at 4μg/ml. The anti-CD14 antibodies were both used at the recommended concentration (20μl/100μl of blood).

Target	Isotype	Clone	Fluorophore	Supplier	Dilution
PR3	Mouse IgG1, κ	PR3G-2	FITC	Hycult	1:50
Control	Mouse IgG1, κ	MOPC-21	FITC	Biolegend	1:250
MPO	Mouse IgG1, κ	MPO-7	APC	Dako	1:12.5
Control	Mouse IgG1, κ	MOPC-21	APC	Biolegend	1:50
CD14	Mouse IgG2a, κ	M5E2	PE	BD	1:6
CD14	Mouse IgG2a, κ	M5E2	APC	BD	1:6

Table 4.1 Anti-human antibodies used for flow cytometry. All antibodies were obtained from commercial sources.

4.3.2 Superoxide dismutase inhibitable ferricytochrome C reduction assay

Neutrophils were isolated from either sodium citrate or lithium heparin anti-coagulated blood using Polymorphprep or Ficoll as described in Section 2.2.6.1 and 2.2.6.2, respectively. The assay was performed as described in Section 2.2.7.1. For the PI3Kβ/δ inhibition experiments cells were primed with TNFα for 15 minutes at 37°C before being pre-incubated with various concentrations of TGX-221 (Cayman Chemicals, Michigan, USA) for 5 minutes. The appropriate concentration of inhibitor was added, diluted in HBH, together with the appropriate stimuli to the wells of the 96 well plates before the addition of the cells. As the TGX-221 was dissolved in ethanol, an

equal concentration of ethanol was added both to the cells and to the wells that did not have inhibitor, to serve as a vehicle control.

4.3.3 DHR123 assay

Neutrophils were isolated from heparinised blood using Ficoll as described in Section 2.2.6.2, with assays being performed as described in Section 2.2.7.2. For the GCSF priming assays the rhodamine 123 production, and by extension the reactive oxygen species production, was determined as follows: The median fluorescent intensity (MFI) of the unprimed/GCSF primed control sample was subtracted from the MFI of the unprimed/GCSF primed ANCA stimulated sample. This was to compensate for any non-specific rhodamine-123 production. This number was then divided by the MFI of the unprimed unstimulated cells. As the flow cytometer settings were not kept constant between donors, this was necessary to standardise the results and thus allow comparison.

For whole blood assays, heparinised blood was taken and assays were carried out as follows: Whole blood was loaded with 70μg/ml DHR123 together with 5μg/ml cytochalasin B and 2 mM sodium azide. This was incubated in the dark for 10 minutes at 37˚C. Blood was incubated with or without 2ng/ml TNFα for 30 minutes at 37˚C with gentle mixing at 5 minute intervals. 100μl of blood was added to each FACS tube and stimulated with 5μg/ml monoclonal anti-PR3 or anti-MPO IgG for 1 hour at 37˚C. Control IgG was used as a negative control and fMLP as a positive control for cell activation. The reaction was stopped by incubation on ice for 5-10 minutes. The blood was then stained with CD14 APC at 20μl/100μl of blood to allow monocytes to be identified. Red cells were lysed using BD FACSLyse as previously described. The remaining cells were finally resuspended in a small volume of PBS (~300μl) and kept on ice and in the dark until measurement.

4.3.4 Determining the effect of GCSF on mouse neutrophil activation

Mice were bled from the saphenous vein four days after injection with 30μg human pegylated GCSF (Neulasta®, from Amgen, Cambridge, UK) or PBS. They were then injected intraperitoneally with control PBS or with 10μg of LPS from *E. coli*, Serotype R515 (Enzo Life Sciences), and bled again from the saphenous vein 2 hours later. Flow cytometry was performed as described in Section 4.3.1 and using the antibodies shown in Table 4.2.

Target	Isotype	Clone	Fluorophore	Supplier	Dilution
Ly6G	Rat (Lew) IgG2b, κ	IA8	Alexafluor700	BD	1:200
CD11b	Rat (Lew) IgG2b, κ	M1/70	FITC	BD	1:100
CD11c	Hamster IgG	N418	PE	BD	1:62.5
CD62L	Rat IgG2a, κ	MEL-14	Pacific Blue	Biolegend	1:80

Table 4.2 Anti-mouse antibodies used for flow cytometry. All antibodies were obtained from commercial sources.

4.3.5 Statistics

Statistics were performed using Graphpad Prism software (Graphpad Software Inc, La Jolla, CA, USA). Data was analysed using paired t tests or one-way ANOVAs as indicated.

4.3.5 Acknowledgements

I would like to thank Dr. Reena Popat for her assistance in gathering the data, she kindly performed the experiments on 4 of the donors, presented in Figure 4.10 and Figure 4.11.

4.4 Results: ANCA antigens are expressed on the surface of whole blood neutrophils and monocytes

4.4.1 PR3 and MPO are present on the surface of whole blood neutrophils and monocytes

Several studies have demonstrated, using flow cytometry, that PR3 is expressed on the surface of isolated neutrophils that have been primed with TNFα, and this was confirmed (Fig 4.1. A). Furthermore, the typical bimodal pattern of PR3 expression was present. Similarly, MPO has been shown to be expressed on the surface of TNFα primed neutrophils that have been isolated from whole blood, and this was also confirmed (Fig 4.1. B) As discussed in Chapter 3, however, neutrophils are thought to be particularly sensitive cells and it has been shown that different methods of neutrophil isolatation lead to different expression of various neutrophil activation markers. It is therefore possible that the isolation of neutrophils also changes their expression of membrane bound PR3 and MPO. In order to test this, blood was taken from a number of healthy volunteers and either stained immediately or after incubation at 37°C with or without 2ng/ml TNFα. As whole blood was used it was possible to examine PR3 and MPO expression on the surface of both neutrophils (Fig 4.2 and 4.3) and monocytes (Fig 4.4 and 4.5). Neutrophils were identified based on their forward and side scatter profile, while monocytes were identified as CD14 expressing cells. Whole blood, resting neutrophils, in this case defined as cells that had been stained as soon as the blood was taken, expressed PR3 on their membranes (Fig 4.2. B). Incubation at 37°C marginally increased the surface expression of PR3 (Fig 4.2. C), while priming with TNFα appeared to downregulate membrane PR3 expression (Fig 4.2. D), both when compared to neutrophils incubated at 37°C (*$p<0.05$), and interestingly, with resting neutrophils (Fig 4.2 A). With regards to the whole blood monocytes, PR3 was expressed on the membranes of both resting (Fig 4.4. B), and primed, cells (Fig 4.4. C, D). Notably, priming with TNFα, and not incubation at 37°C alone, appeared to increase the levels of membrane bound PR3, although this did not quite significance ($p<0.0629$

using a paired t test, Fig 4.4. A). MPO was expressed on the surface of whole blood, resting neutrophils (Fig 4.3. B), and to a similar level, on neutrophils that had been incubated at 37°C for 30 minutes (Fig 4.3 C). Interestingly, the expression level of membrane MPO was significantly decreased following incubation with TNFα ($p<0.01$, Fig 4.3 A, B). Whole blood monocytes in contrast to neutrophils whether resting, incubated, or primed with TNFα, expressed only very low levels of membrane MPO (Fig 4.5 A-D).

4.4.2. ANCA does not induce whole blood neutrophils to undergo respiratory burst

Having identified PR3 and MPO on surface of whole blood neutrophils and monocytes, the next step was to determine if an ANCA induced whole blood respiratory burst assay could be established. Blood was taken from healthy volunteers and a whole blood DHR123 flow cytometry based assay was carried out either without (Fig 4.6 A, Fig 4.7 A) or with (Fig 4.6 B, Fig 4.7 B) TNFα priming as described in Section 4.3.3. Although both whole blood neutrophils (identified based on their forward and side scatter) (Fig 4.6) and monocytes (defined as CD14 positive cells) (Fig 4.7) underwent a respiratory burst in response to fMLP, neither cell type responded to anti-PR3 or anti-MPO ANCA.

4.5. Results: GCSF primes neutrophils for an anti-MPO IgG but not an anti-PR3 IgG induced respiratory burst

4.5.1 Superoxide production by ANCA stimulated neutrophils is not increased by GCSF priming

Neutrophils were isolated from sodium citrate anti-coagulated blood using Polymorphprep and the effect of priming with TNFα, GCSF or both together on ANCA induced superoxide release was examined using the ferricytochrome C reduction assay. Neutrophils were incubated at 37°C for 15 minutes with or without 2ng/ml TNFα, 50ng/ml GCSF or both together before stimulation with either a commercial monoclonal anti-PR3 (Fig 4.8) or

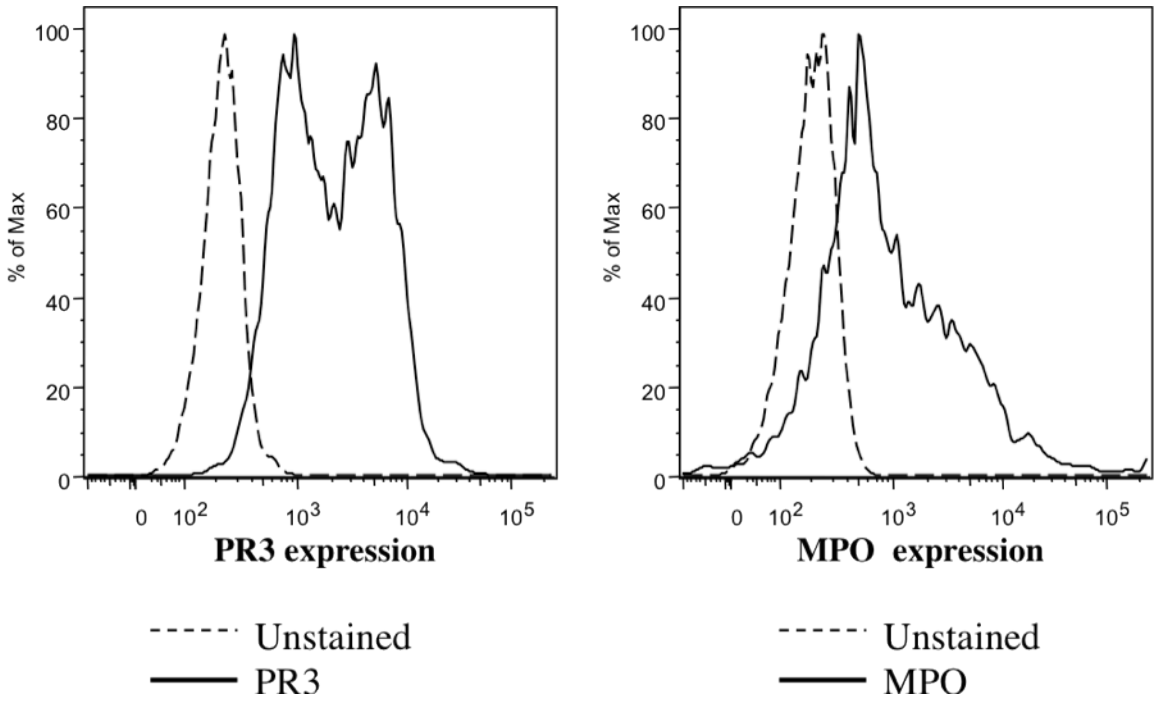

Figure 4.1 PR3 and MPO expression on the surface of isolated neutrophils. Neutrophils were isolated from EDTA anti-coagulated whole blood, taken from a healthy volunteer, using Polymorphprep. (n=1) They were primed with 2ng/ml TNFα for 30 minutes at 37°C before staining.

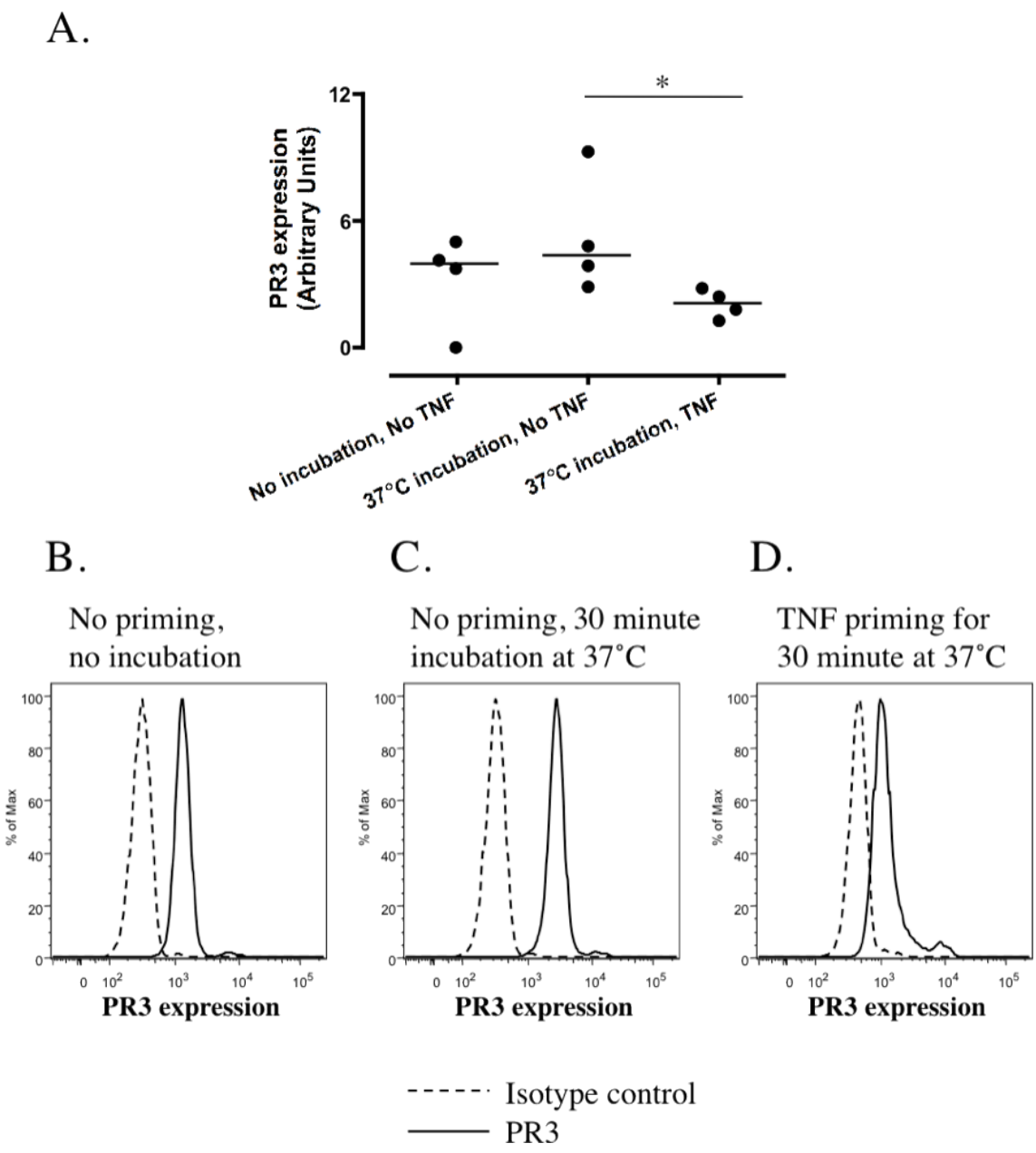

Figure 4.2 PR3 expression on the surface of whole blood neutrophils. EDTA anti-coagulated whole blood from heathly volunteers (n=4) was either stained immediately or incubated at 37˚C for 30 minutes with or without 2ng/ml TNFα. Red cells were lysed using BDFacsLyse. (A) Shows the results from 4 separate experiments with the median of each group shown by the horizontal line, while (B-D) show representative graphs. Arbitrary units were obtained from the median fluorescence intensities (MFI) of the PR3 positive population minus the MFI of the negative isotype control population. * $p<0.05$. Data were logarithmically transformed and analysed using a paired t test.

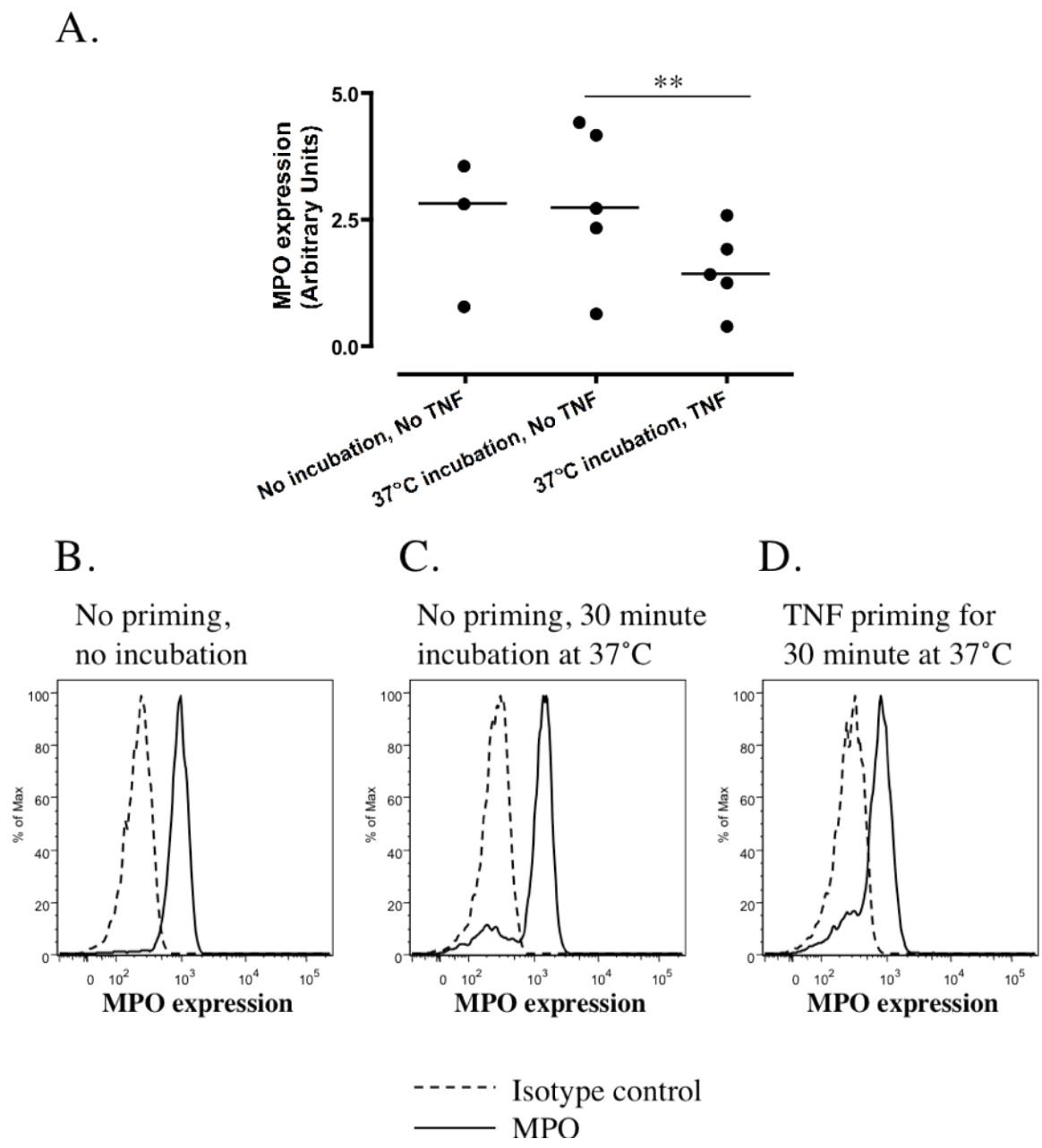

Figure 4.3 MPO expression on the surface of whole blood neutrophils. EDTA anti-coagulated whole blood from heathly volunteers (n=5) was either stained immediately or incubated at 37˚C for 30 minutes with or without 2ng/ml TNFα. Red cells were lysed using BDFacsLyse. (A) Shows the results from between 3 and 5 separate experiments with the median of each group shown by the horizontal line, while (B-D) show representative graphs. Arbitrary units were obtained from the median fluorescence intensities (MFI) of the MPO positive population minus the MFI of the negative isotype control population.
** p< 0.01. Data was analysed using a paired t test.

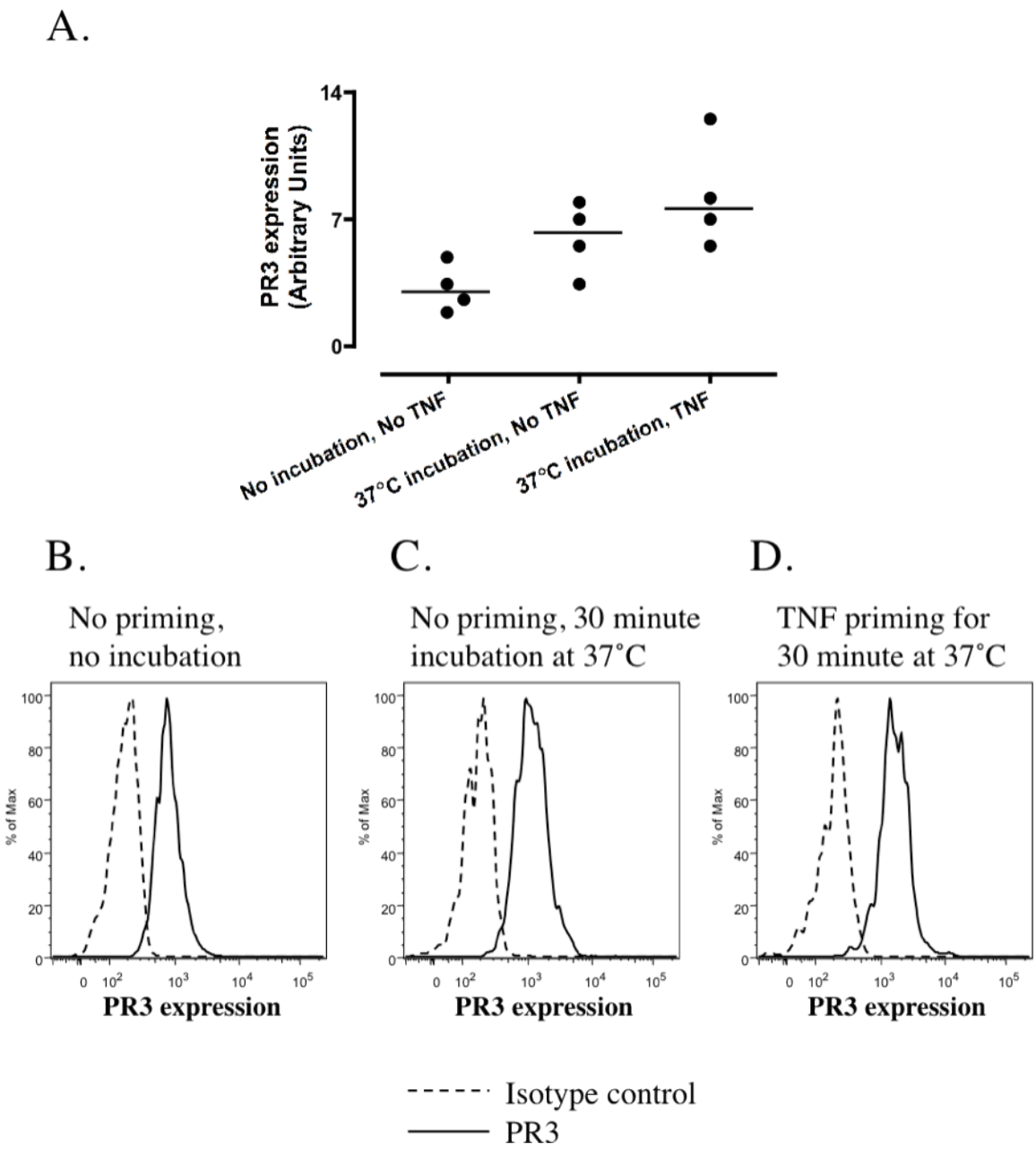

Figure 4.4 PR3 expression on the surface of whole blood monocytes. EDTA anti-coagulated whole blood from heathly volunteers (n=4) was either stained immediately or incubated at 37˚C for 30 minutes with or without 2ng/ml TNFα. Red cells were lysed using BDFacsLyse. (A) Shows the results from 4 separate experiments with the median of each group shown by the horizontal line, while (B-D) show representative graphs. Arbitrary units were obtained from the median fluorescence intensities (MFI) of the PR3 positive population minus the MFI of the negative isotype control population.
Data was analysed using a paired t test.

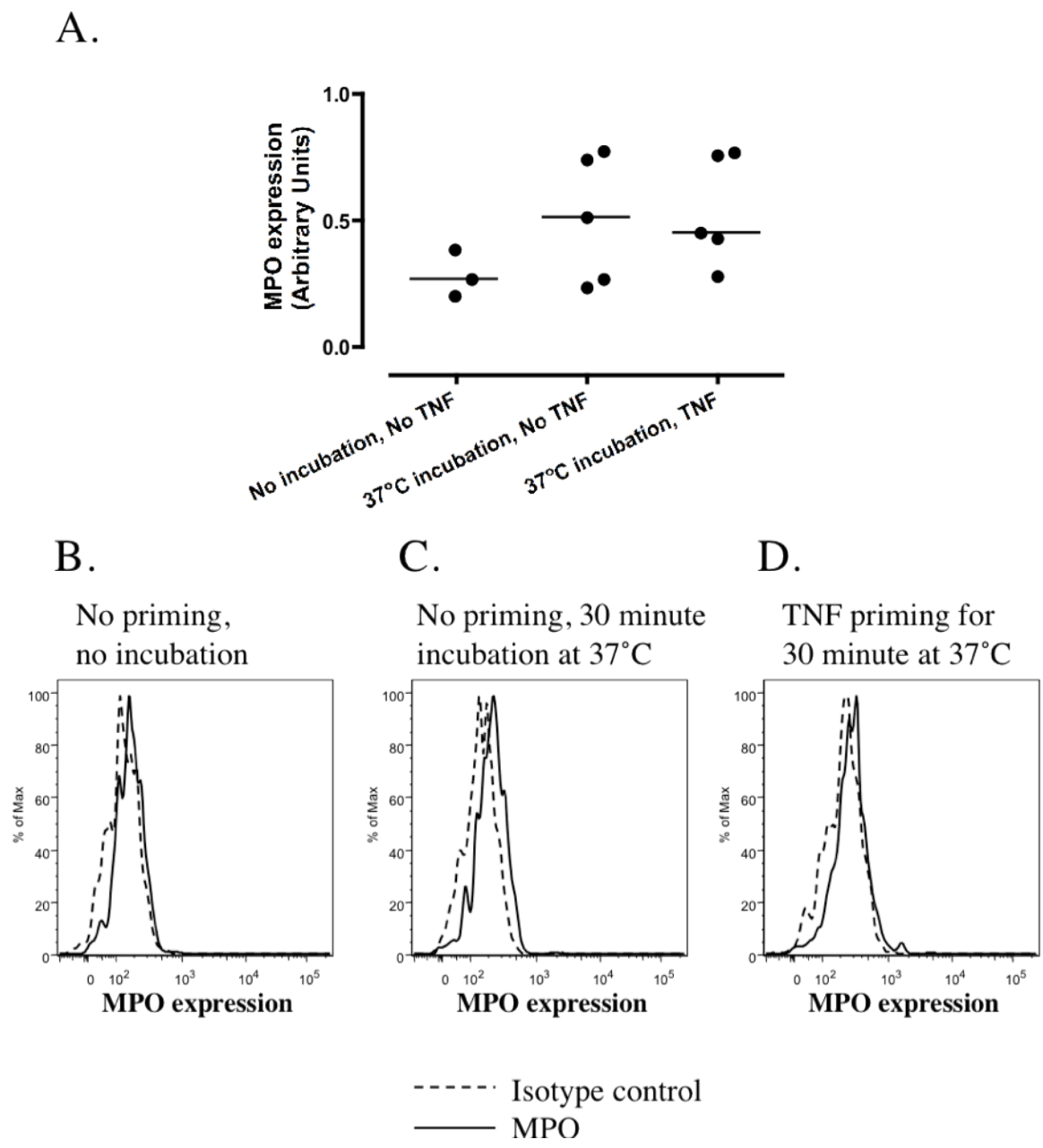

Figure 4.5 MPO expression on the surface of whole blood monocytes. . EDTA anti-coagulated whole blood from heathly volunteers (n=5) was either stained immediately or incubated at 37˚C for 30 minutes with or without 2ng/ml TNFα. Red cells were lysed using BDFacsLyse. (A) Shows the results from between 3 and 5 separate experiments with the median of each group shown by the horizontal line, while (B-D) show representative graphs. Arbitrary units were obtained from the median fluorescence intensities (MFI) of the MPO positive population minus the MFI of the negative isotype control population. Data were analysed using a paired t test.

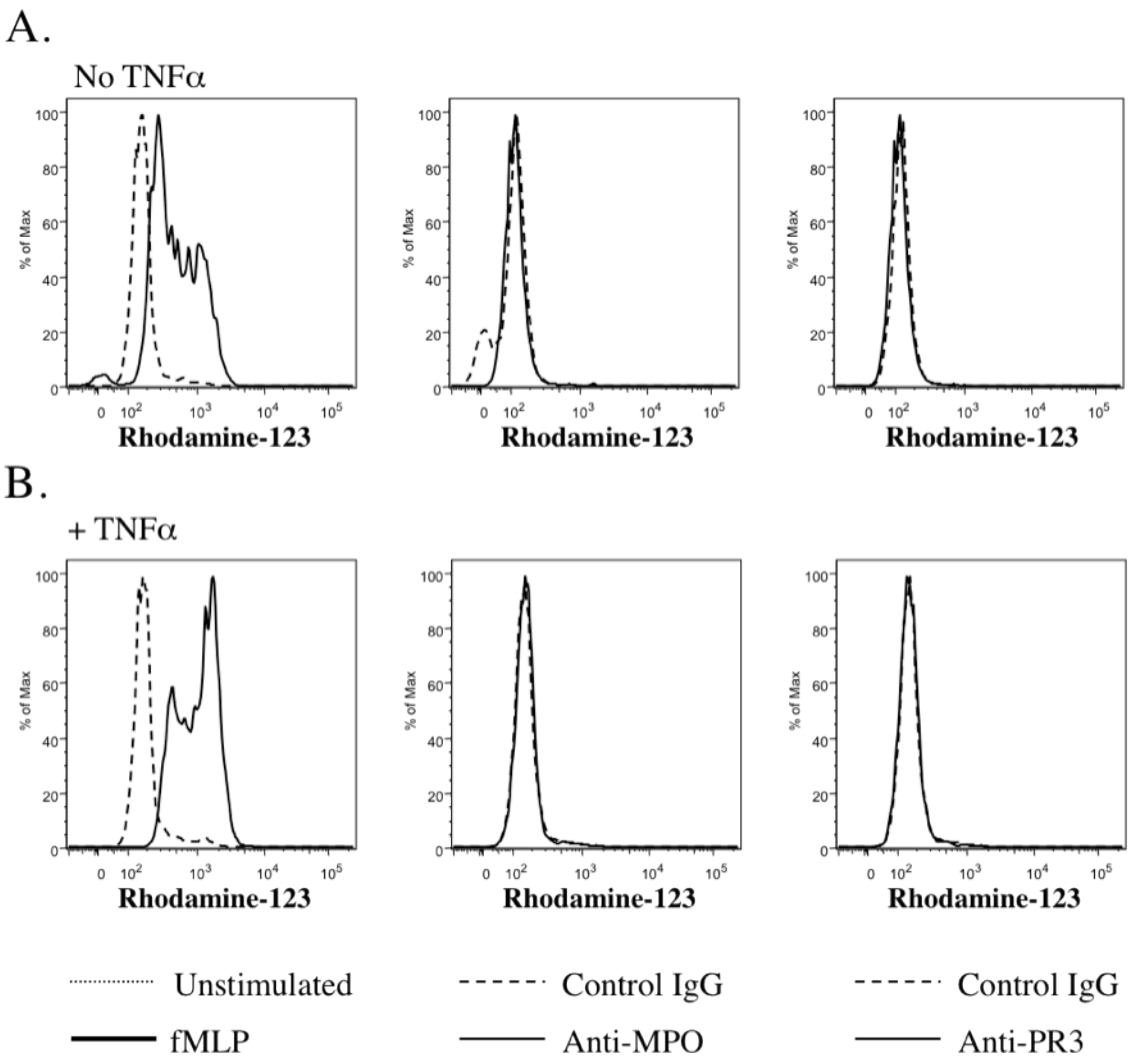

Figure 4.6 Whole blood neutrophils are capable of undergoing respiratory burst in response to fMLP but not ANCA as measured by the conversion of DHR123 into fluorescent rhodamine-123. Heparinised whole blood was primed at 37˚C (A) without or (B) with 2ng/ml TNFα before stimulation with either fMLP or 5μg/ml human monoclonal anti-PR3 (n=1) or anti-MPO IgG (n=1). Red cells were lysed after stimulation using BDFacsLyse.

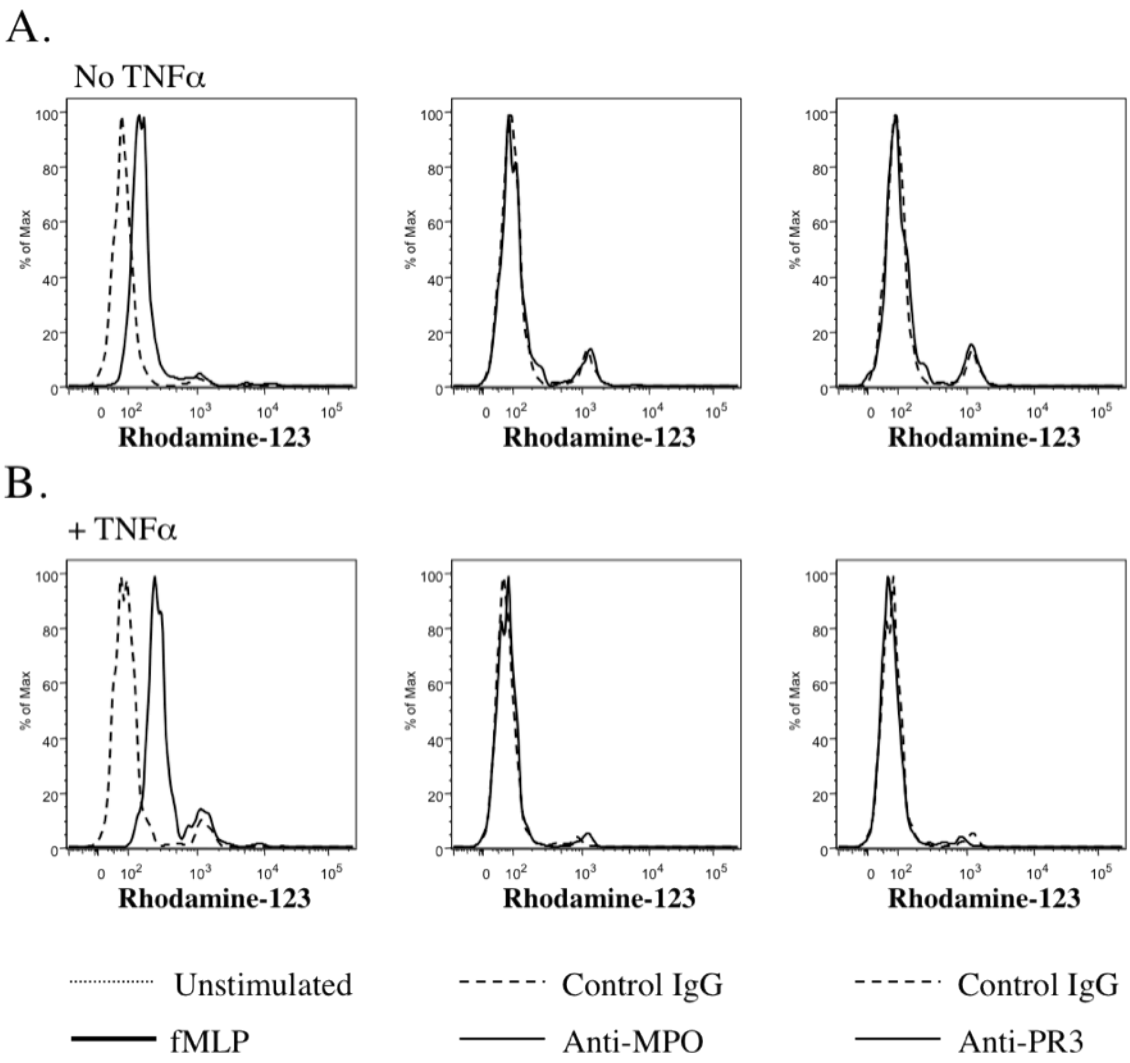

Figure 4.7 Whole blood monocytes are capable of undergoing respiratory burst in response to fMLP but not ANCA as measured by the conversion of DHR123 into fluorescent rhodamine-123. Heparinised whole blood was primed at 37˚C (A) without or (B) with 2ng/ml TNFα before stimulation with either fMLP or 5μg/ml monoclonal human anti-PR3 (n=1) or anti-MPO IgG (n=1). Red cells were lysed after stimulation using BDFacsLyse.

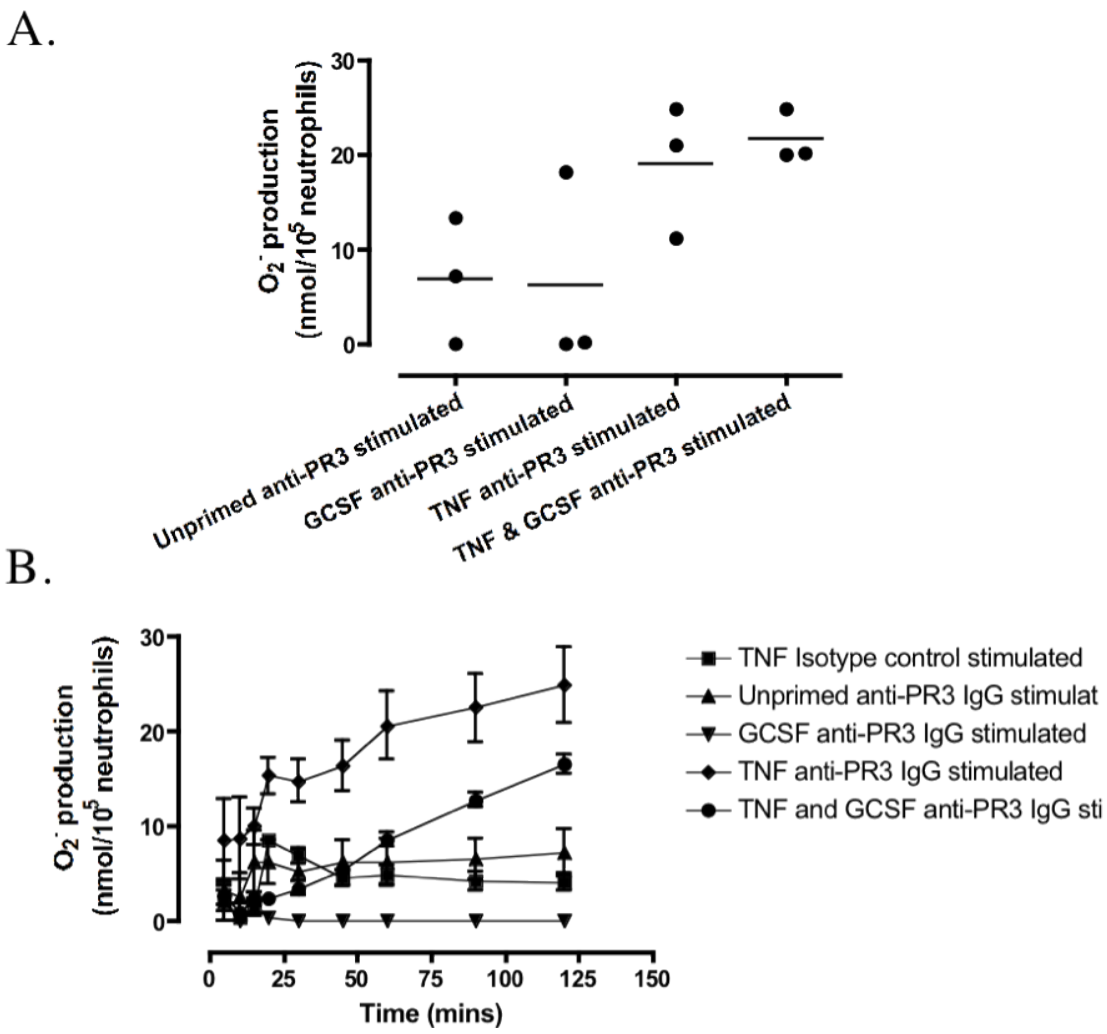

Figure 4.8 The role of GCSF and TNF in the priming of the ANCA induced superoxide release as measured by the superoxide dismutase inhibitable reduction of ferricytochrome C. Unprimed, TNFα primed, GCSF primed or TNFα and GCSF primed neutrophils isolated from sodium citrate anti-coagulated blood using Polymorphprep were stimulated with 5μg/ml of monoclonal human anti-PR3 IgG (n=1) or a relevant control. (A) Shows the results from 3 separate experiments with the median of each group shown by the horizontal line. Arbitrary units were obtained by subtracting the amount of O_2^- produced following the stimulation of neutrophils with the isotype control from the amount of O_2^- produced following stimulation of neutrophils with the anti-PR3 antibodies. (B) Shows a representative graph. Data was analysed using a repeated measures ANOVA with a Dunnett's post test and are presented as mean values ± SEM of triplicate wells.

anti-MPO (Fig 4.9) antibody. An IgG isotype control was included to discount non-specific superoxide production. TNFα primed neutrophils consistently produced greater amounts of superoxide in response to anti-PR3 IgG than either unprimed or GCSF primed cells, although this did not reach statistical significance (Fig 4.8. A). There was no synergistic effect of TNFα and GCSF observed. In fact the neutrophils of 2 of the 3 donors produced slightly less superoxide when compared to those primed with TNFα alone, although the difference was minimal. Similarly, anti-MPO IgG stimulated neutrophils that had been primed with TNFα induced significantly more superoxide than those that were unprimed ($p<0.01$) or primed with GCSF ($p<0.05$). Again, there was no synergistic effect of TNFα and GCSF observed (Fig 4.9. A). Interestingly, the GCSF primed neutrophils of 2 out of 3 donors produced more superoxide than the unprimed neutrophils when stimulated with anti-MPO IgG.

4.5.2 GCSF primes neutrophils for an anti-MPO IgG but not an anti-PR3 IgG induced respiratory burst

For the DHR123 assay neutrophils were isolated from heparinised whole blood using the Ficoll method described in Section 2.2.6.2. Isolated neutrophils were incubated at 37°C for 15 minutes with or without 50ng/ml GCSF, or 2ng/ml TNFα, before stimulation with either a commercial monoclonal anti-PR3 (Fig 4.10) or anti-MPO (Fig 4.11) antibody. Of the 8 donors assessed only 3 showed an increase in anti-PR3 IgG induced rhodamine 123 production as a result of GCSF priming, while all showed an increase in response to TNFα (Fig 4.10). In contrast, 5 out of 8 donors assessed had a noticeable increase in anti-MPO IgG induced rhodamine-123 production as a result of GCSF priming. Overall there was a significant increase in intracellular reactive oxygen species production as a result of priming the neutrophils with GCSF before stimulation with anti-MPO IgG ($p<0.05$, Fig 4.11). Once again neutrophils from all donors showed elevated rhodamine 123 production in response to TNFα. The data for all 8 donors is shown in Figure 4.10 A, and a representative histogram is shown in Figure 4.11 B. To determine whether the effect of GCSF priming on the ANCA

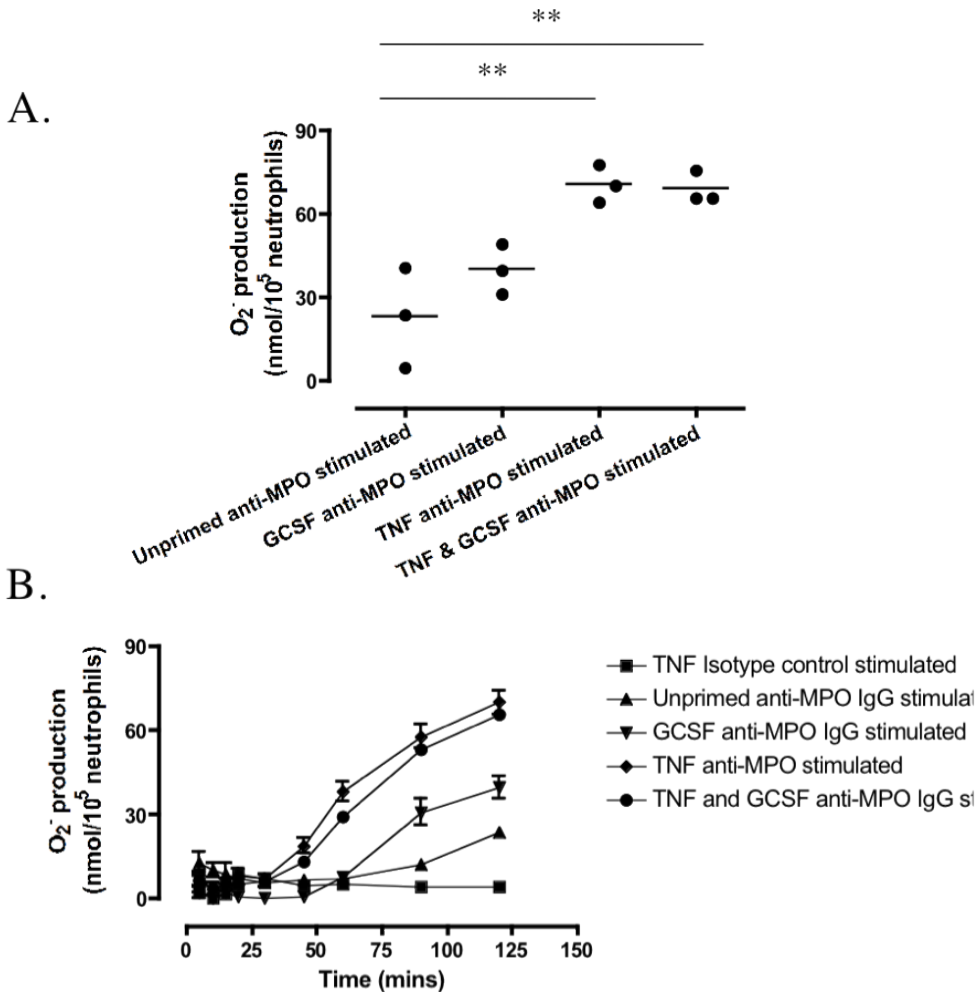

Figure 4.9 The role of GCSF and TNF in the priming of the ANCA induced superoxide release as measured by the superoxide dismutase inhibitable reduction of ferricytochrome C. Unprimed, TNFα primed, GCSF primed or TNFα and GCSF primed neutrophils isolated from sodium citrate anti-coagulated blood using Polymorphprep were stimulated with 10μg/ml of monoclonal human anti-MPO IgG (n=1) or a relevant control. (A) Shows the results from 3 separate experiments with the median of each group shown by the horizontal line. Arbitrary units were obtained by subtracting the amount of O_2^- produced following the stimulation of neutrophils with the isotype control from the amount of O_2^- produced following stimulation of neutrophils with the anti-PR3 antibodies. (B) Shows a representative graph. **p<0.01. Data was analysed using a repeated measures ANOVA with a Dunnett's post test and are presented as mean values ± SEM of triplicate wells.

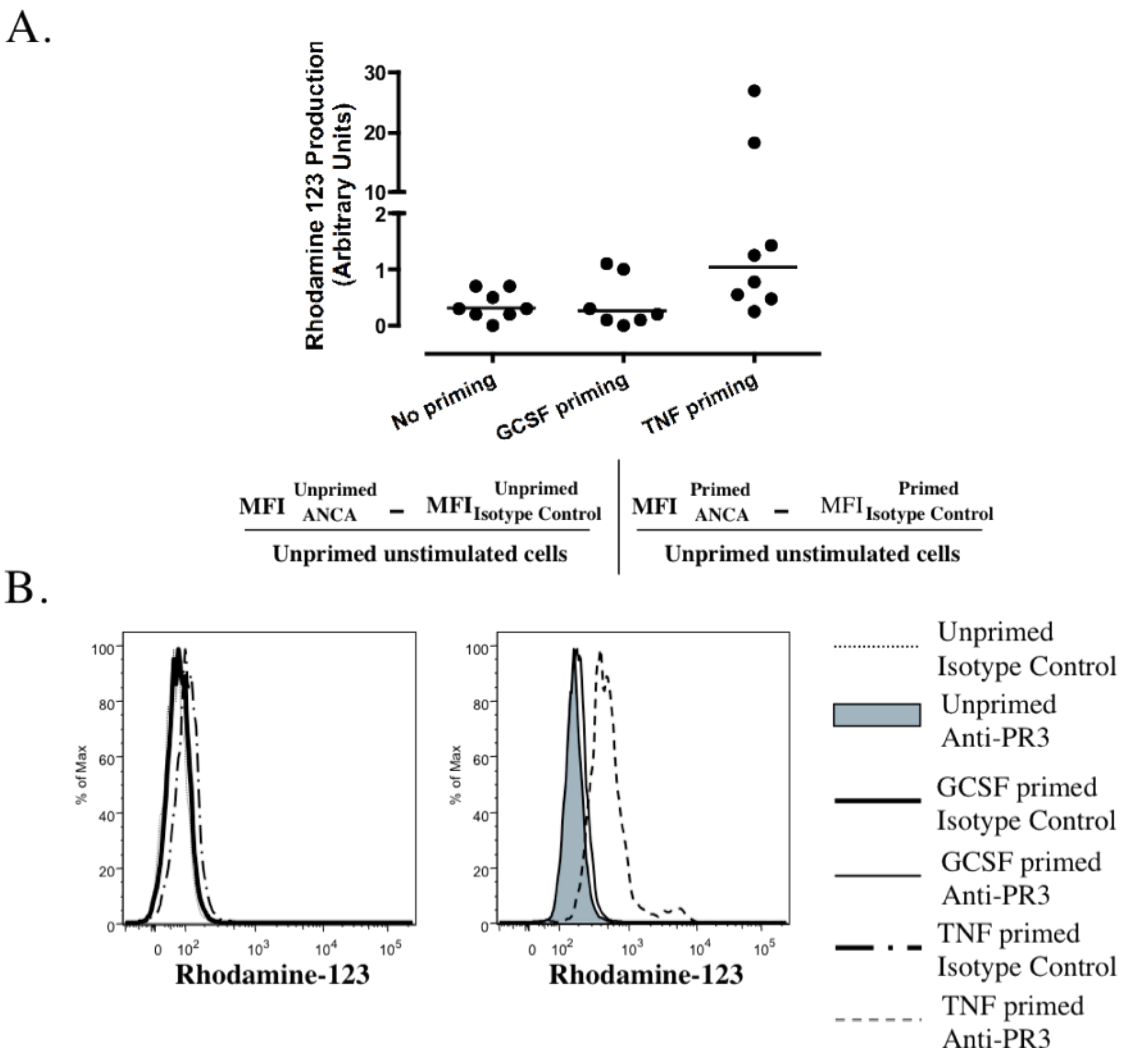

Figure 4.10 The role of GCSF and TNF in the priming of the ANCA induced respiratory burst as measured by the conversion of DHR123 into fluorescent rhodamine-123. Unprimed, GCSF primed and TNFα primed neutrophils isolated from heparinised blood using Ficoll and red cell lysis were stimulated with 5μg/ml of monoclonal human anti-PR3 IgG (n=1) or a relevant control. (A) Shows the results from 8 separate experiments with the median of each group shown by the horizontal line, while (B) shows a representative graph. Arbitrary units were obtained from the median fluorescence intensities (MFI) as indicated in the figure, with data normalised for the MFI of unstained unstimulated cells in each experiment. Data was analysed using a paired t test.

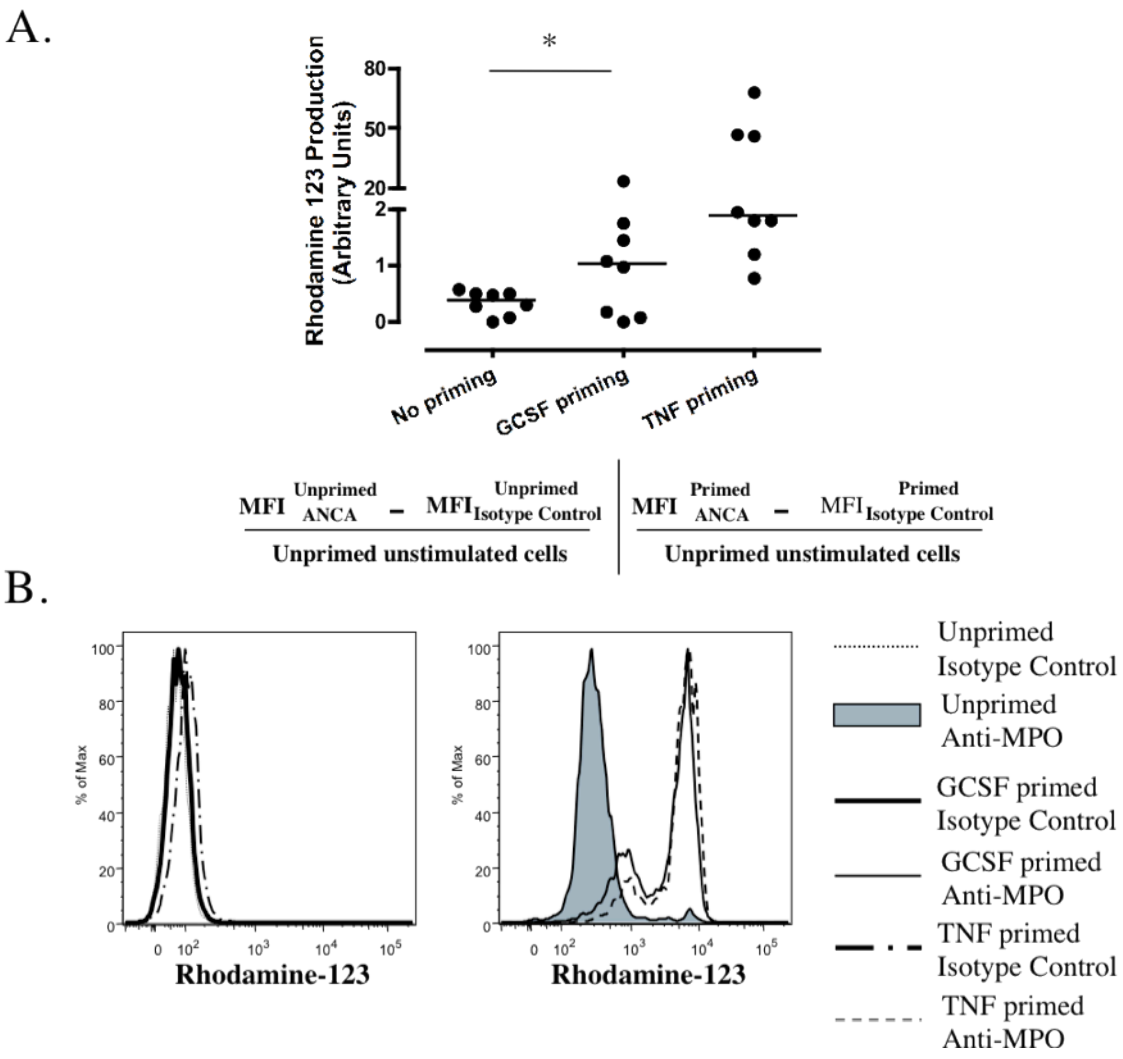

Figure 4.11 The role of GCSF and TNF in the priming of the ANCA induced respiratory burst as measured by the conversion of DHR123 into fluorescent rhodamine-123. Unprimed, GCSF primed and TNFα primed neutrophils isolated from heparinised blood using Ficoll and red cell lysis were stimulated with 1.25 μg/ml of monoclonal human anti-MPO IgG or a relevant control. (A) Shows the results from 8 separate experiments with the median of each group shown by the horizontal line, while (B) shows a representative graph. Arbitrary units were obtained from the median fluorescence intensities (MFI) as indicated in the figure, with data normalised for the MFI of unstained unstimulated cells in each experiment. *$p<0.05$. Data was analysed using a paired t test.

induced response was limited to the specific monoclonal antibodies used, IgG purified from anti-PR3 and anti-MPO ANCA positive patients was also tested. Figure 4.12 shows the result of 8 separate ANCAs, 4 purified from anti-PR3 ANCA positive patients and 4 purified from anti-MPO ANCA positive patients. Data is taken from 2 donors. Patient ANCA induced greater rhodamine-123 production in neutrophils primed either with TNFα or the combination of TNFα and GCSF, although there was no synergistic effect observed. In Figures 4.12 A and C, which show data from the same donor, none of the ANCA used induced a greater response when added to GCSF primed neutrophils as compared to unprimed neutrophils. Conversely, using a different donor, all ANCA induced greater rhodamine 123 production, although in most cases the difference was very small and no statistical significance was reached. There was no difference seen between anti-PR3 antibodies and anti-MPO antibodies in these experiments.

4.5.3 GCSF priming does not alter the surface expression of PR3 or MPO

Neutrophils were isolated from heparinised whole blood using the Ficoll method described in Section 2.2.6.2. Isolated neutrophils were then prepared in the same manner as those used in the respiratory burst assays examining GCSF priming; that is they were incubated at 37°C for 15 minutes with or without 50ng/ml GCSF, or 2ng/ml TNFα, before staining with commercial anti-PR3 and anti-MPO antibodies designed for flow cytometry. The neutrophil donors in for this experiment were chosen based on their strong response to GCSF priming in the experiments described in the previous section.
GCSF priming had no effect on the surface expression of either PR3 or MPO under these conditions (Fig 4.13 A-B). In contrast, and for 3 out of 3 donors, TNFα priming led to the upregulation of both enzymes on the surface of the isolated neutrophils (Fig 4.13 B). Of note, once again, PR3 displayed a bimodal pattern of expression (Fig 4.13 A).

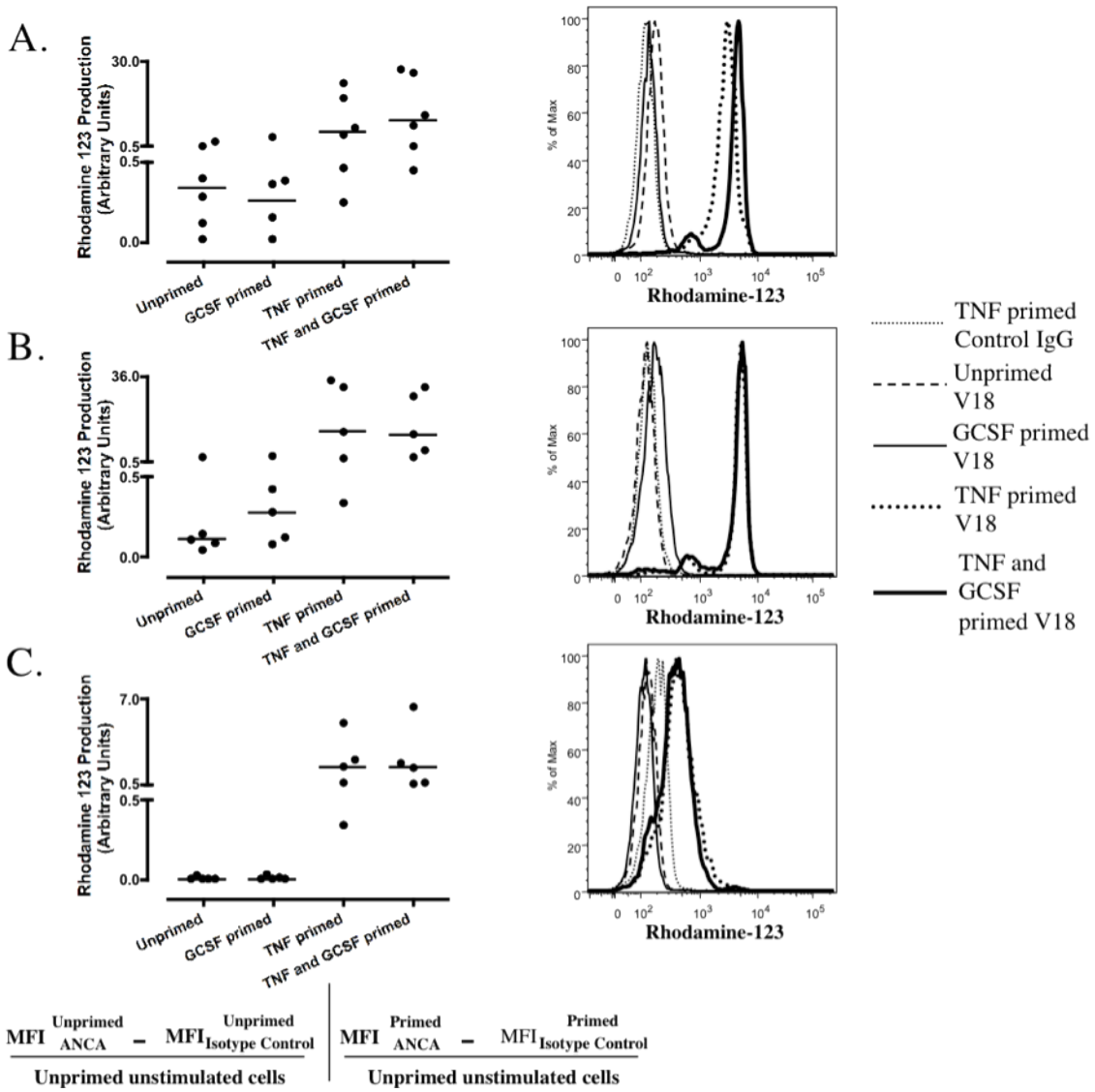

Figure 4.12 The role of GCSF and TNF in the priming of the ANCA induced respiratory burst as measured by the conversion DHR123 into fluorescent rhodamine-123. Unprimed, TNFα primed, GCSF primed or TNFα and GCSF primed neutrophils isolated from heparinised blood using Ficoll and red cell lysis were stimulated with 200μg/ml human ANCA.(n=8). V14, V16, V18 and V21 refer to separate patient derived anti-PR3. antibodies V20, V33, V41 and V45 refer to patient derived anti-MPO antibodies. Plots on the right are representative. (A, C) show data from the same donor on different days. (B) shows data from a separate donor. Arbitrary units were obtained from the median fluorescence intensities (MFI) as indicated in the figure, with data normalised for the MFI of unstained unstimulated cells in each experiment. The dot plots show the median activation (horizontal line).

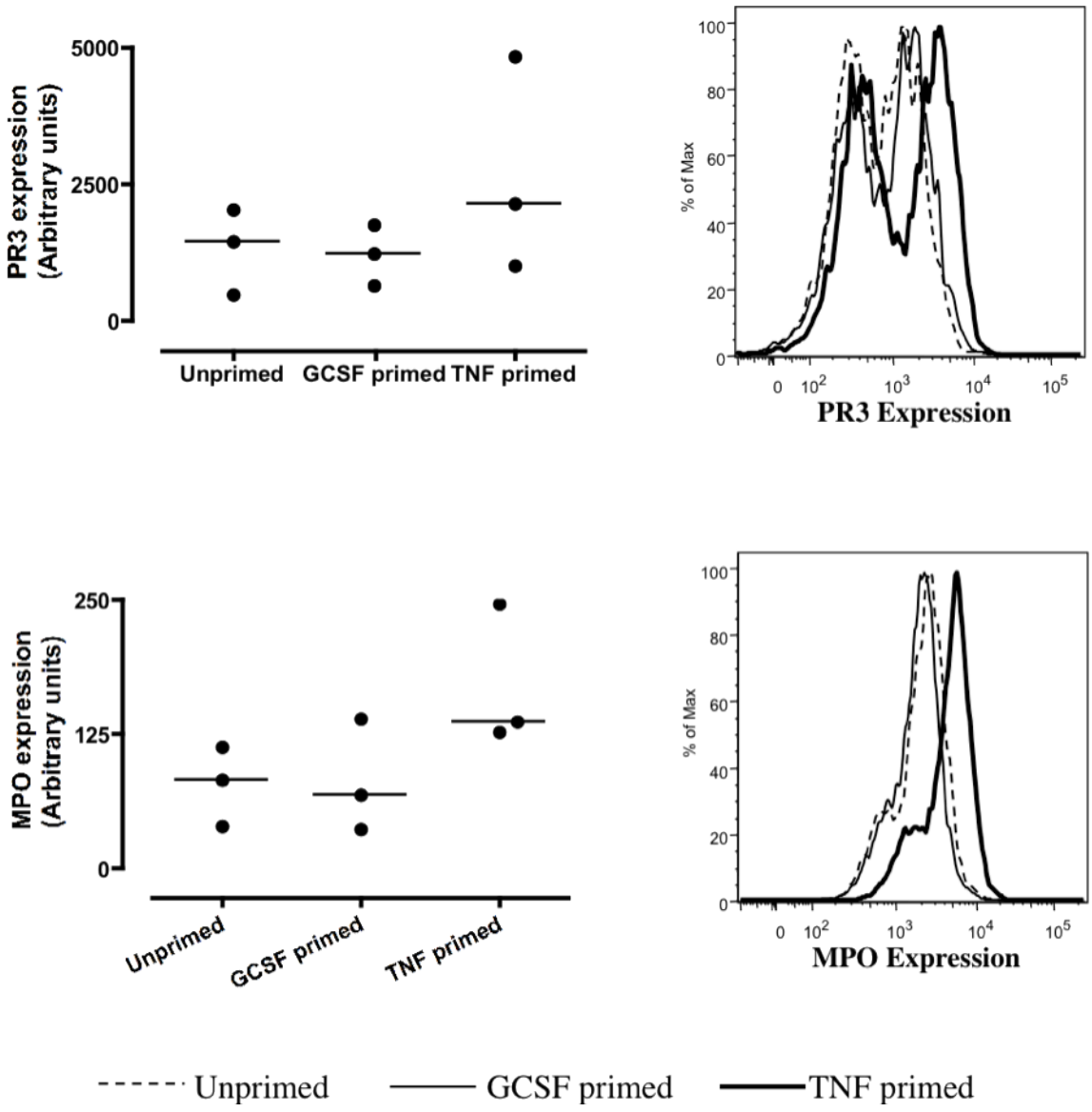

Figure 4.13 The effect of GCSF on the expression of ANCA antigens. Neutrophils were isolated from heparinised blood, drawn from healthy volunteers (n=3), using Ficoll and red cell lysis. They were unprimed, GCSF primed or TNFα primed before being stained for (A) PR3 or (B) MPO surface expression. The dot plots on the left show the median MPO expression (horizontal line).

4.5.4 GCSF primes mouse neutrophils *in vivo*

In addition to priming human neutrophils *in vitro*, the ability of GCSF to prime mouse neutriphils *in vivo* was also examined. Wildtype mice were divided into 4 groups, as indicated in Figure 4.14. Each group was either treated with 30μg of human pegylated GCSF, or a PBS control. After 4 days the mice given either 10μg LPS, or a PBS control. Two hours later the mice were bled and the expression of CD11b, CD11c and CD62L on their neutrophils was assessed. LPS but not GCSF treatment was shown to upregulate CD11b expression on mouse neutrophils (Fig 4.14 A). Importantly, there was no synergistic effect observed as a result of treatment with both GCSF and LPS. In contrast, CD11c was upregulated in mice given GCSF, either alone or in combination with LPS, but not in mice given LPS alone (Fig 4.14 B). Indeed, in mice given only LPS, CD11c levels were no different from that seen in control-treated mice, showing that this upregulation was due to the effect of GCSF. Finally, GCSF and LPS, both individually and in combination, led to to the shedding of CD62L from the surface of mouse neutrophils (Fig 4.14 C)

4.6 Results: PI3Kβ/δ blockade inhibits both ANCA and fMLP induced superoxide release as measured by the superoxide dismutase inhibitable reduction of ferricytochrome C

Neutrophils were isolated from heparinised blood drawn from healthy volunteers and using Ficoll as described. They were treated with 1000nM TGX-221, a PI3Kβ/δ inhibitor, and stimulated with one of the following: 5μg/ml human monoclonal anti-PR3 IgG, 10μg/ml human monoclonal anti-MPO IgG, 10μg/ml human IgG isotype control or 5μg/ml fMLP. It should be noted here that the viability of the cells treated with TGX-221 was not assessed at any point, and this will be discussed in the following section. TGX-221, at 1000nM, completely abolished superoxide release in response to anti-PR3 IgG (Fig 4.15 A) and anti-MPO IgG (Fig 4.15 B). The fMLP induced response was partially inhibited at this concentration of TGX-221 (Fig 4.15 C). To determine whether the effect of TGX-221 on the ANCA induced superoxide release was

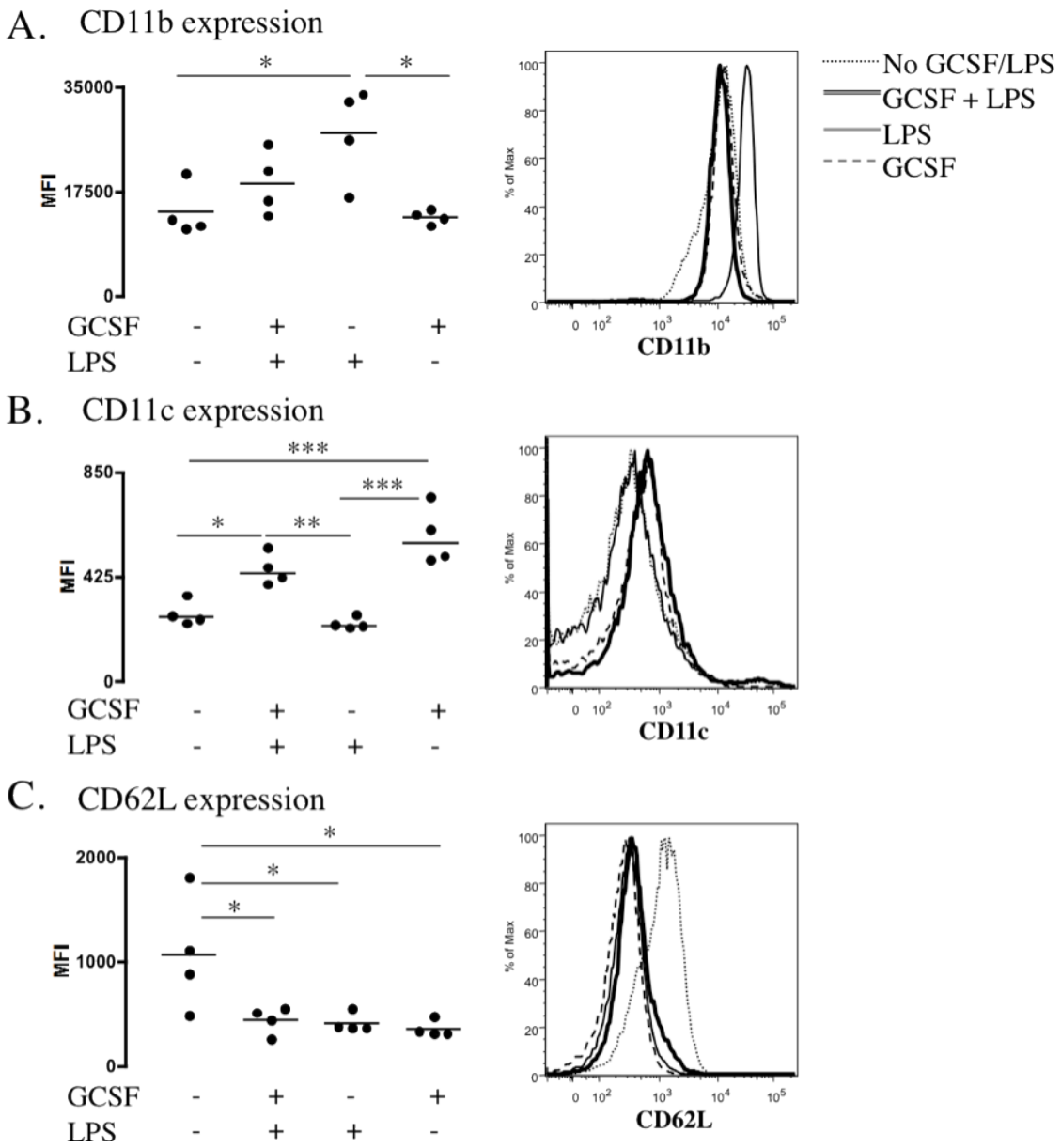

Figure 4.14 The effect of GCSF on mouse neutrophils *in vivo*. Mice were treated with PBS or GCSF for 4 days and then given either LPS or PBS, with blood taken 2 hours later. The 4 groups, each containing 4 mice, were treated as is indicated in the figure. Following treated the mice were culled and the expression of (A) CD11b, (B) CD11c and (C) CD62L on their neutrophils was assessed. Expression levels were obtained after gating on $Ly6G^+$ cells. Data from individual mice, with the median of each group shown by the horizontal line, and a representative flow cytometry plot for each marker is shown. * $p<0.05$, ** $p<0.01$, *** $p<0.001$. Data was analysed using a one-way ANOVA with a Tukey's multiple comparison post test.

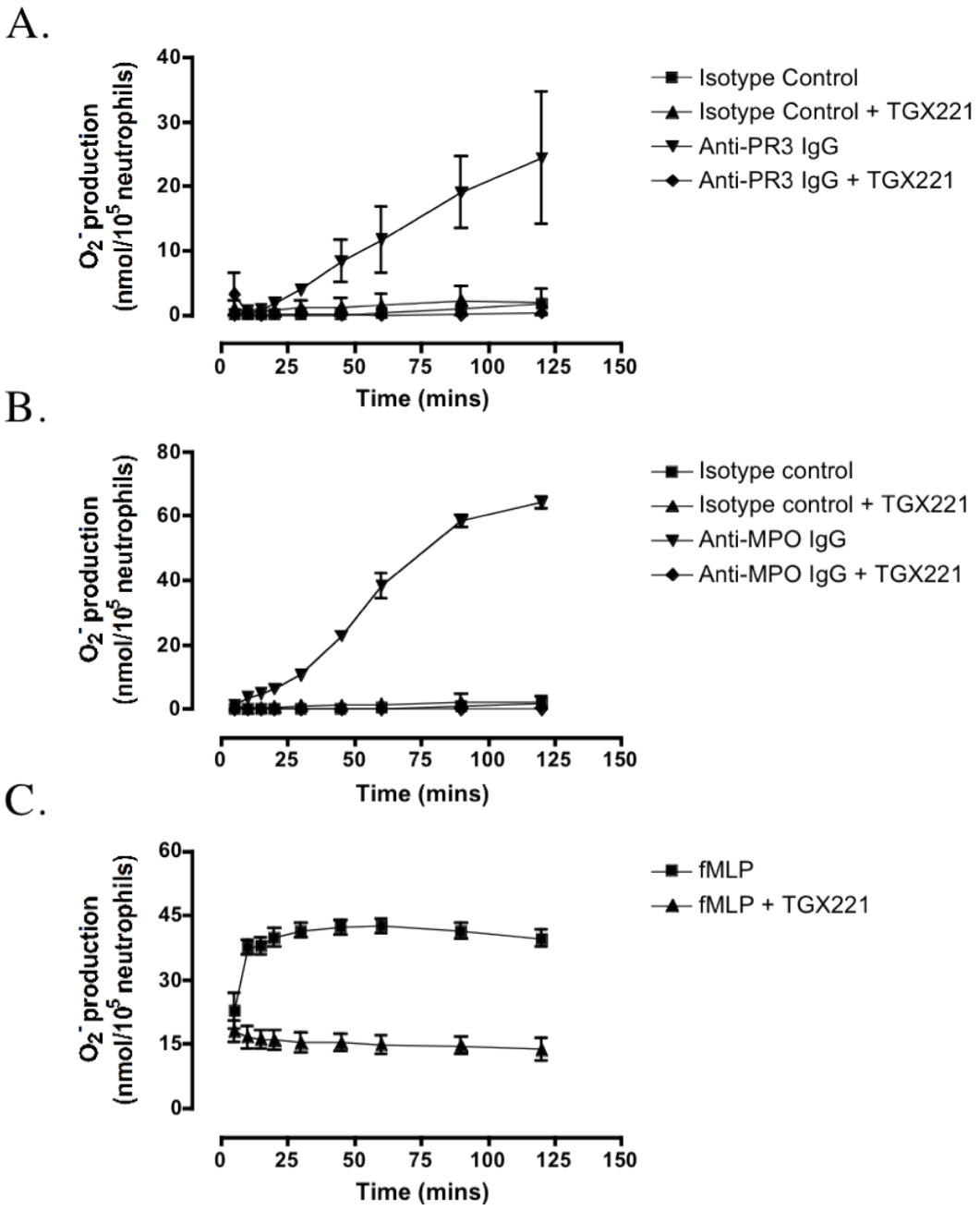

Figure 4.15 TGX-221 inhibits both ANCA and fMLP induced superoxide release as measured by the superoxide dismutase inhibitable reduction of ferricytochrome C. TNFα primed neutrophils were isolated from a healthy volunteer using Ficoll. They were treated with 1000nM TGX-221 or the same dilution of ethanol as the vehicle control before, and during, stimulation with either 5μg/ml human monoclonal anti-PR3 IgG, 10μg/ml human monoclonal anti-MPO IgG (n=1), a relevant IgG control or 5μg/ml fMLP. Data are presented as mean values ± SEM of triplicate wells.

limited to the specific monoclonal antibodies used, IgG purifed from anti-MPO ANCA positive patients was also tested. IgG purified from healthy voluteers was used as a negative control. Although only 1 of the 3 patient purified IgG samples activated the neutrophils to any great extent, it was clear that TGX-221 inhibited the ANCA induced response nonetheless (Fig 4.16). Finally, a dose response experiment was performed using 5 concentrations of TGX-221, ranging from 100nM to 1000nM (Fig 4.17). Anti-MPO IgG induced superoxide release was completely abrogated when TGX-221 was used at concentrations of 500nM and higher (Fig 4.17 A). At a concentration of 250nM, TGX-221 partially inhibited the ANCA induced response. Interestingly, 100nM TGX-221 changed the kinetics of the reaction, slowing down the response but not affecting the overall yield of the superoxide released after 2 hours of anti-MPO IgG stimulation. fMLP induced superoxide release was inhibited to some degree by all concentrations of TGX-221, although the response was never fully abolished (Fig 4.17 B).

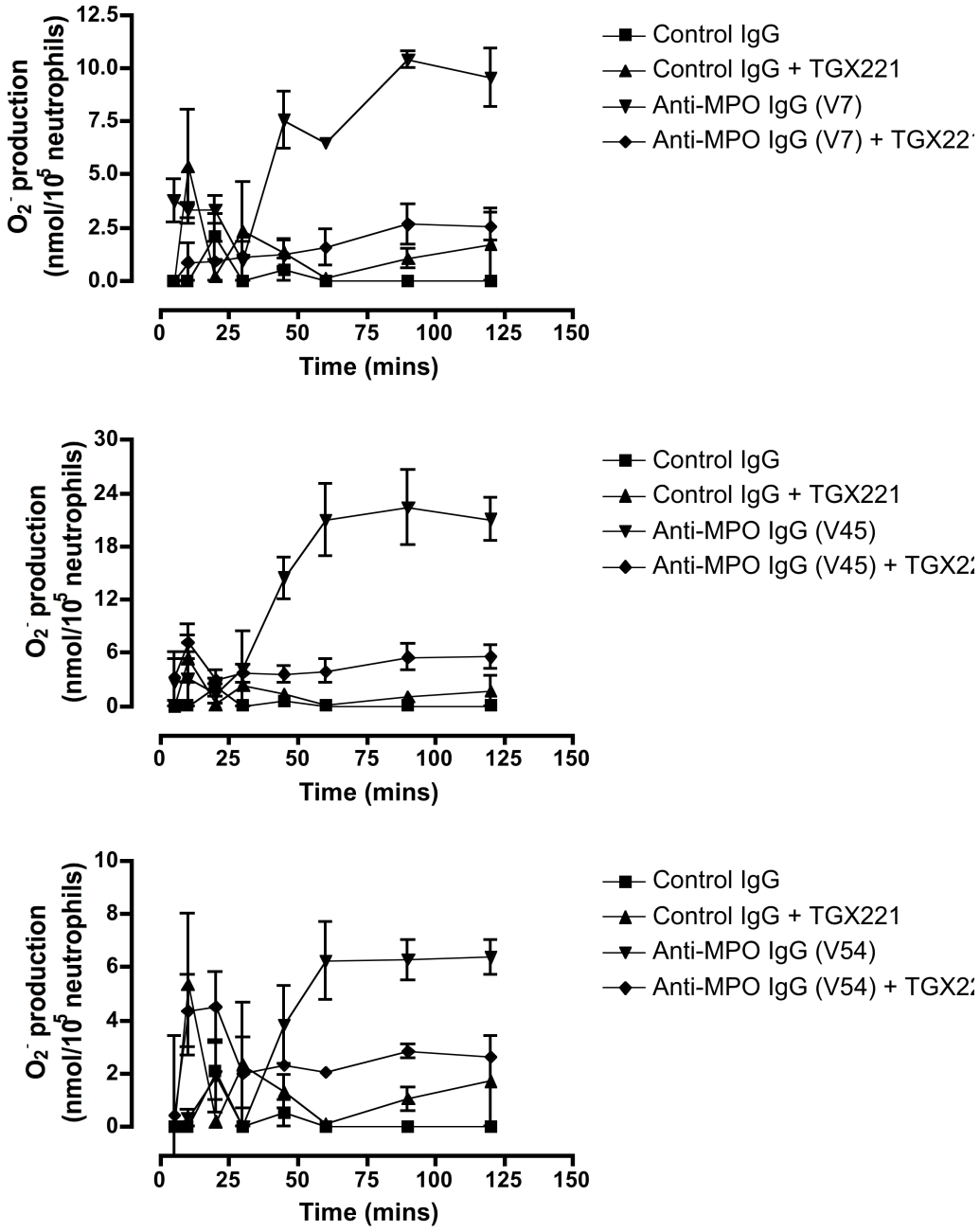

Figure 4.16 TGX-221 inhibits the patient ANCA induced superoxide release as measured by the superoxide dismutase inhibitable reduction of ferricytochrome C. TNFα primed neutrophils were isolated from a healthy volunteer using Ficoll. They were treated with 1000nM TGX-221 or ethanol, as the vehicle control, before, and during, stimulation with 200μg/ml human polyclonal anti-MPO IgG (n=3) or a relevant IgG control (n=1). Data are presented as mean values ± SEM of triplicate wells.

A.

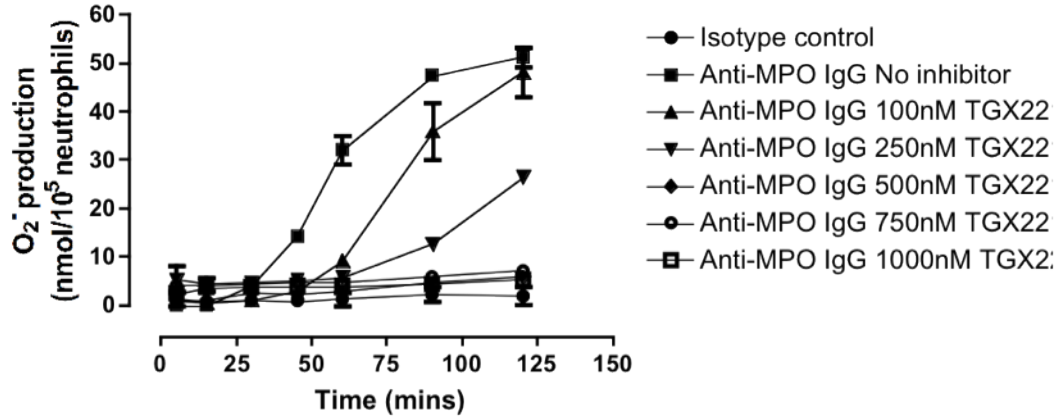

B.

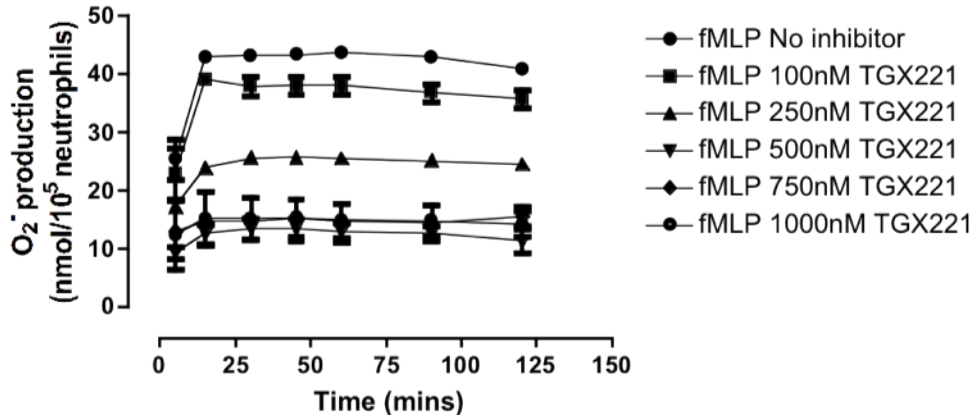

Figure 4.17 TGX-221 inhibition of ANCA induced superoxide release as measured by the superoxide dismutase inhibitable reduction of ferricytochrome C is dose dependent. TNFα primed neutrophils were isolated from a healthy volunteer using Ficoll. They were treated with various concentrations of TGX-221, or ethanol as the vehicle control, before and during stimulation with (A) 10μg/ml monoclonal human anti-MPO IgG (n=1) (B) 5μg/ml fMLP. Data are presented as mean values ± SEM of triplicate wells.

4.7 Discussion

PR3 and MPO expression

The vast majority of research on the membrane expression of ANCA antigens, PR3 and MPO, has been carried out using isolated cells. Some of the problems inherent to this approach have been discussed in Section 3.6 of the previous chapter. Thus, to avoid artefacts associated with cell isolation methods, and to allow both neutrophil and monocyte PR3 and MPO expression to be assessed simultaneously, experiments were carried out using whole blood. Using this system PR3 and MPO were found to be present on the surface of both resting neutrophils (Fig 4.2 and 4.4) and monocytes (Fig 4.3 and 4.5). This is in contrast to a previous study which showed that apoptotic neutrophils, and neutrophils primed by 4 and 8 hour incubation at 37°C, but not unstimulated cells, expressed both PR3 and MPO on their membrane [263]. However, it is in agreement with a later study showing that whole blood, resting neutrophils from patients with GPA, and to a lesser extent neutrophils from healthy controls, expressed PR3 on their membrane surface [264]. Although it cannot be directly compared, as the staining was not done in parallel, it is interesting to note that neutrophils from the same donor had a bimodal expression of PR3 when these cells were isolated (Fig 4.1), but not when they were examined in whole blood (Fig 4.2). The significance of this was not established but is discussed briefly below. What is perhaps most surprising however, is the fact that priming with TNFα did not increase surface expression of either PR3 or MPO on neutrophils. On the contrary, priming appeared to lead to a significant decrease in their expression (Fig 4.2 A and Fig 4.3 A, respectively). This is in direct contrast to what is observed using isolated neutrophils, where TNFα is frequently used to upregulate ANCA antigens and thus increase ANCA induced neutrophil activation [14, 67, 68]. This suggests that the isolation of neutrophils has profound effects on their function, and thus, *in vitro* ANCA assays may not accurately reflect the behaviour of these cells and, by extension, ANCA *in vivo*. Finally, in the case of monocytes, membrane MPO was present,

although almost undetectable, and unchanged by priming (Fig 4.5). In contrast, reasonably high levels of membrane PR3 were found to be expressed by monocytes, and this expression was upregulated in cells that had been primed with TNFα, although this did not reach statistical significance ($p<0.0629$, Fig 4.3). This is consistent with a report that monocytes, isolated together with lymphocytes and identified based on their forward and side scatter characteristics, expressed PR3 on their surface when primed with TNFα for 30 minutes [265].

The role of monocytes in ANCA associated vasculits has not been studied to any great extent. While they express both PR3 and MPO, unlike neutrophils, they have not been shown to be essential for disease pathogenesis.
Using a passive transfer model of disease (Discussed in Chapter 1) mice that were depleted of neutrophils were completely protected from anti-MPO IgG induced NCGN. Under the conditions of this model, monocyte activity was insufficient to cause disease [22]. It is important to note, however, that this is a MPO dependent model of disease, and, as results have shown, MPO is only weakly expressed by monocytes. Although the data on MPO expression relates to human cells, mouse MPO is very similar to human MPO and it is likely, though unconfirmed here, that this holds true for mouse monocytes. Interestingly, the majority of data showing a potential role for monocytes in ANCA associated vasculitis have come from studies of GPA and using anti-PR3 antibodies. For example, monocytes have been shown to be present in the granulomas and glomerular crescents of patients with GPA [266]. Furthermore, increased monocyte activation, as measured by increased neopterin and IL6 production, together with increased surface expression of CD11b and CD64, has been shown to correlate with disease activity in GPA [267]. Finally, *in vitro*, it has been shown that anti-PR3 antibodies can activate monocytes, inducing the release of monocyte chemoattractant protein (MCP)-1 [268], IL8 [265, 269], TNFα, IL1β, IL6 and thromboxane A_2 [269]. These studies, together with a lack of corresponding data for MPA and anti-MPO antibodies, and the strong expression of PR3 but not MPO on the surface of monocytes, suggests that these cells might play an important role the

pathogenesis of anti-PR3 ANCA but not anti-MPO ANCA associated vasculitis.

Despite the presence of PR3 and MPO on the surface of whole blood neutrophils, an ANCA induced whole blood respiratory burst assay could not be established. As previously mentioned, the role of TNFα in potentiating the ANCA induced respiratory burst is generally attributed to its ability to translocate PR3 and MPO from the granules of neutrophils to their cell membranes. However, data in whole blood suggests that TNFα actually downregulates neutrophil ANCA antigen surface expression (Fig 4.2, 4.4). Despite the emphasis on ANCA expression, it is important to note that there is also some evidence that TNFα can play a role in the assembly of the NADPH oxidase system, an enzyme system that is necessary for the neutrophil respiratory burst response [270]. Furthermore, a recent study has suggested that TNFα primes neutrophils for ANCA induced activation, at least partially, through the redistribution and subsequent colocalisation of $gp91^{phox}$, an important component of the NADPH oxidase system, together with β_2-integrins and FcγRIIa on the cell surface [271]. Consequently the whole blood respiratory burst assay was performed both with and without TNFα priming. While, in a limited study, TNFα appeared to increased, but was not essential for, the response to fMLP in both neutrophils and monocytes, it clearly had no effect on the response to either anti-PR3 or anti-MPO IgG (Fig 4.6-4.7). There are a number of reasons why isolated neutrophils, but not whole blood neutrophils, might undergo oxidative burst in response to ANCA. As discussed in chapter 1, data suggests that both the antigen binding region and the Fc portion of the ANCA molecule are important in ANCA signaling. It is therefore possible that antibodies, present in the plasma component of the whole blood and binding transiently to whole blood neutrophil Fc receptors, are preventing the Fc region of the ANCA molecules binding to the neutrophils and thereby activing them. It is also possible that the process of isolating neutrophils primes them for an ANCA induced response. It is unclear what this might mean for *in vivo* ANCA induced neutrophil activation, however, as discussed in Chapter 3 there are various intrinsic issues with *in vitro*

respiratory burst assays as models of ANCA induced neutrophil activation. Alternatively, or perhaps concomitantly, other plasma factors may inhibit ANCA induced neutrophil activation. Antiprotease α1-antitrypsin (A1AT), a physiological inhibitor of PR3 found in plasma, is an example of one such factor. A number of clinical studies have shown a correlation between A1AT deficiency and GPA [272-275]. Furthermore, the addition of A1AT to TNFα primed neutrophils, isolated from healthy controls and stimulated with anti-PR3 antibodies, led to a 47% decrease in the production of reactive oxygen species. For neutrophils isolated from GPA patients, the decrease upon A1AT addition was greater, at 56% [276]. A1AT is thought to bind to PR3 and thus prevent its interaction with ANCA. Therefore, it would be expected that PR3 expression on the surface of cells in whole blood would be undetectable using flow cytometry. However, this is not the case. It has already been noted that neutrophils from the same donor had a bimodal expression of PR3 when these cells were isolated (Fig 4.1) but not when they were examined in whole blood (Fig 4.2). It is possible that this is due to A1AT binding preferentially to the $mPR3^{high}$ population of neutrophils, leaving the $mPR3^{low}$ population to be bound by the anti-PR3 antibody used for flow cytometry. This is, however, unconfirmed. Furthermore, it should not affect the ability of ANCA to induce intracellular reactive oxygen species production in whole blood neutrophils, as the mPR3 pheonotype was shown to be irrelevant when using a DHR123 assay [50, 56]. It has been shown that activated neutrophils and neutrophil products, such as H_2O_2, can inactivate A1AT *in vitro* [277, 278]. In addition, the adhesion of neutrophils to endothelial cells was enough to overcome A1AT inhibition [279]. Therefore, while A1AT may inhibit neutrophil activation as a result of ANCA stimulation *in vitro* it is unlikely to be able to protect against anti-PR3 antibodies *in vivo*.

The role of GCSF in priming ANCA induced oxidative burst

The ability of GCSF to stimulate granulopoiesis has led to its use in treating neutropenia in patients, allowing the rapid production and mobilization of neutrophils into their circulation. As discussed in Chapter 1, the passive

transfer model of ANCA associated vasculitis is very mild when compared to human disease. One possible reason for this is the relatively small population of neutrophils, the key effector cell in ANCA vasculitis, found in mice. Neutrophils comprise approximately 50-70% of the leukocytes in human blood, however, they account for only 10-25% of circulating mouse leukocytes [280]. Therefore, in the hopes of establishing a more severe model of ANCA vasculitis, mice were treated with human GCSF together with LPS and anti-MPO antibodies. Despite only a modest increase in neutrophil numbers, there was a very significant increase in disease severity in mice treated with GCSF [239]. In addition to mobilising neutrophils from the bone marrow, several studies have shown that GCSF primes neutrophils both *in vitro* and *in vivo* (Discussed in Section 4.1). Further to this, GCSF signalling has been shown to activate, PI3K [281] and Akt [282], two signalling molecules thought to be essential for ANCA induced activation of neutrophils [75, 76]. Consequently, a possible role for GCSF in priming ANCA induced neutrophil activation was examined using both the ferricytochrome C reduction assay and the DHR123 assay. GCSF did not appear to prime neutrophils for superoxide release in response to stimulation with an anti-PR3 monoclonal antibody (Fig 4.8). However, it was noted that the GCSF primed neutrophils of all 3 donors tested produced more superoxide than the unprimed neutrophils when stimulated with monoclonal anti-MPO IgG (Fig 4.9). Although this did not reach statistical significance, it suggested that a difference might be seen with a larger number of donors. Believing that the difference might be small, yet physiologically significant, it was decided to switch to the DHR123 assay, as it is more sensitive than the ferricytochrome C reduction assay, and therefore might be better able to distinguish an effect. Indeed, it was found using this assay that neutrophils stimulated with monoclonal anti-MPO IgG produced significantly more reactive oxygen species when first primed with GCSF (Fig 4.11). In contrast, GCSF did not increase the response to monoclonal anti-PR3 IgG (Fig 4.10). Why this GCSF priming effect appears to be specific to anti-MPO antibodies is unclear. Previous studies have shown that, unlike TNFα, GCSF priming does not alter the expression of PR3 or MPO on the surface of neutrophils [237, 283], and this was confirmed under the same conditions

used for the respiratory burst assays (Fig 4.13). Interestingly, the TNFα induced translocation of ANCA antigens to the surface of isolated neutrophils has been shown to be p38 MAPK dependent [76]. Furthermore, it was found that ERK, while activated by TNFα, had no role in TNFα induced ANCA antigen translocation. Therefore, the inability of GCSF to induce PR3 and MPO expression on the surface of isolated neutrophils is consistent with the fact that GCSF has been shown to selectively activate ERK, but not p38 MAPK, in neutrophils [284]. If GCSF priming is not affecting MPO expression, and the signalling molecules known to be both activated by GCSF and thought to play important roles in ANCA vasculitis (PI3K and Akt) are common to both anti-PR3 and anti-MPO induced neutrophil activation, then the reason for the anti-MPO IgG specific GCSF priming response remains to be seen.

The role of GCSF in priming for an anti-MPO ANCA induced response was established using a single monoclonal antibody and was not confirmed using patient samples. This is perhaps unsurprising given that the patient derived ANCA was tested on only 2 donors and, of these, only 1 showed any response (Fig 4.12). The decision to preferentially use the monoclonal antibody was based on the fact that patient derived antibodies are, as discussed in Section 3.6 of the previous chapter, unreliable in their ability to activate neutrophils and, due to the use of whole IgG solutions, less clear in their results.

GCSF primes neutrophils in vivo

Using an anti-MPO antibody transfer model of vasculitis, it was shown that mice given GCSF, in addition to LPS, had significantly greater disease compared to controls [239]. This was likely due, at least in part, to an increase in the number of mouse neutrophils, combined with the ability of GCSF to prime these cells for an anti-MPO antibody induced respiratory burst. However, it is also likely that the ability of GCSF to modulate neutrophil adhesion molecules played an equally important role in exacerbating disease in these mice. Indeed, it has been shown here that GCSF treatment, both

alone and in combination with LPS, serves to increase the expression of CD11c while simultaneously downregulating CD62L (Fig 4.14 B-C). CD11c is a member of the CD18 family of integrins, expressed primarily by monocytes/macrophages, NK cells, DCs and neutrophils. Importantly, TNFα primed neutrophils have been shown to bind to fibrinogen in a CD11c dependent manner [285]. Furthermore, that CD11c, but not CD11b, appeared to be increased by GCSF treatment *in vivo* (Fig 4.14 A-B), suggests that it is the former rather than the latter that has an important role in neutrophil adhesion in the context of ANCA induced disease. Indeed, in a recent study using intravital microscopy, it was shown that, in the context of LPS stimulation, blocking LFA1 but not CD11b prevented the anti-MPO triggered recruitment of neutrophils to glomeruli [25]. CD62L is involved in neutrophil rolling [286] and is characteristically downregulated in response to cell activation [287], likely in preparation for the switch from rolling to firm adhesion and subsequent neutrophil transmigration. Therefore, taken together, these data suggest that GCSF treatment leads to the conversion of neutrophil rolling to firm adhesion, via the induction of CD62L shedding and CD11c upregulation, and in this manner further contributes to anti-MPO IgG induced disease.

PI3Kβ/δ plays a role in ANCA induced superoxide production?

TGX-221 is a potent Class IA PI3K specific inhibitor. The IC_{50} of TGX-221 for each Class I PI3K isotype, as determined in three separate studies, is shown in Table 4.3. Using the ferricytochrome C reduction assay, it has been shown that TGX-221 is capable of inhibiting, though not abolishing, the fMLP induced release of superoxide by isolated neutrophils (Fig 4.15, 4.17). In addition, it has been shown that 1000nM of TGX-221 completely abrogates superoxide release by anti-PR3 and anti-MPO monoclonal IgG (Fig 4.15), and polyclonal patient derived anti-MPO IgG (Fig 4.16). Furthermore, it has been demonstrated that TGX-221 inhibits monoclonal anti-MPO IgG and fMLP induced respiratory burst activation in a dose-dependent manner (Fig 4.17).

When used at 1000nM, TGX-221 inhibits both PI3Kβ and PI3Kδ. The extent to which it also inhibits PI3Kα at this concentration is less certain, as out of 3 separate studies, 1 has reported an IC_{50} of 784nM for TGX-221 against PI3Kα, while 2 have reported an IC_{50} of >1000nM (Table 4.3). However, taking into account that 500nM TGX-221 completely abolished the anti-MPO induced respiratory burst (Figure 4.17A), it is likely that PI3Kα does not play a major role, relative to PI3Kβ and PI3Kδ, in the ANCA induced release of reactive oxygen species by neutrophils. Similarly, based on the results shown in Figure 4.17B, it is likely that Class IA PI3Ks, particularly PI3Kβ and/or PI3Kδ, play prominent roles in the fMLP induced neutrophil respiratory burst. Importantly, however, not even the highest concentration of TGX-221 completely abrogated superoxide generation by treated neutrophils. This result is fits with previous studies showing that fMLP activates neutrophils through both PI3Kδ, which is inhibited here, and PI3Kγ, which is not [254].

Interestingly, neither 100nM nor 250nM of TGX-221 abolished the ANCA induced respiratory burst, although at 100nM TGX-221 did change the kinetics of the response. Indeed, 100nM TGX-221, while not sufficient to affect the overall yield of superoxide released after 2 hours of anti-MPO IgG stimulation, did appear to slow down the response, with superoxide release starting at a later time point and increasing rapidly. At 250nM, TGX-221 almost halved the amount of superoxide generated (51 nmol $O_2^-/10^5$ neutrophils without inhibitor vs 26 nmol $O_2^-/10^5$ neutrophils with 250nM TGX-221, following 2 hours ANCA stimulation). The exact reason for this is unclear and would require further study to be elucidated. However, as the IC_{50} of TGX-221 against PI3Kδ is in the range of 65-211nM (Table 4.3), it is possible that superoxide generation in the presense of both 100nM and 250nM TGX-221 is the result of remaining PI3Kδ activity.

It is important to note that the effect of TXG-221 on neutrophil viability was not tested. It is therefore possible that the results shown are the due to neutrophil death and not specific inhibition of PI3Ks. However, as 10μM TGX-221 (10 times the highest concentration used here) was found to have no toxic effects

on bone marrow derived macrophages, following incubation of up to 40 hours [288], it is unlikely that the results shown are due to TGX-211 cell toxicity.

Taken together, and presuming that TGX-221 is not affecting neutrophil viability, these data suggest that Class IA PI3Ks, particularly, PI3Kβ/δ play an important role in the ANCA induced respiratory burst, and by extension may be important for the pathogenesis of ANCA associated vasculitis.

To date, the majority of research on PI3Ks in ANCA associated vasculitis has focused on PI3Kγ, which, as discussed in Chapter 1, was shown to have an important role in disease pathogenesis. Indeed, the data presented here are in direct contrast to a previous study by Ben-Smith et al., in which ANCA stimulation failed to activate the PI3Kα, PI3Kβ and PI3Kδ catalytic subunit p85, and thus suggested that Class IA PI3Ks do not have a role in ANCA signalling [75]. However, it is likely that this discrepancy is due to the timing of the assays involved. In the study by Ben-Smith et al., p85 activation was examined following 30 seconds, 1 minute and 15 minutes of ANCA stimulation. This is significant as there was little superoxide production, either with out without TGX-221, seen in the first 30 minutes following the addition of ANCA to the neutrophils in the ferricytochrome C reduction assays presented in Figures 4.15-4.17. Thus, it is possible, although it cannot be confirmed without further study, that p85 activation does not occur within the first 15 minutes of ANCA stimulation. Consequently, its activation, likely between 15 and 30 minutes post ANCA addition, was missed by Ben-Smith et al.. Interestingly, it has been shown that fMLP induces biphasic activation of the PI3K pathway in human neutrophils, with the first phase largely dependent on PI3Kγ activation, and the second phase largely dependent on PI3Kδ activation [254]. Further to this, a separate study has shown that PI3Kγ is essential for early fMLP induced reactive oxygen species generation, but is dispensable for the late response to fMLP [250]. In the same study it was suggested that that Class IA PI3Ks might be activated by PI3Kγ, via Ras in the early phase and Src in the late phase. Thus, it is possible that a similar response occurs in ANCA induced neutrophil activation, with PI3Kγ being

important for early ANCA responses, and for the activation of PI3Kβ and/or PI3Kδ, which are in turn essential for late ANCA responses. Consequently, it is possible that both Class IA and Class IB PI3Ks are potential therapeutic targets for the treatment of ANCA associated vasculitis.

α	β	δ	γ	
784	10	65	3240	[254]
>1000	9	211	-	[289]
5000	5	100	>10000	[290]

Table 4.3 The IC_{50}'s (nM) of TGX-221 for the four class I PI3K isoforms as determined by three separate studies.

5.1 Introduction

It has been long established that findings in mice do not always translate to humans. Furthermore, there exist a number of pathogens that simply do not infect small laboratory animals. Therefore humanised mice, in this case mice that possess human immune cells, represent an important tool for the *in vivo* study of human leukocytes, and their roles in both host defence and autoimmunity. As discussed in Chapter 1, there are numerous issues with regards the current animal models of ANCA associated vasculitis that make the prospect of a humanised mouse model attractive. This will be further discussed in Chapter 7.

Despite, or perhaps because of, the continuous efforts to improve the currently available models, the development of humanised mice remains complicated by the fact that there is no consensus on how it should be approached. Factors that must be considered when developing these models include the following: a number of different human cell types can be used to engraft mice, IL2r$\gamma^{-/-}$ mice are available on a number of background strains, mice can be engrafted both as adults and neonates, and there are numerous routes of injection that can be used [129]. To date there have been few studies on the engraftment of humanised mice that have directly compared these factors. Although some investigators use peripheral blood leukocytes to reconstitute mice, human hematopoietic stem cells (HSCs) have been shown to provide better engraftment, and present less risk of the mice developing graft vs host disease. HSCs can be derived from peripheral blood, bone marrow, foetal tissue and umbilical cord blood (UCB). They are capable of differentiating into cells of both the lymphoid and myeloid lineage, depending on the presence or absence of various hematopoietic factors, and are self-renewing, thus allow for long term engraftment [134]. The majority of investigators use $CD34^+$ HSCs derived from UCB to develop humanised mice, and indeed it has been established that HSCs from newborn/foetal sources have greater potential than those from adult sources [291, 292]. Consequently, $CD34^+$ stem cells derived from UCB were chosen to repopulate immunodeficient mice with human immune cells in this study.

The engraftment levels of three strains of immunodeficient mice, all with the IL2rγ$^{-/-}$ mutation, were compared after adoptive transfer of human CD34^{+} cells derived from UCB [128]. In addition, this study examined engraftment in both adult and neonatal mice. The three strains used were as follows: NOD-scid IL2rγ$^{-/-}$, NOD-Rag1$^{-/-}$IL2rγ$^{-/-}$, BALB/c-Rag1$^{-/-}$. Both NOD strains supported higher levels of engraftment than the BALB/c strain, and this was independent of age. However, despite not quite reaching statistical significance, it was observed that NOD-scid IL2rγ$^{-/-}$ mice engrafted as neonates tended to have greater human leukocyte reconstitution when compared to mice engrafted as adults. Interestingly, the main difference seen between neonatal and adult engrafted mice was with regards to their ability to reconstitute lymphocytes. While neonatal mice supported significantly increased T cell development when compared with their adult counterparts, B cell engraftment was higher in adult engrafted mice as compared to mice engrafted as newborns. The development of myeloid lineage cells was not compared. There are many advantages to working with adult mice over neonates. Perhaps most importantly, there is much more leeway with regards timing. Mouse breeding is often unreliable and, as a consequence, it can be difficult to plan experiments with newborn mice. Indeed, there is an ever-present risk that UCB stem cells may become available at time when there are no litters to engraft, or conversely, newborn mice may be available at time when there are no UCB stem cells. In contrast, adult mice are generally engrafted between 6 and 12 weeks, and thus there is generally sufficient time to procure stem cells and carefully plan out experiments. Therefore, few stem cells or mice will go to waste. In addition, newborn mice may not survive to adulthood. Female mice have been known to reject litters and the risk of this is increased when the newborns have been handled. Taking both this, and the fact that T cell development is unlikely to be important for a potential humanised mouse passive transfer model of ANCA vasculitis, adult NOD-scid IL2γ$^{-/-}$ mice were chosen for use in this study.

In this chapter the passive transfer of human neutrophils into NOD-scid IL2γ$^{-/-}$ mice was considered, various methods of CD34^{+} cell isolation from UCB were

tested, purified cells were transferred into conditioned NOD-scid IL2r$\gamma^{-/-}$ mice and the engraftment of these mice was characterised.

5.2 Aims

- To repopulate conditioned NOD-scid IL2$\gamma^{-/-}$ mice with human leukocytes using human haematopoietic stem cells
- To characterise the human leukocytes present in engrafted mice

5.3 Methods

5.3.1 Passive transfer of neutrophils

Neutrophils were isolated from healthy volunteers using Polymorphprep as described in Section 2.2.6.1. Approximately $1x10^7$ neutrophils in 200μl PBS were injected into adult NOD-scid IL2$\gamma^{-/-}$ mice via the lateral tail vein. Mice were bled from the saphenous vein 10 and 60 minutes post transfer and whole blood was stained for the presence of human neutrophils using human CD45 and human CD66b antibodies. A small volume of blood was used to perform whole blood counts using Turk's solution. Flow cytometry was performed as described in Section 5.3.2. Absolute numbers of neutrophils were calculated from flow cytometry data and total leukocyte numbers.

5.3.2 Flow cytometry

Flow cytometry was performed as described in Section 2.2.1. The antibodies used are shown in Table 5.1 and 5.2.

Target	Isotype	Clone	Fluorophore	Supplier	Dilution
CD3	Mouse IgG2a, κ	BW264/56	APC	Miltenyi	1:11
CD19	Mouse IgG1,κ	HIB19	FITC	BD	1:6
CD34	Mouse IgG2a, κ	AC136	PE	Miltenyi	1:11
CD45	Mouse IgG1, κ	HI30	V450	BD	1:101
CD45	Mouse IgG1, κ	HI30	PE-Cy7	BD	1:101
CD66b	Mouse IgM, κ	G10F5	FITC	BD	1:11

Table 5.1 Anti-human antibodies used for flow cytometry. All antibodies were obtained from commercial sources.

Target	Isotype	Clone	Fluorophore	Supplier	Dilution
CD45	Rat (LOU) IgG2b, κ	30-F11	PE	BD	1:500

Table 5.2 Anti-mouse antibodies used for flow cytometry. All antibodies were obtained from commercial sources.

5.3.3 $CD34^+$ isolation from frozen cord blood

Frozen UCB was defrosted as described in Section 2.2.10.1. UCB cells were resuspended in MACS buffer (PBS with 0.5% BSA and 2mM EDTA) and $CD34^+$ cells were purified using the Miltenyi MACS separation system as described in Section 2.2.10.3, with any changes made to this protocol being listed in Table 5.3. The yield and purity of the resulting cell suspension was determined using flow cytometry. Staining was carried out for $CD34^+$ cells and $CD3^+$ contaminating T cells.

5.3.4 $CD34^+$ isolation from fresh cord blood

$CD3^+$ cells were depleted from fresh cord blood as described in Section 2.2.10.2. For some batches of cord blood, the yield and purity of the resulting cell suspension was determined using flow cytometry before the cells were either injected into mice or cryopreserved in 90% FCS and 10% DMSO. For

other batches the cells were resuspended in MACS buffer (PBS with 0.5% BSA and 2mM EDTA) and $CD34^+$ cells were purified using the Miltenyi MACS separation system as described in Section 2.2.10.3 or resuspended in PBS containing 2% FCS and 1mM EDTA with $CD34^+$ cells being purified using StemCell Technolies EasySep separation system (Section 2.2.10. 4).

5.3.5 Engraftment of NOD-scid IL2$\gamma^{-/-}$ mice

Humanised mice were generated as described in Section 2.2.11. Briefly, mice were engrafted by injecting $1x10^5$ human cord blood $CD34^+$ stem cells (either purified as described in Section 2.2.10 or purchased from Lonza, Slough, Berkshire, UK) into 6-12 week old NOD-scid IL2$\gamma^{-/-}$ mice approximately 4 hours post irradiation at 2.4Gy with a Cs-source irradiator.

5.3.5 Characterisation of humanised mice

Reconstitution of human cells in the peripheral blood, bone marrow and spleen of engrafted mice was assessed using flow cytometry at least 8 weeks post adoptive transfer of stem cells. Mouse blood and tissue was collected as described in Section 2.2.13.1.The percentage of mouse and human $CD45^+$ cells was first examined. By gating on the human $CD45^+$ cell population human $CD3^+$ T cells and human $CD19^+$ B cells were then considered.

5.3.6 Statistics

Statistics were performed using Graphpad Prism software (Graphpad Software Inc, La Jolla, CA, USA). Student t tests or one-way/repeated measures ANOVAs were used, as indicated, to analyse the data presented here.

5.4 Results: Passively transferred human neutrophils rapidly disappear from the mouse circulation

Isolated human neutrophils were injected into immunodeficient NOD-scid IL2$\gamma^{-/-}$ mice via the lateral tail vein. The percentage and total number of human neutrophils remaining in the circulation of injected mice was then tested at 10 and 60 minutes post passive transfer. After approximately 10 minutes the percentage of human neutrophils remaining in the peripheral blood of these mice was on average 6.98%, with a standard deviation of 1.89%. After 60 minutes this had decreased to give an average of 2.38%, with a 1.25% standard deviation. A representative flow cytometry plot is shown in Figure 5.1. The flow cytometry data together with total leukocyte counts was used to determine the approximate number of human neutrophils remaining in circulation. Approximately $1x10^7$ neutrophils were injected into each mouse and Table 5.3 shows the total number of neutrophils/ml in the peripheral blood of mice 10 and 60 minutes post transfer. At 10 minutes there were, on average, approximately $1.15x10^5$ neutrophils/ml remaining and this had decrease to $3.9x10^4$ neutrophils/ml after 60 minutes.

5.5 Results: Isolating viable haematopoietic stem cells from umbilical cord blood

5.5.1 $CD34^+$ cells could not be purified for injection into mice from frozen umbilical cord blood

Non-clinical standard, frozen UCB was obtained from The Anthony Nolan Trust. It was defrosted at 37°C and $CD34^+$ cells were purified using the Miltenyi magnetic cell (MACS) separation system. Flow cytometry, staining for both $CD34^+$ and $CD3^+$ cells, was used to determine the purity of the cell preparations. Figure 5.2 shows a representative plot from the purification of one batch of UCB. A small population of $CD34^+$ cells could be seen in the untreated blood, together with a large population of $CD3^+$ T cells. After $CD34^+$

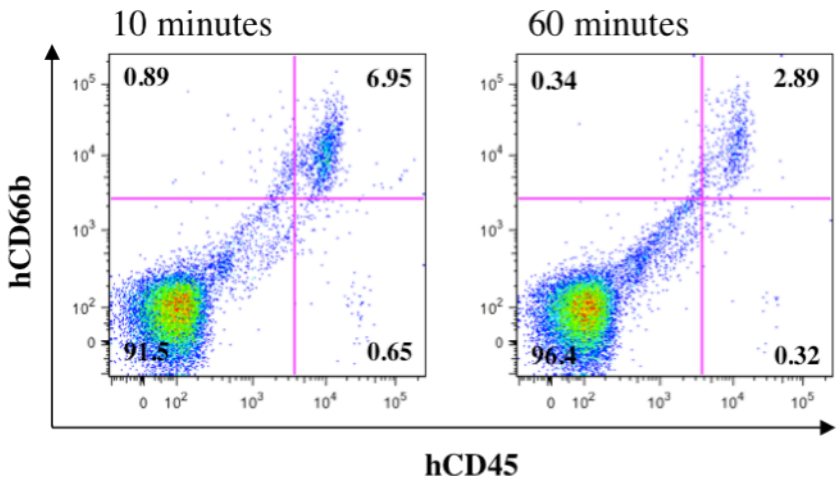

Figure 5.1 Representative plot showing the percent of human $CD45^{+}CD66b^{+}$ neutrophils in the circulation of NOD-scid $IL2\gamma^{-/-}$ mice (n=4) 10 and 60 minutes post adoptive transfer of $1x10^{7}$ human neutrophils isolated from healthy controls.

Mouse	Total no. of circulating human neutrophils 10 minutes post transfer (cells/ml)	Total no. of circulating human neutrophils 60 minutes post transfer (cells/ml)
1	85.400	77,400
2	85,000	17,100
3	173,300	43,350
4	117,300	21,200
Average	115,250	39,763

Table 5.3 The total number of human $CD66b^{+}$ neutrophils remaining in the circulation of NOD-scid $IL2\gamma^{-/-}$ mice (n=4) 10 and 60 minutes post adoptive transfer of $1x10^{7}$ human neutrophils isolated from healthy controls.

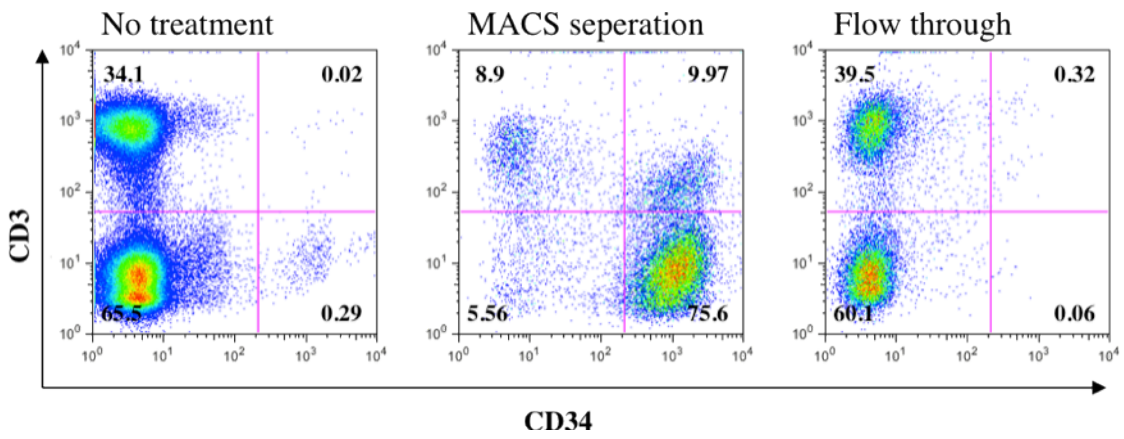

Figure 5.2 Representative flow cytometry data showing $CD34^+$ cell purification using the Miltenyi MACS seperation system from cryopreserved human cord blood obtained from The Anthony Nolan Trust. Data is from Donor 100640 and is representative of 5 separate experiments (See Table 5.4).

cell purification, using MACS separation involving two separate isolation steps, the cell suspension contained approximately 75.6% $CD34^+$ cells and 8.9% contaminating $CD3^+$ T cells. The flow through, containing the cells that were not magnetically labelled and thus passed straight through the separation column, was also examined to ensure no $CD34^+$ cells that could be collected by an extra purification step remained. As can be seen, no $CD34^+$ cells were present in the flow through. Table 5.4 summarises the various attempts to purify $CD34^+$ cells from frozen cord blood. Of the 5 attempts to isolate $CD34^+$ cells from frozen UCB, sufficient purity (>95% $CD34^+$ cells) combined with a sufficiently low percent of $CD3^+$ T cell contamination (<1%) was achieved only once, and in this case the yield was very low ($4x10^5$ cells total, enough to engraft a maximum of 4 mice).

5.5.2 $CD3^+$ cells were successfully depleted from fresh umbilical cord blood

Non-clinical standard, fresh UCB was obtained from the National Blood Service, Oxford and Collindale. In order to produce a cell suspension containing $CD34^+$ cells that could safely be injected into mice, $CD34^+$ cell isolation using the Miltenyi MACS separation system was compared to $CD3^+$ cell depletion using RosetteSep followed by $CD34^+$ cell purification using the EasySep system. As can be seen in Figure 5.3, MACS separation alone did not provide a sufficiently pure (comprising >95% $CD34^+$ cells and <1% $CD3^+$ cells) cell suspension. RosetteSep, on the other hand, effectively depleted all $CD3^+$ T cells from the UCB, and when this was followed by $CD34^+$ cell purification using EasySep, a cell suspension with 84% $CD34^+$ cells and less than 1% $CD3^+$ T cells was achieved. Furthermore, the yield was acceptable ($2.1x10^6$ cells total, enough to engraft approximately 20 mice) (Table 5.5). As T cell contamination, and subsequent graft vs host disease, is the biggest concern with regards to injecting mice with whole UBC cells it was decided that CD3 depleted UCB cells would be sufficient to engraft mice as suggests by both Brehm et al. [128] and Lang et al. [293]. Table 5.5 summarises the fresh UCB batches processed.

Donor ID	No. of cells through column ($x10^8$)	Yield (Cells total)	$CD34^+$ cells (%)	$CD3^+$ cells (%)	Notes on protocol
100640	2	$2x10^6$	75.6	8.9	2 x through column
100728	5	$2x10^6$	88.2	1.9	3 x through column
100672	8	$7x10^5$	55.3	13.8	2 x through column, EDTA in MACS buffer replaced with ACD/A
100730	1.75	$4x10^5$	98.1	0.35	3 x through column, returned to EDTA for MACS buffer
100720	3.5	$2x10^5$	94	2.2	3 x through column

Table 5.4 List of $CD34^+$ cell purifications using the Miltenyi MACS seperation system from cryopreserved human cord blood obtained from The Anthony Nolan Trust. All Donor identification numbers begin G2212 09.

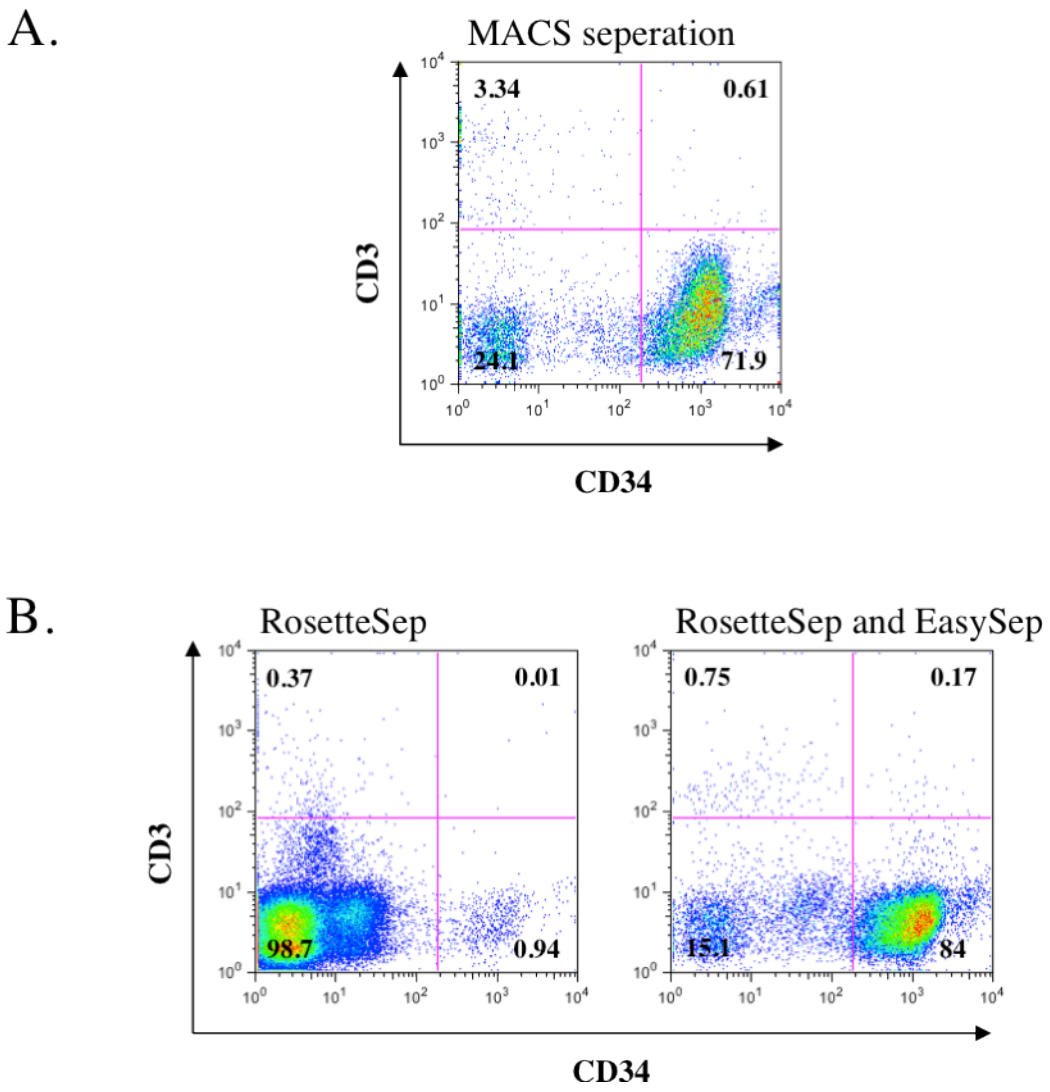

Figure 5.3 Comparing $CD34^+$ cell isolation using (A) the Miltenyi MACS cell seperation system with (B) $CD3^+$ cell depletion using RosetteSep followed by $CD34^+$ cell purification using EasySep (n=1). Data is from Donor 166 (See Table 5.5).

Donor ID	Total no. nucleated cells ($x10^8$)	Yield (Cells total)	$CD34^+$ cells (%)	$CD3^+$ cells (%)	Protocol
166	7.76	$2.4x10^6$	76.8	1.85	Miltenyi MACS separtion
166	7.76	$2.1x10^6$	84	<1	RosetteSep $CD3^+$ cell depletion followed by EasySep $CD34^+$ cell purification
182	8.65	$7.5x10^7$	1.2	<1	RosetteSep $CD3^+$ cell depletion
205	6.80	$3.5x10^8$	0.27	<1	RosetteSep $CD3^+$ cell depletion
231	3.50	$1.8x10^8$	0.97	<1	RosetteSep $CD3^+$ cell depletion
478G	7.31	$2.32x10^8$	0.8	<1	RosetteSep $CD3^+$ cell depletion

Table 5.5 List of fresh human cord blood obtained from NBS, Oxford and Colindale. All donor identification numbers begin G180 105 127 with the exception of the donor 478G the sole cord blood received from Colindale NBS and beginning G180 110 218.

5.6 Results: Generating humanised mice

5.6.1 Humanised mice possess similar levels of human cells at 8 and 12 weeks post engraftment

The majority of studies using humanised mice assess engraftment 12 weeks post transfer of HSCs. To determine whether this was the earliest time point at which engrafted mice possessed human cells, irradiated NOD-scid IL2$\gamma^{-/-}$ mice were injected intravenously with either human $CD3^+$ cell depleted UCB cells (Fig 5.4) or isolated $CD34^+$ stem cells obtained from Lonza (Fig 5.5), and assessed using flow cytometry, 4, 8 and 12 weeks later. Mice engrafted with CD3 depleted UCB had low levels of human $CD45^+$ cells in their circulation at all time points tested (Fig 5.4). Importantly the average percentage of human $CD45^+$ cells more than doubled between 4 and 8 weeks post engraftment (Mean 2.45% vs 5.59%). Although this was not a statistically significant increase it is very suggestive. In contrast, there was little change in the level of human cells between 8 and 12 weeks post engraftment (Mean 5.59% vs 4.94%). Mice that received isolated $CD34^+$ stem cells possessed relatively high levels, when compared to the CD3 depleted UCB cell engrafted mice, of human $CD45^+$ leukocytes in their circulation at all time points tested. These mice had significantly more human $CD45^+$ cells in their peripheral blood at 8 weeks post engraftment when compared to their levels at 4 weeks post engraftment (Mean 27.04% vs 7.54%). Consistent with CD3 depleted UCB cell engrafted mice, there was little difference seen in the percentage of human cells between 8 and 12 weeks post engraftment (mean 27.04% vs 26.02%).

5.6.2 NOD-scid IL2$\gamma^{-/-}$ mice engrafted with $CD34^+$ stem cells (from Lonza) had enhanced leukocyte reconstitution when compared with mice engrafted with CD3 depleted umbilical cord blood cells

Table 5.6 shows a summary of mice engrafted during this project. It includes the number of mice in each group, the cells used to reconstitute them and the

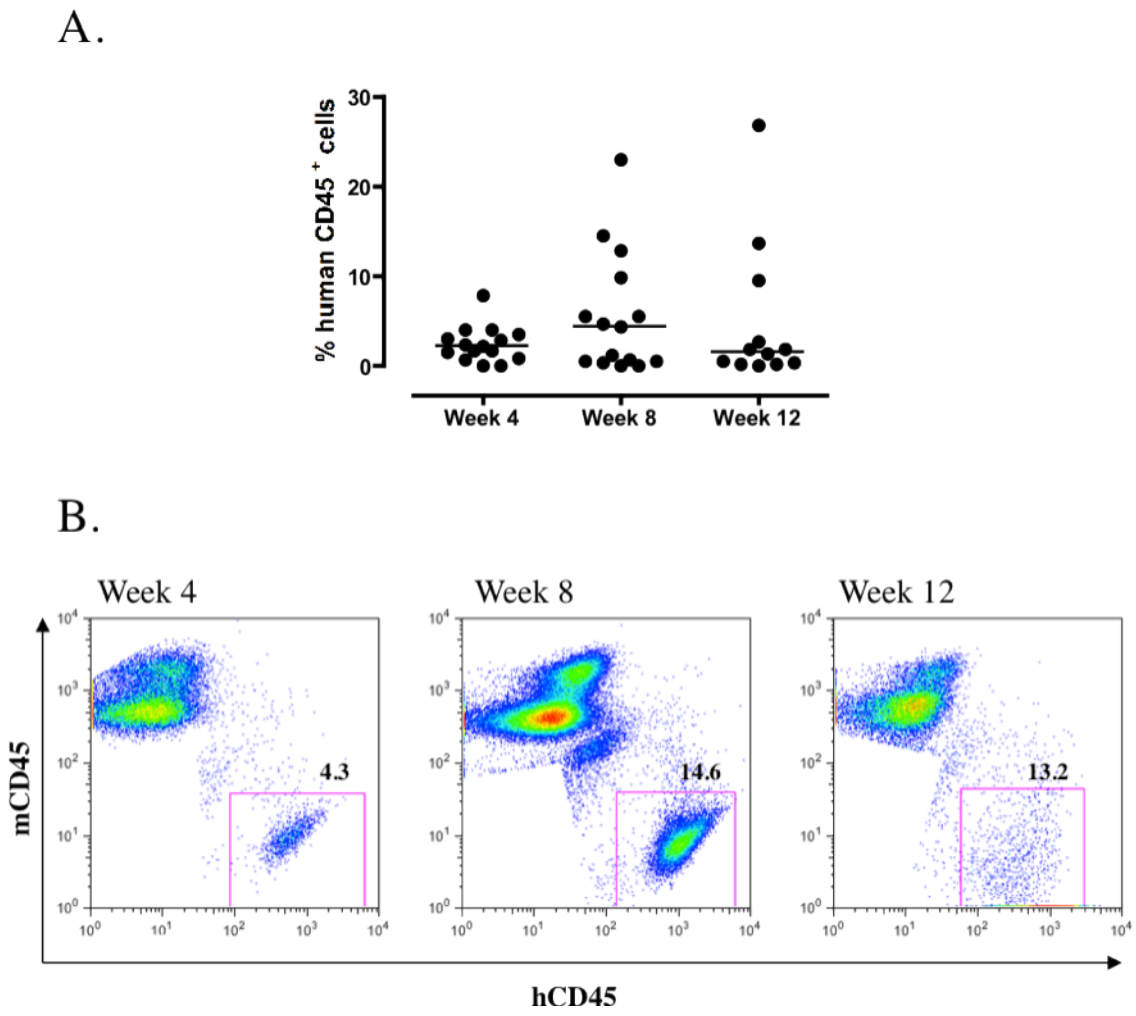

Figure 5.4 Time course of peripheral blood engraftment of human (h)CD45$^+$ cells using CD3$^+$ cells depleted cord blood cells. (A) Combined data from Group 2 (n=5 at weeks 4 and 8, n=3 at week 12) and Group 5.1 (n=10 at weeks 4 and 8, n=9 at week 12) with the median of each group shown by the horizontal line. (B) Representative plots from a single mouse from Group 2. mCD45 refers to mouse CD45$^+$ cells. See Table 5.6 for further information on groups of mice shown.

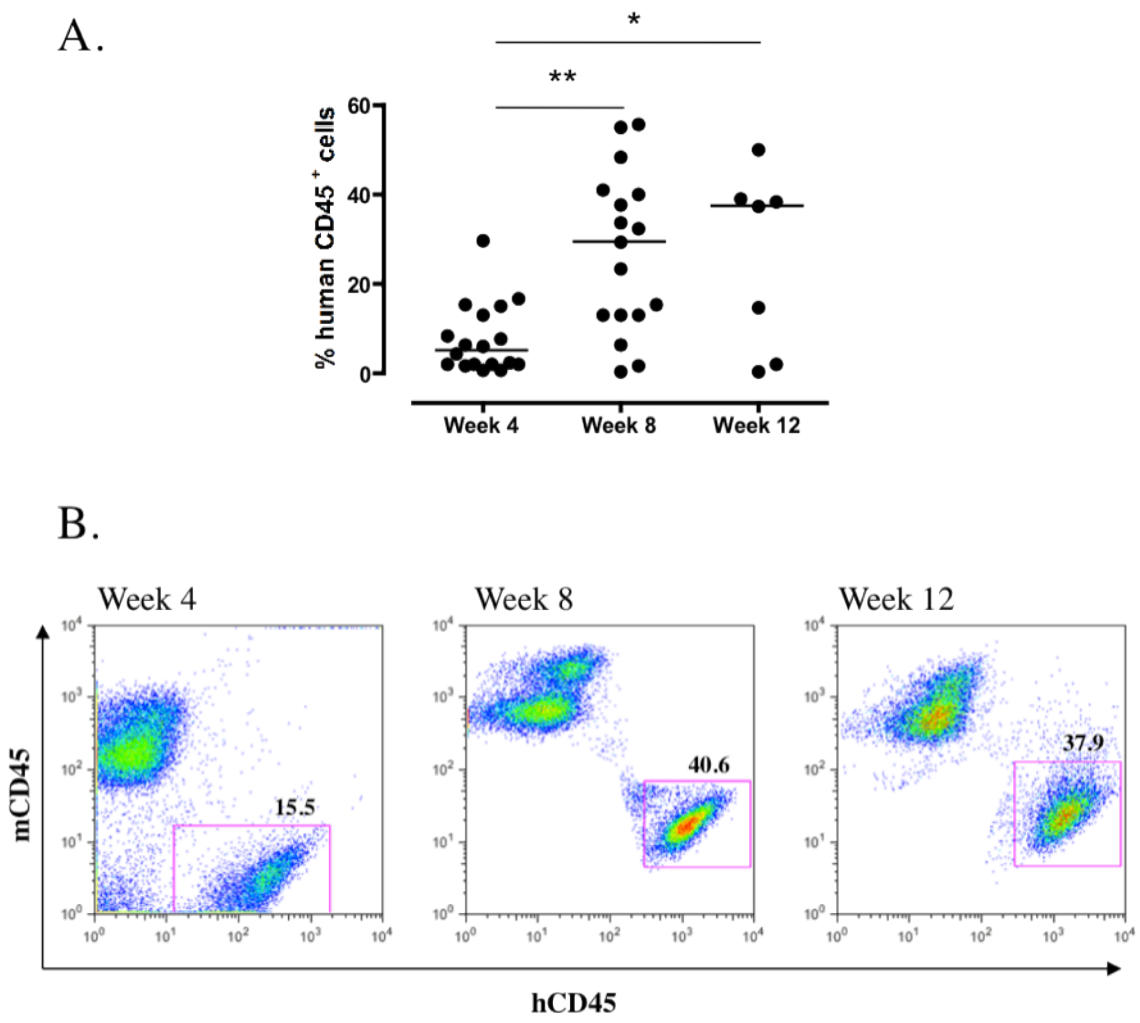

Figure 5.5 Time course of peripheral blood engraftment of human (h)CD45$^+$ cells using CD34$^+$ cells obtained from Lonza. (A) Combined data from Group 1 (n=8 at week 4 and n=7 at weeks 8 and 12) and Group 5.1 (n=10 at weeks 4 and 8, n=0 at week 12) with the median of each group shown by the horizontal line.. (B) Representative plots from a single mouse from Group 1. mCD45 refers to mouse CD45$^+$ cells. See Table 5.6 for further information on groups of mice shown. *p<0.05, **p<0.01. Data was analysed using a one-way ANOVA with a Tukey's multiple comparison post test.

Mouse Group No.	No. of mice engrafted/No. of mice surviving to end point	CD34 positive cells used	Mean engraftment (% human $CD45^+$ cells)
1	8/7	Purchased from Lonza, Lot 091254A	22.8 ± 20.5
2	6/3	CD3 positive cell depleted cord blood from donor 182	16.7 ± 9.09
3	7/6	CD3 positive cell depleted cord blood from donor 205	0.8 ± 1.06 Week 8
4	7/7	CD3 positive cell depleted cord blood from donor 231	1.4 ± 2.51 Week 5
5.1	12/10	Purchased from Lonza, Lot OF3018	22.9 ± 12.4 Week 9
5.2	10/10	CD3 positive cell depleted cord blood from donor 231	4.14 ± 4.37 Week 9
6	9/8	CD3 positive cell depleted cord blood from donor 478G	15.4 ± 16
7	10/7	Purchased from Lonza, Lot 080026B	15.1±5.38
8.1	19/14	Purchased from Lonza, Lot OF4518	32.4±22.5
8.2	14/9	Purchased from Lonza, Lot OF4444	23.9±29.4
9	15/15	Purchased from Lonza, Lot OF4518	60.3±17.4 Week 8
10	14/9	Purchased from Lonza, Lot IF3299	19.3±18.6 Week 25
11	10/6	Purchased from Lonza, Lot IF3269	60.3±17.4 Week 21
12	18/13	Purchased from Lonza, Lot IF3299	0.53 ± 0.77
13	8/5	Purchased from Lonza, Lot IF3269	64.2±5.52 Week 9
14	10/8	Purchased from Lonza, Lot OF4444	51.8 ± 10

Table 5.6 Humanised mice generated. All engraftment data is from peripheral blood 12 weeks post engraftment unless otherwise stated. All mice received approximately $1x10^5$ $CD34^+$ cells with the exception of those in Group 12 who received $5x10^4$ cells (Due to a low availability of $CD34^+$ cells at the time of engraftment). All $CD34^+$ cells purchased from Lonza were derived from cord blood with the exception of Lot 080026B, which were bone marrow derived. Mean is given as ± standard deviation.

average percentage of human $CD45^+$ cells in their peripheral blood 12 weeks (unless otherwise stated) post adoptive transfer of human $CD34^+$ HSCs. It is clear from these data that mice engrafted with isolated $CD34^+$ cells obtained from Lonza had a higher level of human $CD45^+$ cell reconstitution than mice engrafted with CD3 depleted UCB cells. This was confirmed by the comparison of two groups of mice engrafted side-by-side, with one group receiving $CD34^+$ Lonza cells and one group receiving CD3 depleted UCB cells (Fig 5.6). The mice were assessed together at 9 weeks post engraftment. The mice that received Lonza cells had significantly higher levels of human leukocyte engraftment as measured by the percentage of human $CD45^+$ cells present in their peripheral blood.

5.6.3 NOD-scid IL2$\gamma^{-/-}$ mice reconstituted with $CD34^+$ stem cells had human T and B cells in their bone marrow, spleen and peripheral blood 12 weeks post engraftment

Humanised mice reconstituted with isolated human $CD34^+$ cells (Group 1 Table 5.6) were sacrificed 12 weeks post engraftment and their bone marrow and spleens were harvested for analysis. Concurrently, blood was collected from the axillary vessels under terminal anaesthesia. Human $CD45^+$ cells were present in the bone marrow, spleens and circulation of all mice tested (Fig 5.7). Furthermore, there were considerably more human leukocytes present in the bone marrow and spleen of these mice than in the blood (Mean 26.07% vs 59.81% vs 49.62%) (Fig 5.7 A). Having demonstrated that human $CD45^+$ cells repopulate conditioned NOD-scid IL2$\gamma^{-/-}$ mice that have received human HSCs, it was decided to further identify the human cells present. The majority of human $CD45^+$ cells found in these mice were $CD19^+$ B cells (Fig 5.8). They accounted for on average 75.4%, 87.7% and 60.32% of the human cells in the bone marrow, spleen and blood, respectively. Notably, there were more B cells found in the found in the spleen than in the bone marrow or peripheral blood and in the bone marrow than in the blood (Fig 5.8 A). Together with B cells, $CD3^+$ T cells were found to be present in the spleen

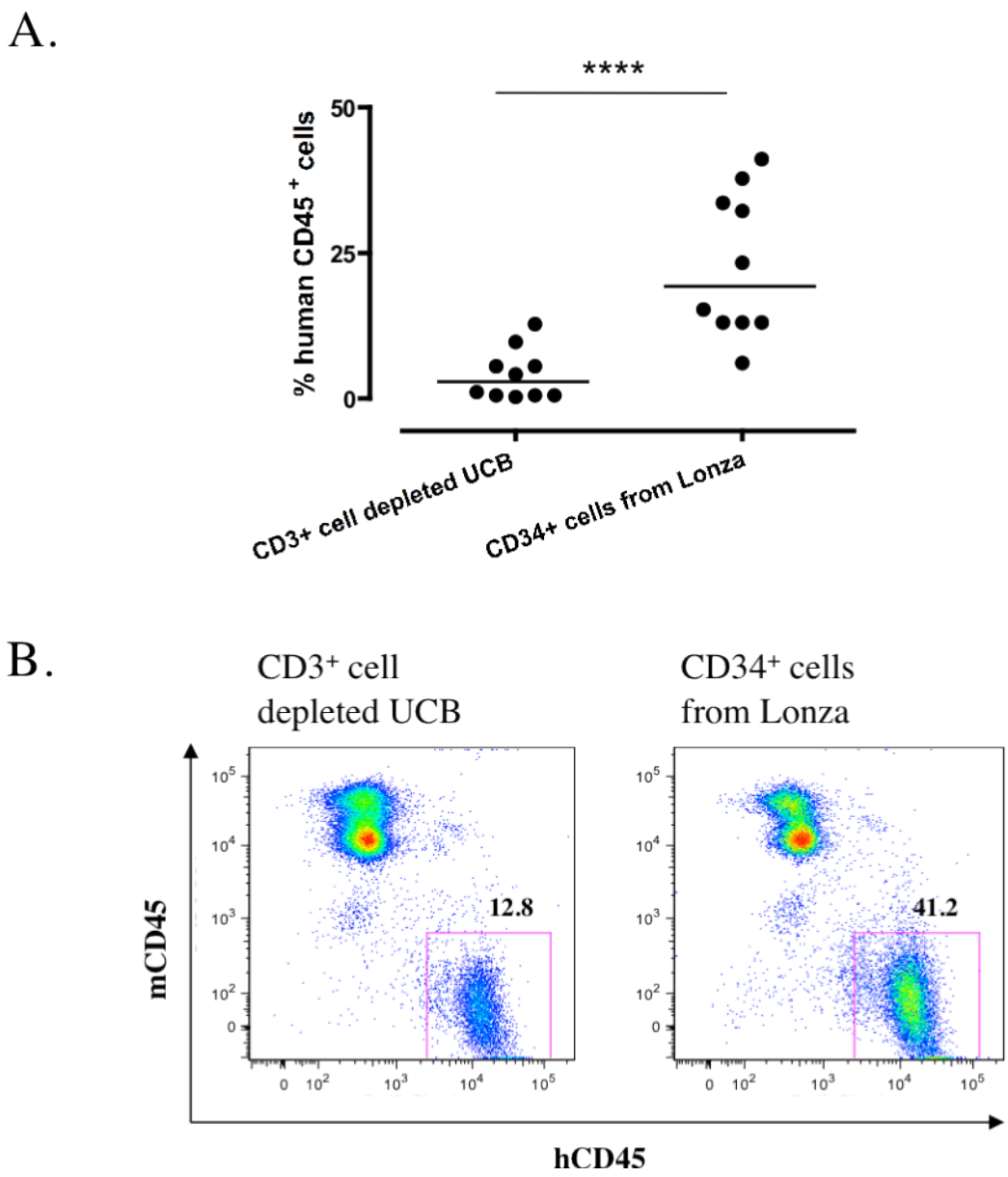

Figure 5.6 Comparison of two groups of mice engrafted side-by-side with one group receiving $CD34^+$ Lonza cells and one group receiving CD3 depleted UCB cells. The mice where from group 5.1 (n=10) and 5.2 (n=10) respectively. See table 5.6 for more information. The mice were assessed together at 9 weeks post engraftment. (A) Percentage of human $CD45^+$ cells in the peripheral blood of these mice. with the median values of each group shown by the horizontal line. (B) Representative plots. ****p<0.0001. Data was analysed using an unpaired t test.

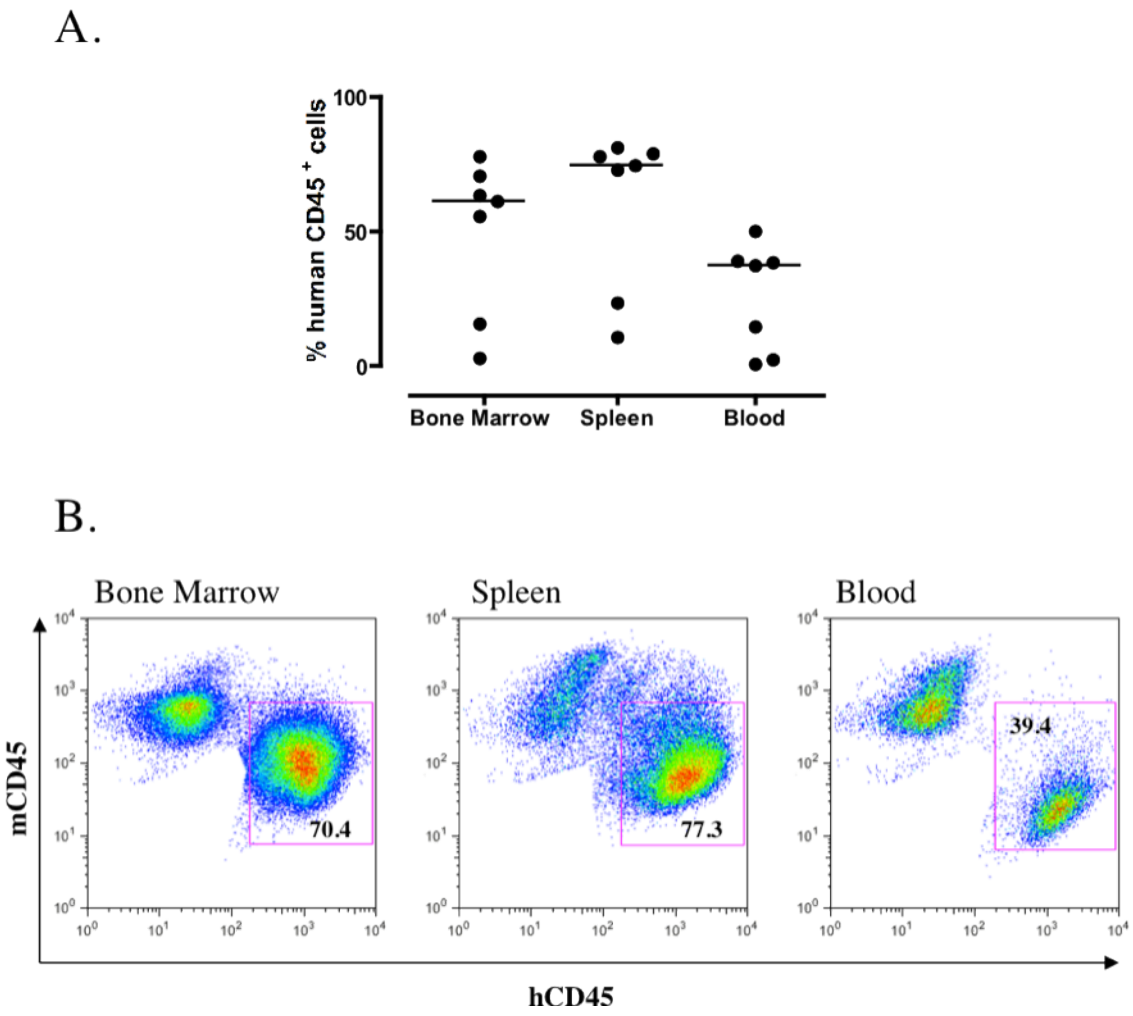

Figure 5.7 Engraftment of human (h)CD45^{+} cells. (A) Combined data from Group 1 (n=7) with the median of each group shown by the horizontal line. (B) Representative plots from single mouse from Group 1. mCD45 refers to mouse CD45^{+} cells. See Table 5.6 for further information on Group 1.

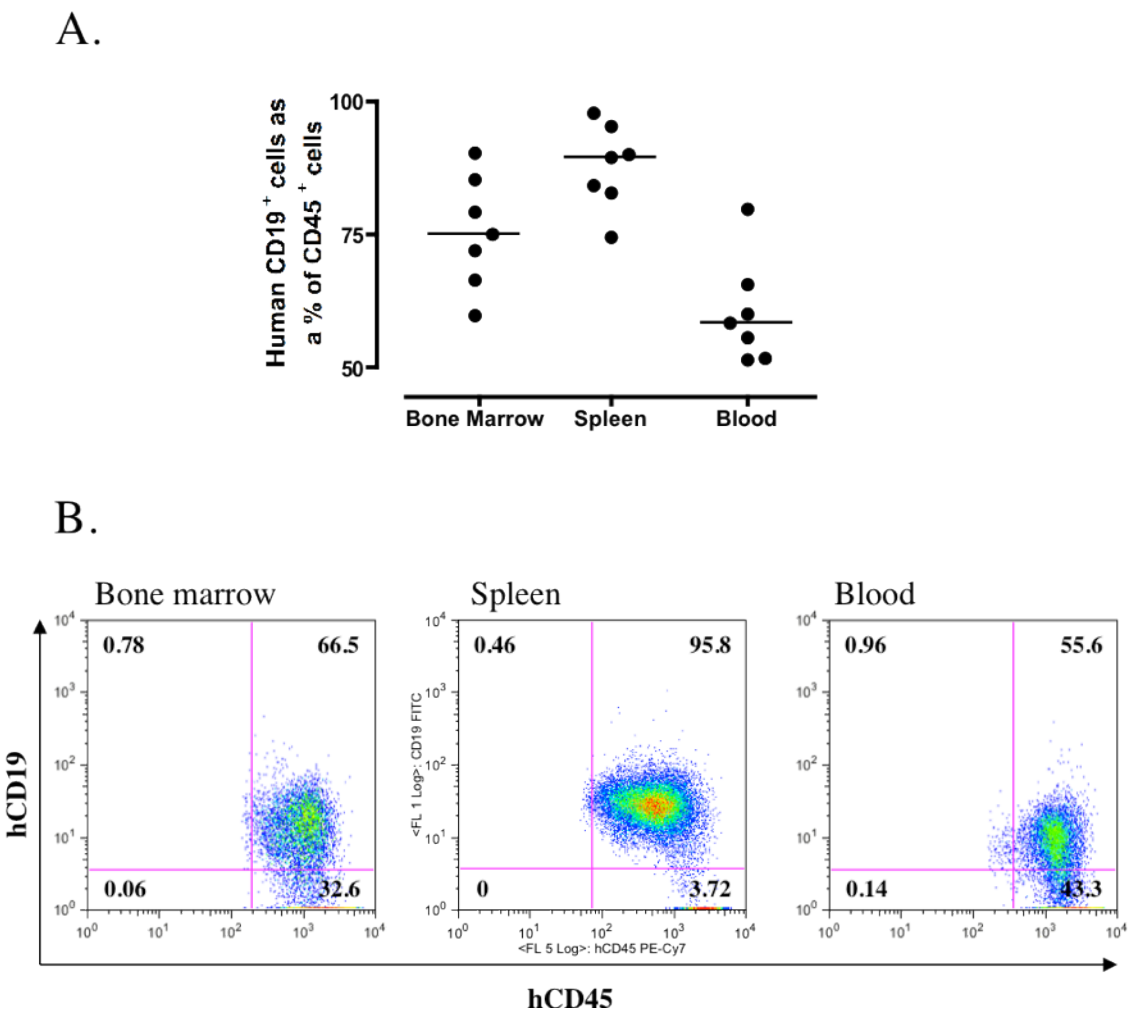

Figure 5.8 Engraftment of human (h)CD19$^+$ cells as a percent of human CD45$^+$ cells. (A) Data from Group 1 (n=7) with the median of the groups shown by the horizotal line. (B) Representative plots from a single mouse from Group 1. mCD45 refers to mouse CD45$^+$ cells. See Table 5.6 for further information on Group 1.

and blood but not, to any great extent, the bone marrow of mice tested (Fig 5.9). On average, humanised mice had 0.49%, 4.71% and 9.95% T cells in their bone marrow, spleen and blood, respectively. There were far more T cells found in the spleen and blood of mice compared to the bone marrow (Fig 5.9 A).

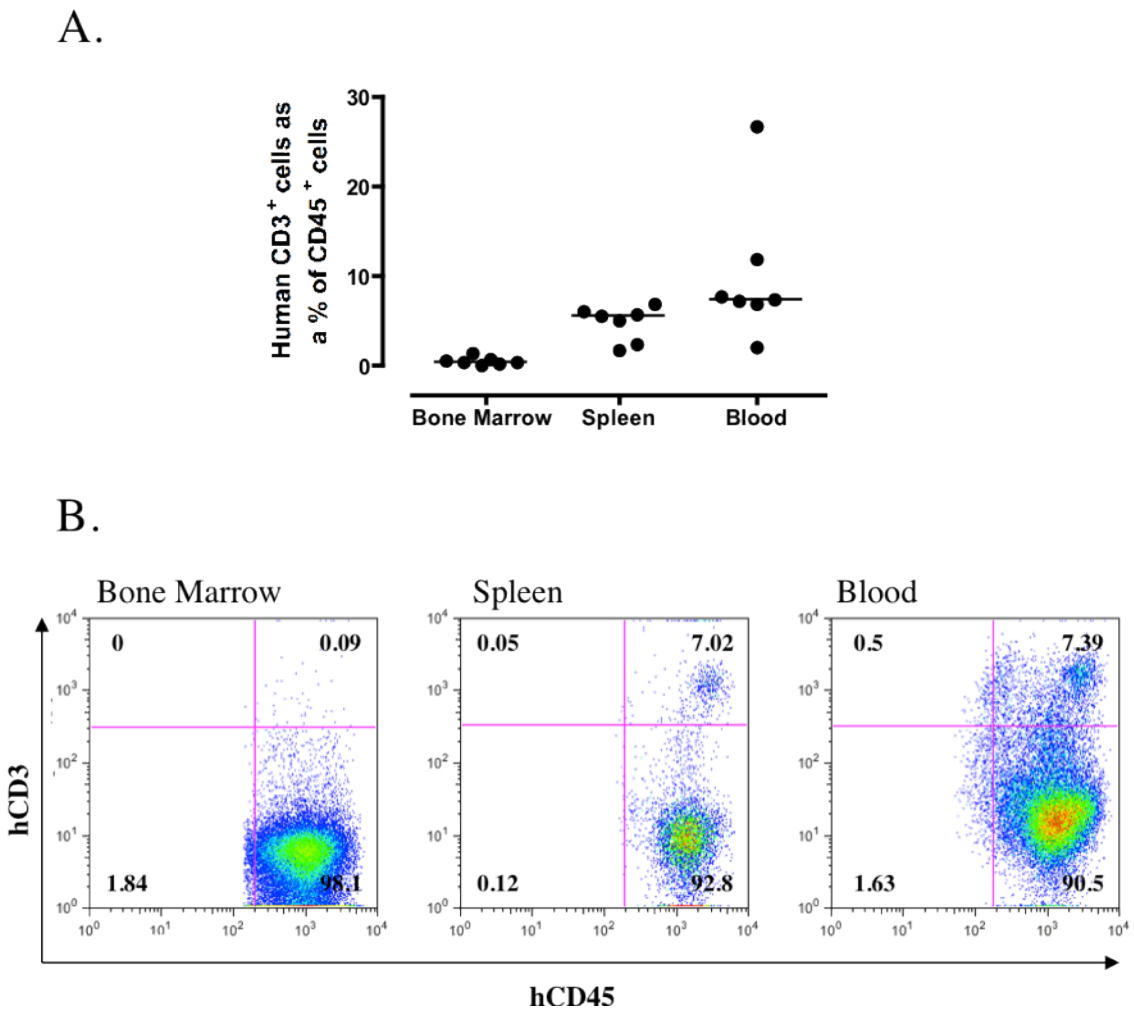

Figure 5.9 Engraftment of human (h)CD3$^+$ cells as a percent of human CD45$^+$ cells. (A) Data from Group 1 (n=7) with the median of the groups shown by the horizotal line. (B) Representative plots from a single mouse from Group 1. mCD45 refers to mouse CD45$^+$ cells. See Table 5.4 for further information on Group 1.

5.7 Discussion

Passive transfer of human neutrophils

The failure to develop a murine model of anti-PR3 induced ANCA associated vasculitis has largely been attributed to differences between murine and human PR3, the most important of which is thought to be the former's inaccessibility to circulating anti-PR3 antibodies. Thus the development of a mouse model with human neutrophils present in the peripheral blood would provide a potential tool for the study of anti-PR3 antibodies *in vivo*. To investigate what would perhaps be the simplest way of achieving such a goal, human neutrophils were passively transferred directly into the circulation of mice. Isolated human neutrophils injected into the lateral tail vein of immunodeficient mice were rapidly cleared from the circulation (Fig 5.1). Although the whereabouts of the infused neutrophils was not investigated, it is likely that they were cleared from the circulation by the bone marrow, liver and spleen. Indeed, following the intravenous injection of radiolabelled neutrophils into mice, high levels of radioactivity were detected in these organs [294]. Furthermore it was demonstrated that, in mice, each of these organs was responsible for approximately 30% of neutrophil clearance from the peripheral blood under homeostatic conditions [295]. Further to this, radiolabelled neutrophils infused into human volunteers, both with and without sepsis, were revealed to be cleared from the circulation by the bone marrow, liver and spleen over the 24 hour period post passive transfer [296].

It is not only their rapid clearance from the circulation that makes the passive transfer of human neutrophils into mice unsuitable for their study *in vivo*. Indeed, in addition to this neutrophils are very short-lived cells with a half-life of only 6-8 hours. Therefore, even if they were not cleared rapidly, human neutrophils would disappear from mouse circulation within a relatively short space of time. Consequently, to overcome this, mice would require daily injections of neutrophils if longer studies were to be performed. Thus, instead of a passive transfer model, a mouse model that constantly generates, and replaces, human neutrophils is required.

Humanised mice

Human immune cells are present in mice reconstituted with human HSCs for up to twelve months [127, 149]. The lack of human progenitor renewal, itself due to the lack of a maintence pool of human HSCs, may be responsible for the eventual disappearance of human cells from these mice [148]. As human cells are present for an extended period of time, humanised mice may provide an effective tool to study human neutrophils *in vivo* and this will be discussed at length in the following chapter. In this chapter, the generation of mice with human lymphocytes present in their bone marrow, spleen and circulation was investigated.

As discussed in Section 5.1, human UCB was chosen to repopulate irradiated NOD-scid IL2$\gamma^{-/-}$ mice with human cells. Thus, establishing a source of human HSCs was the first step in the generation of humanised mice. As procuring cord blood samples directly from women is both difficult, and time consuming, it was decided to purchase non-clinical grade UCB samples from The Anthony Nolan Trust and the National Blood Service, Oxford and Collindale. Initially, cryopreserved UCB was obtained from The Anthony Nolan Trust. The use of frozen UCB allowed greater control over the timing of sample processing. Using the Miltenyi MACS separation system, $CD34^+$ HSCs were purified from frozen UCB. However, the cell suspensions obtained from this were thought to be insufficiently pure (Table 5.4). That is they appeared to contain more than 1% $CD3^+$ T cells, and thus, if injected into mice would likely induce graft vs host disease. In hindsight, it is possible that a proportion of the $CD3^+$ cells were actually dead. Indeed, dead cells may bind non-specifically to MACS microbeads (Manufacturers Protocol). However, as no dead cell stain was used, it is difficult to be completely certain of the viability of the $CD3^+$ cells identified in Figure 5.2 and Table 5.4. Thus, believing that $CD34^+$ cells suitable for injection into mice could not be isolated from frozen cord blood, fresh cord blood was obtained from the National Blood Service. In the initial experiment UCB from a single donor was divided into two equal parts. One part was used to test $CD34^+$ cell separation using the MACS system, while the other half was used to test $CD3^+$ cell depletion using RosetteSep followed

by magnetic $CD34^+$ cell selection using EasySep (Fig 5.3). Contaminating $CD3^+$ T cells (>1% of the total cell suspension) remained after MACS separation; however, they were completely absent after treatment with RosetteSep CD3 depletion cocktail. $CD34^+$ cell selection using EasySep was then used to give a cell suspension comprising approximately 84% $CD34^+$ cells. It has been suggested that T cell depleted cord blood may be more efficient than isolated $CD34^+$ cells when it comes to repopulating conditioned NOD-scid $IL2\gamma^{-/-}$ mice with human immune cells [128, 293]. Therefore, and taking into account the time and expense required to isolate $CD34^+$ cells, it was decided that $CD3^+$ cell depleted UCB cells would be used to engraft mice. At approximately the same time, though not in parallel, it was decided that $CD34^+$ cells derived from UCB would be purchased from Lonza and used to generate humanised mice. Both CD3 depleted UCB cells (Fig 5.4) and $CD34^+$ cells from Lonza (Fig 5.5) gave rise to human $CD45^+$ cells in the peripheral blood of irradiated NOD-scid $IL2\gamma^{-/-}$ mice as early as 4 weeks post engraftment. Mice engrafted with the $CD3^+$ cell depleted UCB cells did not see a significant increase in their percentage of human $CD45^+$ cells over time (Fig 5.3). In contrast, mice engrafted using the enriched $CD34^+$ stem cells showed a significant increase in their human leukocyte levels at 8 weeks compared to 4 weeks post engraftment. These levels then stayed fairly constant between 8 and 12 weeks post engraftment (Fig 5.4). Importantly, the mice that were reconstituted using enriched $CD34^+$ cells showed enhanced engraftment compared to their counterparts that received $CD3^+$ cell depleted UCB cells, although this was not formally compared in this experiment. In order to confirm this observation, two groups of mice were engrafted side-by-side; with one group receiving $CD34^+$ Lonza cells and one group receiving CD3 depleted UCB cells (Fig 5.6). The mice were then assessed together at 9 weeks post engraftment. The results showed that mice reconstituted with enriched $CD34^+$ cells from Lonza had significantly higher levels of human leukocytes in their circulation compared to mice reconstituted with $CD3^+$ cell depleted UCB cells. The reason for this is unclear, however, it may be related to the age of the cord blood (It was a minimum of 24 hours before isolation of $CD34^+$ cells could be performed). Regardless, it was decided that for future

experiments, isolated $CD34^+$ cells purchased from Lonza would be used for the generation of humanised mice.

Due to differing levels of engraftment, human cells of the lymphoid lineage have been more extensively studied than cells of the myeloid lineage in humanised mice (Discussed in detail in Chapter 1). As a consequence of this, early attempts to characterise the humanised mice in this study focused on the identification of human $CD19^+$ B cells and human $CD3^+$ T cells.
Mice were exsanguinated at 12 weeks post engraftment and their bone marrow and spleens were harvested for analysis. Human $CD45^+$ cells were identified in the bone marrow, spleen and peripheral blood of all mice tested (Fig 5.7). Consistent with their roles in leukocyte production and storage, the bone marrow and the spleen of all mice tested contained a large numbers of $CD45^+$ cells. Furthermore, the majority of human $CD45^+$ cells found, in the bone marrow, spleen and peripheral blood, were $CD19^+$ B cells (Fig 5.8). $CD3^+$ T cells were found to be present in the spleen and blood but not the bone marrow of mice tested. As T cells are generated in the thymus and not the bone marrow the lack of T cells in the bone marrow of these mice was unsurprising. In fact, it was the presence of T cells in both the spleen and the peripheral blood of these mice that was surprising. Indeed, previous study has shown that NOD-scid $IL2\gamma^{-/-}$ mice engrafted with HSC as adults do not support engraftment of human T cells [128]. The reason for this discrepancy is unclear, however, as the mice were healthy and the percentage of human T cells was still relatively low it seems unlikely to be due to T cell contamination of the $CD34^+$ cell preparation used to engraft the mice.

It has been shown that human leukocytes, primarily lymphocytes, are reconstituted in adult irradiated NOD-scid $IL2\gamma^{-/-}$ mice engrafted with enriched $CD34^+$ stem cells. The reconstitution of human myeloid cells, with a particular focus on neutrophils, will be discussed in the following chapters.

6.1 Introduction

Neutrophils are one of the most important cells in the host defence against pathogens. They are the first leukocytes to be mobilised in response to infection and they serve to launch the immune response [297]. Importantly, neutropenia leads to sepsis and death [298]. Although they are essential for our survival, neutrophils can also cause unwanted inflammation and pathology during systemic infection or autoimmune disease. Therefore, an understanding of neutrophil biology in health and disease is a priority in medical research. Unfortunately neutrophils are short-lived cells that are easily activated and thus are difficult to study *in vitro* (Discussed in Chapter 3 and Chapter 4). To further complicate matters significant differences in human and mouse neutrophils have been found. For example, there are important differences in the roles and structure of key molecules such as serine proteases [299]. Indeed, as mention in Chapter 1, and discussed further in Chapter 7, it is likely that it is the differences between human and mouse PR3 that prevents the development of a mouse model of anti-PR3 ANCA associated vasculitis. Therefore, the development of humanised mice with functional human neutrophils may be an important step in advancing our ability to study these cells.

Up until this point, neutrophils in humanised mouse models have received relatively little attention. In one report, human neutrophils, defined as $CD66b^{+}CD10^{+}$ cells, were identified in humanised mice using the zymosan induced air pouch model of inflammation [300]. Another report identified neutrophils, defined as $CD15^{+}CD14^{-}$ cells, in the bone marrow and spleen of human HSC engrafted mice [301]. Neutrophils were also identified in the bone marrow of the thrombopoeitin knockin mice, as $CD33^{+}CD66^{hi}$ cells [302]. In a more recent study, the differentiation of human myeloid subsets was studied in NOD-scid $IL2\gamma^{-/-}$ mice engrafted as neonates [165]. Granulocytes identified in the bone marrow and spleen of these mice included $CD15^{+}CD33^{low}$HLA-DR^{-} neutrophils, $CD117^{-}CD123^{+}CD203c^{+}$ basophils and $CD117^{+}CD123^{+}CD203c^{+}$HLA-$DR^{-}$ mast cells.

It is important to note that in each of these studies neutrophils were identified based on their expression of a different set of surface markers. Indeed, this is an important issue as the majority of neutrophil surface markers are also expressed by other granulocytes. Consequently, care must be taken when attempting to identify neutrophils in humanised mice.

CD66b is a single chain GPI-linked member of the carcinoembryonic antigen (CEA) family of Ig domain containing glycoproteins [303]. It is expressed exclusively on granulocytes (neutrophils, eosinophils and basophils) where it is thought to mediate cell-cell adhesion. Indeed, the cross-linking of CD66b with monoclonal antibodies can stimulate the adhesion of neutrophils to endothelial cells in an integrin dependent manner [304]. Furthermore, CD66b molecules have been shown to be involved in regulating the adhesion and activation of eosinophils [305].

CD16 (FcγRIII) is a low affinity IgG receptor and is a member of the same family as CD64 (FcγRI) and CD32 (FcγRII). There are two CD16 isotypes: CD16a is a transmembrane molecule with a distinct cytoplasmic domain found on monocytes/macrophages, NK cells, mast cells, T cells and T- and B-cell progenitors, while CD16b is a GPI linked molecule thought to be found exclusively on neutrophils [306, 307]. While CD66b is expressed by granulocytes (not including mast cells), neutrophils are the only one of these cells widely believed to also express CD16. Indeed, the presence of CD16 on neutrophils, and its usual absence on eosinophils and basophils, is the basis of the use of CD16-negative selection for the separation of these cells from neutrophils [308, 309]. Therefore, cells that express both CD66b and CD16 can be defined as neutrophils. Finally, CD16 appears late during neutrophil development and thus can be used as a rough marker of neutrophil maturation [307].

In this chapter the reconstitution of functional human neutrophils in humanised mice was examined. Human GCSF was used to mobilise neutrophils from the

bone marrow into the peripheral blood and the response of these neutrophils to inflammatory stimuli was tested both *in vivo* and *in vitro*.

6.2 Aims

- To identify human neutrophils in a humanised mouse model
- To expand the population of human neutrophils
- To investigate the functional responses, both *in vivo* and *in vitro*, of human neutrophils reconstituted in humanised mice

6.3 Methods

6.3.1 Engraftment of NOD-scid IL2$\gamma^{-/-}$ mice

Humanised mice were generated as described in Section 2.2.11. Briefly, mice were engrafted by injecting $1x10^5$ human cord blood $CD34^+$ stem cells, purchased from Lonza, into 6-12 week old NOD-scid IL2$\gamma^{-/-}$ mice approximately 4 hours post irradiation at 2.4Gy with a Cs-source irradiator.

6.3.2 Flow cytometry

Mouse blood and tissue was collected as described in Section 2.2.13.1 and flow cytometry was performed as described in Section 2.2.1. The antibodies used are shown in Table 6.1 and 6.2. Absolute numbers of human and mouse cells were calculated from whole blood counts, performed as described in Section 2.2.2, and flow cytometry data

Target	Isotype	Clone	Fluorophore	Supplier	Dilution
CD11b	Mouse IgG1, κ	ICRF44	APC	BD	1:6
CD16	Mouse IgG1, κ	3G8	APC	BD	1:20
CD16	Mouse IgG1, κ	3G8	PerCP-Cy5.5	BD	1:20
CD45	Mouse IgG1, κ	HI30	V450	BD	1:101
CD62L	Mouse IgG1, κ	DREG-56	PerCP-Cy5.5	Biolegend	1:6
CD63	Mouse IgG1, κ	H5C6	PE	BD	1:6
CD66b	Mouse IgM, κ	G10F5	FITC	BD	1:12
CD66b	Mouse IgM, κ	G10F5	PE	Biolegend	1:12
CD66b	Mouse IgM, κ	G10F5	PerCP-Cy5.5	Biolegend	1:20
PR3	Mouse IgG1, κ	PR3G-2	FITC	Hycult	1:50
Control	Mouse IgG1, κ	MOPC-21	FITC	Biolegend	1:250
MPO	Mouse IgG1, κ	MPO-7	APC	Dako	1:12.5
Control	Mouse IgG1, κ	MOPC-21	APC	Biolegend	1:50

Table 6.1 Anti-human antibodies used for flow cytometry. All antibodies were obtained from commercial sources.

Target	Isotype	Clone	Fluorophore	Supplier	Dilution
CD45	Rat (LOU) IgG2b, κ	30-F11	FITC	BD	1:250
Ly-6G	Rat (LEW) IgG2b, κ	IA8	AlexaFluor 700	BD	1:200

Table 6.2 Anti-mouse antibodies used for flow cytometry. All antibodies were obtained from commercial sources.

6.3.3 Expansion of human neutrophils *in vivo*

Mice were bled from the saphenous vein between 2 and 6 months post engraftment and given 50μg human pegylated GCSF (Neulasta ®, from Amgen, Cambridge, UK) subcutaneously. Five days later the mice were bled again from the saphenous vein their engraftment levels were assessed using flow cytometry.

6.3.4 Measuring activation of human neutrophils *in vivo*

Mice were bled via the saphenous vein and then treated with 50μg human pegylated GCSF (Neulasta ®, from Amgen, Cambridge, UK). 5 days later they were rebled and then given 10μg highly purified LPS from *E.coli*, Serotype R515 (Enzo Life Sciences, Exeter, UK) intraperitoneally. Two hours later the mice were bled from the axillary vessels under terminal anaesthesia and their lungs were either harvested for flow cytometric analysis as described in Section 2.2.13 or collected for histological analysis as described in Section 2.2.16. All blood was taken into lithium heparin tubes. Total leukocyte counts were obtained as described in Section 2.2.2.

6.3.5 Immunofluorescence staining

Frozen lung sections were cut and stained as described in Section 2.2.17 using the antibodies shown in Table 6.3.

Target	Isotype	Clone	Fluorophore	Supplier	Dilution
Human CD66b	IgG1	80H3	NA	Serotec	1:100
Mouse IgG	Goat IgG Fc fragment specific	-	Dylight 488	Jackson's ImmunoResearch	1:100

Table 6.3 Antibodies used for immunofluorescence staining. All antibodies were obtained from commercial sources.

6.3.6 Neutrophil functional assays

Respiratory burst assays were carried as described in Section 2.2.7. Due to the significant spectral overlap between A) rhodamine 123 and FITC and B) rhodamine 123 and PE, human CD45-V450 and human CD66b-PerCP-Cy5.5 were used flow cytometry (See Table 6.1). Degranulation assays were carried

out as described in Section 2.2.8. Neutrophils were identified as human $CD45^+CD66b^+$ cells for both assays.

6.3.7 Staining for human PR3 and MPO

Immunostaining was performed as described in Section 2.2.14. Flow cytometry was carried out as described in Section 6.3.2. For flow cytometry data, neutrophils were identified as human $CD45^+CD66b^+$ cells.

6.3.8 Statistics

Statistics were performed using Graphpad Prism software (Graphpad Software Inc, La Jolla, CA, USA). Where two data sets from the same mouse were compared a paired t test was used, and for more than two data sets from the same mouse a repeated measures ANOVA with Dunnett's post test was used. For data from different mice an unpaired t test was used.

6.4 Results: Human neutrophils are mobilised in peripheral blood of humanised mice in response to human GCSF

6.4.1 Treatment with human GCSF increases the number of human neutrophils present in the peripheral blood of humanised mice

As established in the previous chapter, NOD-scid $IL2\gamma^{-/-}$ mice reconstituted with human $CD34^+$ UCB HSCs purchased from Lonza had high levels of human $CD45^+$ cells present in both their peripheral blood and bone marrow. To determine the percentage of these human cells that comprised human $CD66b^+$ granulocytes, humanised mice were sacrificed at 12 weeks post engraftment and their blood and bone marrow cells were assessed using flow cytometry. On average 60.33% of the leukocytes present in their peripheral blood of the humanised mice were of human origin (Fig 6.1 A). Of these human $CD45^+$ cells less than 0.4%, on average, were also positive for human CD66b (Fig 6.1 B). Notably, significantly more human leukocytes were found in the bone marrow than in the peripheral blood of these mice (Mean 75.34%).

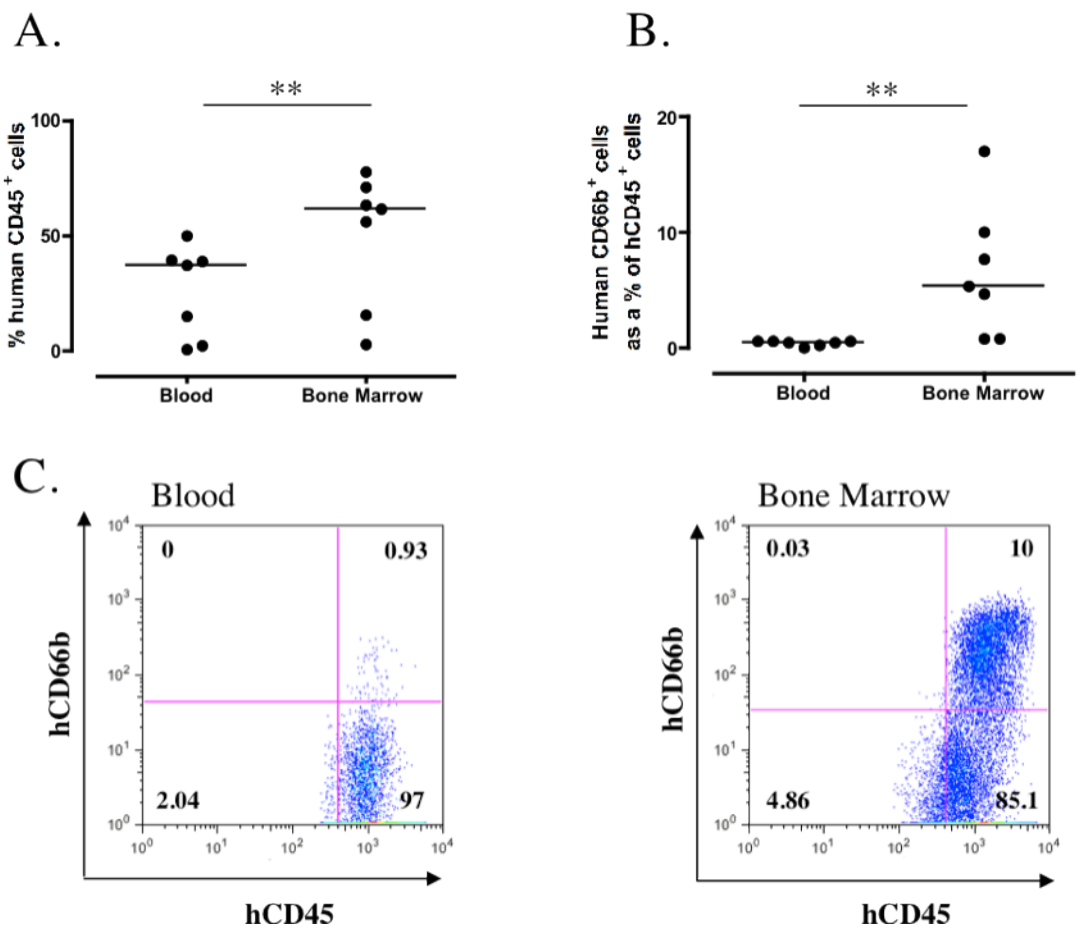

Figure 6.1 Reconstitution of human granulocytes in the peripheral blood and bone marrow of humanised mice. (A) Engraftment of human (h)CD45$^+$ cells. (B-C) Engraftment of hCD66b$^+$ granulocytes as a percent of human CD45$^+$ cells. (B) Data for all mice, with the median of each group indicated by the horizontal line, together with (C) representative FACS plots are shown.

More importantly, however, human $CD66b^+$ granulocytes represented a significantly higher percentage of the human $CD45^+$ cells in this compartment (Mean 6.62% of the human $CD45^+$ cells) (Figure 6.1 B). Representative flow cytometry plots show the staining for human $CD45^+CD66b^+$ cells (Fig 6.1 C). Humanised mice at least 8 weeks post engraftment were injected, subcutaneously, with 50μg human pegylated GCSF in order to determine if these bone marrow human granulocytes could be mobilised into the peripheral blood (Fig 6.2). A human CD16 antibody was included in the staining to allow the identification of mature human neutrophils. Before GCSF treatment human $CD66b^+CD16^+$ neutrophils accounted for less that 1% of the human $CD45^+$ cells present in the peripheral blood of these mice (Mean 0.17%). This represented an average of $1.76x10^3$ total human neutrophils per mouse (Fig 6.2 A). The same mice were then assessed 5 days post GCSF and were to found have significantly more human neutrophils present in their peripheral blood. On average, 2.29% of human $CD45^+$ cells were also positive for human CD66b and CD16 post GCSF. This represented a new average of $16.28x10^3$ total human neutrophils per mouse. Representative flow cytometry plots show the staining for human $CD45^+CD66b^+CD16^+$ cells pre and post GCSF (Fig 6.2 B). This data was reanalysed to exclude the CD16 marker and thus show the effect of GCSF on the total human granulocyte population (Fig 6.3). Before GCSF treatment human $CD66b^+$ granulocytes accounted for approximately 0.25% of the human $CD45^+$ cells present in the peripheral blood of these mice. This represented an average of $3.04x10^3$ total human granulocytes per mouse (Fig 6.3 A). On average, 2.57% of human $CD45^+$ cells were also positive for human CD66b post GCSF. This represented an average of $18.57x10^3$ total human granulocytes per mouse. Representative flow cytometry plots show the staining for human $CD45^+CD66b^+$ cells pre and post GCSF (Fig 6.3 C). As can be inferred from a comparison of these two figures, and is confirmed in Table 6.4, the majority of human granulocytes (Mean±SEM 86.14±1.97%) in the peripheral blood of mice post GCSF are in fact positive for both CD66b and CD16 and thus can be characterised as mature neutrophils. Consequently, neutrophils will be defined as $CD66b^+$ cells in the rest of this chapter.

6.4.2 Human GCSF cross-reacts with mouse cells

The number of human and mouse $CD45^+$ cells were assessed both before and after GCSF administration (Fig 6.4). While GCSF treatment led to a dramatic decline in the percentage of human $CD45^+$ cells that comprised the leukocytes in the peripheral blood of these mice, it has no affect on the absolute number of human cells present (Mean $1.18x10^6$ human $CD45^+$ cells before GCSF vs $1.32x10^6$ human $CD45^+$ cells post GCSF) (Fig 6.4 A). In contrast, both the percentage and absolute numbers of mouse $CD45^+$ cells were significantly higher post GCSF treatment (Fig 6.4 B). Representative flow cytometry plots show the staining for human and mouse $CD45^+$ cells both before and after GCSF (Fig 6.4 C). An expansion in the number of peripheral blood mouse neutrophils in response to human GCSF was thought to be responsible for the increase in mouse $CD45^+$ cells. To investigate this, the total number of mouse $CD45^+$ leukocytes and $Ly6G^+$ neutrophils present in peripheral blood of humanised mice was assessed before and after GCSF treatment (Fig 6.5). The absolute numbers of mouse $CD45^+$ cells was significantly higher post GCSF administration (Fig 6.5 A). Importantly, this was mirrored by a similarly significant increase in the number of mouse $Ly6G^+$ neutrophils (Fig 6.5 B). Representative flow cytometry plots show the staining for mouse $CD45^+Ly6G^+$ cells, which was used to determine absolute numbers of mouse neutrophils both before and after GCSF (Fig 6.5 C)

6.5 Results: Human neutrophils present in the peripheral blood of humanised mice undergo functional responses *in vivo*

6.5.1 Human neutrophils respond to GCSF and LPS *in vivo* by augmenting their expression of activation markers

In order to establish if human neutrophils respond to inflammatory stimuli in an appropriate manner *in vivo*, the level of expression of four neutrophil

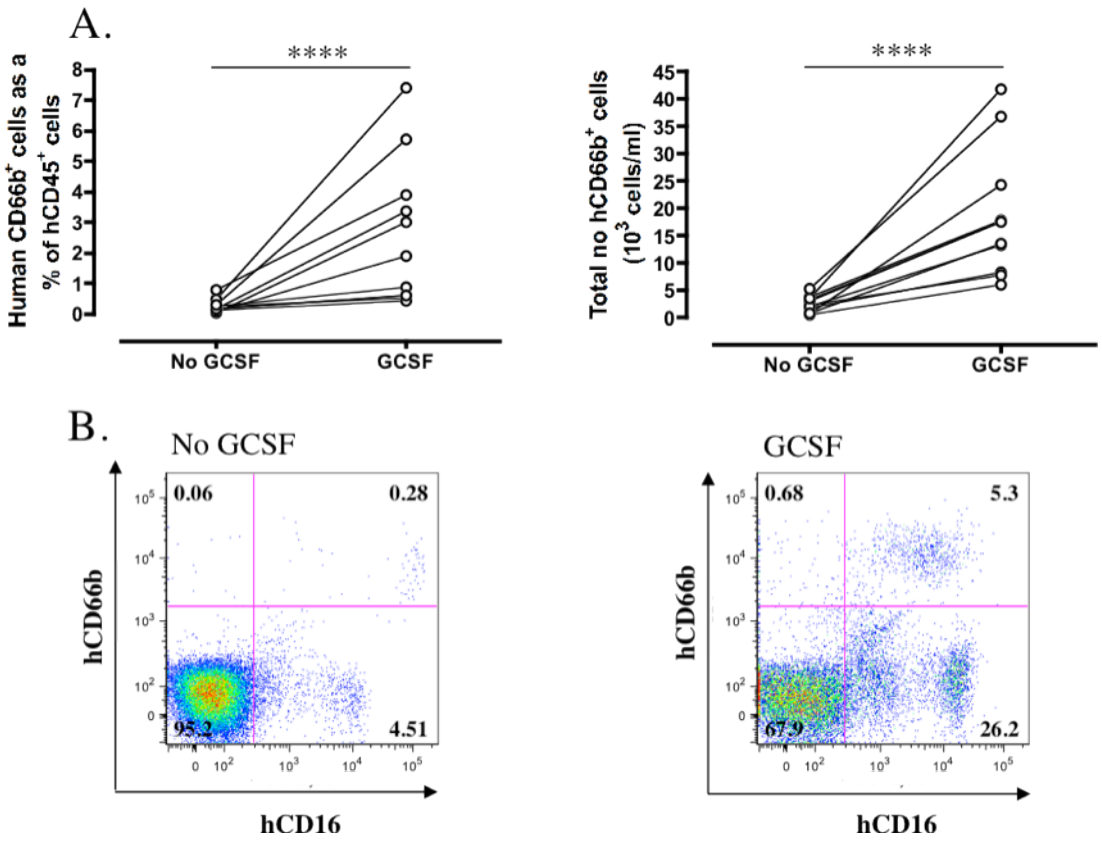

Figure 6.2 Human $CD66b^{+}CD16^{+}$ mature neutrophils in the peripheral blood of mice (n=11) before and after 5 days of GCSF administration. (A) Data are shown as a percent of human $CD45^{+}$ cells and as absolute numbers , with (B) representative FACs plots. **** $p<0.001$. Data was analysed using a paired t test.

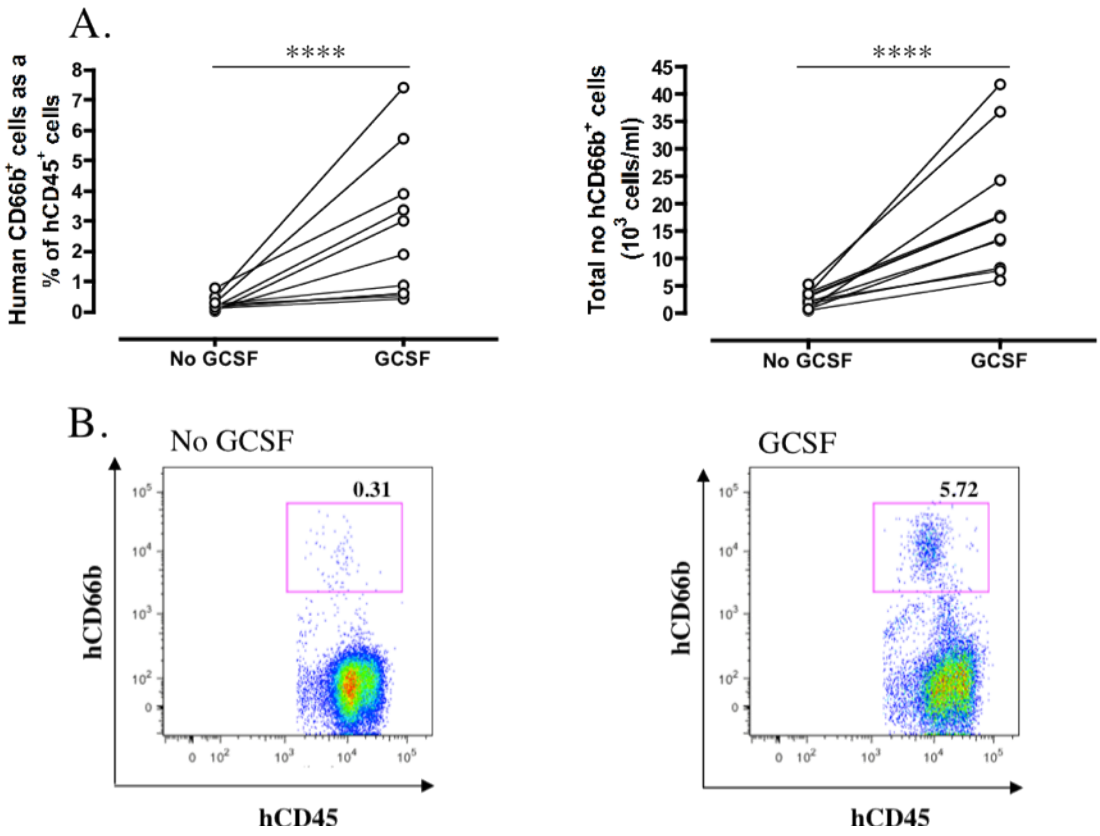

Figure 6.3 CD66b$^+$ granulocytes in the peripheral blood of mice (n=11) before and after 5 days of GCSF administration. (A) Data are shown as a percent of human CD45$^+$ cells and as absolute numbers, with (B) representative FACs plots. **** p<0.001. Data was analysed using a paired t test.

Mouse	Total no. of human $CD66b^+$ granulocytes ($x10^3$)	Total no. of human $CD66b^+CD16^+$ neutrophils ($x10^3$)	$CD66b^+CD16^+$ neutrophils as a percent of $CD66b^+$ granulocytes
1	17.70	13.38	75.58
2	8.34	6.76	81.13
3	7.68	6.65	86.67
4	17.43	13.71	78.68
5	17.56	14.16	80.64
6	6.05	5.39	89.03
7	23.18	11.18	84.91
8	41.81	39.34	94.10
9	13.18	12.99	95.21
10	24.18	21.51	88.96
11	36.72	34.03	92.66
Mean±SEM	18.57±3.49	16.28±3.35	86.14±1.97

Table 6.4 Total number of granulocytes, defined as $CD66b^+$ cells, and mature neutrophils, defined as $CD66b^+CD16^+$ cells, in the peripheral blood of humanised mice post 5 day treatment with human GCSF. The percent of human granulocytes comprising neutrophils reconstituted in these mice is shown on the far right.

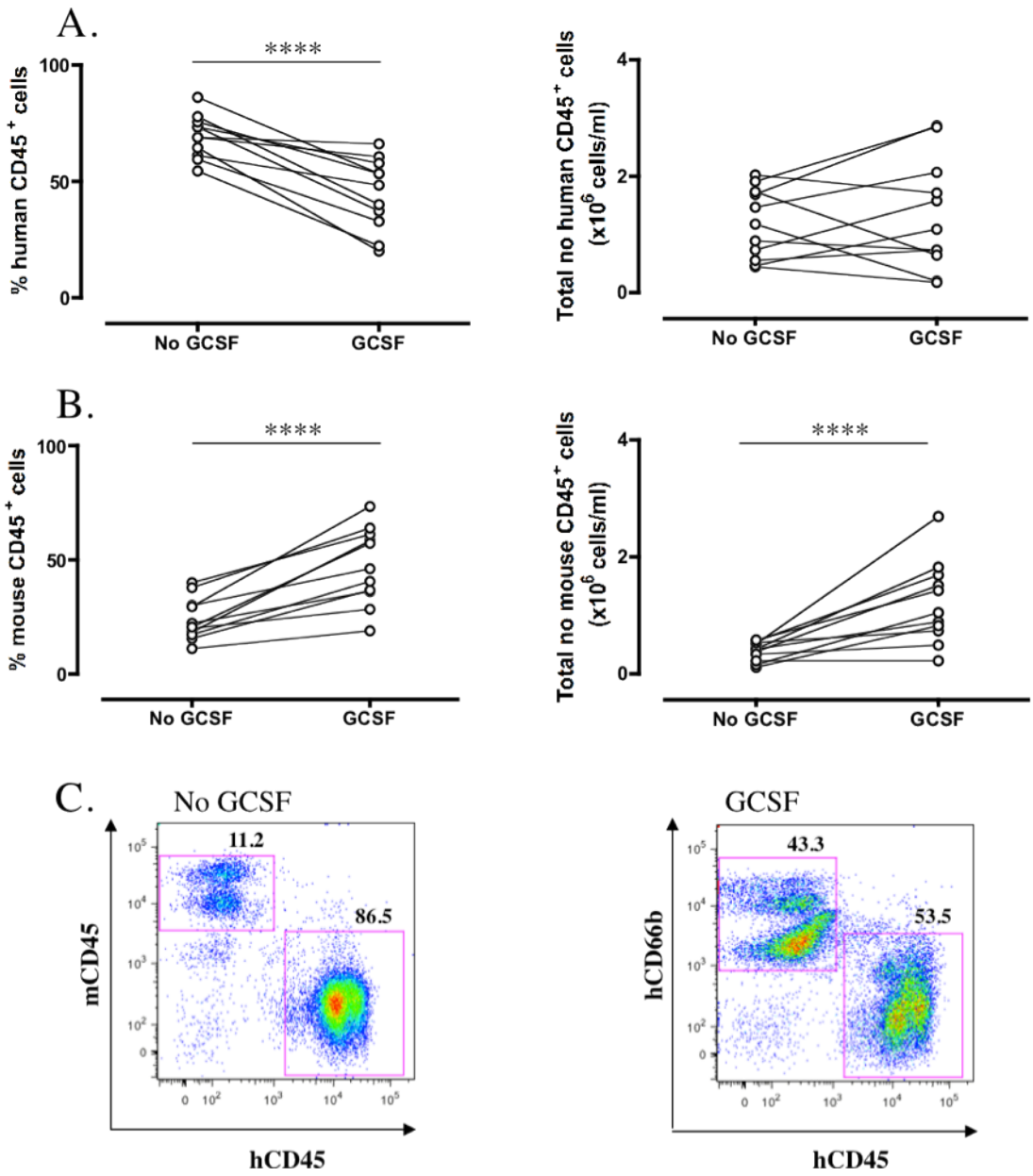

Figure 6.4 The effect of GCSF on (A) human and (B) mouse $CD45^+$ leukocytes in the peripheral blood of humanised mice (n=11) before and after 5 days of GCSF treatment. Data are shown as a percent of total leukocytes and as absolute numbers, with (C) showing representative FACs plots.**** $p<0.001$. Data was analysed using a paired t test.

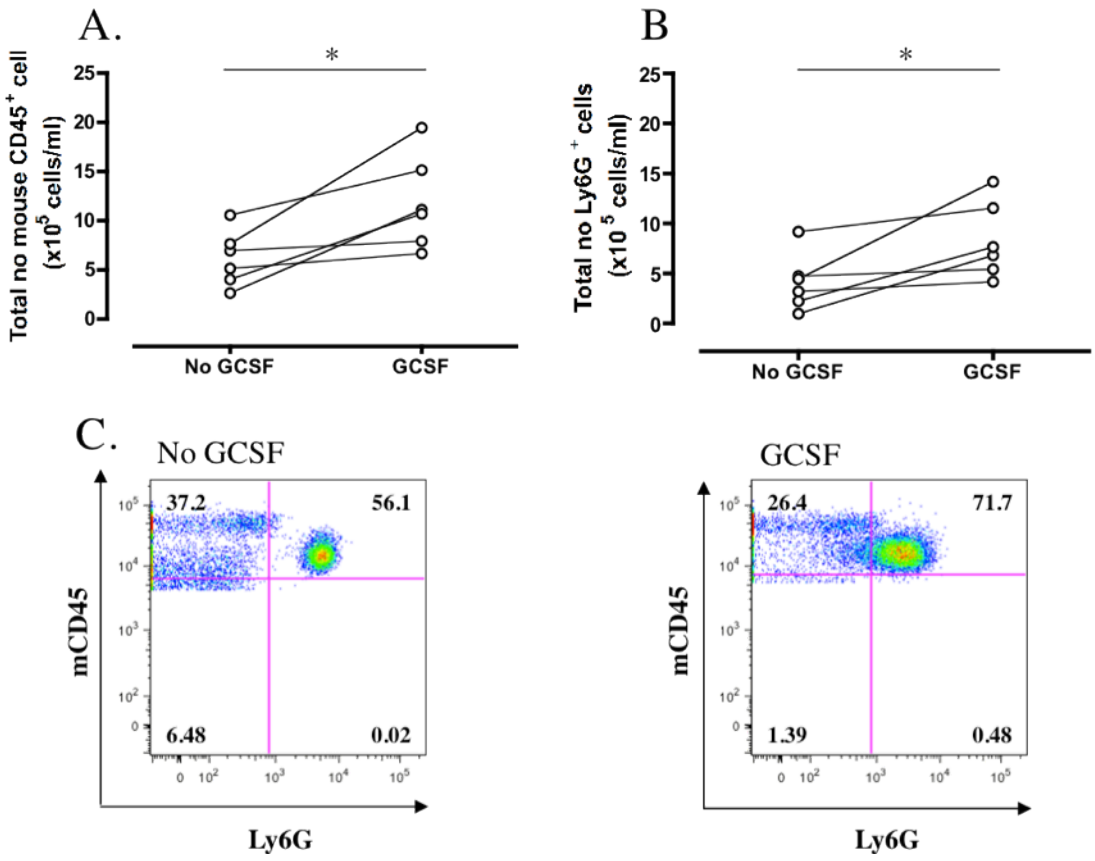

Figure 6.5 The increase in the number of mouse CD45$^+$ cells in humanised mice (n=7) in response to GCSF correlates with an increase in the number of mouse Ly6G$^+$ neutrophils. (A) Absolute numbers of mouse CD45 positive cells (B) Absolute numbers of mouse Ly6G$^+$ neutrophils (C) Representative FACs plots. * $p<0.05$. Data was analysed using a paired t test.

activation markers was measured, using flow cytometry, before and after 5 days of GCSF treatment, and 2 hours post subsequent LPS or PBS administration. It should be noted that flow cytometer settings were kept constant for this study, and although the pre and post GCSF samples were collected on different days, activation marker expression was analysed at the same time using Flowjo software. Furthermore, gates on the human $CD45^+CD66b^+$ cells were synchronised, thus ensuring there were identical gates in place for samples taken both before and after stimulation.

In addition to being a granulocyte marker, CD66b is upregulated in both primed and activated neutrophils. Therefore, CD66b expression in human $CD45^+CD66b^+$ cells before and after GCSF administration was assessed. As shown in Figure 6.6 A, CD66b was significantly upregulated post GCSF treatment. Importantly, the administration of LPS, but not PBS, resulted in a further and significant increase in the surface expression of CD66b (Fig 6.6 B). Concurrently, human CD11b expression was assessed and found to be significantly increased post GCSF (Fig 6.7 A). Subsequent LPS, but not PBS, administration resulted in a further, though not statistically significant, upregulation in CD11b expression (Fig 6.7 B). In addition to this, CD62L was found to be significantly downregulated in human neutrophils post GCSF treatment (Fig 6.8A). Notably, the administration of LPS, but not PBS, resulted in a further, and significant, shedding of CD62L by human neutrophils (Fig 6.8 B). Finally, the expression of human CD63 was examined and found to be significantly increased post GCSF (Fig 6.9 A). Surface bound CD63 expression was higher on the neutrophils of mice that had received LPS than on the neutrophils of mice that had received PBS (Fig 6.9 B).

6.5.2 Human neutrophils sequester in the lungs of humanised mice in response to LPS

The ability of human neutrophils to migrate to the lungs of humanised mice in response to LPS was investigated. Neutrophils were identified by human CD66b immunofluorescence staining of lung tissue taken at the end of the

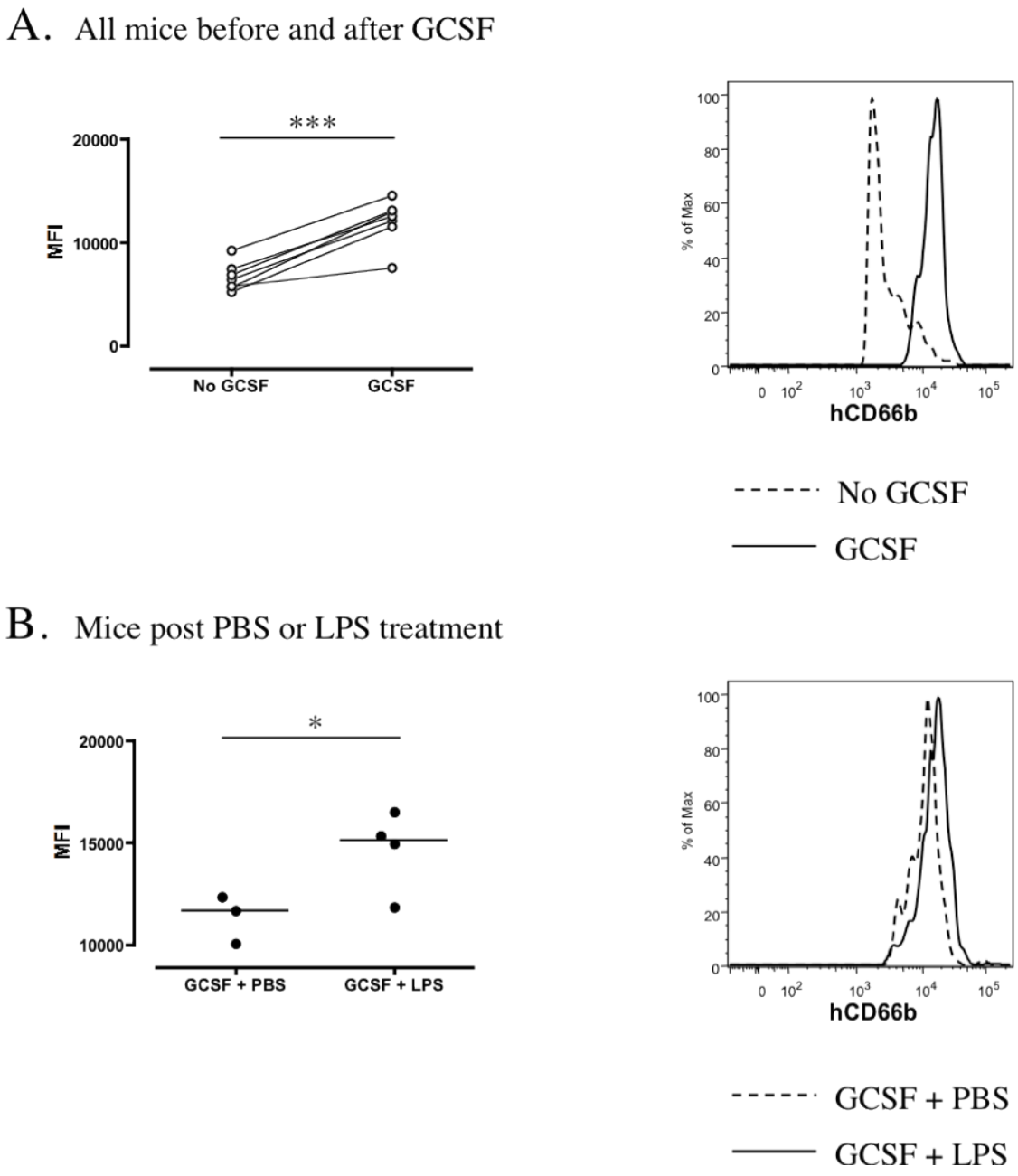

Figure 6.6 CD66b expression in peripheral blood neutrophils before and after (A) GCSF in all mice (n=7), and then either after subsequent (B) PBS (n=3) or LPS (n=4). Data for individual mice are shown on the left, with the median of each group indicated by the horizontal line, and representative histograms are shown on the right. *p<0.05, ***p<0.001. Data shown in (A) was analysed using a paired t test, while data shown in (B) was analysed using an unpaired t test.

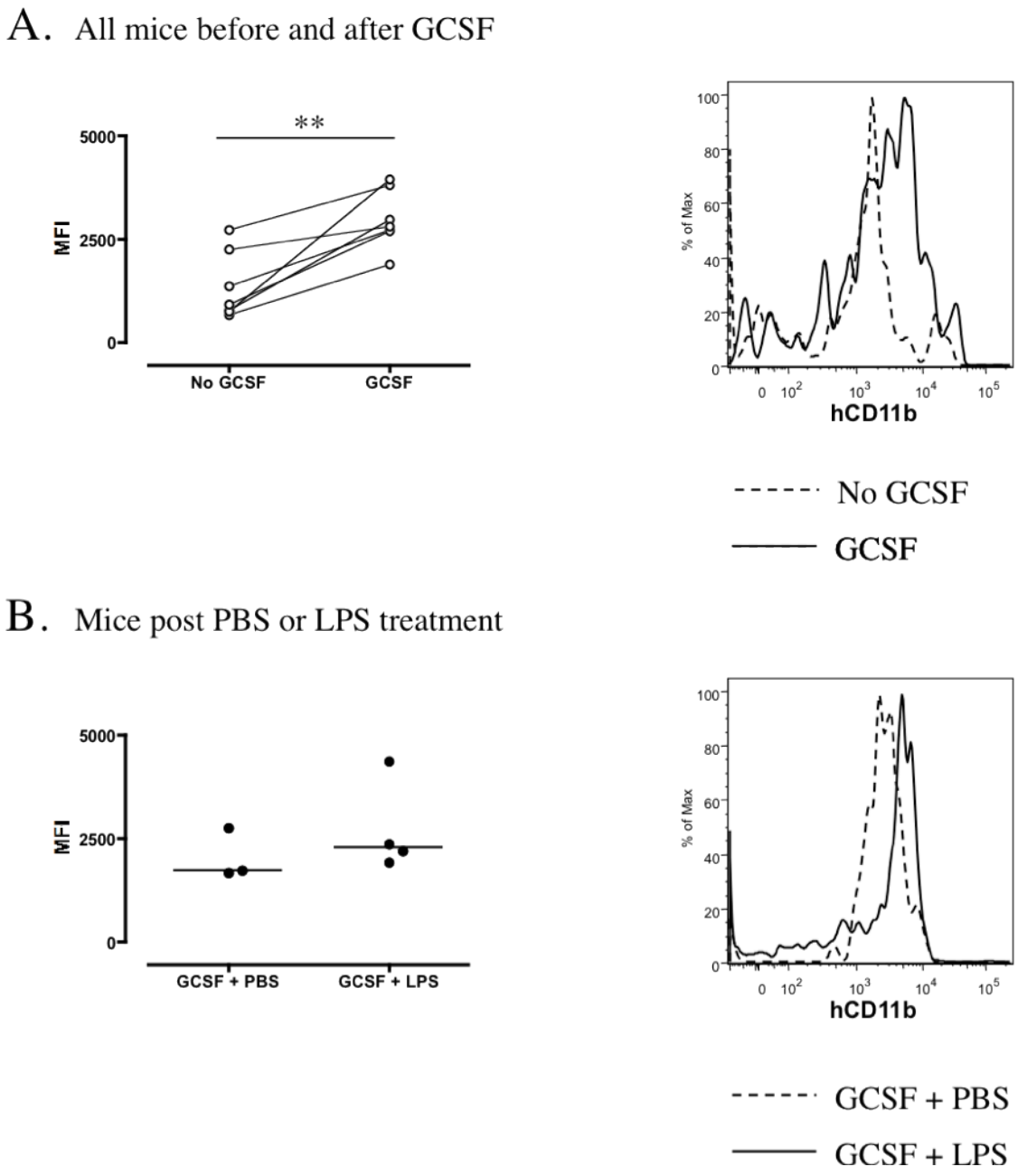

Figure 6.7 CD11b expression in peripheral blood neutrophils before and after (A) GCSF in all mice (n=7), and then either after subsequent (B) PBS (n=3) or LPS (n=4). Data for individual mice are shown on the left, with the median of each group indicated by the horizontal line, and representative histograms are shown on the right. **p<0.01. Data shown in (A) was analysed using a paired t test, while data shown in (B) was analysed using an unpaired t test.

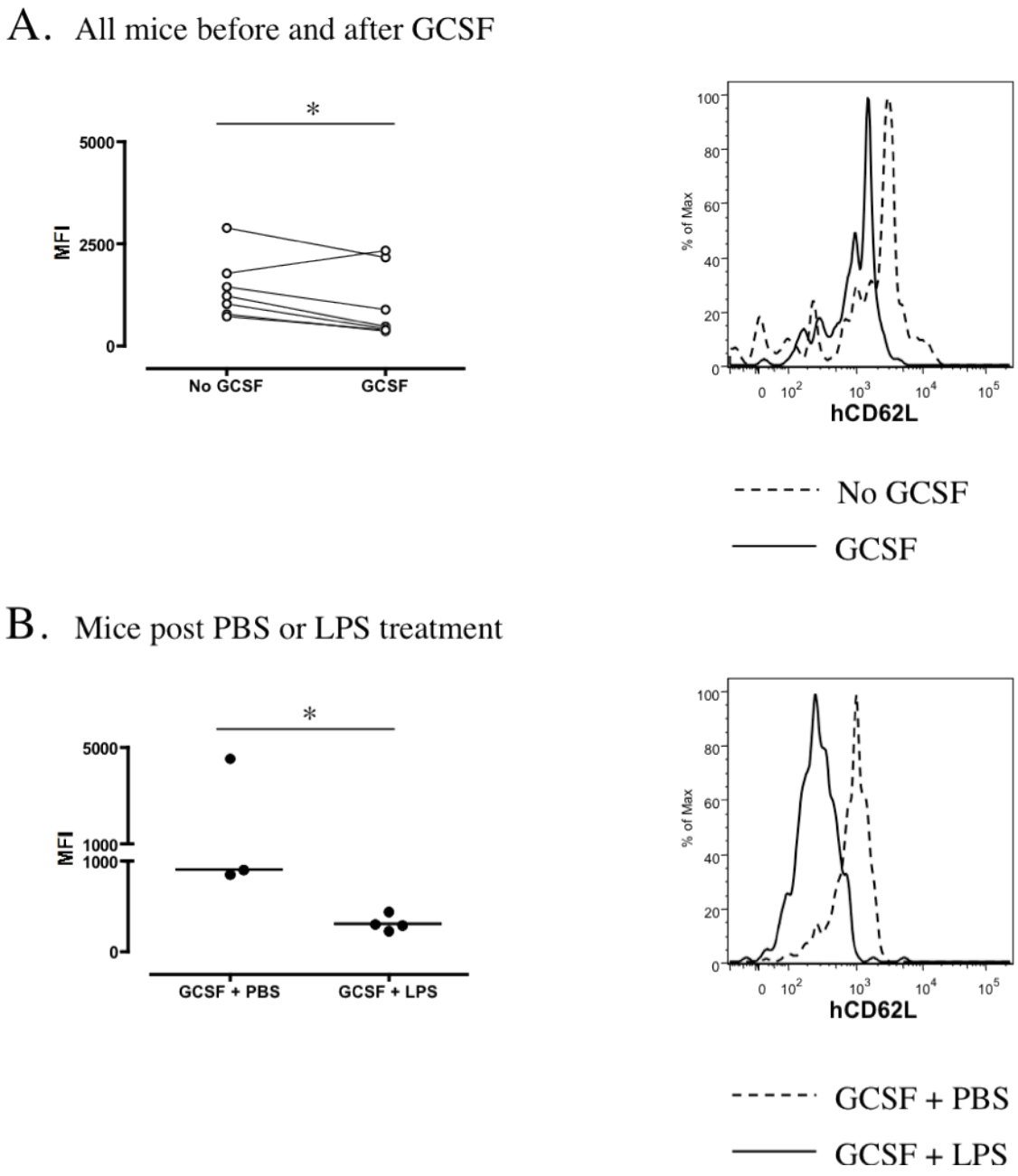

Figure 6.8 CD62L expression in peripheral blood neutrophils before and after (A) GCSF in all mice (n=7), and then either after subsequent (B) PBS (n=3) or LPS (n=4). Data for individual mice are shown on the left, with the median of each group indicated by the horizontal line, and representative histograms are shown on the right. *p<0.05. Data shown in (A) was analysed using a paired t test, while data shown in (B) was analysed using an unpaired t test.

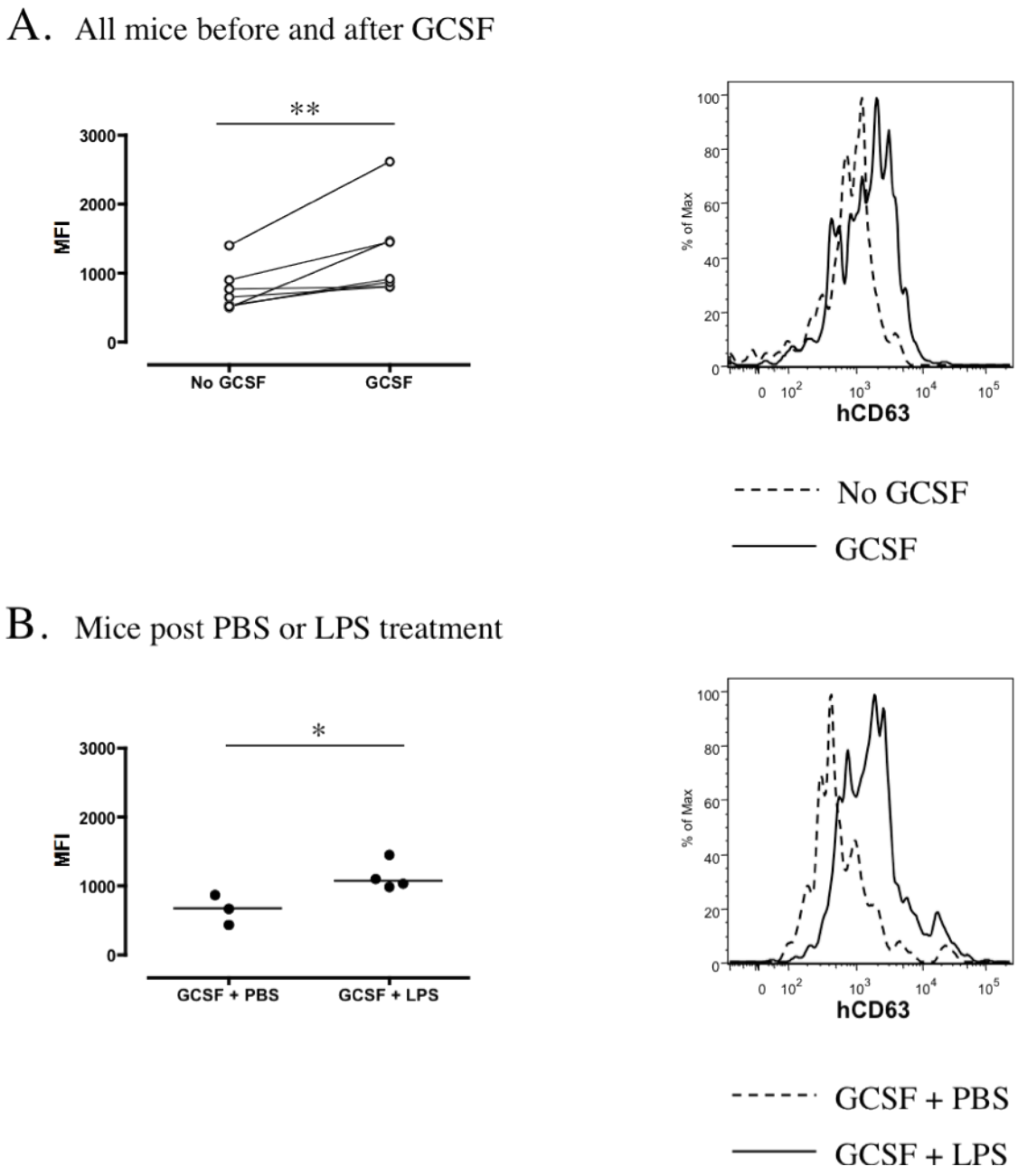

Figure 6.9 CD63 expression in peripheral blood neutrophils before and after (A) GCSF in all mice (n=7), and then either after subsequent (B) PBS (n=3) or LPS (n=4). Data for individual mice are shown on the left, with the median of each group indicated by the horizontal line, and representative histograms are shown on the right. *p<0.05, **p<0.01. Data shown in (A) was analysed using a paired t test, while data shown in (B) was analysed using an unpaired t test.

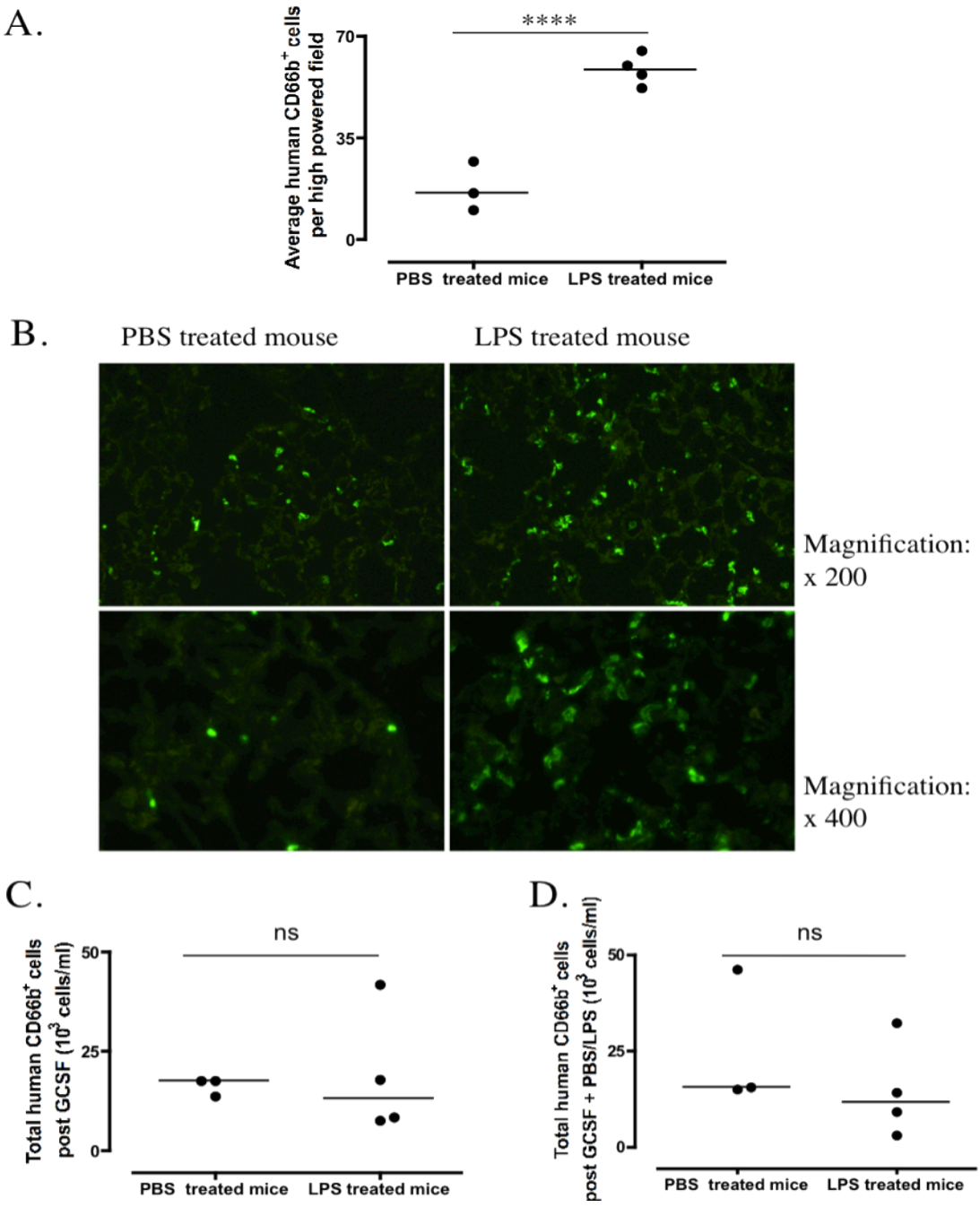

Figure 6.10 CD66b$^+$ human neutrophils in the lungs of mice 5 days post GCSF treatment and 2 hours post PBS (n=3) or LPS (n=4) administration. (A) Average number of human neutrophils per high powered field (B) Representative lung tissue showing immunofluorescence staining for CD66b. (C-D) Total number of peripheral blood neutrophils 5 days post GCSF (C) and 2 hours after subsequent LPS or PBS administration (D). ****p<0.0001. Data was analysed using an unpaired t test. The dot plots show the median values of the populations (horizontal line).

experiment described in Section 6.5.1. Neutrophil numbers and representative histology are shown in Figure 6.10 A-B. There were significantly more neutrophils seen in the lungs of mice receiving LPS compared to those given PBS (Fig 6.10 A). Furthermore, neutrophils were seen in the alveolar capillaries and were not located in the air spaces (Fig 6.10 B). When the total number of peripheral blood human neutrophils were compared in these two groups there was no difference observed either post GCSF pre LPS/PBS (Fig 6.10 C) or post GCSF and LPS/PBS (Fig 6.10 D). Finally, the activation status of human neutrophils, as measured by expression of CD66b, CD11b, CD62L and CD63, found in collagenase-digested lungs were assessed using flow cytometry (Fig 6.11). Lung neutrophils taken from mice that had received LPS expressed significantly more human CD66b than their counterparts taken from PBS treated mice (Fig 6.11 A). There was no difference in the expression of hCD11b (Fig 6.11 B), hCD62L (Fig 6.11 C) or hCD63 (Fig 6.11 D).

6.6 Results: Peripheral blood human neutrophils from humanised mice undergo respiratory burst and degranulate in response to fMLP and *E.coli in vitro*

The ability of human neutrophils generated by humanised mice to exhibit functional responses *in vitro* was examined. In order to avoid the complications and potential artifacts of neutrophil isolation whole blood assays were chosen for this purpose. It must be noted that all mice received human pegylated GCSF 5 days before the assays were performed. Whole blood human neutrophils from humanised mice underwent respiratory burst, as measured by the generation of rhodamine 123, in response to both fMLP and opsonised *E.coli* (Fig 6.12). While there was an increase in rhodamine 123 production in response to fMLP in 3 out of 4 mice, overall this did not reach statistical significance ($p=0.07$). In contrast, the human neutrophils from all mice produced more rhodamine 123 when stimulated with opsonised *E.coli* and this was statistically significant. Degranulation was measured by the upregulation of human CD63, CD66b and CD11b on the surface of human whole blood neutrophils. As shown in Figure 6.13, there was a significant

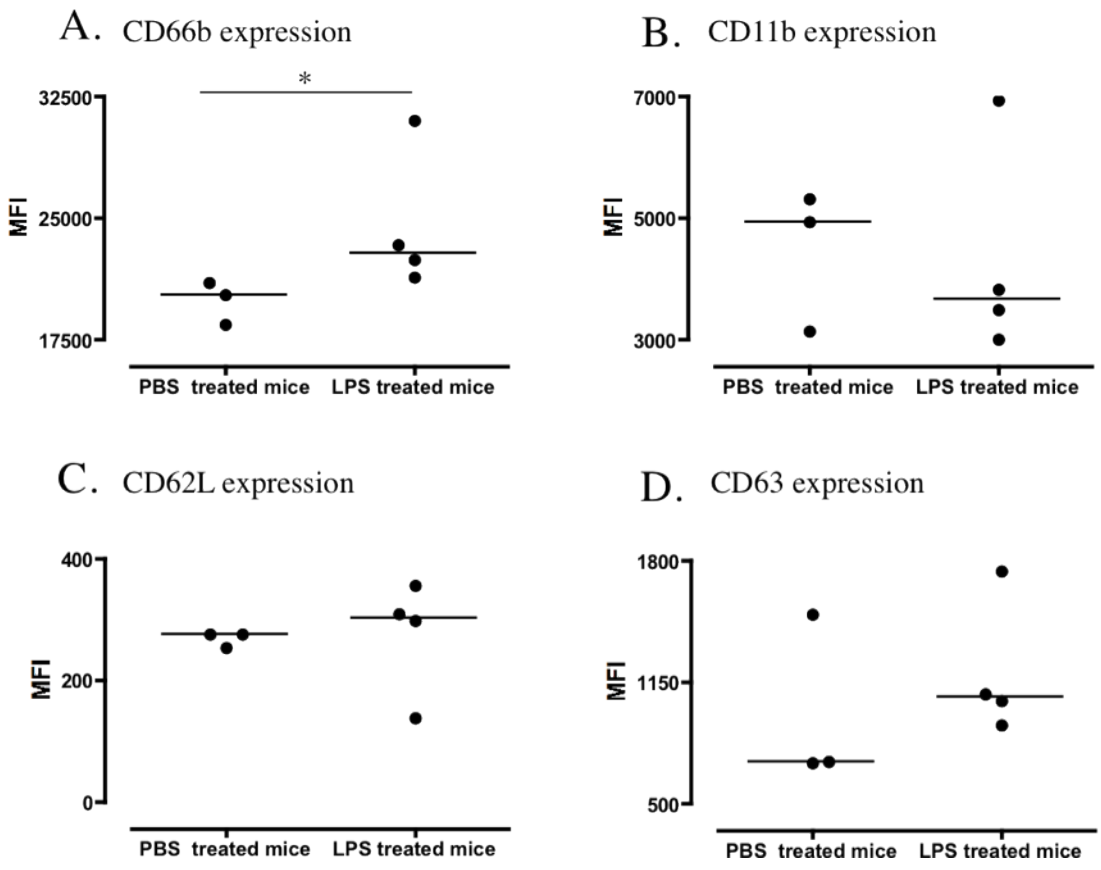

Figure 6.11 Phenotype of human $CD45^{+}CD66b^{+}$ neutrophils obtained from digested lung tissue showing expression of CD66b, CD11b, CD62L and CD63 in the same PBS (n=3) or LPS (n=4) treated mice from figure 6.10. *$p<0.05$. Data was analysed using an unpaired t test. The dot plots show the median expression levels (horizontal line).

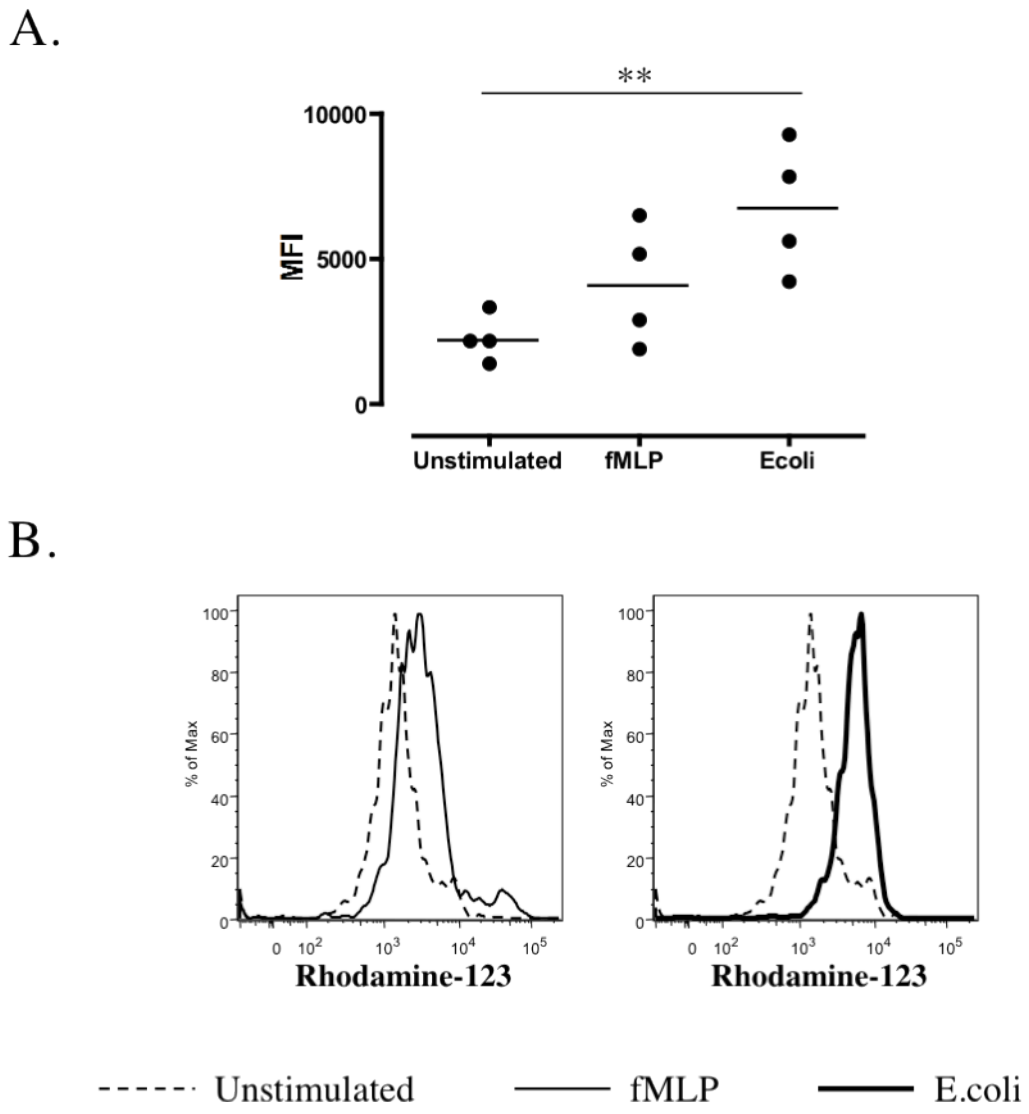

Figure 6.12 A respiratory burst shown by rhodamine 123 generation in response to fMLP or *E.coli* in a whole blood assay. All mice (n=4) had received GCSF 5 days prior to obtaining blood for the assays, and all data shown was obtained after gating on $hCD45^{+}hCD66^{+}$ cells. (A) Shows data for each individual mouse, with the median indicated by the horizontal line and (B) shows representative histograms. **p<0.01. Data was analysed using a repeated measures ANOVA with a Dunnett's post test.

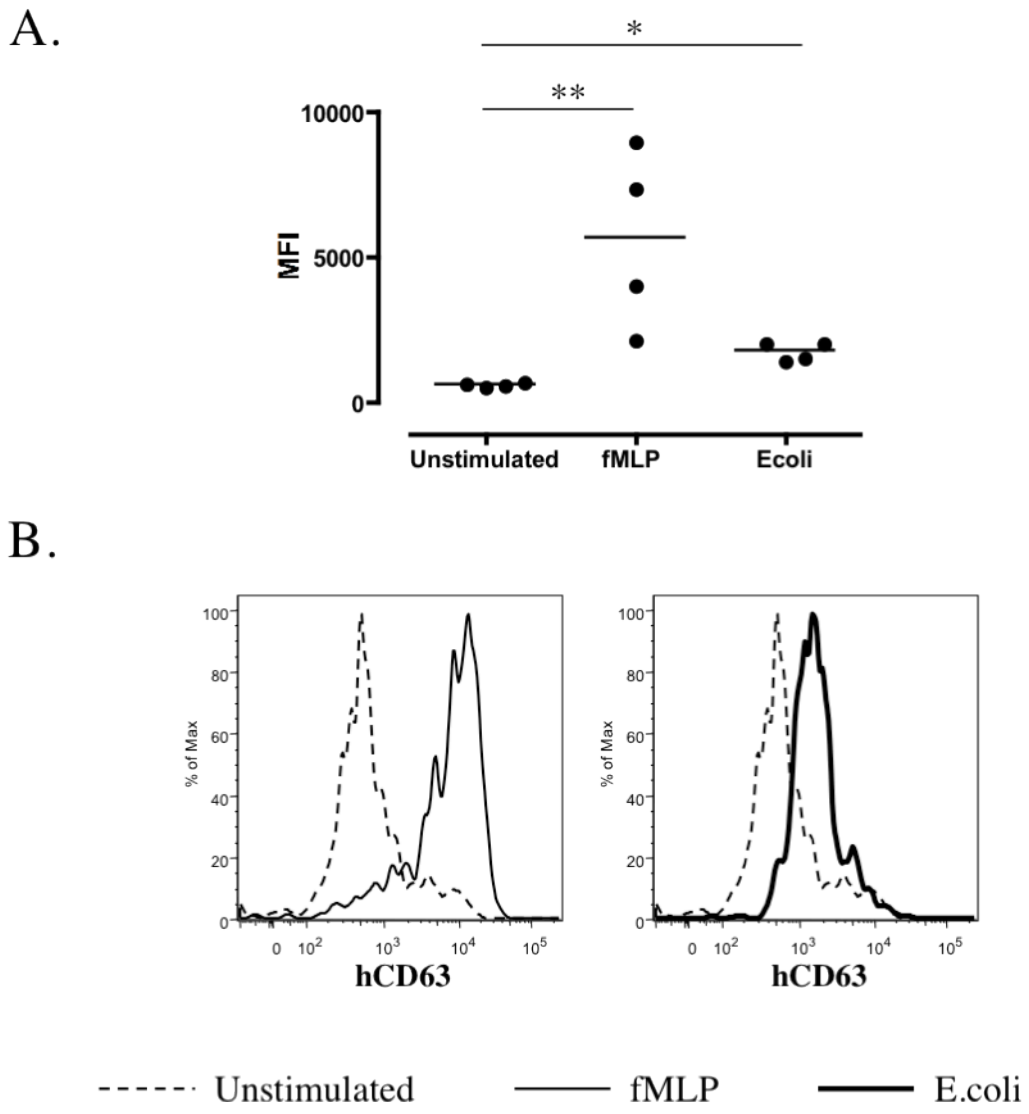

Figure 6.13 Expression of CD63 in response to fMLP or *E.coli* in a whole blood assay. All mice (n=4) had received GCSF 5 days prior to obtaining blood for the assays, and all data shown was obtained after gating on $hCD45^+hCD66^+$ cells. (A) Shows data for each individual mouse, with the median indicated by the horizontal line and (B) shows representative histograms. *p<0.05, ** p<0.01. Data was analysed using a repeated measures ANOVA with a Dunnett's post test.

increase in human CD63 in response to both fMLP and opsonised *E.coli*, though it was more marked for fMLP. Similarly, there was a significant increase in the surface expression of human CD66b in response to fMLP (Fig 6.14). However, CD66b expression was unchanged following stimulation with opsonised *E.coli*. Furthermore, while there was an increase in CD11b expression on the surface of human neutrophils in response to fMLP in 3 out of 4 mice, overall this did not reach statistical significance (p=0.059) (Fig 6.15). Finally, opsonised *E.coli* did not appear to induce human CD11b upregulation.

6.7 Results: Human neutrophils derived from the bone marrow of humanised mice express the ANCA antigens PR3 and MPO

The expression of human PR3 and MPO by human neutrophils generated by humanised mice was investigated. Bone marrow cells from HSC engrafted mice that had not received GCSF were fixed in ethanol and immunofluorescent staining for human PR3 and MPO was performed. Neutrophils were identified based on their morphology with the help of Hoeshst dye, which stains nuclei blue. Representative immunofluorescent staining demonstrating the present of human neutrophils expressing both PR3 and MPO is shown in Figure 6.16 A. In addition to this, flow cytometry was performed, gating on $hCD45^{+}CD66b^{+}$ cells, in order to confirm the presence of PR3 and MPO on the surface of human neutrophils (Fig 6.16 B).

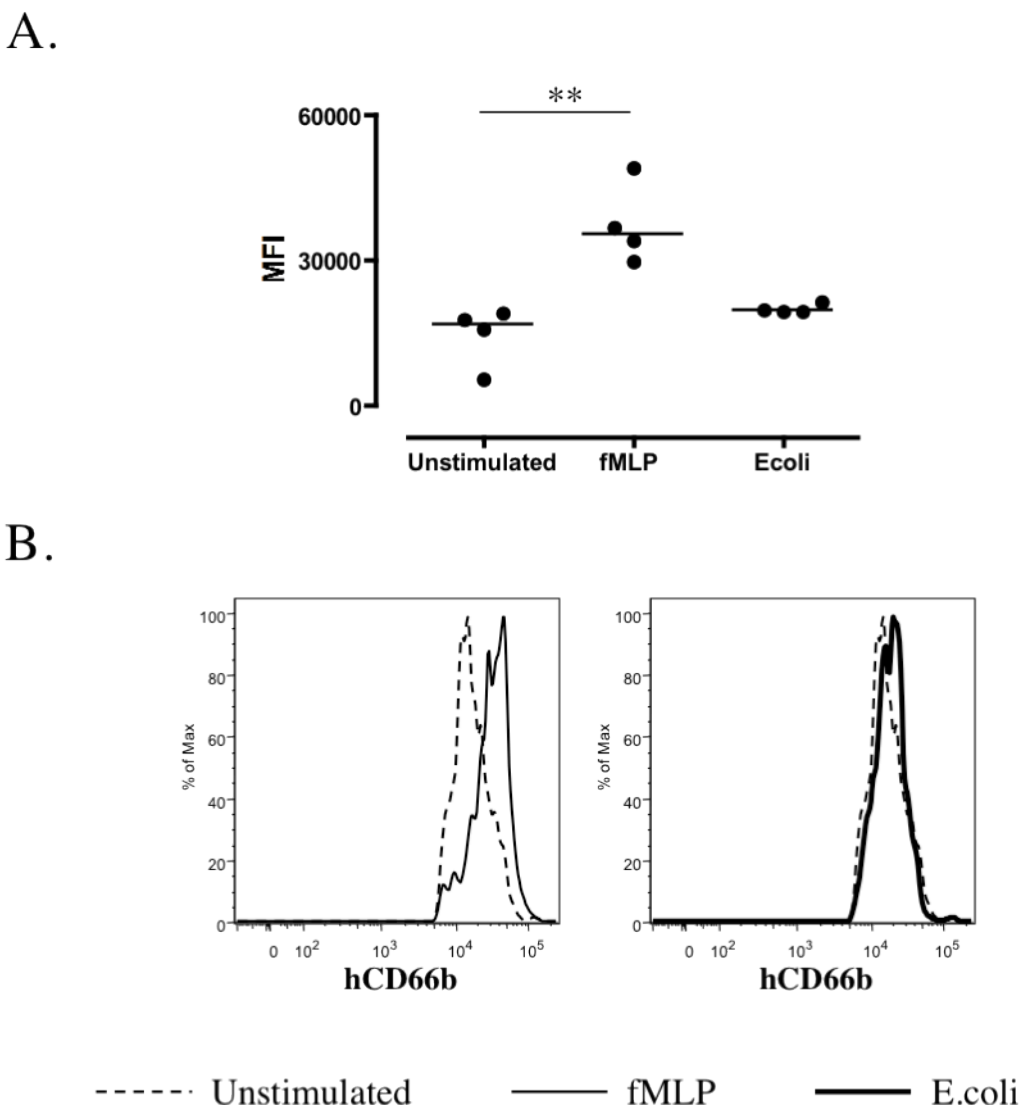

Figure 6.14 Expression of CD66b in response to fMLP or *E.coli* in a whole blood assay. All mice (n=4) had received GCSF 5 days prior to obtaining blood for the assays, and all data shown was obtained after gating on $hCD45^{+}hCD66^{+}$ cells. (A) Shows data for each individual mouse, with the median indicated by the horizontal line and (B) shows representative histograms. ** $p<0.01$. Data was analysed using a repeated measures ANOVA with a Dunnett's post test.

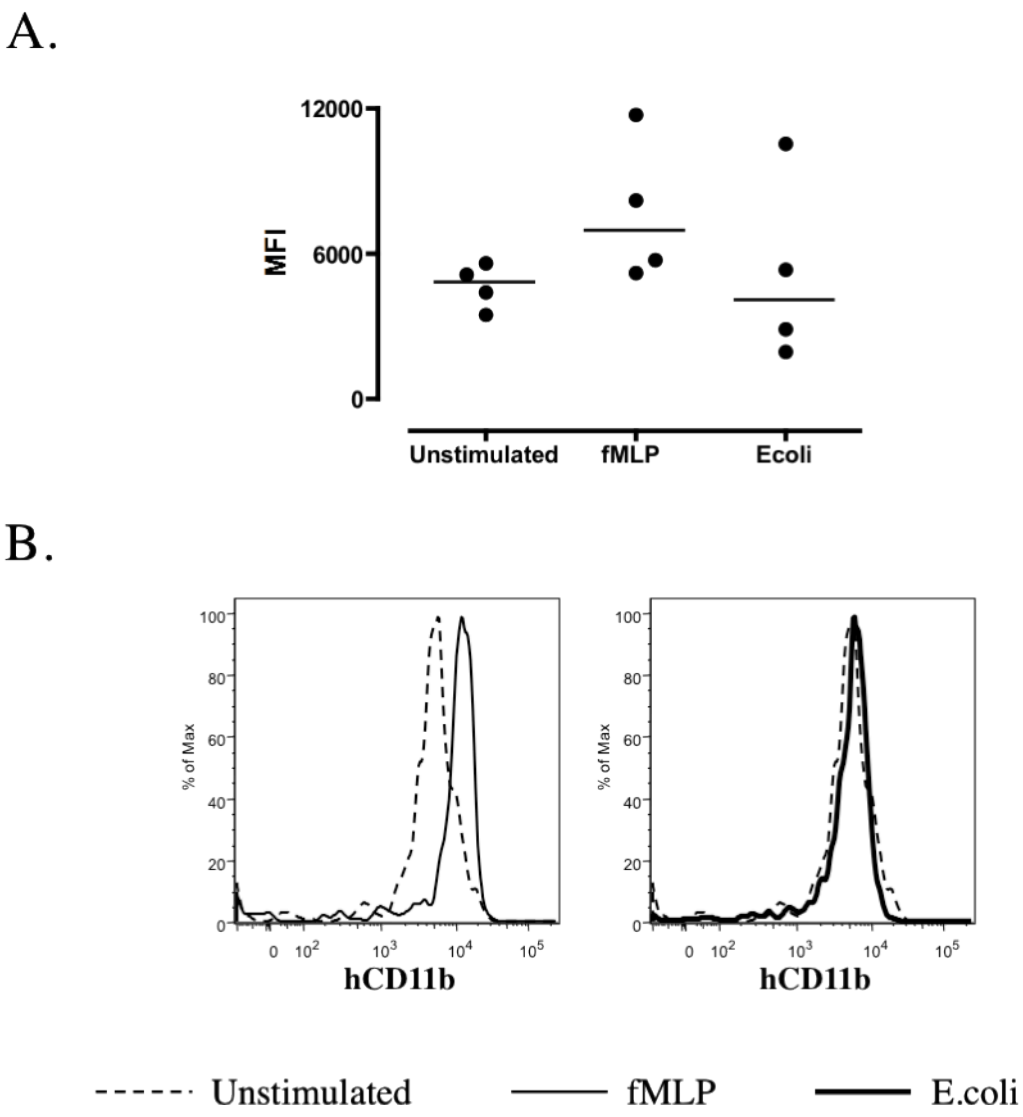

Figure 6.15 Expression of CD11b in response to fMLP or *E.coli* in a whole blood assay. All mice (n=4) had received GCSF 5 days prior to obtaining blood for the assays, and all data shown was obtained after gating on $hCD45^{+}hCD66^{+}$ cells. (A) Shows data for each individual mouse, with the median indicated by the horizontal line and (B) shows representative histograms. Data was analysed using a repeated measures ANOVA with a Dunnett's post test.

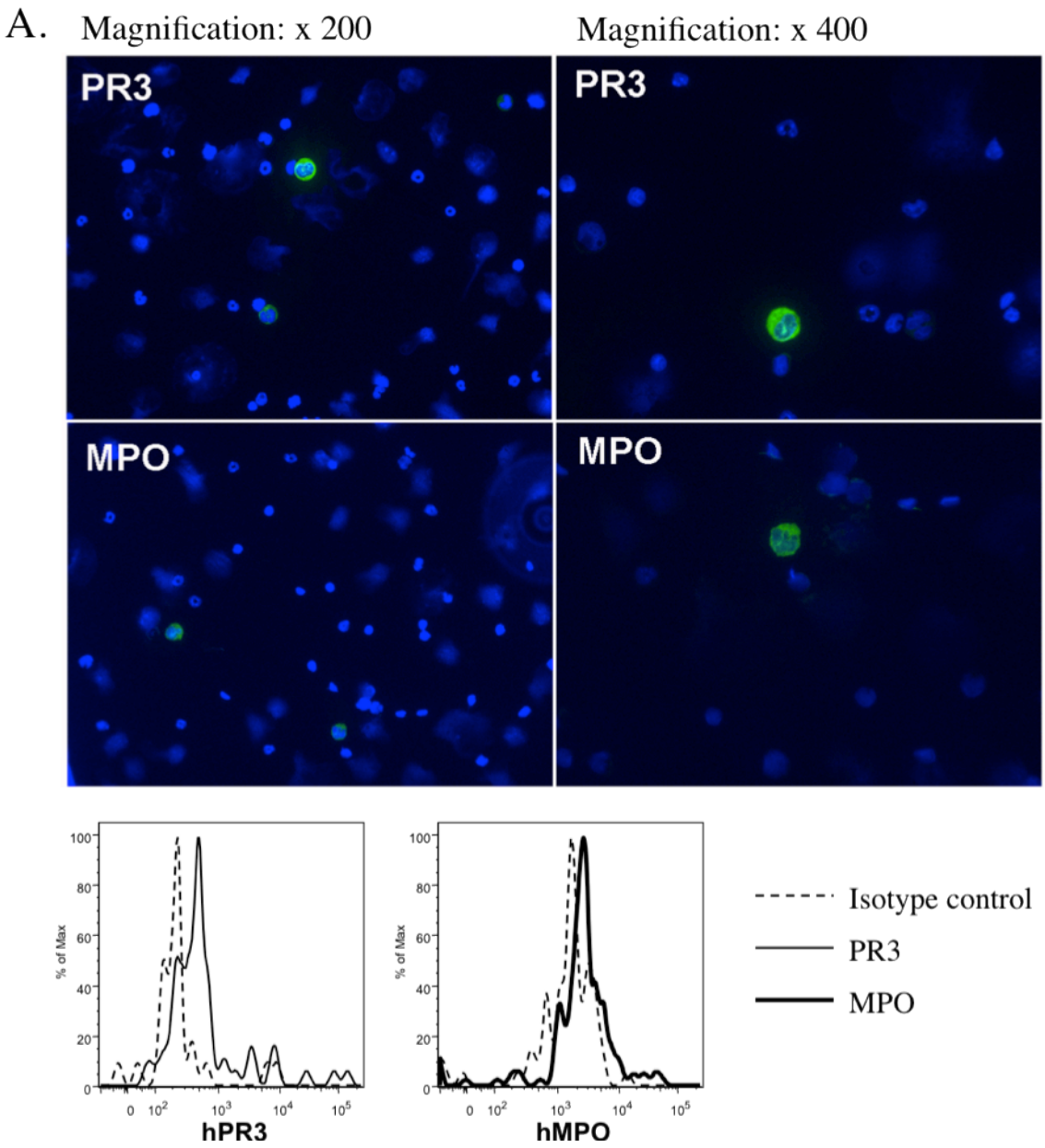

Figure 6.16 Human PR3 and MPO expression in bone marrow derived human CD66b$^+$ neutrophils in humanised mice. (A) Ethanol fixed bone marrow derived neutrophils showing immunofluorescence staining for human PR3 and MPO (Green). Hoechst dye (Blue) was used to stain the nuclei of the cells. Images are representative of 3 separate experiments (B) Human PR3 and MPO on the surface of human neutrophils as measured by flow cytometry and with gating on hCD45$^+$CD66b$^+$ cells (n=1)

6.8 Discussion

The role of GCSF in mobilising human neutrophils generated in humanised mice from the bone marrow into the circulation

Human granulocyte reconstitution in humanised mice is poor. While human granulocytes accounted for, on average, 6.62% of human cells in the bone marrow of humanised mice, they constituted, on average, only 0.4% of the human cells present in the peripheral blood (Fig 6.1). The relatively low frequency of human granulocytes both in the bone marrow and in the circulation is most likely due to an inadequate cytokine environment. Previous strategies to improve myeloid engraftment in humanised mice have included the transient expression of human cytokines through injection of viral vectors, the construction of transgenic mice with human transgenes, and the generation of knockin mice expressing human homologues of murine genes (Discussed in Chapter 1). The role of GCSF in neutrophil differentiation, mobilisation and activation has previously been discussed (Chapter 4). Since neutrophils are short-lived cells that develop rapidly when required, and long acting human GCSF is readily available, the more straightforward approach of direct injection of the cytokine protein was chosen for the purpose of expanding the population of peripheral blood neutrophils. In addition to being relatively easy from a technical standpoint, using this approach ensured that all mice had similar levels of cytokine, which may not be the case with the use of viral vectors for cytokine gene expression. As demonstrated, this strategy led to a dramatic increase in the number of peripheral blood circulating neutrophils, defined as $CD45^+CD66b^+CD16^+$ cells (Fig 6.2). It must be noted here that there was a decrease in the fluorescent intensity of the CD16 staining, however, this is agreement with previously published data [310]. These results correspond with those of a recent study in which it was demonstrated that humanised mouse bone marrow derived human $CD45^+CD33^+$ cells, which comprise neutrophils, monocytes and DCs, expressed the GCSF receptor [165]. In addition, it was shown that GCSF induced STAT3 and STAT5 phosphorylation in these cells *in vitro*. This is an important finding as STAT3 is thought to be essential for GCSF mediated

granulopoeisis, while STAT5 plays a role in the proliferation and survival of mature neutrophils. Finally, it was shown in this study that humanised mice treated with recombinant human GCSF for 5 days had an increase in the frequency of human $CD45^+CD15^+CD33^{low}$ neutrophils present in their circulation. Thus, this study together with the data shown here confirm that human bone marrow derived neutrophils generated in humanised mice are mobilised from the bone marrow into the peripheral blood in a similar manner to normal human neutrophils.

In addition to mobilising human granulocytes from the bone marrow of humanised mice into their circulation (Fig 6.2, 6.3), human GCSF also led to an increase in both the percentage and absolute number of mouse cells composing the population of leukocytes in the humanised mouse peripheral blood (Fig 6.4). This resulted in a corresponding decrease in the percentage of human $CD45^+$ cells, while leaving their total number largely unaffected. Given that human and mouse GCSF are approximately 76% identical at the amino acid level, and that the two proteins show species cross reactivity [311-313] it was theorised that the increase in the number of mouse cells was due to the mobilisation of mouse neutrophils from the bone marrow into the peripheral blood in response to GCSF. This was confirmed by the addition of an antibody against mouse neutrophil marker Ly6G in the analysis of a different group of mice that had received GCSF for 5 days (Fig 6.5). In this group, the increase in the number of mouse $CD45^+$ cells was closely mirror by an increase in the number of mouse $Ly6G^+$ cells present in the mouse peripheral blood.

GCSF and LPS induce humananised mouse human neutrophil activation in vivo

Technical difficulties, such as compensation issues and the instability of tandem conjugate fluorescent antibodies, arise when performing multicolour flow cytometry involving more than six colours. Consequently, and taking into account the importance of examining a wide range of neutrophil activation markers, it was decided to determine if, for the purpose of this study, CD66b

alone could be used to identify neutrophils. To achieve this, the data from the initial GCSF induced neutrophil mobilisation experiments (Fig 6.2) were reanalysed to exclude the CD16 marker (Fig 6.3). This allowed the number of human neutrophils ($CD45^+CD66b^+CD16^+$) present in the peripheral blood post GCSF to be expressed as a percentage of the total number of granulocytes ($CD45^+CD66b^+$)(Table 6.4). As can be seen the vast majority of $CD66b^+$ cells were also $CD16^+$ (Mean±SEM 86.14±1.97%) and thus the majority of granulocytes present in the peripheral blood post GCSF were in fact neutrophils. Furthermore, if it is taken into account that CD16 is only present on neutrophils during the last stages of development [307] then it is also possible that some of the $CD66b^+CD16^-$ cells are in fact immature neutrophils. Given both the normally small percentage of eosinophils (1-4%) and basophils (0.5-1%) present in the human circulation, and the low frequency of human basophils (0.1%) [165] found in the bone marrow and spleen of humanised mice, this is likely. Therefore, CD66b was used to identify neutrophils when investigating their ability to respond to stimuli *in vivo* and *in vitro*.

Neutrophils possess a wide array of activation markers, four of which were investigated using flow cytometry in the course of this study. Due to its abundance in the intracellular stores of neutrophils and its upregulation in response a variety of inflammatory stimuli, CD66b is not only a surface marker but also an activation marker for neutrophils [307]. Similarly, CD63 is present in the azurophilic granules of neutrophils and is translocated to the surface of activated cells [314]. Finally, both CD62L (L selectin) and CD11b are involved in neutrophil adhesion. CD62L, like other selectins, mediates the initial attachment of leukocytes to endothelial cells [286]. It is characteristically downregulated, or shed, in response to cell activation [287]. CD11b is a β_2-integrin that associates with CD18 to form Mac-1. Mac-1 mediates the firm adhesion of neutrophils to endothelial cells and is involved in the transmigration of neutrophils to sites of inflammation [287]. It is present in the membranes of secretory, gelatinase and specific granules of neutrophils [315] and is characteristically upregulated in activated cells.

For the study of neutrophil activation in response to GCSF *in vivo*, flow cytometer settings were kept constant and the expression of activation markers both before and after stimulation was analysed together using Flowjo software. Gates on the human $CD45^+CD66b^+$ cells were synchronised, thus ensuring there were identical gates in place for samples taken both before and after stimulation. All mice in this study received GCSF for 5 days. They were then divided into two groups with some given LPS and some PBS as a control. The expression of activation markers between the LPS and the PBS groups was compared 2 hours post administration with samples both run and analysed together. CD66b, CD11b and CD63 showed increased expression post GCSF (Fig 6.6. 6.7 and 6.9 respectively). Concurrently, CD62L expression was downregulated (Fig 6.8). This is entirely consistent with previous findings for these markers in humans [316, 317]. Furthermore, subsequent LPS but not PBS administration resulted in a significant increase in CD66b and CD63 expression and with further shedding of CD62L (Fig 6.6. 6.8 and 6.9, respectively). There was an upregulation in CD11b in response to LPS, however, when compared to PBS treated mice this was not statistically significant (Fig 6.7). It is possible that total CD11b expression, as measured here, was a poorly chosen marker of humanised mouse human neutrophil activation. Indeed, it has been shown *in vivo* that conformational activation of CD11b on mouse neutrophils can occur in the absence of total CD11b upregulation [318]. In addition, it was shown that, if present, the upregulation of total CD11b on mouse neutrophils *in vivo* is both mild and short lived. In contrast, a subpopulation of neutrophils was found to persistently express increased levels of the CD11b activation epitope CBRM1/5. Thus, it is likely that CD11b mobilisation from intracellular reservoirs and CD11b activation can be regulated independently by neutrophils in vivo, and that CBRM1/5 expression is a more sensitive marker of circulating neutrophil activation than total CD11b expression [318]. Despite this, taken together these results demonstrate that human neutrophils reconstituted by humanised mice are activated *in vivo* in a manner similar to normal human neutrophils.

Gram-negative sepsis is a major cause of mortality. Regardless of the source of sepsis a prominent pulmonary neutrophil influx often occurs and this lung

injury may be the major cause of death [319]. Consequently, the ability of neutrophils to traffic to the lungs in response to LPS was examined. There were significantly more neutrophils found in the lungs of mice receiving LPS than in those receiving PBS. Furthermore, the neutrophils were located in the alveolar capillaries and not found in the air spaces (Fig 6.10). Importantly, when the total numbers of peripheral blood neutrophils were compared, there was no difference found between mice receiving LPS or PBS. This confirms that neutrophils had migrated to the lung in response to LPS and the difference in numbers did not reflect differences in peripheral blood numbers. The mechanisms of neutrophil sequestration in the lung in response to sepsis are not fully understood although current data obtained in fully murine models suggests that stimulation of TLR4 on endothelial cells plays a key role [320], and that it may be selectin and β_2 integrin independent [320, 321]. This fits with the data showing that human neutrophils, taken from the lungs of mice that had received LPS, expressed similar levels of CD11b, CD62L and CD63, as those that received PBS (Fig 6.11 B-D). Interestingly, there was significantly more CD66b expressed on the human neutrophils taken from the lungs of LPS treated mice than on their counterparts taken from PBS treated mice (Fig 6.11 A). Given the already established role of CD66b in neutrophil-endothelial cell adhesion [304], this perhaps suggests a role for CD66b in neutrophil sequestration in the lung in response to LPS. Although, it must also be noted that there was an increase in CD66b levels in peripheral blood neutrophils of LPS treated mice, and so the neutrophils in the lungs could merely be representative of those in the circulation. In addition, it must also be taken into account that peripheral blood neutrophils from mice that had received LPS expressed higher levels of CD11b and CD63 together with lower levels of CD62L. Therefore, it is possible that these cells are preferentially trapped in the lungs and that CD11b, CD63 and CD62L are important despite previous reports in fully murine systems [320, 321].

Human neutrophils reconstituted by humanised mice undergo respiratory burst and degranulation in vitro

The role of neutrophils in host defence, and in tissue damage, is based on

their ability to, upon activation, a) produce highly toxic reactive oxygen species and b) to release proteolytic enzymes from intracellular storage granules. Therefore, using whole blood neutrophils from mice treated with GCSF for 5 days, the ability of human neutrophils generated by humanised mice to undergo respiratory burst and degranulation was examined. Human neutrophils stimulated with fMLP and opsonised *E.coli* produced intracellular reactive oxygen species as measure by the production of rhodamine 123 (Fig 6.12). The respiratory burst in response to opsonised *E.coli* was more robust than the response to fMLP. This is perhaps unsurprising given that *E.coli* is a strong particulate stimulus while fMLP is a low soluble stimulus.

Degranulation is frequently measured by the release of granular contents such as MPO, lysozyme and neutrophil elastase. This approach, however, would require the purification of human neutrophils from humanised mouse bone marrow or blood. Fortunately, degranulation can also be measured by the selective upregulation of granule membrane molecules such as CD63 (azurophilic granules), CD66b (secondary granules) and CD11b (secretory, gelatinase and specific granules) [314, 322]. This is made possible by the fact that the granule membrane containing these markers fuses with the plasma membrane thus leading to an increase in their surface expression [314]. Using this, degranulation can be measured by flow cytometry, and thus human neutrophil specific degranulation can be examined without the need to isolate the cells. Humanised mouse human neutrophils underwent degranulation in response to both fMLP and opsonised *E.coli*. There was a significant increase in human CD63 in response to both fMLP and *E.coli* (Fig 6.13). Similarly, there was a significant increase in the surface expression of human CD66b in response to fMLP, although there was no response to *E.coli* (Fig 6.14). Finally, while there was an increase in CD11b expression on the surface of human neutrophils in response to fMLP in 3 out of 4 mice, overall this did not quite reach statistical significance ($p=0.059$) (Fig 6.15).

Neutrophils release their granules in the following order: secretory vesicles > tertiary granules > secondary granules > azurophilic granules [323]. Therefore

it would be expected that if *E.coli* induces the upregulation of CD63, the result of the release of azurophilic granules, then it must also induce the upregulation of CD66b and CD11b, indicating the release of secondary and tertiary granules, and secretory vesicles. However, this was not observed. The likely reason for this discrepancy is the variability of CD66b and CD11b expression on the surface of humanised mouse human neutrophils, combined with small mouse cohorts. CD63 expression on the surface of humanised mouse human neutrophils is relatively low and, furthermore, there is very little variability in CD63 expression between mice (Fig 6.13). Thus even a small increase in expression appears to be statistically significant. In contrast, CD66b and CD11b appear to be highly expressed on the surface of humanised mouse human neutrophils and, importantly, the levels of expression of these two molecules vary between mice (Fig 6.14 and Fig 6.15, respectively). Thus, although there may be an increase in the expression of CD66b and CD11b in response to *E.coli*, it does not reach statistical significant due to the variance. It is likely, had more mice been available, that a larger sample size would have overcome this variability and led to statistical significance being achieved. Similarly, the variability of CD11b expression between mice may explain why the increase in CD11b expression, in contrast to the increase in CD66b and CD63 expression, in response to fMLP was not found to be statistically significant.

Despite these technical issues, together these data indicate that human neutrophils in the peripheral blood of humanised mice are capable of undergoing respiratory burst and degranulation in response to inflammatory stimuli.

Human PR3 and MPO expression by human neutrophils reconstituted by humanised mice

The ultimate goal in establishing a humanised mouse model with functional human neutrophils present in the peripheral blood is to allow the development of an *in vivo* model of anti-PR3 induced ANCA associated vasculitis. Therefore, the expression of human PR3, and to a lesser extent human MPO,

by human neutrophils generated by humanised mice is of the upmost importance. To investigate the expression of human PR3 and MPO, immunofluorescent staining of ethanol fixed humanised mouse bone marrow neutrophils was performed. The ethanol fixation and subsequent staining of neutrophils for PR3 and MPO produces characteristic staining patterns. Antibodies against PR3 produce a diffusely cytoplasmic, internuclear staining pattern (c-ANCA) while antibodies against MPO generally produce a perinuclear staining pattern with some nuclear extension (p-ANCA). These patterns are artefacts of the ethanol fixation process and are related to the charge of the protein in question [324, 325]. Using human monoclonal antibodies, PR3 and MPO were found to be present in a small percentage of humanised mouse neutrophils (Fig 6.16 A). Furthermore, the antibody against human PR3 produced a perinuclear staining pattern. The staining pattern produced by the anti-MPO antibody was somewhat indistinct, however, it did appear to be cytoplasmic with some nuclear extension. It must be noted that human neutrophils were identified based on their reactivity with antibodies specific for human proteins. Therefore, as there may have been some cross reactivity with the mouse proteins, the presence of PR3 and MPO on human neutrophils was confirmed using flow cytometry. PR3 and MPO were both found to be expressed on the surface of TNFα primed human neutrophils ($CD45^+CD66b^+$ cells) in humanised mouse bone marrow (Fig 6.16 B). These data, together with the data showing that humanised mouse human neutrophils respond to inflammatory stimuli both *in vivo* and *in vitro*, suggest these cells have all the components required to induce disease when activated by human anti-PR3 and/or anti-MPO antibodies *in vivo*. This will be discussed in the following chapter.

7.1 Introduction

Attempts to develop models of anti-PR3 ANCA induced vasculitis, and thus provide evidence of a pathogenic role for anti-PR3 antibodies in disease development, have remained largely unsuccessful (Discussed in depth in Chapter 1). One possible reason for this is that murine PR3 is functionally more similar to both human and mouse neutrophil elastase than to human PR3 [104]. Consequently, human anti-PR3 antibodies do not recognise mouse PR3. Furthermore, PR3 is unlikely to be present on the surface of mouse neutrophils, and thus, likely remains unavailable to circulating anti-PR3 antibodies, whether of mouse or human origin. Evidence suggests that this is in fact the case, as PR3 is undetectable on the surface of freshly isolated mouse neutrophils [101]. Interestingly, in the same study PR3 was detected on the surface of peritoneal exodate neutrophils. This, however, is likely to be an artefact and a consequence of the activating effects of the isolation method used, which involved the mice receiving 1ml of a 9% sterile casein solution via intraperitoneal injection. Peritoneal cells were then isolated 3 hours later by peritoneal gavage. Thus the lack of circulating neutrophils expressing PR3 must be overcome if a mouse model of anti-PR3 associated vasculitis is to be established. One possible approach to this issue is to use the humanised mouse model described in the previous chapter. In addition to having circulating, functional, and already primed human neutrophils present in their peripheral blood, these mice express PR3, which is recognised by human anti-PR3 antibodies, on the human neutrophils they reconstitute. Thus, this model not only provides the opportunity to establish a role of anti-PR3 antibodies in disease induction, but it also provides the possibility of directly demonstrating a role for human anti-PR3 antibodies derived from patients in the pathogenesis of ANCA associated vasculitis.

As discussed in Chapter 1, the passive transfer of anti-MPO antibodies raised in $MPO^{-/-}$ mice results in the development of a mild necrotising cresentic glomerulonephritis in wildtype mice. In addition, LPS was shown to exacerbate disease in this model. Therefore, in this chapter, the ability of

patient derived anti-MPO and anti-PR3 antibodies passively transferred into humanised mice, that had also been administered human GCSF and LPS, to induce a disease similar to ANCA associated vasculitis was examined.

7.2 Aim

- To induce cresentic glomerulonephritis and/or pulmonary haemorrhage in humanised mice by the passive transfer of human anti-PR3 antibodies

7.3 Methods

All plasma samples, from both patients and healthy controls, were taken with informed consent and ethical approval (NRES committee London—London Bridge 09/H084/72).

7.3.1 Generation of humanised mice

Humanised mice were generated as described in Section 2.2.11. Briefly, mice were engrafted by injecting $1x10^5$ human cord blood CD34 positive stem cells, purchased from Lonza, into 6-12 week old NOD-scid IL2$\gamma^{-/-}$ mice approximately 4 hours post irradiation at 2.4Gy with a Cs-source irradiator.

7.3.2 Antibody purification

Human IgG from either healthy controls or ANCA positive patients was purified using ammonium sulphate precipitation followed by Protein G antibody purification as described in Section 2.2.3.1. IgG was stored at at -20°C and a concentration of either 20mg/ml or 50mg/ml until use.

7.3.3 PR3/MPO capture ELISA

ELISAs for antibodies against PR3 and MPO were carried out using the Weislab Capture PR3 and MPO ELISA Kits as described in Section 2.2.5. Purified antibody was diluted in PBS to give a final concentration of 20μg/ml per test. Serum was diluted 1:100 in PBS before testing.

7.3.4 Flow cytometry

Mouse blood was collected either from the saphenous vein of conscious mice or from the axillary vessels of mice under terminal anaesthesia as described in Section 2.2.13.1. Flow cytometry was performed as described in Section 2.2.1. The antibodies used are shown in Table 7.1 and 7.2. Absolute numbers of human and mouse cells were calculated from whole blood counts, performed as described in Section 2.2.2, and flow cytometry data.

Target	Isotype	Clone	Fluorophore	Supplier	Dilution
CD14	Mouse IgG2a, κ	M5E2	APC	BD	1:6
CD16	Mouse IgG1, κ	3G8	PerCP-Cy5.5	BD	1:20
CD45	Mouse IgG1, κ	HI30	V450	BD	1:101
CD66b	Mouse IgM, κ	G10F5	PE	Biolegend	1:12

Table 7.1 Anti-human antibodies used for flow cytometry. All antibodies were obtained from commercial sources.

Target	Isotype	Clone	Fluorophore	Supplier	Dilution
CD45	Rat (LOU) IgG2b, κ	30-F11	FITC	BD	1:250

Table 7.2 Anti-mouse antibodies used for flow cytometry. All antibodies were obtained from commercial sources.

7.3.5 Inducing disease

Two separate experiments were carried in the hope of inducing disease in humanised mice. In both cases, humanised mice between 8 and 12 weeks post engraftment were matched based on the absolute number of human neutrophils and monocytes present in their peripheral blood. In the first experiment (Section 7.4) mice were treated as follows:

Day 0-Engrafted mice received 6μg GCSF subcutaneously, 10μg LPS intraperitoneally and 4mg IgG (either control of patient derived ANCA) via the lateral tail vein

Day 1 and 2-Mice received 6μg GCSF subcutaneously

Day 3-Mice received 6μg GCSF subcutaneously and 10μg LPS intraperitoneally

Day 4 and 5-Mice received 6μg GCSF subcutaneously

Day 6-Mice received 6μg GCSF subcutaneously and were placed in metabolic cages overnight for urine collection

Day 7-

1. Mice were exsanguinated and their blood collected into heparin tubes for flow cytometric analysis and into eppendorfs for serum collection
2. Their kidneys and lungs were harvested for histological analysis

While in the second experiment (Section 7.5) mice were treated as follows:

Day 0-Engrafted mice received 50μg pegylated GCSF subcutaneously, 10μg LPS intraperitoneally and 4mg IgG (either control of patient derived ANCA) via the lateral tail vein

Day 3-Mice received 10μg LPS intraperitoneally

Day 6-Mice were placed in metabolic cages overnight for urine collection

Day 7-

1. Mice were exsanguinated and their blood collected into heparin tubes for flow cytometric analysis and into eppendorfs for serum collection
2. Their kidneys and lungs were harvested for histological analysis

7.3.6 Albuminuria measurement

Mice were housed in metabolic cages for 24 hours for urine collections. The urine albumin concentration was measure by ELISA using a mouse albumin ELISA quantisation set from Bethyl Laboratories as described in Section 2.2.18. Urine albumin was then calculated by multiplying the concentration of albumin in each sample, as measured by ELISA (μg/ml), by the volume of urine collected over the 24-hour period.

7.3.7 Urine creatinine measurement

Urine creatinine was measured with the help of Dr N Dalton and Dr C Turner in the Department of Paediatric Biochemistry at St. Thomas' Hospital by mass spectrometry as described in Section 2.2.19.

7.3.8 Histology

Kidney and lungs were collected and histology performed as described in Section 2.2.16. All of the PAS stained sections of lungs and kidneys from both of the experiments described here were reviewed by Prof Terry Cook (Imperial College), an expert clinical and experimental renal pathologist, who confirmed there were no significant abnormalities.

7.4.9 Statistics

Statistics were performed using Graphpad Prism software (Graphpad Software Inc, La Jolla, CA, USA). Paired t tests, as indicated, were used to the analyse data presented here.

7.4.10 Acknowledgements

I would like to thank Simon Freeley for kindly sectioning and staining lung and kidney tissue for histological analysis for this chapter. I would also like to thank Prof Terry Cook for kindly reviewing the histology for this chapter.

7.4 Results: Neither human anti-PR3 nor anti-MPO antibodies induced disease in the humanised mouse model

Mice were engrafted as previously described with $CD34^+$ cells either derived from human bone marrow or human UCB. In either case the $CD34^+$ cells were purchased from Lonza. Between 8 and 12 weeks later mice were divided into three groups based primarily on the total number of human $CD45^+$ leukocytes (Fig 7.1 A), $CD45^+CD66b^+$ neutrophils (Fig 7.1 B) and $CD45^+CD14^+$ monocytes (Fig 7.1 C) present in their peripheral blood. The first group would go on to receive control IgG, the second group would go on to receive anti-PR3 IgG and the final group would go on to receive anti-MPO IgG as indicated in Figure 7.1. IgG from 6 individual patients, 3 positive for anti-PR3 ANCA and 3 positive for anti-MPO ANCA, was chosen based on the severity of disease present in the patient from which they were derived (Table 7.3) and on their ability to bind to MPO and PR3 as measure by ELISA (Fig 7.2). Due to the variability of the neutrophil respiratory burst induced by patient derived ANCA, combined with technical difficulties experienced in performing these assays during this period (Discussed in Chapter 3), the ability of these ANCA to activate neutrophils *in vitro* was not taken into account. Control IgG was derived from a healthy volunteer (L2) and as shown in Figure 7.2 did not bind to either PR3 or MPO.

Table 7.4 shows a summary of the mice used in this experiment including the IgG administered, the mouse group number (which refers to the source of $CD34^+$ cells used for engraftment and can be cross referenced with Table 5.6) and the percentage of human leukocytes, neutrophils and monocytes present in their circulation. There were 7 groups of mice all together, a control group containing 5 mice and one group comprising 3 mice for each of the patient ANCA samples tested. Each mouse received 6μg GCSF (Neupogen®) together with 4m IgG and 10μg LPS. They were boosted daily with 6μg GCSF and received a single boost of 10μg LPS 3 days after the first. On day 6 mice were place in metabolic cages for 24 hour, to allow urine collection, and following this the mice were culled and their kidneys and lungs were

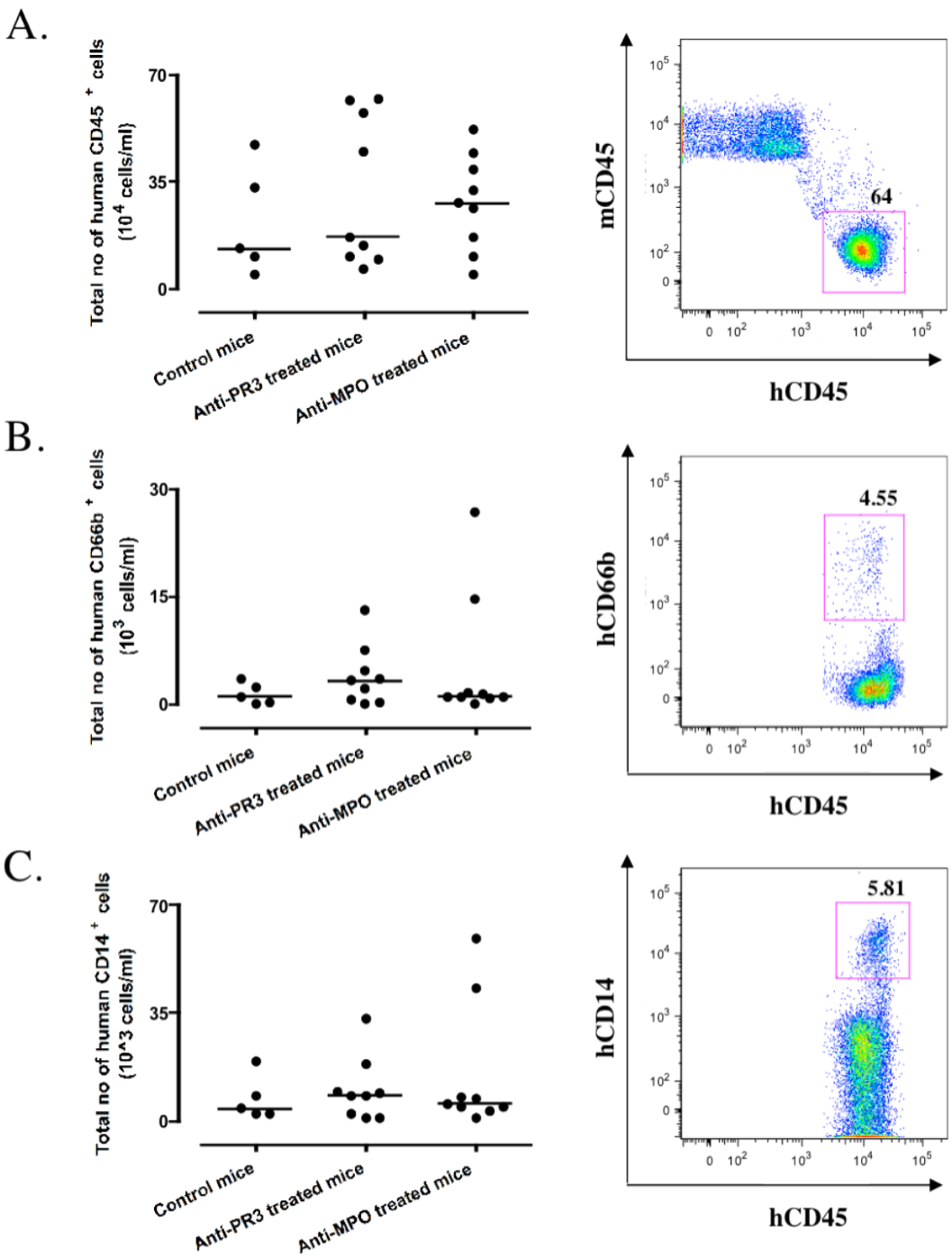

Figure 7.1 Engraftment of human cells. Total number of human (A) $CD45^+$ leukocytes (B) $CD66b^+$ neutrophils and (C) $CD14^+$ monocytes in the peripheral blood of humanised mice (n=5 for control mice, n=10 for anti-PR3 treated mice and n=10 for anti-MPO treated mice) are shown on the left. Representative flow cytometry plots used to calculate total numbers are shown on the right. The dot plots show the median population (horizontal line).

Sample ID	Renal BVAS	Total BVAS	Renal Biopsy	Non-renal Features	O_2^- Production (nmol/10^5 cells above control)	Rhodamine-123 production (MFI above control)
V3*	12	31	No	Chest/ns/ent/skin	1±1	56
V5*	12	32	Yes	Eyes/ns/abdo	1±1	195
V8*	12	14	Yes	No	5±2	32
V7**	12	20	No	Chest/ent	15±3	9
V26**	12	22	Yes	Ent/chest	9±1	0
V30**	12	18	No	Chest	18±1	6020

Table 7.3 Information on ANCA used in an attempt to induce disease. ANCA was derived from patients that had evidence of active renal involvement, which was confirmed by renal biopsy in most cases. Clinical evidence of other tissue involvement (ent-ear, nose or throat, ns-nervous system, abdo-abdomen) is also indicated. BVAS-Birmingham Vasculitis Activity Score. * anti-PR3 ANCA, **anti-MPO ANCA. V26 was from a patient positive for both anti-MPO and anti-PR3 antibodies

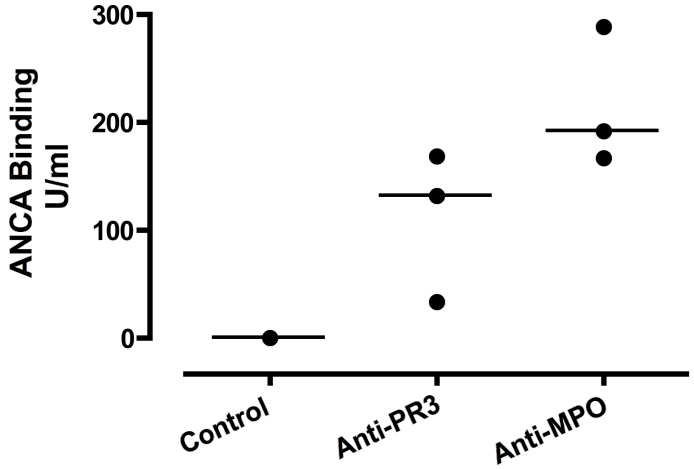

Figure 7.2 PR3 and MPO Capture ELISA results showing the binding of antibody used in an attempt to induce disease. Antibody was tested at a concentration of 20μg/ml. The median binding is shown (horizontal line).

IgG	Mouse Group No.	% $hCD45^+$ cells	% $hCD66b^+$ cells	% $hCD14^+$ cells
L2	7	13.2	0.83	3
L2	7	8.09	0.22	4.83
L2	8.1	52.4	0.5	1.73
L2	8.1	33.2	1.05	5.81
L2	8.2	15	0.29	2.08
V3	8.2	68.9	0.76	1.44
V3	8.2	7.54	0.7	2.49
V3	8.2	64	0.38	1.65
V5	8.1	56.3	1.66	4.09
V5	8.1	68.4	2.13	5.38
V5	8.2	8.72	0.25	1
V7	7	24.2	0.62	2.73
V7	7	13.1	0.79	3.04
V7	8.1	39	0.39	1.95
V8	7	14.1	2.09	4.9
V8	7	20.3	2.34	5.81
V8	7	12.6	0.2	1.84
V26	8.1	6.8	0.23	2.38
V26	8.1	47.	0.19	1.35
V26	8.2	17.5	0.42	1.74
V30	8.1	46.7	0.55	2.01
V30	8.1	40.4	6.03	13.3
V30	8.1	40.5	4.55	13.3

Table 7.4 Summary of ANCA and mice used in the experiment to induce disease in humanised mice. Each mouse received 4mg of IgG intravenously. For data on mouse groups used refer to Table 5.6

harvested. There were no histological signs of disease in either the kidneys or the lungs of mice receiving anti-PR3 or anti-MPO IgG (Fig 7.3). Furthermore, there was no difference in the levels of albumin over 24 hours in the urine of mice receiving patient derived ANCA when compared with those receiving control antibody (Fig 7.4 A). As there was some doubt about the urine collection, due to an issue with the metabolic cages the urine:creatinine ratio was measured and found to be similar in all mice regardless of whether they received anti-PR3, anti-MPO or control IgG (Fig 7.4 B). In addition, there was no haematuria detected in any of the mice tested. The presence of anti-PR3 and anti-MPO IgG in the circulation of the relevant mice at the end point of the experiment was confirmed, for the majority of mice, using a PR3 and a MPO capture ELISA (Fig 7.5).

7.5 Results: Human anti-PR3 antibodies did not induce disease in the humanised mouse model

For the first experiment IgG from patients positive for either anti-MPO or anti-PR3 was transferred into humanised mice. As none of the anti-PR3 nor anti-MPO IgG preparations used appeared to induce disease, IgG from two further anti-PR3 positive patients, with particularly severe disease, was used in a second attempt to assess the pathogenicity of patient ANCA. Mice were engrafted as previously described with $CD34^+$ cells from human UCB obtained from Lonza. Approximately 12 weeks later they were divided into three groups based primarily on the total number of human $CD45^+$ leukocytes (Fig 7.6 A), $CD45^+CD66b^+$ neutrophils (Fig 7.6 B) and $CD45^+CD14^+$ monocytes (Fig 7.6 C) present in their circulation. The first group would go on to receive control IgG while the second and third groups would go on to receive anti-PR3 IgG derived from two individual patients (V14 and V31) as indicated. Patient IgG was chosen based on the severity of disease present in the patient from which they were derived, and in the case of V31 on the patients high anti-PR3 titres (Table 7.5). Due to the variability of the neutrophil respiratory burst induced by patient derived ANCA, combined with technical difficulties experienced in performing these assays during this period

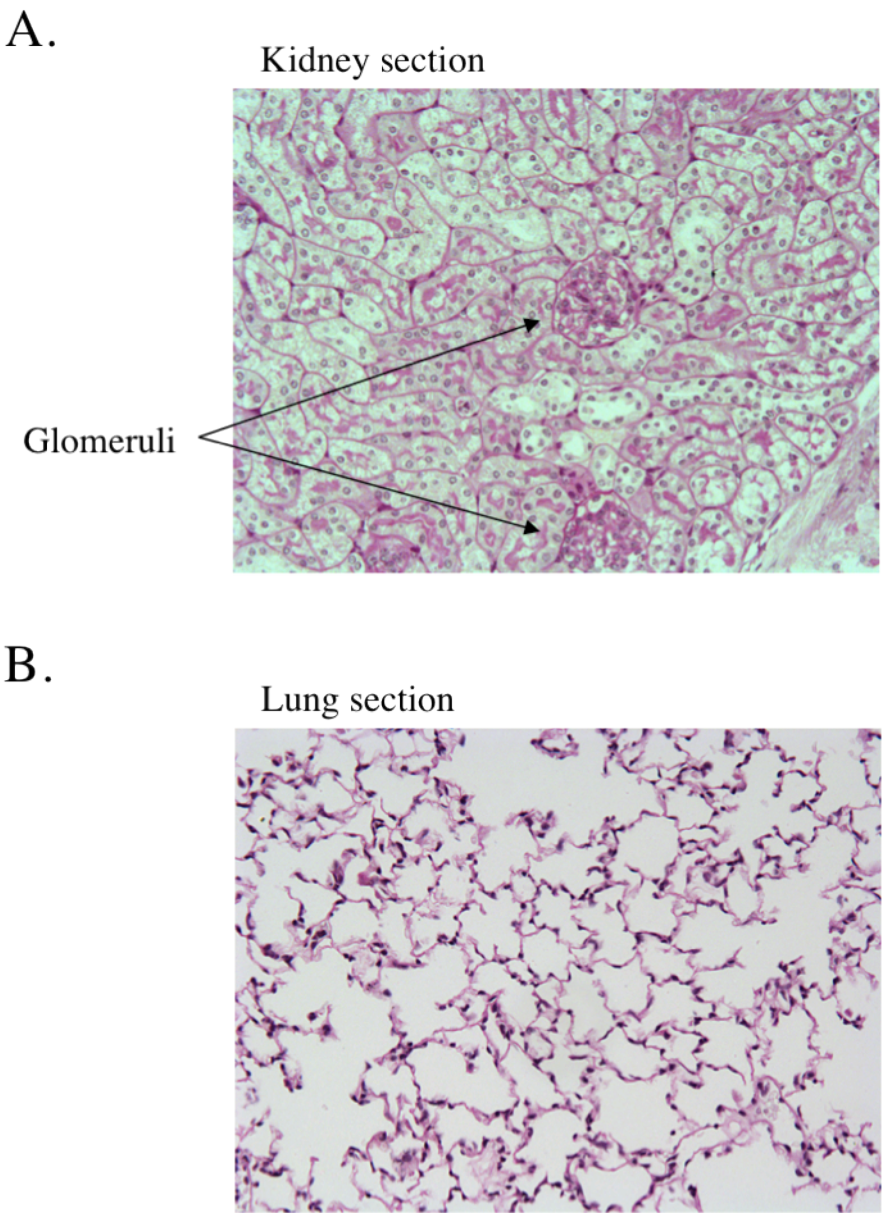

Figure 7.3 PAS staining of (A) a kidney section and (B) a lung section showing no abnormalities. Magnification is x 400 on a BX51 fluorescent microscope (Olympus, Southend-on-sea, UK).

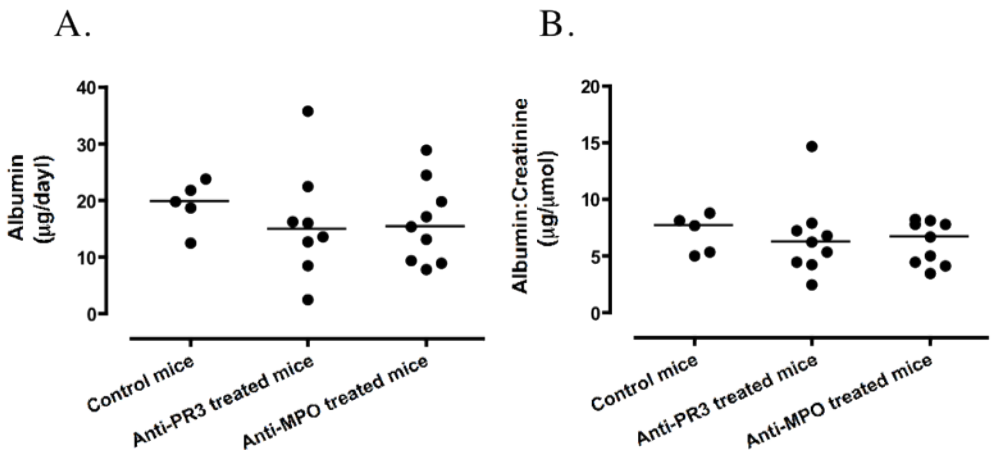

Figure 7.4 Functional readouts from mice receiving purified control (n=5), anti-PR3 (n=9) or anti-MPO antibody (n=10). (A) Albuminuria over the 24 hour period 6 days post human control antibody or ANCA administration to engrafted NOD-scid IL2$\gamma^{-/-}$ mice treated with GCSF and LPS. (B) Urine albumin:creatinine ratios over the 24 hour period 7 days post human control antibody or ANCA administration to engrafted NOD-scid IL2$\gamma^{-/-}$ mice treated with GCSF and LPS. The dot plots show the median levels (horizontal line).

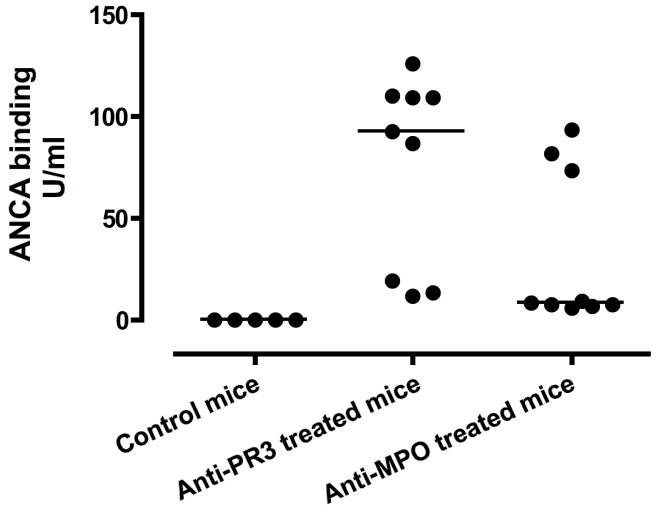

Figure 7.5 MPO and PR3 Capture ELISA results showing the binding of antibody remaining in mouse (n=5 for control antibody treated mice, n=9 for anti-PR3 treated muce and n=10 for anti-MPO treated mice) serum 7 days post transfer. Serum was diluted 1:100. The median binding is shown (horizontal line).

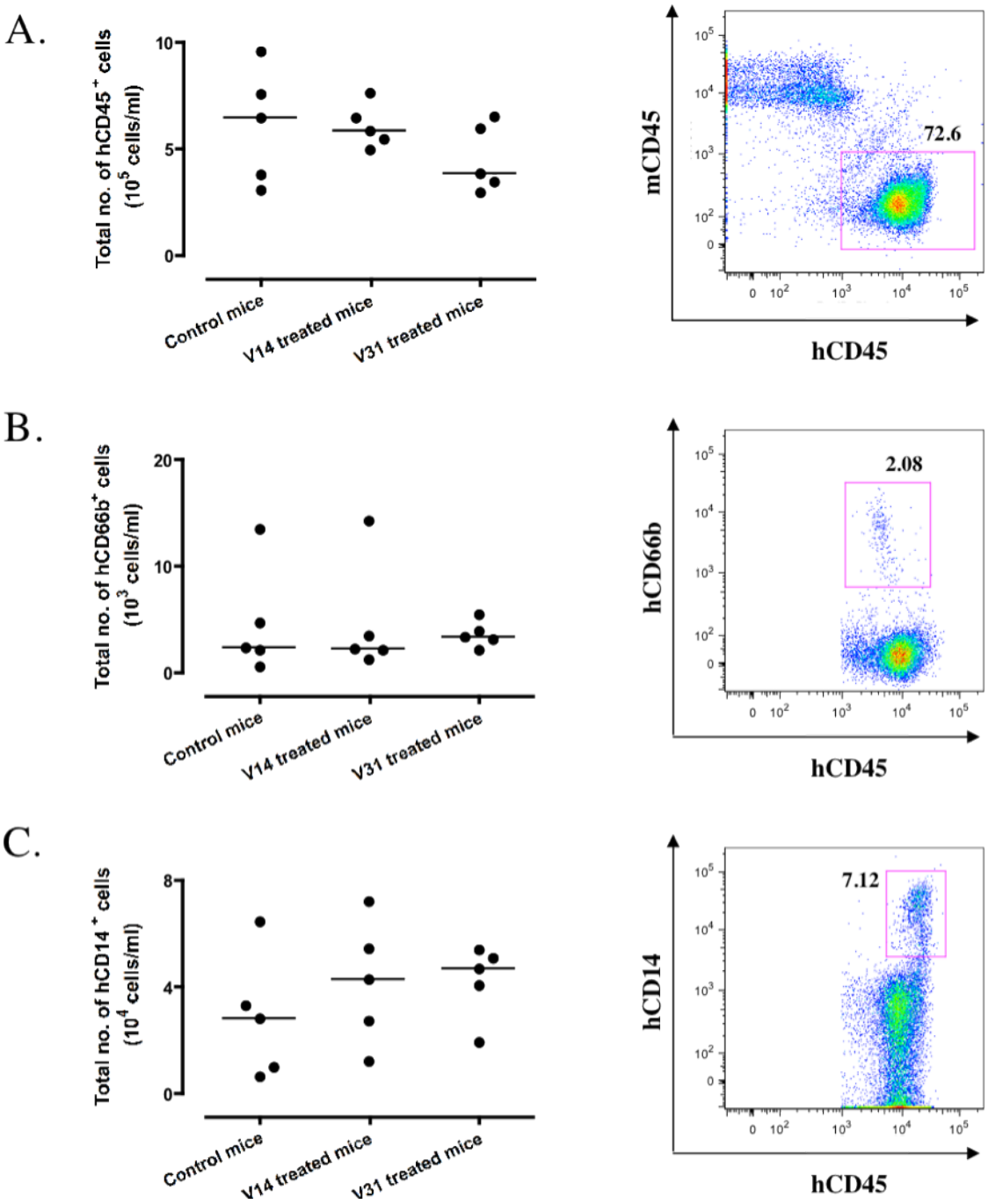

Figure 7.6 Engraftment of human cells. Total number of human (A) $CD45^+$ leukocytes (B) $CD66b^+$ neutrophils and (C) $CD14^+$ monocytes in the peripheral blood of humanised mice (n=5 for control mice, n=5 for anti-PR3 treated mice and n=5 for anti-MPO treated mice) are shown on the left. Representative flow cytometry plots used to calculate total numbers are shown on the right. The dot plots show the median population (horizontal line).

(Discussed in Chapter 3), the ability of these ANCA to activate neutrophils *in vitro* was not taken into account. However, in hindsight V14 consistently induced a strong neutrophil respiratory burst as measured by rhodamine 123 production. Control IgG was the combination of IgG derived from 2 healthy volunteers (L1 + 2). Table 7.6 shows a summary of the mice used in this experiment including the IgG administered, the mouse group number (which refers to the source of $CD34^+$ cells used for engraftment and can cross referenced with Table 5.6) and the percentage of human leukocytes, neutrophils and monocytes present in their circulation. There were 3 groups of mice, one control group and two test groups, each comprising 5 mice. Each mouse received 50μg pegylayed GCSF (Neulasta®), this was in contrast to the previous experiment in which the mice received 6μg GCSF (Neupogen®) daily from day 0-6, together with 10mg IgG (more than twice that given in the previous experiment) and 10μg LPS. They received a single boost of 10μg LPS 3 days after the first. On day 6 mice were place in metabolic cages for 24 hour, to allow urine collection, and the following day they were culled and their kidney and lungs were harvested. There were no histological signs of disease in either the kidneys or the lungs of mice receiving anti-PR3 IgG (Not shown, See figure 7.3 for representative histology). Furthermore, there was no difference in the levels of albumin over 24 hours in the urine of mice receiving patient derived ANCA when compared with those receiving control antibody (Fig 7.7). In addition, only 1 of the 10 mice receiving anti-PR3 antibody, and none of the mice receiving control antibody, had haematuria.

In this second experiment flow cytometry was performed in order to confirm the presence of human cells, particularly mature neutrophils, in these humanised mice both before and 7 days after treatment with GCSF, LPS and human IgG (Fig 7.8-7.10). As expected, based on the results from Chapter 6, in which GCSF treatment led to a significant increase in the number of mouse neutrophils and a concurrent decrease in the percentage of human cells, there was a significant decrease in the percentage of human $CD45^+$ cells in the peripheral blood of mice treated with GCSF, LPS and human IgG. Surprisingly, however, this corresponded with a significant decline in the total

Sample ID	Renal BVAS	Total BVAS	Renal Biopsy	Non-renal Features	O_2^- Production (nmol/10^5 cells above control)	Rhodamine-123 production (MFI above control)
V14	12	21	Yes	Ent	0	2719
V31	12	15	Yes	No	No data	No data

Table 7.5 Information on ANCA used in an attempt to induce disease. ANCA was derived from patients that had evidence of active renal involvement, which was confirmed by renal biopsy in most cases. Clinical evidence of other tissue involvement (ent-ear, nose or throat) is also indicated. BVAS-Birmingham Vasculitis Activity Score.

IgG	Mouse Group No.	% $hCD45^+$ cells	% $hCD66b^+CD16^+$ cells	% $hCD14^+$ cells
L1 + 2	9	75.9	0.61	8.51
L1 + 2	9	43	2.08	5.09
L1 + 2	9	50.3	0.25	2.96
L1 + 2	9	61.5	0.19	2.07
L1 + 2	9	63.2	0.57	2.62
V14	9	69.5	1.87	9.45
V14	9	41.1	0.43	2.47
V14	9	65.1	0.6	7.31
V14	9	54.3	0.41	9.98
V14	9	58.7	0.19	4.18
V31	9	76.5	0.88	14.1
V31	9	66.4	0.92	8.49
V31	9	72.6	0.48	7.12
V31	9	68.6	0.63	5.65
V31	9	49.5	1.33	13.7

Table 7.6 Summary of ANCA and mice used in the experiment to induce disease in humanised mice. Each mouse received 10mg of IgG intravenously. For data on mouse groups used refer to Table 5.6.

number of human $CD45^+$ cells in the circulation (Fig 7.8 A). In contrast, both the percentage and absolute number of mouse $CD45^+$ cells was significantly increased 7 days after GCSF, LPS and IgG administration (7.8 B). Representative flow cytometry plots show the staining for human and mouse $CD45^+$ cells (Fig 7.8 C). Of the human $CD45^+$ cells present in the peripheral blood of these mice before GCSF, LPS and human IgG treatment, on average 0.87% were mature human neutrophils, defined as $CD66b^+CD16^+$ cells. Post treatment this had increased; with human neutrophils accounting for, on average, 2.64% of the human $CD45^+$ cell population (Fig 7.9 A). Representative flow cytometry plots show the staining for human $CD45^+CD66b^+CD16^+$ cells (Fig 7.9 B). Interestingly, two separate populations of human neutrophils could be identified both before and after GCSF, LPS and human IgG administration. These were a $CD66b^+CD16^{dim}$ population and a $CD66b^+CD16^+$ population. Concurrently, the percentage and absolute number of human monocytes, defined as human $CD45^+CD14^+$ cells, were significantly higher 7 days post GCSF, LPS and human IgG (Fig 7.10). Importantly, as shown in Figure 7.10 B, these monocytes could be divided into three subpopulations: $CD14^{dim}CD16^+$, $CD14^+CD16^+$ and $CD14^+CD16^{dim/-}$.

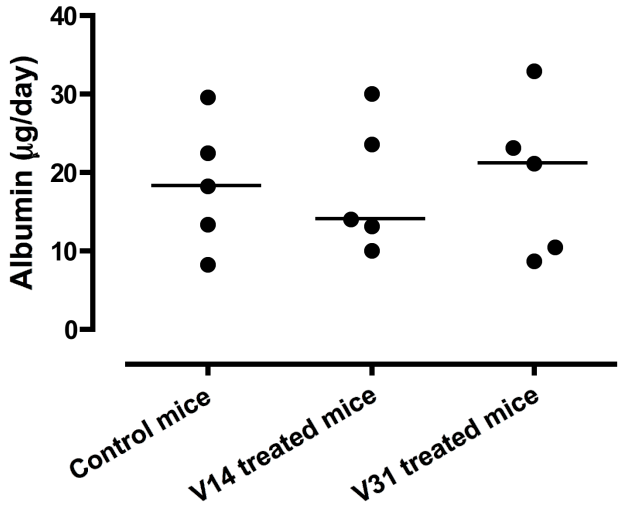

Figure 7.7 Albuminuria over the 24 hour period 6 days post human control antibody (n=5) or ANCA (n=10) administration to engrafted NOD-scid IL2$\gamma^{-/-}$ mice treated with GCSF and LPS. The dot plots show the median levels (horizontal line).

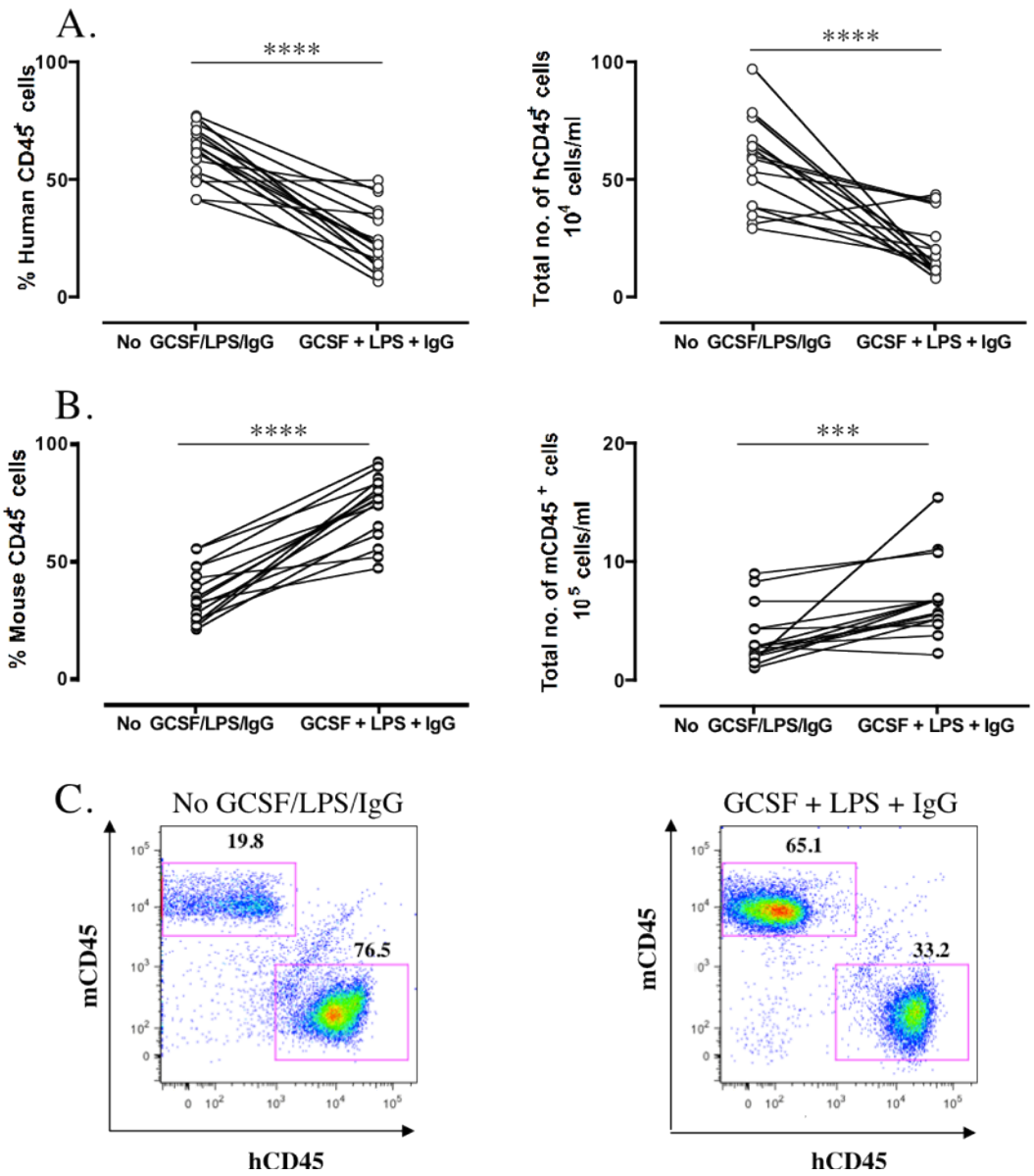

Figure 7.8 Human cell engraftment pre and post disease induction. Mice (n=15) were bled from the saphenous vein and given 50μg pegylated GCSF subcutaneously, 10μg LPS intraperitoneally and 10mg human IgG intravenously. They received a second dose of LPS 3 days later. On day 7 they were culled and bled via the axillary vessels. (A) Human and (B) mouse $CD45^+$ leukocytes are shown as a percent of the total leukocytes and as absolute numbers. (C) Shows representative FACs plots.***p<0.001, ****p<0.0001. Data was analysed using a paired t test.

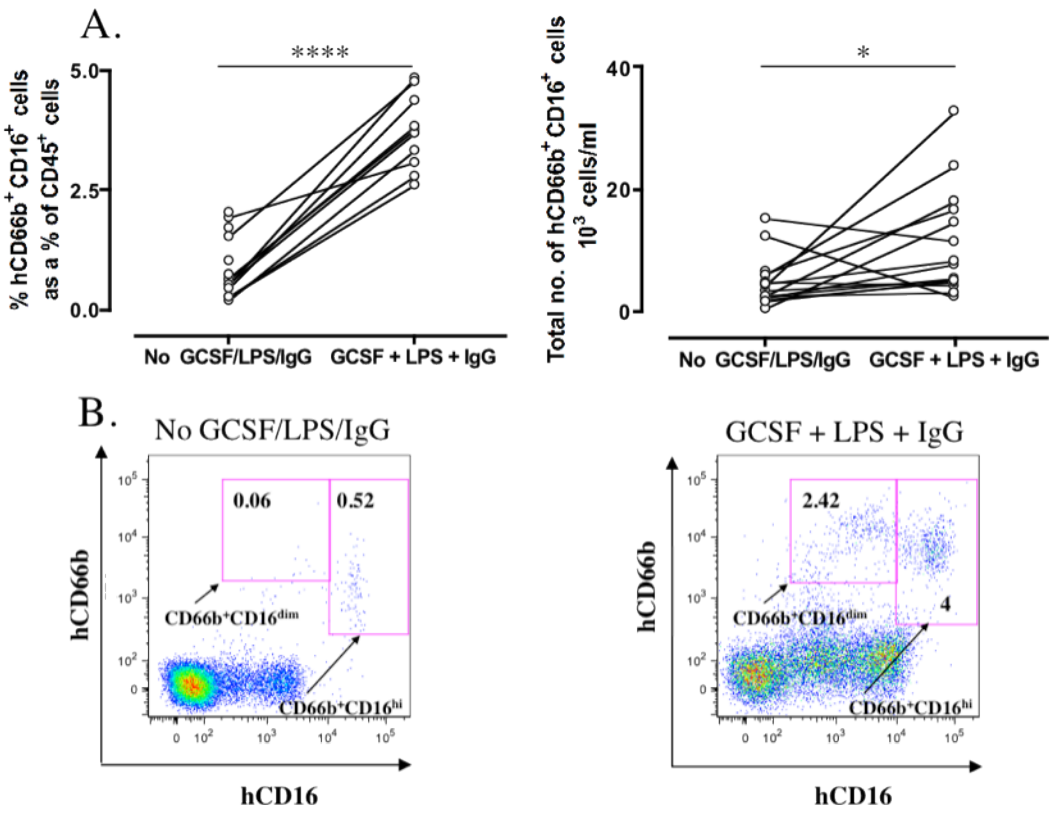

Figure 7.9 Human $CD45^+CD66b^+CD16^+$ cells in humanised mice (n=15) pre and post disease induction. Mice were bled from the saphenous vein and given 50μg pegylated GCSF subcutaneously, 10μg LPS intraperitoneally and 10mg human IgG intravenously. They received a second dose of LPS 3 days later. On day 7 they were culled and bled via the axillary vessels. (A) Data from each individual mouse (B) Representative FACs plots. *p<0.05. **** p<0,0001. Data was analysed using a paired t test.

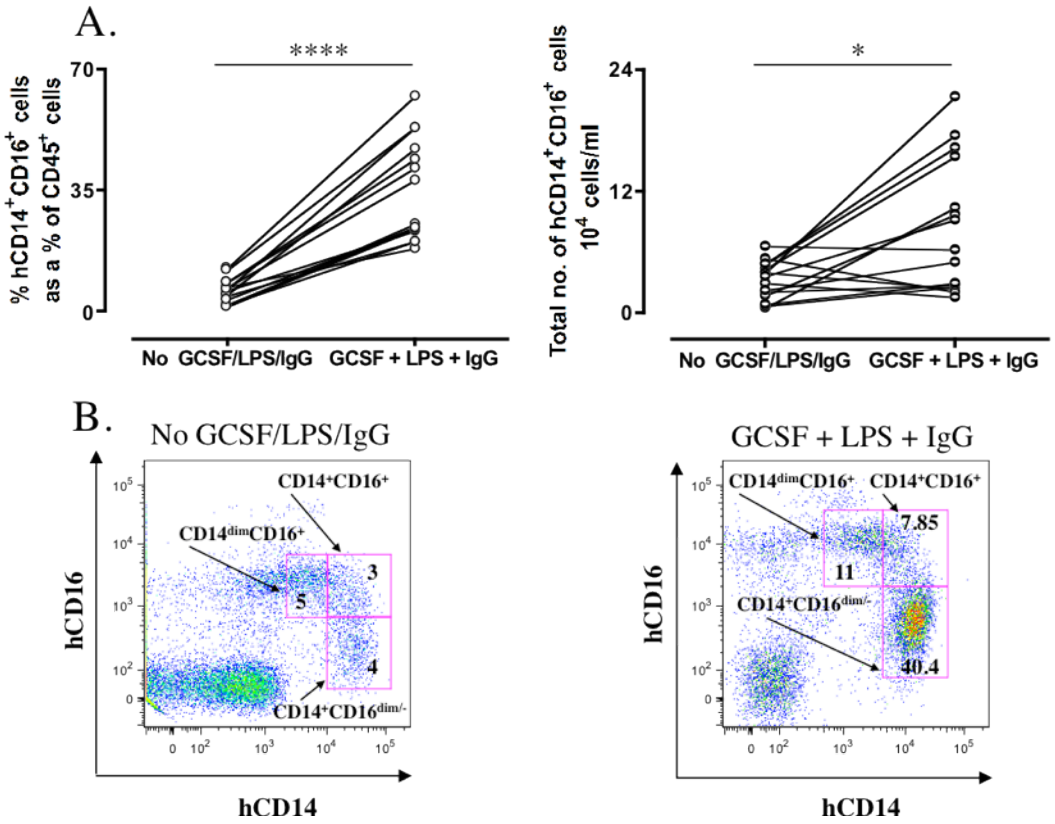

Figure 7.10 Human $CD45^+CD14^+CD16^+$ cells in humanised (n=15) mice pre and post disease induction. Mice were bled from the saphenous vein and given 50μg pegylated GCSF subcutaneously, 10μg LPS intraperitoneally and 10mg human IgG intravenously. They received a second dose of LPS 3 days later. On day 7 they were culled and bled via the axillary vessels. (A) Data for individual mice (B) Representative FACs plots. Multiple populations of monocytes can be identified as indicated. *p<0.05. **** p<0.0001. Data was analysed using a paired t test.

7.6 Discussion

A humanised mouse model of ANCA associated vasculitis

Despite two separate attempts, the passive transfer of patient derived ANCA failed to induce pathological changes in the kidneys or lungs of humanised mice. Consistent with this, anti-PR3 and anti-MPO antibodies also failed to induce proteinuria or haematuria. Mice in these experiments were matched based primarily on their reconstitution of human neutrophils, however, the overall engraftment of human cells and the number of human monocytes present was also taken into account (Fig 7.1 and 7.6). As established in Chapter 4, it is possible that monocytes play a role in the pathogenesis of anti-PR3, if not anti-MPO, induced ANCA associated vasculitis. In order to increase the chances of inducing disease and to provide a proinflammatory environment, which is thought to be required for the pathogenesis of ANCA associated vasculitis (Chapter 1), all humanised mice in these experiments were administered GCSF and LPS, alongside either human anti-PR3, anti-MPO or control IgG. In the previous chapter human GCSF was shown to expand, and partially activate, the population of human neutrophils found in humanised mice, while LPS was shown to further activate these human neutrophils and maximise their recruitment to the lungs. In addition, GCSF has been shown to prime human neutrophils for activation by anti-MPO antibodies (Fig 4.11). Furthermore, GCSF acting in synergy with LPS has been shown to exacerbate disease in wildtype mice receiving anti-MPO antibodies via passive transfer [239]. Indeed, LPS itself has been shown to activate endothelial cells [93, 94] and, through its induction of TNFα production, exacerbate disease in the passive transfer model of anti-MPO induced glomeronephritis [23]. Thus, although the humanised mice appeared to have all the components necessary to support disease induction by the passive transfer of anti-PR3 or anti-MPO antibodies, a humanised mouse model of ANCA-associated vasculitis could not be established. This in contrast to a recent study by Little et al., in which patient derived anti-PR3 IgG induced mild pathology, including focal pulmonary haemorrhage and mild

renal abnormalities, together with proteinuria and hematuria in a humanised mouse model [326]. There are numerous possible reasons for the failure of the model described here and the relatively mild disease found in the Little et al. model:

a) The number of human neutrophils present in the circulation of the humanised mouse model may be limiting. Relatively speaking, there are very few human neutrophils reconstituted by these mice. While there are $>1.5x10^6$ neutrophils/ml found in healthy humans, there are on average only $1.62x10^4$ human neutrophils/ml in the peripheral blood of humanised mice post GCSF (data from Table 6.4). Thus, as neutrophils are the key effector cells in disease pathogenesis, their relative lack may be responsible for the absence of disease in this model.

The main difference between the humanised mouse model described here and that employed by Little et al. is the source of the HSCs used to reconstitute the NOD-scid IL2$\gamma^{-/-}$ mice. While human UCB CD34$^+$ cells were used in this study, Little et al., engrafted mice using mobilised CD34$^+$ human bone marrow derived HSCs. It has been shown previously that HSCs from newborn/foetal sources have greater potential for repopulating immunodeficient mice than those from adult sources [291, 292]. However, this was with regards to overall human engraftment and focused primarily on the reconstitution of lymphoid lineage cells. Therefore it is possible, though it cannot be confirmed as the absolute number of cells were not provided in the Little et al. study, that mice engrafted with bone marrow derived HSCs reconstituted a higher number of human neutrophils than those engrafted with UCB HSCs. If this is the case it may help explain why disease, though mild, was present in the humanised mice used in the Little et al. study.

b) Although human neutrophils from UCB CD34$^+$ cell engrafted mice were shown to be capable of responding to opsonised *E.coli* and fMLP *in vitro* (Fig 6.12-6.15), there is no evidence that these cells can be activated by anti-PR3 or anti-MPO antibodies, despite data showing that both PR3 and MPO are

indeed expressed by these cells (Fig 6.16). This lack of data is primarily due to technical difficulties involved the use of ANCA assays. As discussed in Chapter 4, there is currently no whole blood assay that can be performed to assess the ability of ANCA to activate neutrophils and therefore neutrophils must be isolated for ANCA activation studies. There are several reasons why this might present difficulties with regards to humanised mice. As noted above, human neutrophils in humanised mice are relatively rare and thus isolating sufficient numbers would be difficult. In addition, the donor dependent variability of neutrophils seen with healthy human volunteers is likely to translate to humanised mice. Taking both of these issues into account, a large number of humanised mice would be required to properly test human neutrophil responses to ANCA. Thus, due to the limited number of humanised mice, a consequence of the time and expense required to generate them, this study was not feasible in the time allotted. Finally, neutrophils are sensitive cells and are activated by cell separation to some extent regardless of the method used, meaning that results *in vitro* might not accurately reflect the situation *in vitro* (Discussed in Chapter 3).

c) Due to the variability of the neutrophil respiratory burst induced by patient derived ANCA, combined with technical difficulties experienced in performing these assays during this period (Discussed in Chapter 3), the ability of ANCA to activate neutrophils *in vitro* was not taken into account when choosing patient IgG to induce disease. However, it must be noted that both V14 and V30 were later found to consistently induce a strong neutrophil respiratory burst as measured by rhodamine-123 production, if not by superoxide production (Table 7.5). Despite this, mice receiving IgG for patient V14 had no signs of disease. In contrast, Little et al., specifically chose to inject mice with anti-PR3 antibodies that had been shown to induce a strong respiratory burst and degranulation response in neutrophils isolated from human volunteers. It is therefore possible that the ability of ANCA to activate neutrophils in the humanised model is dependent on the anti-PR3 and anti-MPO antibodies used. Indeed this would be consistent with the variability found between ANCA derived from different patients to induce neutrophil activation *in vitro*. If

this is the case it is likely that the testing a larger number of patient derived ANCAs would lead to the development of disease in some mice. This potentially raises questions as to whether patient derived ANCA is in itself pathogenic. If this were the case then it would be expected that all ANCA would be capable of inducing disease. Having said that however, and as discussed in Chapter 3, it is possible that it is simply the use of whole IgG solutions that is the problem. ELISA results are insufficient to quantify the percentage of anti-PR3 or anti-MPO specific antibodies in a whole IgG solution. Therefore, it is impossible to be sure how much ANCA each mouse is actually receiving. In addition, it is possible that ANCA purified from patients may differ in regards to its subclass, epitope specificity and affinity, leading to differences in its ability to interact with neutrophils and thus induce disease in these mice.

d) Concern has been raised with regards to the ability of human cells generated in mice to transmigrate to sites of inflammation, and once there to adequately adhere to mouse endothelial cells. The data from Chapter 4 suggests that this is not an issue for human neutrophils, at least not with regards to their ability to respond to LPS by migrating to the lungs where they can bind to vasculature. Despite this, there are numerous interactions that may be required for disease pathogenesis that cannot occur in the mouse system due to a lack of cross reactivity between mice and human proteins, combined with the limited number of human cells available to compensate for this.

e) Although humanised mouse neutrophils have been shown to respond as normal human neutrophils thus far, they have not been fully phenotyped or tested. Therefore, it is possible that there are yet undiscovered defects in these cells, perhaps with regards signalling, that prevents them functioning as proper human neutrophils.

It is likely that no single point discussed is wholly responsible for the absence of disease in the model shown here, and for the relatively mild disease

observed in the model established by Little et al, but instead it is due to a combination of these issues.

It should be noted here that while it is possible that some strains of mice might be resistant to NCGN, previous results showning robust disease in NOD-scid mice [103] suggest that this is not a problem for associated with mice of this background strain.

Human neutrophil and monocyte subpopulations generated by humanised mice

Flow cytometry confirmed that human cells, including neutrophils and monocytes, remained in the circulation of humanised mice 7 days after treatment with GCSF, LPS and human IgG (Fig 7.8-7.10). Indeed, post treatment the number of human neutrophils and monocytes had increased, although, unexpectedly the absolute number of human leukocytes had declined (Fig 7.8). The decrease in the number of human $CD45^+$ cells in the peripheral blood 7 days post GCSF, LPS and human IgG administration cannot be fully explained, however, it is possible that the loss of cell numbers in due to LPS induced apoptosis of lymphocytes [327, 328], which account for the majority of human cells present in the peripheral blood of engrafted mice. Interestingly, two separate populations of human neutrophils could be identified after GCSF, LPS and human IgG administration. These were a $CD66b^+CD16^{dim}$ population and a $CD66b^+CD16^+$ population (Fig 7.9). The importance of this is unknown, however, it is likely that the $CD16^{dim}$ population represents less mature neutrophils that have been recently released into the circulation from the bone marrow. This is supported by the fact that this population is not present before GCSF, LPS and human IgG administration [329]. Alternatively they are neutrophils that are undergoing apoptosis and have thus downregulated their CD16 expression [330].

Perhaps more importantly however, at least with regards to understanding the engraftment of humanised mice, monocytes could be divided into three

subpopulations: $CD14^{dim}CD16^{+}$, $CD14^{+}CD16^{+}$ and $CD14^{+}CD16^{dim/-}$ (Fig 7.10). This is in keeping with human monocyte populations where these subsets have been identified and studied with each one demonstrating a specific function. $CD14^{dim}CD16^{+}$ monocytes do not produce TNFα or IL1β in response to LPS but instead have been shown to patrol blood vessels where they respond specifically to viruses and nucleic acids [331]. $CD14^{+}CD16^{+}$ monocytes are often referred to as proinflammatory monocytes and express high levels of CX4CR1, low levels of CCR2 and are the main producers of TNFα and IL1β in response to LPS. Finally, $CD14^{+}CD16^{dim/-}$ monocytes, the largest of the subsets, express low levels of CX4CR1, high levels of CCR2 and produce IL10 in preference to TNFα in response to LPS [332]. Notably, with regards ANCA associated vasculitis, there was no difference in the relative proportions of monocyte subsets observed between patients and healthy controls, although there was an increase in the percentage of monocytes expressing TLR4 [333].

8.1 Summary of results

Chapter 3

This chapter detailed the development of the neutrophil assays and ANCA purifications that would be used throughout this project. Using both commercial monoclonal, and patient purified polyclonal, anti-PR3 and anti-MPO antibodies, two respiratory burst assays to measure the ANCA-induced activation of neutrophils were established. These assays had not been used previously in my host laboratory. The superoxide dismutase inhibitible ferricytochrome C reduction assay measures extracellular superoxide release, while the DHR123 assay primarily measures intracellular reactive oxygen species production. In addition, the purification of patient ANCA was optimised, with the removal of fibrin and other impurities from patient plasma using sodium chloride precipitation found to be more efficient than the same process using ammonium sulphate. This chapter closed with a summary of the patient ANCA purified in the course of this project, focussing primarily on the inability of a large number of these patient derived antibodies to induce neutrophil activation in both respiratory burst assays.

Chapter 4

Chapter 4 was roughly divided into three sections, each focussing on a different aspect of human neutrophil and/or monocyte behaviour with regards to the study of ANCAs and their antigens. The first section dealt with the expression of human PR3 and MPO on the surface of human neutrophils and monocytes in whole blood. Importantly, both PR3 and MPO were found to be present on the surface of unprimed whole blood neutrophils. In contrast, only PR3 was found to be expressed at reasonably high levels on the surface of whole blood monocytes. Interestingly, priming with TNFα did not upregulate the expression of PR3 or MPO on the surface of whole blood neutrophils. On the contrary, it appeared to significantly downregulate the expression of both these proteins. With regards monocytes, pretreatement with TNFα was found

to upregulate PR3 membrane expression. Despite detectable PR3 and MPO on the surface of whole blood neutrophils and monocytes, stimulation with neither anti-PR3 nor anti-MPO IgG induced cell activation as measured by the reactive oxygen species dependent oxidation of dihydrorhodamine-123 into fluorescent rhodamine-123.

The second section focussed on determining whether GCSF may have a role in potentiating the ANCA induced activation of neutrophils. Interestingly, it was found that GCSF primes isolated neutrophils for anti-MPO, but not anti-PR3, induced neutrophil activation as measure by the production of rhodamine-123. Furthermore, it was shown that this was not the result of a GCSF induced upregulation of MPO on the surface of the cell. Finally, it was shown that GCSF primed mouse neutrophils *in vivo*, and this relates to results obtained from an *in vivo* passive transfer model of anti-MPO IgG induced NCGN, in which GCSF treatment was found to exacerbate disease [239].

The third and final section examined the role of Class IA PI3K in the ANCA induced activation of neutrophils. Using a specific inhibitor, TGX-221, it was shown that the loss PI3Kβ/δ activity profoundly, and negatively, affected the ANCA induced respiratory burst, thus suggesting a role for this molecule in ANCA associated vasculitis pathogenesis.

Chapter 5

This chapter focussed on the establishment of a humanised mouse model. It was found that commercially available umbilical cord blood derived $CD34^+$ stem cells provided higher human cell engraftment in adult irradiated NOD-scid $IL2\gamma^{-/-}$ mice than $CD3^+$ cell depleted umbilical cord blood cells derived in house. Furthermore, it was shown that engrafted mice reconstituted high levels of human $CD45^+$ leukocytes by 8 weeks post transfer of stem cells, and that these levels did not appear to increase further by 12 weeks. In addition, it was confirmed that these mice possessed human T cells and B cells in their bone marrow, spleens and peripheral blood.

Chapter 6

Chapter 6 concerns itself with the reconstitution of human neutrophils by humanised mice. Humanised mice, between 2 and 6 months post engraftment, were found to reconstitute human $CD45^+CD66b^+$ neutrophils at very low levels, with these cells comprising, on average, less than 1% of the total human $CD45^+$ cells in their peripheral blood. Treatment of these mice with human pegylated GCSF for 5 days increased the number of human neutrophils, with these cells comprising, on average, 2.6% of the human peripheral blood cells post treatment. Furthermore, GCSF served to prime the human neutrophils *in vivo*, as measured by CD66b, CD63 and CD11b upregulation, together with CD62L shedding. In addition, the human neutrophils of mice that received subsequent LPS treatment showed further CD66b and CD63 upregulation, as well as further CD62L shedding. Importantly, LPS was also shown to induce human neutrophil trafficking to the lungs. Taken together these results showed that reconstituted human neutrophils were responsive to inflammatory stimuli *in vivo*. In addition, humanised mouse human neutrophils were shown to undergo respiratory burst and degranulation in response to fMLP and *E.coli* stimulation *in vitro*. Finally, human neutrophils reconstituted by humanised mice were shown to express human PR3 and MPO.

Chapter 7

The final results chapter details attempts to induce anti-PR3 and anti-MPO IgG associated disease in humanised mice. Despite the presence of functional human neutrophils, these mice did not show signs of disease when administered LPS, GCSF and patient derived ANCA, elements shown to work together to induce disease in a purely mouse model of anti-MPO IgG associated NCGN [23, 239]. Two separate experiments were carried out, differing in both the patient derived ANCAs used and the concentration administered. The engraftment levels of the mice were tested both before and after the experiments, with human monocytes confirmed to be present in the peripheral blood of mice in the second experimental group. Interestingly, it

was shown that different subsets of human monocytes were present, and that these responded to GCSF, LPS and IgG treatment by significantly increasing in number.

8.2 Limitations and implications

In vitro results: ANCA and it's antigens

The results detailed in chapter 3 and 4 are based on the *in vitro* study of cells, together with, either polyclonal antibodies derived from human blood, or monoclonal antibodies. The main limitation found with regards polyclonal patient derived ANCA, is that not all patient ANCA activates the neutrophil respiratory burst *in vitro*, and of those that do less than 21% induce a notably strong response (based on results using the more sensitive DHR123 assay). It is difficult to say whether this is due to a) the assays used, b) an issue arising from the neutrophil isolation techniques employed or c) the antibody preparation itself. Each of these potential issues, however, will be addressed below:

a) It is possible that ANCA does not mediate enthothelial cell damage via the respiratory burst, and, if that is indeed the case, the ability or inability of ANCA to induce the release of reactive oxygen species is largely irrelevant. Indeed, results, available in abstract form, from a mouse with neutrophils that lack the ability to undergo a respiratory burst suggest that this may be the case [220]. As this has not been confirmed however, the neutrophil respiratory burst remains a major readout of ANCA induced neutrophil activation.

b) That the process of isolation affects the activation status of neutrophils is well documented, and has already been discussed in some detail (Chapter 3 and 4). As demonstrated in Chapter 3, neutrophils isolated using Polymorphprep did not undergo activation in response to ANCA, as measured by the DHR123 assay. However, when neutrophils were isolated using a modified Ficoll method, a robust ANCA induced response could be achieved, again using a DHR123 assay. This suggests that the way in which the

neutrophils are purified has a profound affect on their ability to respond to ANCA. Therefore, it is possible that a larger number of patient purified ANCA might activate neutrophils if the right isolation technique was found. However, it also suggests that it is possible that the *in vitro* activation of neutrophils by ANCA is unphysiological to the point of irrelevance.

The expression of PR3 and MPO on human neutrophils in whole blood was examined in Chapter 4 with both of these ANCA antigens found to be present on the membrane of resting neutrophils. Indeed, in contrast to results with isolated cells [14, 26, 67, 68], TNFα was not only unnecessary for PR3 and MPO expression, but actually significantly downregulated their expression. This result further suggests that ANCA assays using isolated neutrophils do not reflect the *in vivo* behaviour of these cells.

c) The use of whole IgG preparations is a limitation in and of itself. Although patients possess a wide array of antibodies with varying specificities, for *in vitro* assays it would be useful to have antibodies specific for the ANCA antigens. This would allow greater certainty with regards the response being the result of anti-PR3 or anti-MPO antibodies, as opposed to a yet undiscovered antibody specific to another antigen that may be unique to patients, as well as allowing a more precise control over the concentration of ANCA added to the cells. This particular limitation is overcome here by the use of monoclonal anti-PR3 and anti-MPO antibodies, however, as these antibodies have mouse Fc receptors and are specific for one particular epitope, they do not accurately reflect patient ANCA. Furthermore, with recent work showing that IgA may also play a role in ANCA associated vasculitis [73], focussing solely on anti-PR3 and anti-MPO IgG is somewhat limiting.

It is clear that ANCA assays, like all assays, have a number of intrinsic limitations that must be taken into account when interpreting data. However, with appropriate controls, and *in vivo* data to confirm *in vitro* results, they can provide a wealth of information on ANCA:antigen interactions, and subsequent pathogenic responses. Indeed using these assays, GCSF and

PI3Kβ/δ have been implicated in ANCA associated vasculitis (Chapter 4). With regards GCSF, this cytokine has been shown to prime neutrophils for an anti-MPO IgG induced response, and its ability to exacerbate disease has been confirmed *in vivo* using a passive transfer model of ANCA induce NCGN [239]. Thus, the combination of *in vitro* and *in vivo* results strongly suggest that GCSF should be given with great caution to neutropenic patients suffering from ANCA associated vasculitis.

In vivo results: Humanised mouse models

Both anti-PR3 and anti-MPO antibodies have been shown to activate neutrophils *in vitro*. However, while, at the outset of this project, it had already been confirmed that anti-MPO antibodies are capable of inducing NCGN in mice (Discussed in Chapter 1), there had been little corresponding *in vivo* data to confirm the pathogenicity of anti-PR3 antibodies. It must be noted however, that with the recent publication by Little et al. showing that anti-PR3 antibodies induce mild disease in humanised mice, this is no longer the case [326]. As the difficulties involved in developing an animal model of anti-PR3 induced disease is often attributed to the differences in human and mouse PR3, particularly the lack of PR3 on mouse neutrophil membranes [299], it was thought, at the beginning of this project, that the development of a humanised mouse model with functional human neutrophils expressing PR3 had the potential to overcome this issue, and thus could be used to establish a disease model. Furthermore, and representing an advancement on the current models, a humanised mouse model could be used to study human neutrophil:ANCA interactions *in vivo*. However, despite the successful establishment of a humanised mouse model with functional human neutrophils expressing PR3 and MPO, the passive transfer of patient ANCA together with a proinflammatory stimuli, in the form of exogenous human GCSF and LPS, failed to induce pathology in this study. This is in contrast to the previously mentioned study by Little et al. in which anti-PR3 antibodies together with LPS induced disease [326].

There are number of potential reasons for the lack of success of this model, and these are discussed in detail in Chapter 7. However, even had anti-PR3 IgG induced disease in the humanised mice, or indeed, if the existing model established by Little et al. could be optimised to provide a more robust disease model, a number of limitations would still need to be faced. First and foremost of these are complications involved in examining human cells interacting with a mouse environment, particularly with regards mouse endothelium. It is likely that human leukocyte:mouse cell interactions differ from human neutrophil:human cell interactions, and thus results may not be directly translatable. However, it is possible that the transplantation of further human tissues into mice could partially overcome this issue. In addition, the full functionality of humanised mouse human neutrophils remains to be seen. While they appear to mirror all human neutrophil responses tested thus far, it is still possible that they have defects that have yet to be identified. In addition, the lack of available knockout mice would make the study of signalling difficult using this model. Finally, disease induced by the passive transfer of anti-PR3 and anti-MPO IgG, as proposed here, would provide a model of antibody induced disease without any cellular component. Furthermore, as T and B cell response remain suboptimal in humanised mice, it is unlikely that an autoimmune model could be developed in the near future.

Although a humanised mouse model of ANCA associated vasculitis was not established, data showing that humanised mice reconstitute a population of functional human neutrophils represents an important advancement in the study of humanised mouse models. That said, it must be noted that the system described here remains limited by the low numbers of neutrophils found in the peripheral blood, even following GCSF administration. However, the confirmation that humanised mice can support human neutrophil reconstitution, may serve as the basis for further improvements to this *in vivo* model of the human immunity.

8.3 Future work

As mentioned above the use of whole IgG preparations in ANCA studies may be at least partially responsible for the inability of a large number of patient derived ANCA to induce neutrophil activation *in vitro*. In addition, the use of whole IgG preparations may also have been partially responsible for the lack of disease observed in humanised mice. Therefore, affinity purifying patient plasma would provide polyclonal anti-PR3 or anti-MPO specific patient antibody, and thus may allow more potent neutrophil activation. However, even if this did not turn out to be the case, the use of antibodies of known concentration and specificity would allow for more controlled assay conditions, and this would beneficial to the study of ANCA.

PI3Kβ/δ have been implicated in the pathogenesis of ANCA associated vasculitis, with the inhibition of this molecule preventing the ANCA induced activation of neutrophils (Chapter 4). However, this result is preliminary, and much work is still required in order to determine if PI3Kβ/δ does have a role in ANCA signalling. Not only do the *in vitro* results presented here need to be confirmed, both in the ferricytochrome C assay as well as in a separate assay, but *in vivo* confirmation would also be necessary before PI3Kβ/δ could be said to be important, or indeed unimportant, in ANCA pathogenesis. As both PI3Kβ and PI3Kδ deficient mice have already been derived [253, 334], a passive transfer, or a bone marrow transplant, model of anti-MPO induced NCGN could be used to address the need for *in vivo* data, and thus determine if PI3Kβ, PI3Kδ or both represent potential therapeutic targets in ANCA associated vasculitis treatment.

The low number of human neutrophils reconstituted by humanised mice is a limiting factor with regards the use of this model. Thus, increasing the number of human neutrophils reconstituted represents an important avenue for future research, both with regards to improving humanised mouse models in general, and in successfully establishing a humanised mouse model of ANCA associated vasculitis specifically. As discussed in Chapter 1, the use of mice

transgenic for human cytokines has led to improvements in human cell engraftment. Thus, it is possible that with the correct mixture of human cytokines present, including human GCSF, greater human neutrophil engraftment could be achieved. In addition, it is likely that mouse innate immune cells that remain present post human cell engraftment play a role in preventing substantial human myeloid cell engraftment. With regards neutrophils, this may be related to regulatory systems, which serve to prevent the release of excessive numbers of neutrophils from the bone marrow into the circulation [335]. In this scenario, mouse neutrophils would be preferentially released into the circulation with human neutrophils retained in the bone marrow. Indeed, this might fit with the need for exogenous human GCSF to induce the release of human neutrophils, and thus provide peripheral blood human neutrophils for study. To test this theory, and to potentially improve human neutrophil engrafment, a mouse specific neutrophil depletion antibody could be used to remove mouse neutrophils from the circulation, and thus allow for the release of human neutrophils from bone marrow storage.

While a humanised mouse model with functional human neutrophils was established, using the passive transfer of patient ANCA into these mice failed to induce disease. Despite this, the humanised model described in this thesis still has the potential to allow the study of human neutrophils *in vivo*, both with regards to normal human neutrophil behaviour and, more specifically, with regards human neutrophil:ANCA interactions. For example, the use of intravital microscopy could provide data on the behaviour human neutrophils *in vivo*, with the use of blocking strategies allowing the elucidation of molecular mechanism involved in the adhesion of these cells to the endothelium. However, for this to be achieved some method of identifying human cells would first need to be established. The transduction of human $CD34^+$ cells with green fluorescent protein (GFP) prior to engraftment has already be shown [336], and it is possible that this technique may be modified to allow the reconstitution of human neutrophils with a GFP tag. This would most likely involve a significant amount of time to achieve and thus, in the short term, injecting engrafted mice with fluorescently labelled antibodies

would allow the identification of human neutrophils using intravital microscopy techniques. In addition, and as mentioned earlier, it would be preferable to have human endothelium present in these mice and, as human skin has already been successfully transplanted into NOD-scid IL2$\gamma^{-/-}$ mice [133], this should be possible. Thus, despite it's limitations, this model may still allow us to probe human neutrophil responses *in vivo*, both with regards to their ability to confer protection, and induce pathology. Furthermore, these humanised mice may provide a model to test therapeutic interventions that target human neutrophils.

8.4 Concluding remarks

This thesis was divided into two interconnected sections. The first was concerned with establishing assays and antibody purifications, which could then be used in the pursuit of the main goal of the thesis, and the focus of the second section, which was attempting to establish a novel model of ANCA associated vasculitis. Although the main goal of the thesis was not achieved in the manner set out, various important, and novel, discoveries were reported. These include:

- The discovery that PR3 and MPO are expressed on the surface of resting human neutrophils, and, importantly, that TNFα negatively regulates their expression

- The discovery that GCSF potentiates the anti-MPO induced respiratory burst in a manner independent of membrane MPO expression.

- The novel finding that GCSF, given *in vivo*, induces CD11c upregulation by mouse neutrophils

- The discovery that PI3Kβ/δ inhibition prevents the ANCA induced respiratory burst, and thus may have a role in ANCA associated vasculitis pathogenesis

- The discovery that humanised mice have functional human neutrophils that expand in number in response to human GCSF, are activated by human GCSF and LPS, migrate to the lungs in response to LPS and are capable of undergoing robust effector responses *in vitro*

- The discovery that the passive transfer of patient ANCA does not induce disease in humanised mice. Whether this is due to limitations associated with the humanised mouse model and/or the ANCA preparations used, or whether this may suggest that ANCA are not pathogenic in and of themselves, remains to be seen.

Thus, results arising from this work provide many future avenues of research both in the field of ANCA associated vasculitis, and with regard the study of human neutrophils *in vivo*.

1. **Booth, A.D., et al., *Outcome of ANCA-associated renal vasculitis: a 5-year retrospective study.* Am J Kidney Dis, 2003. 41(4): p. 776-84.**
2. **Walton, E.W., *Giant-cell granuloma of the respiratory tract (Wegener's granulomatosis).* Br Med J, 1958. 2(5091): p. 265-70.**
3. **Hamour, S., A.D. Salama, and C.D. Pusey, *Management of ANCA-associated vasculitis: Current trends and future prospects.* Ther Clin Risk Manag, 2010. 6: p. 253-64.**
4. **Jennette, J.C., et al., *Pathogenesis of antineutrophil cytoplasmic autoantibody-associated small-vessel vasculitis.* Annu Rev Pathol, 2013. 8: p. 139-60.**
5. **Hoffman, G.S., et al., *Wegener granulomatosis: an analysis of 158 patients.* Ann Intern Med, 1992. 116(6): p. 488-98.**
6. **Davies, D.J., et al., *Segmental necrotising glomerulonephritis with antineutrophil antibody: possible arbovirus aetiology?* Br Med J (Clin Res Ed), 1982. 285(6342): p. 606.**
7. **van der Woude, F.J., *Anticytoplasmic antibodies in Wegener's granulomatosis.* Lancet, 1985. 2(8445): p. 48.**
8. **Stegeman, C.A., *Anti-neutrophil cytoplasmic antibody (ANCA) levels directed against proteinase-3 and myeloperoxidase are helpful in predicting disease relapse in ANCA-associated small-vessel vasculitis.* Nephrol Dial Transplant, 2002. 17(12): p. 2077-80.**
9. **Sanders, J.S., et al., *Prediction of relapses in PR3-ANCA-associated vasculitis by assessing responses of ANCA titres to treatment.* Rheumatology (Oxford), 2006. 45(6): p. 724-9.**
10. **Finkielman, J.D., et al., *Antiproteinase 3 antineutrophil cytoplasmic antibodies and disease activity in Wegener granulomatosis.* Ann Intern Med, 2007. 147(9): p. 611-9.**
11. **Falk, R.J. and J.C. Jennette, *Anti-neutrophil cytoplasmic autoantibodies with specificity for myeloperoxidase in patients with systemic vasculitis and idiopathic necrotizing and crescentic glomerulonephritis.* N Engl J Med, 1988. 318(25): p. 1651-7.**
12. **Ludemann, J., B. Utecht, and W.L. Gross, *Anti-neutrophil cytoplasm antibodies in Wegener's granulomatosis recognize an elastinolytic enzyme.* J Exp Med, 1990. 171(1): p. 357-62.**
13. **Franssen, C.F., et al., *Antiproteinase 3- and antimyeloperoxidase-associated vasculitis.* Kidney Int, 2000. 57(6): p. 2195-206.**
14. **Falk, R.J., et al., *Anti-neutrophil cytoplasmic autoantibodies induce neutrophils to degranulate and produce oxygen radicals in vitro.* Proc Natl Acad Sci U S A, 1990. 87(11): p. 4115-9.**
15. **Van Rossum, A.P., et al., *Human anti-neutrophil cytoplasm autoantibodies to proteinase 3 (PR3-ANCA) bind to neutrophils.* Kidney Int, 2005. 68(2): p. 537-41.**
16. **Charles, L.A., et al., *Antibodies against granule proteins activate neutrophils in vitro.* J Leukoc Biol, 1991. 50(6): p. 539-46.**
17. **Brooks, C.J., et al., *IL-1 beta production by human polymorphonuclear leucocytes stimulated by anti-neutrophil cytoplasmic autoantibodies: relevance to systemic vasculitis.* Clin Exp Immunol, 1996. 106(2): p. 273-9.**

18. **Kessenbrock, K., et al., *Netting neutrophils in autoimmune small-vessel vasculitis.* Nat Med, 2009. 15(6): p. 623-5.**
19. **Ewert, B.H., J.C. Jennette, and R.J. Falk, *Anti-myeloperoxidase antibodies stimulate neutrophils to damage human endothelial cells.* Kidney Int, 1992. 41(2): p. 375-83.**
20. **Savage, C.O., et al., *Autoantibodies developing to myeloperoxidase and proteinase 3 in systemic vasculitis stimulate neutrophil cytotoxicity toward cultured endothelial cells.* Am J Pathol, 1992. 141(2): p. 335-42.**
21. **Brouwer, E., et al., *Neutrophil activation in vitro and in vivo in Wegener's granulomatosis.* Kidney Int, 1994. 45(4): p. 1120-31.**
22. **Xiao, H., et al., *The role of neutrophils in the induction of glomerulonephritis by anti-myeloperoxidase antibodies.* Am J Pathol, 2005. 167(1): p. 39-45.**
23. **Huugen, D., et al., *Aggravation of anti-myeloperoxidase antibody-induced glomerulonephritis by bacterial lipopolysaccharide: role of tumor necrosis factor-alpha.* Am J Pathol, 2005. 167(1): p. 47-58.**
24. **Sanders, J.S., et al., *Risk factors for relapse in anti-neutrophil cytoplasmic antibody (ANCA)-associated vasculitis: tools for treatment decisions?* Clin Exp Rheumatol, 2004. 22(6 Suppl 36): p. S94-101.**
25. **Kuligowski, M.P., et al., *Antimyeloperoxidase antibodies rapidly induce alpha-4-integrin-dependent glomerular neutrophil adhesion.* Blood, 2009. 113(25): p. 6485-94.**
26. **Kettritz, R., et al., *Role of mitogen-activated protein kinases in activation of human neutrophils by antineutrophil cytoplasmic antibodies.* J Am Soc Nephrol, 2001. 12(1): p. 37-46.**
27. **Summers, S.A., et al., *Intrinsic renal cell and leukocyte-derived TLR4 aggravate experimental anti-MPO glomerulonephritis.* Kidney Int, 2010. 78(12): p. 1263-74.**
28. **Campanelli, D., et al., *Cloning of cDNA for proteinase 3: a serine protease, antibiotic, and autoantigen from human neutrophils.* J Exp Med, 1990. 172(6): p. 1709-15.**
29. **Campanelli, D., et al., *Azurocidin and a homologous serine protease from neutrophils. Differential antimicrobial and proteolytic properties.* J Clin Invest, 1990. 85(3): p. 904-15.**
30. **Kao, R.C., et al., *Proteinase 3. A distinct human polymorphonuclear leukocyte proteinase that produces emphysema in hamsters.* J Clin Invest, 1988. 82(6): p. 1963-73.**
31. **Gabay, J.E., et al., *Antibiotic proteins of human polymorphonuclear leukocytes.* Proc Natl Acad Sci U S A, 1989. 86(14): p. 5610-4.**
32. **Odeberg, H. and I. Olsson, *Mechanisms for the microbicidal activity of cationic proteins of human granulocytes.* Infect Immun, 1976. 14(6): p. 1269-75.**
33. **Bank, U., et al., *Evidence for a crucial role of neutrophil-derived serine proteases in the inactivation of interleukin-6 at sites of inflammation.* FEBS Lett, 1999. 461(3): p. 235-40.**
34. **Csernok, E., et al., *Transforming growth factor-beta (TGF-beta) expression and interaction with proteinase 3 (PR3) in anti-neutrophil***

cytoplasmic antibody (ANCA)-associated vasculitis. **Clin Exp Immunol, 1996. 105(1): p. 104-11.**

35. **Tal, T., M. Sharabani, and I. Aviram, *Cationic proteins of neutrophil azurophilic granules: protein-protein interaction and blockade of NADPH oxidase activation.* J Leukoc Biol, 1998. 63(3): p. 305-11.**
36. **Padrines, M., et al., *Interleukin-8 processing by neutrophil elastase, cathepsin G and proteinase-3.* FEBS Lett, 1994. 352(2): p. 231-5.**
37. **Robache-Gallea, S., et al., *In vitro processing of human tumor necrosis factor-alpha.* J Biol Chem, 1995. 270(40): p. 23688-92.**
38. **Coeshott, C., et al., *Converting enzyme-independent release of tumor necrosis factor alpha and IL-1beta from a stimulated human monocytic cell line in the presence of activated neutrophils or purified proteinase 3.* Proc Natl Acad Sci U S A, 1999. 96(11): p. 6261-6.**
39. **Bank, U., et al., *Selective proteolytic cleavage of IL-2 receptor and IL-6 receptor ligand binding chains by neutrophil-derived serine proteases at foci of inflammation.* J Interferon Cytokine Res, 1999. 19(11): p. 1277-87.**
40. **Renesto, P., et al., *Proteinase 3. A neutrophil proteinase with activity on platelets.* J Immunol, 1994. 152(9): p. 4612-7.**
41. **Renesto, P., et al., *Specific inhibition of thrombin-induced cell activation by the neutrophil proteinases elastase, cathepsin G, and proteinase 3: evidence for distinct cleavage sites within the aminoterminal domain of the thrombin receptor.* Blood, 1997. 89(6): p. 1944-53.**
42. **Witko-Sarsat, V., et al., *Presence of proteinase 3 in secretory vesicles: evidence of a novel, highly mobilizable intracellular pool distinct from azurophil granules.* Blood, 1999. 94(7): p. 2487-96.**
43. **Baggiolini, M., et al., *The polymorphonuclear leukocyte.* Agents Actions, 1978. 8(1-2): p. 3-10.**
44. **Klebanoff, S.J., *Iodination of bacteria: a bactericidal mechanism.* J Exp Med, 1967. 126(6): p. 1063-78.**
45. **Klinke, A., et al., *Myeloperoxidase attracts neutrophils by physical forces.* Blood, 2011. 117(4): p. 1350-8.**
46. **Deimann, W., *Endogenous peroxidase activity in mononuclear phagocytes.* Prog Histochem Cytochem, 1984. 15(2): p. 1-58.**
47. **Csernok, E., et al., *Ultrastructural localization of proteinase 3, the target antigen of anti-cytoplasmic antibodies circulating in Wegener's granulomatosis.* Am J Pathol, 1990. 137(5): p. 1113-20.**
48. **Halbwachs-Mecarelli, L., et al., *Bimodal distribution of proteinase 3 (PR3) surface expression reflects a constitutive heterogeneity in the polymorphonuclear neutrophil pool.* FEBS Lett, 1995. 374(1): p. 29-33.**
49. **Schreiber, A., F.C. Luft, and R. Kettritz, *Membrane proteinase 3 expression and ANCA-induced neutrophil activation.* Kidney Int, 2004. 65(6): p. 2172-83.**
50. **Hu, N., et al., *Coexpression of CD177 and membrane proteinase 3 on neutrophils in antineutrophil cytoplasmic autoantibody-associated systemic vasculitis: anti-proteinase 3-mediated neutrophil activation***

is independent of the role of CD177-expressing neutrophils. Arthritis Rheum, 2009. 60(5): p. 1548-57.

51. Witko-Sarsat, V., et al., *A large subset of neutrophils expressing membrane proteinase 3 is a risk factor for vasculitis and rheumatoid arthritis.* J Am Soc Nephrol, 1999. 10(6): p. 1224-33.
52. Hajjar, E., et al., *Computational prediction of the binding site of proteinase 3 to the plasma membrane.* Proteins, 2008. 71(4): p. 1655-69.
53. Bauer, S., et al., *Proteinase 3 and CD177 are expressed on the plasma membrane of the same subset of neutrophils.* J Leukoc Biol, 2007. 81(2): p. 458-64.
54. von Vietinghoff, S., et al., *NB1 mediates surface expression of the ANCA antigen proteinase 3 on human neutrophils.* Blood, 2007. 109(10): p. 4487-93.
55. Korkmaz, B., et al., *Catalytic activity and inhibition of wegener antigen proteinase 3 on the cell surface of human polymorphonuclear neutrophils.* J Biol Chem, 2009. 284(30): p. 19896-902.
56. Jerke, U., et al., *Complement receptor Mac-1 is an adaptor for NB1 (CD177)-mediated PR3-ANCA neutrophil activation.* J Biol Chem, 2011. 286(9): p. 7070-81.
57. David, A., et al., *Interaction of proteinase 3 with CD11b/CD18 (beta2 integrin) on the cell membrane of human neutrophils.* J Leukoc Biol, 2003. 74(4): p. 551-7.
58. David, A., R. Fridlich, and I. Aviram, *The presence of membrane Proteinase 3 in neutrophil lipid rafts and its colocalization with FcgammaRIIIb and cytochrome b558.* Exp Cell Res, 2005. 308(1): p. 156-65.
59. Lau, D., et al., *Myeloperoxidase mediates neutrophil activation by association with CD11b/CD18 integrins.* Proc Natl Acad Sci U S A, 2005. 102(2): p. 431-6.
60. Kain, R., et al., *A novel class of autoantigens of anti-neutrophil cytoplasmic antibodies in necrotizing and crescentic glomerulonephritis: the lysosomal membrane glycoprotein h-lamp-2 in neutrophil granulocytes and a related membrane protein in glomerular endothelial cells.* J Exp Med, 1995. 181(2): p. 585-97.
61. Karlsson, K. and S.R. Carlsson, *Sorting of lysosomal membrane glycoproteins lamp-1 and lamp-2 into vesicles distinct from mannose 6-phosphate receptor/gamma-adaptin vesicles at the trans-Golgi network.* J Biol Chem, 1998. 273(30): p. 18966-73.
62. Kain, R., et al., *Molecular mimicry in pauci-immune focal necrotizing glomerulonephritis.* Nat Med, 2008. 14(10): p. 1088-96.
63. Roth, A.J., et al., *Anti-LAMP-2 antibodies are not prevalent in patients with antineutrophil cytoplasmic autoantibody glomerulonephritis.* J Am Soc Nephrol, 2012. 23(3): p. 545-55.
64. Kain, R., et al., *High prevalence of autoantibodies to hLAMP-2 in anti-neutrophil cytoplasmic antibody-associated vasculitis.* J Am Soc Nephrol, 2012. 23(3): p. 556-66.

65. **Kettritz, R., J.C. Jennette, and R.J. Falk, *Crosslinking of ANCA-antigens stimulates superoxide release by human neutrophils.* J Am Soc Nephrol, 1997. 8(3): p. 386-94.**
66. **Keogan, M.T., et al., *Activation of normal neutrophils by anti-neutrophil cytoplasm antibodies.* Clin Exp Immunol, 1992. 90(2): p. 228-34.**
67. **Porges, A.J., et al., *Anti-neutrophil cytoplasmic antibodies engage and activate human neutrophils via Fc gamma RIIa.* J Immunol, 1994. 153(3): p. 1271-80.**
68. **Mulder, A.H., et al., *Activation of granulocytes by anti-neutrophil cytoplasmic antibodies (ANCA): a Fc gamma RII-dependent process.* Clin Exp Immunol, 1994. 98(2): p. 270-8.**
69. **Reumaux, D., et al., *Effect of tumor necrosis factor-induced integrin activation on Fc gamma receptor II-mediated signal transduction: relevance for activation of neutrophils by anti-proteinase 3 or anti-myeloperoxidase antibodies.* Blood, 1995. 86(8): p. 3189-95.**
70. **Yang, J.J., et al., *Expression profile of leukocyte genes activated by anti-neutrophil cytoplasmic autoantibodies (ANCA).* Kidney Int, 2002. 62(5): p. 1638-49.**
71. **Williams, J.M., et al., *Activation of the G(i) heterotrimeric G protein by ANCA IgG F(ab')2 fragments is necessary but not sufficient to stimulate the recruitment of those downstream mediators used by intact ANCA IgG.* J Am Soc Nephrol, 2003. 14(3): p. 661-9.**
72. **Nolan, S.L., et al., *Mechanisms of ANCA-mediated leukocyte-endothelial cell interactions in vivo.* J Am Soc Nephrol, 2008. 19(5): p. 973-84.**
73. **Kelley, J.M., et al., *IgA and IgG antineutrophil cytoplasmic antibody engagement of Fc receptor genetic variants influences granulomatosis with polyangiitis.* Proc Natl Acad Sci U S A, 2011. 108(51): p. 20736-41.**
74. **Radford, D.J., J.M. Lord, and C.O. Savage, *The activation of the neutrophil respiratory burst by anti-neutrophil cytoplasm autoantibody (ANCA) from patients with systemic vasculitis requires tyrosine kinases and protein kinase C activation.* Clin Exp Immunol, 1999. 118(1): p. 171-9.**
75. **Ben-Smith, A., et al., *Antineutrophil cytoplasm autoantibodies from patients with systemic vasculitis activate neutrophils through distinct signaling cascades: comparison with conventional Fcgamma receptor ligation.* Blood, 2001. 98(5): p. 1448-55.**
76. **Kettritz, R., et al., *Phosphatidylinositol 3-kinase controls antineutrophil cytoplasmic antibodies-induced respiratory burst in human neutrophils.* J Am Soc Nephrol, 2002. 13(7): p. 1740-9.**
77. **Chen, Q., et al., *Akt phosphorylates p47phox and mediates respiratory burst activity in human neutrophils.* J Immunol, 2003. 170(10): p. 5302-8.**
78. **Hewins, P., et al., *Activation of Syk in neutrophils by antineutrophil cytoplasm antibodies occurs via Fcgamma receptors and CD18.* J Am Soc Nephrol, 2004. 15(3): p. 796-808.**
79. **Williams, J.M., et al., *Antineutrophil cytoplasm antibody-stimulated neutrophil adhesion depends on diacylglycerol kinase-catalyzed***

phosphatidic acid formation. **J Am Soc Nephrol, 2007. 18(4): p. 1112-20.**

80. **Polzer, K., et al., *Selective p38MAPK isoform expression and activation in antineutrophil cytoplasmatic antibody-associated crescentic glomerulonephritis: role of p38MAPKalpha.* Ann Rheum Dis, 2008. 67(5): p. 602-8.**
81. **van der Veen, B.S., et al., *Effects of p38 mitogen-activated protein kinase inhibition on anti-neutrophil cytoplasmic autoantibody pathogenicity in vitro and in vivo.* Ann Rheum Dis, 2011. 70(2): p. 356-65.**
82. **Schreiber, A., et al., *Phosphoinositol 3-kinase-gamma mediates antineutrophil cytoplasmic autoantibody-induced glomerulonephritis.* Kidney Int, 2010. 77(2): p. 118-28.**
83. **Li, Z., et al., *Roles of PLC-beta2 and -beta3 and PI3Kgamma in chemoattractant-mediated signal transduction.* Science, 2000. 287(5455): p. 1046-9.**
84. **Hirsch, E., et al., *Central role for G protein-coupled phosphoinositide 3-kinase gamma in inflammation.* Science, 2000. 287(5455): p. 1049-53.**
85. **Sasaki, T., et al., *Function of PI3Kgamma in thymocyte development, T cell activation, and neutrophil migration.* Science, 2000. 287(5455): p. 1040-6.**
86. **Xiao, H., et al., *Alternative complement pathway in the pathogenesis of disease mediated by anti-neutrophil cytoplasmic autoantibodies.* Am J Pathol, 2007. 170(1): p. 52-64.**
87. **Huugen, D., et al., *Inhibition of complement factor C5 protects against anti-myeloperoxidase antibody-mediated glomerulonephritis in mice.* Kidney Int, 2007. 71(7): p. 646-54.**
88. **Schreiber, A., et al., *C5a receptor mediates neutrophil activation and ANCA-induced glomerulonephritis.* J Am Soc Nephrol, 2009. 20(2): p. 289-98.**
89. **Neumann, I., et al., *SCG/Kinjoh mice: a model of ANCA-associated crescentic glomerulonephritis with immune deposits.* Kidney Int, 2003. 64(1): p. 140-8.**
90. **Jethwa, H.S., et al., *False-positive myeloperoxidase binding activity due to DNA/anti-DNA antibody complexes: a source for analytical error in serologic evaluation of anti-neutrophil cytoplasmic autoantibodies.* Clin Exp Immunol, 2000. 121(3): p. 544-50.**
91. **Jethwa, H.S., et al., *Restriction in V kappa gene use and antigen selection in anti-myeloperoxidase response in mice.* J Immunol, 2000. 165(7): p. 3890-7.**
92. **Xiao, H., et al., *Antineutrophil cytoplasmic autoantibodies specific for myeloperoxidase cause glomerulonephritis and vasculitis in mice.* J Clin Invest, 2002. 110(7): p. 955-63.**
93. **Giorgini, A., et al., *Toll-like receptor 4 stimulation triggers crescentic glomerulonephritis by multiple mechanisms including a direct effect on renal cells.* Am J Pathol, 2010. 177(2): p. 644-53.**

94. **Brown, H.J., et al., *Toll-like receptor 4 ligation on intrinsic renal cells contributes to the induction of antibody-mediated glomerulonephritis via CXCL1 and CXCL2.* J Am Soc Nephrol, 2007. 18(6): p. 1732-9.**
95. **Schreiber, A., et al., *Bone marrow-derived cells are sufficient and necessary targets to mediate glomerulonephritis and vasculitis induced by anti-myeloperoxidase antibodies.* J Am Soc Nephrol, 2006. 17(12): p. 3355-64.**
96. **Ruth, A.J., et al., *Anti-neutrophil cytoplasmic antibodies and effector CD4+ cells play nonredundant roles in anti-myeloperoxidase crescentic glomerulonephritis.* J Am Soc Nephrol, 2006. 17(7): p. 1940-9.**
97. **Gan, P.Y., et al., *Th17 cells promote autoimmune anti-myeloperoxidase glomerulonephritis.* J Am Soc Nephrol, 2010. 21(6): p. 925-31.**
98. **Little, M.A., et al., *Antineutrophil cytoplasm antibodies directed against myeloperoxidase augment leukocyte-microvascular interactions in vivo.* Blood, 2005. 106(6): p. 2050-8.**
99. **Little, M.A., et al., *Experimental autoimmune vasculitis: an animal model of anti-neutrophil cytoplasmic autoantibody-associated systemic vasculitis.* Am J Pathol, 2009. 174(4): p. 1212-20.**
100. **Nasso, M., et al., *Genetically detoxified pertussis toxin induces Th1/Th17 immune response through MAPKs and IL-10-dependent mechanisms.* J Immunol, 2009. 183(3): p. 1892-9.**
101. **Pfister, H., et al., *Antineutrophil cytoplasmic autoantibodies against the murine homolog of proteinase 3 (Wegener autoantigen) are pathogenic in vivo.* Blood, 2004. 104(5): p. 1411-8.**
102. **van der Geld, Y.M., et al., *Rats and mice immunised with chimeric human/mouse proteinase 3 produce autoantibodies to mouse Pr3 and rat granulocytes.* Ann Rheum Dis, 2007. 66(12): p. 1679-82.**
103. **Primo, V.C., et al., *Anti-PR3 immune responses induce segmental and necrotizing glomerulonephritis.* Clin Exp Immunol, 2010. 159(3): p. 327-37.**
104. **Wiesner, O., et al., *Differences between human proteinase 3 and neutrophil elastase and their murine homologues are relevant for murine model experiments.* FEBS Lett, 2005. 579(24): p. 5305-12.**
105. **Moreno, C., et al., *Creation and characterization of a renin knockout rat.* Hypertension, 2011. 57(3): p. 614-9.**
106. **Zanjani, E.D., G. Almeida-Porada, and A.W. Flake, *The human/sheep xenograft model: a large animal model of human hematopoiesis.* Int J Hematol, 1996. 63(3): p. 179-92.**
107. **Zanjani, E.D., *The human sheep xenograft model for the study of the in vivo potential of human HSC and in utero gene transfer.* Stem Cells, 2000. 18(2): p. 151.**
108. **Ganick, D.J., et al., *Inability of intravenously injected monocellular suspensions of human bone marrow to establish in the nude mouse.* Int Arch Allergy Appl Immunol, 1980. 62(3): p. 330-3.**
109. **Bosma, G.C., R.P. Custer, and M.J. Bosma, *A severe combined immunodeficiency mutation in the mouse.* Nature, 1983. 301(5900): p. 527-30.**

110. **Mosier, D.E., et al.,** ***Transfer of a functional human immune system to mice with severe combined immunodeficiency.*** **Nature, 1988. 335(6187): p. 256-9.**
111. **McCune, J.M., et al.,** ***The SCID-hu mouse: murine model for the analysis of human hematolymphoid differentiation and function.*** **Science, 1988. 241(4873): p. 1632-9.**
112. **Lapidot, T., et al.,** ***Cytokine stimulation of multilineage hematopoiesis from immature human cells engrafted in SCID mice.*** **Science, 1992. 255(5048): p. 1137-41.**
113. **Greiner, D.L., R.A. Hesselton, and L.D. Shultz,** ***SCID mouse models of human stem cell engraftment.*** **Stem Cells, 1998. 16(3): p. 166-77.**
114. **Shultz, L.D., et al.,** ***Multiple defects in innate and adaptive immunologic function in NOD/LtSz-scid mice.*** **J Immunol, 1995. 154(1): p. 180-91.**
115. **Hesselton, R.M., et al.,** ***High levels of human peripheral blood mononuclear cell engraftment and enhanced susceptibility to human immunodeficiency virus type 1 infection in NOD/LtSz-scid/scid mice.*** **J Infect Dis, 1995. 172(4): p. 974-82.**
116. **Lowry, P.A., et al.,** ***Improved engraftment of human cord blood stem cells in NOD/LtSz-scid/scid mice after irradiation or multiple-day injections into unirradiated recipients.*** **Biol Blood Marrow Transplant, 1996. 2(1): p. 15-23.**
117. **Pflumio, F., et al.,** ***Phenotype and function of human hematopoietic cells engrafting immune-deficient CB17-severe combined immunodeficiency mice and nonobese diabetic-severe combined immunodeficiency mice after transplantation of human cord blood mononuclear cells.*** **Blood, 1996. 88(10): p. 3731-40.**
118. **Manz, M.G.,** ***Human-hemato-lymphoid-system mice: opportunities and challenges.*** **Immunity, 2007. 26(5): p. 537-41.**
119. **Shultz, L.D., F. Ishikawa, and D.L. Greiner,** ***Humanized mice in translational biomedical research.*** **Nat Rev Immunol, 2007. 7(2): p. 118-30.**
120. **Sugamura, K., et al.,** ***The interleukin-2 receptor gamma chain: its role in the multiple cytokine receptor complexes and T cell development in XSCID.*** **Annu Rev Immunol, 1996. 14: p. 179-205.**
121. **Cao, X., et al.,** ***Defective lymphoid development in mice lacking expression of the common cytokine receptor gamma chain.*** **Immunity, 1995. 2(3): p. 223-38.**
122. **DiSanto, J.P., et al.,** ***Lymphoid development in mice with a targeted deletion of the interleukin 2 receptor gamma chain.*** **Proc Natl Acad Sci U S A, 1995. 92(2): p. 377-81.**
123. **Ohbo, K., et al.,** ***Modulation of hematopoiesis in mice with a truncated mutant of the interleukin-2 receptor gamma chain.*** **Blood, 1996. 87(3): p. 956-67.**
124. **Jacobs, H., et al.,** ***PIM1 reconstitutes thymus cellularity in interleukin 7- and common gamma chain-mutant mice and permits thymocyte maturation in Rag- but not CD3gamma-deficient mice.*** **J Exp Med, 1999. 190(8): p. 1059-68.**

125. **Ito, M., et al., *NOD/SCID/gamma(c)(null) mouse: an excellent recipient mouse model for engraftment of human cells.* Blood, 2002. 100(9): p. 3175-82.**
126. **Traggiai, E., et al., *Development of a human adaptive immune system in cord blood cell-transplanted mice.* Science, 2004. 304(5667): p. 104-7.**
127. **Ishikawa, F., et al., *Development of functional human blood and immune systems in NOD/SCID/IL2 receptor {gamma} chain(null) mice.* Blood, 2005. 106(5): p. 1565-73.**
128. **Brehm, M.A., et al., *Parameters for establishing humanized mouse models to study human immunity: analysis of human hematopoietic stem cell engraftment in three immunodeficient strains of mice bearing the IL2rgamma(null) mutation.* Clin Immunol, 2010. 135(1): p. 84-98.**
129. **Pearson, T., D.L. Greiner, and L.D. Shultz, *Creation of "humanized" mice to study human immunity.* Curr Protoc Immunol, 2008. Chapter 15: p. Unit 15 21.**
130. **van Rijn, R.S., et al., *A new xenograft model for graft-versus-host disease by intravenous transfer of human peripheral blood mononuclear cells in RAG2-/- gammac-/- double-mutant mice.* Blood, 2003. 102(7): p. 2522-31.**
131. **Shultz, L.D., et al., *Humanized mice as a preclinical tool for infectious disease and biomedical research.* Ann N Y Acad Sci. , 2011. 1245: p. 50-54.**
132. **King, M.A., et al., *Human peripheral blood leucocyte non-obese diabetic-severe combined immunodeficiency interleukin-2 receptor gamma chain gene mouse model of xenogeneic graft-versus-host-like disease and the role of host major histocompatibility complex.* Clin Exp Immunol, 2009. 157(1): p. 104-18.**
133. **Sagoo, P., et al., *Human regulatory T cells with alloantigen specificity are more potent inhibitors of alloimmune skin graft damage than polyclonal regulatory T cells.* Sci Transl Med, 2011. 3(83): p. 83ra42.**
134. **Metcalf, D., *On hematopoietic stem cell fate.* Immunity, 2007. 26(6): p. 669-73.**
135. **Melkus, M.W., et al., *Humanized mice mount specific adaptive and innate immune responses to EBV and TSST-1.* Nat Med, 2006. 12(11): p. 1316-22.**
136. **Wege, A.K., et al., *Functional and phenotypic characterization of the humanized BLT mouse model.* Curr Top Microbiol Immunol, 2008. 324: p. 149-65.**
137. **Stoddart, C.A., et al., *Superior human leukocyte reconstitution and susceptibility to vaginal HIV transmission in humanized NOD-scid IL-2Rgamma(-/-) (NSG) BLT mice.* Virology, 2011. 417(1): p. 154-60.**
138. **Huntington, N.D. and J.P. Di Santo, *Humanized immune system (HIS) mice as a tool to study human NK cell development.* Curr Top Microbiol Immunol, 2008. 324: p. 109-24.**
139. **Chen, Q., M. Khoury, and J. Chen, *Expression of human cytokines dramatically improves reconstitution of specific human-blood lineage***

cells in humanized mice. **Proc Natl Acad Sci U S A, 2009. 106(51): p. 21783-8.**

140. Huntington, N.D., et al., *IL-15 transpresentation promotes both human T-cell reconstitution and T-cell-dependent antibody responses in vivo.* Proc Natl Acad Sci U S A, 2011. 108(15): p. 6217-22.

141. Pek, E.A., et al., *Characterization and IL-15 dependence of NK cells in humanized mice.* Immunobiology, 2011. 216(1-2): p. 218-24.

142. Andre, M.C., et al., *Long-term human CD34+ stem cell-engrafted nonobese diabetic/SCID/IL-2R gamma(null) mice show impaired CD8+ T cell maintenance and a functional arrest of immature NK cells.* J Immunol, 2010. 185(5): p. 2710-20.

143. Huntington, N.D., et al., *IL-15 trans-presentation promotes human NK cell development and differentiation in vivo.* J Exp Med, 2009. 206(1): p. 25-34.

144. Kwant-Mitchell, A., et al., *Development of functional human NK cells in an immunodeficient mouse model with the ability to provide protection against tumor challenge.* PLoS One, 2009. 4(12): p. e8379.

145. Watanabe, Y., et al., *The analysis of the functions of human B and T cells in humanized NOD/shi-scid/gammac(null) (NOG) mice (hu-HSC NOG mice).* Int Immunol, 2009. 21(7): p. 843-58.

146. Matsumura, T., et al., *Functional CD5+ B cells develop predominantly in the spleen of NOD/SCID/gammac(null) (NOG) mice transplanted either with human umbilical cord blood, bone marrow, or mobilized peripheral blood CD34+ cells.* Exp Hematol, 2003. 31(9): p. 789-97.

147. Baenziger, S., et al., *Disseminated and sustained HIV infection in CD34+ cord blood cell-transplanted Rag2-/-gamma c-/- mice.* Proc Natl Acad Sci U S A, 2006. 103(43): p. 15951-6.

148. Garcia, S. and A.A. Freitas, *Humanized mice: Current states and perspectives.* Immunol Lett, 2012. 146(1-2): p. 1-7.

149. Watanabe, S., et al., *Hematopoietic stem cell-engrafted NOD/SCID/IL2Rgamma null mice develop human lymphoid systems and induce long-lasting HIV-1 infection with specific humoral immune responses.* Blood, 2007. 109(1): p. 212-8.

150. Gorantla, S., et al., *Human immunodeficiency virus type 1 pathobiology studied in humanized BALB/c-Rag2-/-gammac-/- mice.* J Virol, 2007. 81(6): p. 2700-12.

151. Gorantla, S., et al., *CD8+ cell depletion accelerates HIV-1 immunopathology in humanized mice.* J Immunol, 2010. 184(12): p. 7082-91.

152. van Lent, A.U., et al., *IL-7 enhances thymic human T cell development in "human immune system" Rag2-/-IL-2Rgammac-/- mice without affecting peripheral T cell homeostasis.* J Immunol, 2009. 183(12): p. 7645-55.

153. Choudhary, S.K., et al., *Latent HIV-1 infection of resting CD4(+) T cells in the humanized Rag2(-)/(-) gammac(-)/(-) mouse.* J Virol, 2012. 86(1): p. 114-20.

154. Billerbeck, E., et al., *Development of human CD4+FoxP3+ regulatory T cells in human stem cell factor-, granulocyte-macrophage colony-*

stimulating factor-, and interleukin-3-expressing NOD-SCID IL2Rgamma(null) humanized mice. **Blood, 2011. 117(11): p. 3076-86.**

155. Hiramatsu, H., et al., *Complete reconstitution of human lymphocytes from cord blood CD34+ cells using the NOD/SCID/gammacnull mice model.* Blood, 2003. 102(3): p. 873-80.

156. Yajima, M., et al., *T cell-mediated control of Epstein-Barr virus infection in humanized mice.* J Infect Dis, 2009. 200(10): p. 1611-5.

157. Takahashi, M., et al., *Comprehensive evaluation of leukocyte lineage derived from human hematopoietic cells in humanized mice.* J Biosci Bioeng, 2012. 113(4): p. 529-35.

158. Strowig, T., et al., *Priming of protective T cell responses against virus-induced tumors in mice with human immune system components.* J Exp Med, 2009. 206(6): p. 1423-34.

159. Shultz, L.D., et al., *Generation of functional human T-cell subsets with HLA-restricted immune responses in HLA class I expressing NOD/SCID/IL2r gamma(null) humanized mice.* Proc Natl Acad Sci U S A, 2010. 107(29): p. 13022-7.

160. Jaiswal, S., et al., *Dengue virus infection and virus-specific HLA-A2 restricted immune responses in humanized NOD-scid IL2rgammanull mice.* PLoS One, 2009. 4(10): p. e7251.

161. Danner, R., et al., *Expression of HLA class II molecules in humanized NOD.Rag1KO.IL2RgcKO mice is critical for development and function of human T and B cells.* PLoS One, 2011. 6(5): p. e19826.

162. Legrand, N., et al., *Humanized mice for modeling human infectious disease: challenges, progress, and outlook.* Cell Host Microbe, 2009. 6(1): p. 5-9.

163. Rathinam, C., et al., *Efficient differentiation and function of human macrophages in humanized CSF-1 mice.* Blood, 2011. 118(11): p. 3119-28.

164. Willinger, T., et al., *Human IL-3/GM-CSF knock-in mice support human alveolar macrophage development and human immune responses in the lung.* Proc Natl Acad Sci U S A, 2011. 108(6): p. 2390-5.

165. Tanaka, S., et al., *Development of mature and functional human myeloid subsets in hematopoietic stem cell-engrafted NOD/SCID/IL2rgammaKO mice.* J Immunol, 2012. 188(12): p. 6145-55.

166. Namikawa, R., et al., *Infection of the SCID-hu mouse by HIV-1.* Science, 1988. 242(4886): p. 1684-6.

167. Sato, K. and Y. Koyanagi, *The mouse is out of the bag: insights and perspectives on HIV-1-infected humanized mouse models.* Exp Biol Med (Maywood), 2011. 236(8): p. 977-85.

168. Sun, Z., et al., *Intrarectal transmission, systemic infection, and CD4+ T cell depletion in humanized mice infected with HIV-1.* J Exp Med, 2007. 204(4): p. 705-14.

169. Nie, C., et al., *Selective infection of CD4+ effector memory T lymphocytes leads to preferential depletion of memory T lymphocytes in R5 HIV-1-infected humanized NOD/SCID/IL-2Rgammanull mice.* Virology, 2009. 394(1): p. 64-72.

170. **Jiang, Q., et al., *FoxP3+CD4+ regulatory T cells play an important role in acute HIV-1 infection in humanized Rag2-/-gammaC-/- mice in vivo.* Blood, 2008. 112(7): p. 2858-68.**
171. **Sato, K., et al., *Dynamics of memory and naive CD8+ T lymphocytes in humanized NOD/SCID/IL-2Rgammanull mice infected with CCR5-tropic HIV-1.* Vaccine, 2010. 28 Suppl 2: p. B32-7.**
172. **Brainard, D.M., et al., *Induction of robust cellular and humoral virus-specific adaptive immune responses in human immunodeficiency virus-infected humanized BLT mice.* J Virol, 2009. 83(14): p. 7305-21.**
173. **Ince, W.L., et al., *Evolution of the HIV-1 env gene in the Rag2-/-gammaC-/- humanized mouse model.* J Virol, 2010. 84(6): p. 2740-52.**
174. **Sato, K., et al., *Remarkable lethal G-to-A mutations in vif-proficient HIV-1 provirus by individual APOBEC3 proteins in humanized mice.* J Virol, 2010. 84(18): p. 9546-56.**
175. **Choudhary, S.K., et al., *Suppression of human immunodeficiency virus type 1 (HIV-1) viremia with reverse transcriptase and integrase inhibitors, CD4+ T-cell recovery, and viral rebound upon interruption of therapy in a new model for HIV treatment in the humanized Rag2-/-{gamma}c-/- mouse.* J Virol, 2009. 83(16): p. 8254-8.**
176. **Kumar, P., et al., *T cell-specific siRNA delivery suppresses HIV-1 infection in humanized mice.* Cell, 2008. 134(4): p. 577-86.**
177. **Denton, P.W., et al., *Antiretroviral pre-exposure prophylaxis prevents vaginal transmission of HIV-1 in humanized BLT mice.* PLoS Med, 2008. 5(1): p. e16.**
178. **Denton, P.W., et al., *Systemic administration of antiretrovirals prior to exposure prevents rectal and intravenous HIV-1 transmission in humanized BLT mice.* PLoS One, 2010. 5(1): p. e8829.**
179. **Ramer, P.C., et al., *Mice with human immune system components as in vivo models for infections with human pathogens.* Immunol Cell Biol, 2011. 89(3): p. 408-16.**
180. **Islas-Ohlmayer, M., et al., *Experimental infection of NOD/SCID mice reconstituted with human CD34+ cells with Epstein-Barr virus.* J Virol, 2004. 78(24): p. 13891-900.**
181. **Yajima, M., et al., *A new humanized mouse model of Epstein-Barr virus infection that reproduces persistent infection, lymphoproliferative disorder, and cell-mediated and humoral immune responses.* J Infect Dis, 2008. 198(5): p. 673-82.**
182. **White, R.E., et al., *EBNA3B-deficient EBV promotes B cell lymphomagenesis in humanized mice and is found in human tumors.* J Clin Invest, 2012. 122(4): p. 1487-502.**
183. **Ma, S.D., et al., *A new model of Epstein-Barr virus infection reveals an important role for early lytic viral protein expression in the development of lymphomas.* J Virol, 2011. 85(1): p. 165-77.**
184. **Ma, S.D., et al., *An Epstein-Barr Virus (EBV) Mutant with Enhanced BZLF1 Expression Causes Lymphomas with Abortive Lytic EBV Infection in a Humanized Mouse Model.* J Virol, 2012. 86(15): p. 7976-87.**
185. **Bente, D.A., et al., *Dengue fever in humanized NOD/SCID mice.* J Virol, 2005. 79(21): p. 13797-9.**

186. **Kuruvilla, J.G., et al.,** ***Dengue virus infection and immune response in humanized RAG2(-/-)gamma(c)(-/-) (RAG-hu) mice.*** **Virology, 2007. 369(1): p. 143-52.**
187. **Mota, J. and R. Rico-Hesse,** ***Humanized mice show clinical signs of dengue fever according to infecting virus genotype.*** **J Virol, 2009. 83(17): p. 8638-45.**
188. **Subramanya, S., et al.,** ***Targeted delivery of small interfering RNA to human dendritic cells to suppress dengue virus infection and associated proinflammatory cytokine production.*** **J Virol, 2010. 84(5): p. 2490-501.**
189. **Takaki, T., et al.,** ***HLA-A*0201-restricted T cells from humanized NOD mice recognize autoantigens of potential clinical relevance to type 1 diabetes.*** **J Immunol, 2006. 176(5): p. 3257-65.**
190. **Siegler, U., et al.,** ***Activated natural killer cells from patients with acute myeloid leukemia are cytotoxic against autologous leukemic blasts in NOD/SCID mice.*** **Leukemia, 2005. 19(12): p. 2215-22.**
191. **Flavell, D.J., et al.,** ***The anti-CD20 antibody rituximab augments the immunospecific therapeutic effectiveness of an anti-CD19 immunotoxin directed against human B-cell lymphoma.*** **Br J Haematol, 2006. 134(2): p. 157-70.**
192. **Dewan, M.Z., et al.,** ***Rapid tumor formation of human T-cell leukemia virus type 1-infected cell lines in novel NOD-SCID/gammac(null) mice: suppression by an inhibitor against NF-kappaB.*** **J Virol, 2003. 77(9): p. 5286-94.**
193. **Watanabe, M., et al.,** ***A novel NF-kappaB inhibitor DHMEQ selectively targets constitutive NF-kappaB activity and induces apoptosis of multiple myeloma cells in vitro and in vivo.*** **Int J Cancer, 2005. 114(1): p. 32-8.**
194. **Ntatsaki, E., R.A. Watts, and D.G. Scott,** ***Epidemiology of ANCA-associated vasculitis.*** **Rheum Dis Clin North Am, 2010. 36(3): p. 447-61.**
195. **Babior, B.M., R.S. Kipnes, and J.T. Curnutte,** ***Biological defense mechanisms. The production by leukocytes of superoxide, a potential bactericidal agent.*** **J Clin Invest, 1973. 52(3): p. 741-4.**
196. **Hohn, D.C. and R.I. Lehrer,** ***NADPH oxidase deficiency in X-linked chronic granulomatous disease.*** **J Clin Invest, 1975. 55(4): p. 707-13.**
197. **McCord, J.M. and I. Fridovich,** ***Superoxide dismutase. An enzymic function for erythrocuprein (hemocuprein).*** **J Biol Chem, 1969. 244(22): p. 6049-55.**
198. **Protnay, G.I., et al.,** ***The effect of physiological doses of thyroxine on carrier-mediated ADP uptake by liver mitochondria from thyroidectomized rats.*** **Biochem Biophys Res Commun, 1973. 55(1): p. 17-21.**
199. **Emmendorffer, A., et al.,** ***A fast and easy method to determine the production of reactive oxygen intermediates by human and murine phagocytes using dihydrorhodamine 123.*** **J Immunol Methods, 1990. 131(2): p. 269-75.**

200. **Rothe, G., et al., *Flow cytometric measurement of the respiratory burst activity of phagocytes using dihydrorhodamine 123.* J Immunol Methods, 1991. 138(1): p. 133-5.**
201. **Cullen, G.E. and D.D. Van Slyke, *Determination of the fibrin, globulin, and albumin nitrogen of blood plasma.* J Biol Chem, 1920. 41: p. 587-597.**
202. **Wingfield, P., *Protein precipitation using ammonium sulfate.* Curr Protoc Protein Sci, 2001. Appendix 3: p. Appendix 3F.**
203. **Bjorck, L. and G. Kronvall, *Purification and some properties of streptococcal protein G, a novel IgG-binding reagent.* J Immunol, 1984. 133(2): p. 969-74.**
204. **Freitas, M., et al., *Isolation and activation of human neutrophils in vitro. The importance of the anticoagulant used during blood collection.* Clin Biochem, 2008. 41(7-8): p. 570-5.**
205. **Macey, M.G., et al., *Expression of functional antigens on neutrophils. Effects of preparation.* J Immunol Methods, 1992. 149(1): p. 37-42.**
206. **Darzynkiewicz, Z., L. Staiano-Coico, and M.R. Melamed, *Increased mitochondrial uptake of rhodamine 123 during lymphocyte stimulation.* Proc Natl Acad Sci U S A, 1981. 78(4): p. 2383-7.**
207. **Bruhns, P., *Properties of mouse and human IgG receptors and their contribution to disease models.* Blood, 2012. 119(24): p. 5640-9.**
208. **Van Der Geld, Y.M., P.C. Limburg, and C.G. Kallenberg, *Characterization of monoclonal antibodies to proteinase 3 (PR3) as candidate tools for epitope mapping of human anti-PR3 autoantibodies.* Clin Exp Immunol, 1999. 118(3): p. 487-96.**
209. **Silva, F., et al., *Discrimination and variable impact of ANCA binding to different surface epitopes on proteinase 3, the Wegener's autoantigen.* J Autoimmun, 2010. 35(4): p. 299-308.**
210. **Bruner, B.F., et al., *Anti-neutrophil cytoplasmic antibodies target sequential functional proteinase 3 epitopes in the sera of patients with Wegener's granulomatosis.* Clin Exp Immunol, 2010. 162(2): p. 262-70.**
211. **Mulder, A.H., C.A. Stegeman, and C.G. Kallenberg, *Activation of granulocytes by anti-neutrophil cytoplasmic antibodies (ANCA) in Wegener's granulomatosis: a predominant role for the IgG3 subclass of ANCA.* Clin Exp Immunol, 1995. 101(2): p. 227-32.**
212. **Jayne, D.R., A.P. Weetman, and C.M. Lockwood, *IgG subclass distribution of autoantibodies to neutrophil cytoplasmic antigens in systemic vasculitis.* Clin Exp Immunol, 1991. 84(3): p. 476-81.**
213. **Brouwer, E., et al., *Predominance of IgG1 and IgG4 subclasses of anti-neutrophil cytoplasmic autoantibodies (ANCA) in patients with Wegener's granulomatosis and clinically related disorders.* Clin Exp Immunol, 1991. 83(3): p. 379-86.**
214. **Harper, L., et al., *IgG from myeloperoxidase-antineutrophil cytoplasmic antibody-positive patients stimulates greater activation of primed neutrophils than IgG from proteinase 3-antineutrophil cytosplasmic antibody-positive patients.* Arthritis Rheum, 2001. 44(4): p. 921-30.**

215. Segelmark, M. and J. Wieslander, *IgG subclasses of antineutrophil cytoplasm autoantibodies (ANCA).* Nephrol Dial Transplant, 1993. 8(8): p. 696-702.

216. Mellbye, O.J., T.E. Mollnes, and L.S. Steen, *IgG subclass distribution and complement activation ability of autoantibodies to neutrophil cytoplasmic antigens (ANCA).* Clin Immunol Immunopathol, 1994. 70(1): p. 32-9.

217. Colman, R., et al., *Chimeric antibodies to proteinase 3 of IgG1 and IgG3 subclasses induce different magnitudes of functional responses in neutrophils.* Ann Rheum Dis, 2007. 66(5): p. 676-82.

218. Hussain, A., et al., *Chimeric IgG4 PR3-ANCA induces selective inflammatory responses from neutrophils through engagement of Fcgamma receptors.* Immunology, 2009. 128(2): p. 236-44.

219. Pankhurst, T., et al., *Immunoglobulin subclass determines ability of immunoglobulin (Ig)G to capture and activate neutrophils presented as normal human IgG or disease-associated anti-neutrophil cytoplasm antibody (ANCA)-IgG.* Clin Exp Immunol, 2011. 164(2): p. 218-26.

220. Schreiber, A., *The protective role of NADPH oxidase in ANCA-induced vasculitis* The Fifteenth International Vasculitis & ANCA Workshop, 2011.

221. Bansal, P.J. and M.C. Tobin, *Neonatal microscopic polyangiitis secondary to transfer of maternal myeloperoxidase-antineutrophil cytoplasmic antibody resulting in neonatal pulmonary hemorrhage and renal involvement.* Ann Allergy Asthma Immunol, 2004. 93(4): p. 398-401.

222. Csernok, E., et al., *Membrane surface proteinase 3 expression and intracytoplasmic immunoglobulin on neutrophils from patients with ANCA-associated vasculitides.* Adv Exp Med Biol, 1993. 336: p. 45-50.

223. Csernok, E., et al., *Activated neutrophils express proteinase 3 on their plasma membrane in vitro and in vivo.* Clin Exp Immunol, 1994. 95(2): p. 244-50.

224. Condliffe, A.M., E. Kitchen, and E.R. Chilvers, *Neutrophil priming: pathophysiological consequences and underlying mechanisms.* Clin Sci (Lond), 1998. 94(5): p. 461-71.

225. Hewins, P., et al., *IL-18 is upregulated in the kidney and primes neutrophil responsiveness in ANCA-associated vasculitis.* Kidney Int, 2006. 69(3): p. 605-15.

226. Semerad, C.L., et al., *G-CSF is an essential regulator of neutrophil trafficking from the bone marrow to the blood.* Immunity, 2002. 17(4): p. 413-23.

227. Avalos, B.R., *Molecular analysis of the granulocyte colony-stimulating factor receptor.* Blood, 1996. 88(3): p. 761-77.

228. Wolfler, A., et al., *A functional single-nucleotide polymorphism of the G-CSF receptor gene predisposes individuals to high-risk myelodysplastic syndrome.* Blood, 2005. 105(9): p. 3731-6.

229. Lee, J., et al., *G-CSF and GM-CSF concentrations and receptor expression in peripheral blood leukemic cells from patients with chronic myelogenous leukemia.* Ann Clin Lab Sci, 2008. 38(4): p. 331-7.

230. **Demetri, G.D. and J.D. Griffin, *Granulocyte colony-stimulating factor and its receptor.* Blood, 1991. 78(11): p. 2791-808.**
231. **Yuo, A., et al., *Recombinant human granulocyte colony-stimulating factor as an activator of human granulocytes: potentiation of responses triggered by receptor-mediated agonists and stimulation of C3bi receptor expression and adherence.* Blood, 1989. 74(6): p. 2144-9.**
232. **Yong, K.L. and D.C. Linch, *Differential effects of granulocyte- and granulocyte-macrophage colony-stimulating factors (G- and GM-CSF) on neutrophil adhesion in vitro and in vivo.* Eur J Haematol, 1992. 49(5): p. 251-9.**
233. **Wang, J.M., et al., *Chemotactic activity of recombinant human granulocyte colony-stimulating factor.* Blood, 1988. 72(5): p. 1456-60.**
234. **Weisbart, R.H. and D.W. Golde, *Physiology of granulocyte and macrophage colony-stimulating factors in host defense.* Hematol Oncol Clin North Am, 1989. 3(3): p. 401-9.**
235. **Roilides, E., et al., *Granulocyte colony-stimulating factor enhances the phagocytic and bactericidal activity of normal and defective human neutrophils.* J Infect Dis, 1991. 163(3): p. 579-83.**
236. **Lopez, A.F., et al., *Activation of granulocyte cytotoxic function by purified mouse colony-stimulating factors.* J Immunol, 1983. 131(6): p. 2983-8.**
237. **Treweeke, A.T., K.A. Aziz, and M. Zuzel, *The role of G-CSF in mature neutrophil function is not related to GM-CSF-type cell priming.* J Leukoc Biol, 1994. 55(5): p. 612-6.**
238. **Carulli, G., *Effects of recombinant human granulocyte colony-stimulating factor administration on neutrophil phenotype and functions.* Haematologica, 1997. 82(5): p. 606-16.**
239. **Freeley, S.J., et al., *Granulocyte colony stimulating factor exacerbates anti-neutrophil cytoplasmic antibody vasculitis.* Annals of Rheumatic Diseases 2012. Accepted for publication.**
240. **Engelman, J.A., J. Luo, and L.C. Cantley, *The evolution of phosphatidylinositol 3-kinases as regulators of growth and metabolism.* Nat Rev Genet, 2006. 7(8): p. 606-19.**
241. **Hawkins, P.T., et al., *PI3K signaling in neutrophils.* Curr Top Microbiol Immunol, 2010. 346: p. 183-202.**
242. **Vanhaesebroeck, B., et al., *Synthesis and function of 3-phosphorylated inositol lipids.* Annu Rev Biochem, 2001. 70: p. 535-602.**
243. **Guillermet-Guibert, J., et al., *The p110beta isoform of phosphoinositide 3-kinase signals downstream of G protein-coupled receptors and is functionally redundant with p110gamma.* Proc Natl Acad Sci U S A, 2008. 105(24): p. 8292-7.**
244. **Traynor-Kaplan, A.E., et al., *An inositol tetrakisphosphate-containing phospholipid in activated neutrophils.* Nature, 1988. 334(6180): p. 353-6.**
245. **Vieira, O.V., et al., *Distinct roles of class I and class III phosphatidylinositol 3-kinases in phagosome formation and maturation.* J Cell Biol, 2001. 155(1): p. 19-25.**

246. **Smith, D.F., et al., *Leukocyte phosphoinositide-3 kinase {gamma} is required for chemokine-induced, sustained adhesion under flow in vivo.* J Leukoc Biol, 2006. 80(6): p. 1491-9.**
247. **Ellson, C., et al., *PtdIns3P binding to the PX domain of p40phox is a physiological signal in NADPH oxidase activation.* EMBO J, 2006. 25(19): p. 4468-78.**
248. **Vanhaesebroeck, B., et al., *The emerging mechanisms of isoform-specific PI3K signalling.* Nat Rev Mol Cell Biol, 2010. 11(5): p. 329-41.**
249. **Suire, S., et al., *Gbetagammas and the Ras binding domain of p110gamma are both important regulators of PI(3)Kgamma signalling in neutrophils.* Nat Cell Biol, 2006. 8(11): p. 1303-9.**
250. **Fumagalli, L., et al., *Class I phosphoinositide-3-kinases and SRC kinases play a nonredundant role in regulation of adhesion-independent and -dependent neutrophil reactive oxygen species generation.* J Immunol, 2013. 190(7): p. 3648-60.**
251. **Weaver, K.L., et al., *Effect of dietary fatty acids on inflammatory gene expression in healthy humans.* J Biol Chem, 2009. 284(23): p. 15400-7.**
252. **Boyle, K.B., et al., *Class IA phosphoinositide 3-kinase beta and delta regulate neutrophil oxidase activation in response to Aspergillus fumigatus hyphae.* J Immunol, 2011. 186(5): p. 2978-89.**
253. **Kulkarni, S., et al., *PI3Kbeta plays a critical role in neutrophil activation by immune complexes.* Sci Signal, 2011. 4(168): p. ra23.**
254. **Condliffe, A.M., et al., *Sequential activation of class IB and class IA PI3K is important for the primed respiratory burst of human but not murine neutrophils.* Blood, 2005. 106(4): p. 1432-40.**
255. **Sadhu, C., et al., *Selective role of PI3K delta in neutrophil inflammatory responses.* Biochem Biophys Res Commun, 2003. 308(4): p. 764-9.**
256. **Sadhu, C., et al., *Essential role of phosphoinositide 3-kinase delta in neutrophil directional movement.* J Immunol, 2003. 170(5): p. 2647-54.**
257. **Puri, K.D., et al., *Mechanisms and implications of phosphoinositide 3-kinase delta in promoting neutrophil trafficking into inflamed tissue.* Blood, 2004. 103(9): p. 3448-56.**
258. **Pinho, V., et al., *Tissue- and stimulus-dependent role of phosphatidylinositol 3-kinase isoforms for neutrophil recruitment induced by chemoattractants in vivo.* J Immunol, 2007. 179(11): p. 7891-8.**
259. **Hannigan, M., et al., *Neutrophils lacking phosphoinositide 3-kinase gamma show loss of directionality during N-formyl-Met-Leu-Phe-induced chemotaxis.* Proc Natl Acad Sci U S A, 2002. 99(6): p. 3603-8.**
260. **Tang, W., et al., *A PLCbeta/PI3Kgamma-GSK3 signaling pathway regulates cofilin phosphatase slingshot2 and neutrophil polarization and chemotaxis.* Dev Cell, 2011. 21(6): p. 1038-50.**
261. **Ellson, C.D., et al., *Neutrophils from p40phox-/- mice exhibit severe defects in NADPH oxidase regulation and oxidant-dependent bacterial killing.* J Exp Med, 2006. 203(8): p. 1927-37.**

262. Lehmann, K., et al., *PI3Kgamma controls oxidative bursts in neutrophils via interactions with PKCalpha and p47phox.* Biochem J, 2009. 419(3): p. 603-10.

263. Yang, J.J., et al., *Target antigens for anti-neutrophil cytoplasmic autoantibodies (ANCA) are on the surface of primed and apoptotic but not unstimulated neutrophils.* Clin Exp Immunol, 2000. 121(1): p. 165-72.

264. Abdel-Salam, B., et al., *Autoantibodies to neutrophil cytoplasmic antigens (ANCA) do not bind to polymorphonuclear neutrophils in blood.* Kidney Int, 2004. 66(3): p. 1009-17.

265. Ralston, D.R., et al., *Antineutrophil cytoplasmic antibodies induce monocyte IL-8 release. Role of surface proteinase-3, alpha1-antitrypsin, and Fcgamma receptors.* J Clin Invest, 1997. 100(6): p. 1416-24.

266. Ferrario, F. and M.P. Rastaldi, *Necrotizing-crescentic glomerulonephritis in ANCA-associated vasculitis: the role of monocytes.* Nephrol Dial Transplant, 1999. 14(7): p. 1627-31.

267. Muller Kobold, A.C., C.G. Kallenberg, and J.W. Tervaert, *Monocyte activation in patients with Wegener's granulomatosis.* Ann Rheum Dis, 1999. 58(4): p. 237-45.

268. Casselman, B.L., et al., *Antibodies to neutrophil cytoplasmic antigens induce monocyte chemoattractant protein-1 secretion from human monocytes.* J Lab Clin Med, 1995. 126(5): p. 495-502.

269. Hattar, K., et al., *Wegener's granulomatosis: antiproteinase 3 antibodies induce monocyte cytokine and prostanoid release-role of autocrine cell activation.* J Leukoc Biol, 2002. 71(6): p. 996-1004.

270. Kim, Y.S., et al., *TNF-induced activation of the Nox1 NADPH oxidase and its role in the induction of necrotic cell death.* Mol Cell, 2007. 26(5): p. 675-87.

271. Reumaux, D., et al., *Priming by tumor necrosis factor-alpha of human neutrophil NADPH-oxidase activity induced by anti-proteinase-3 or anti-myeloperoxidase antibodies.* J Leukoc Biol, 2006. 80(6): p. 1424-33.

272. Savige, J.A., et al., *Alpha 1-antitrypsin deficiency and anti-proteinase 3 antibodies in anti-neutrophil cytoplasmic antibody (ANCA)-associated systemic vasculitis.* Clin Exp Immunol, 1995. 100(2): p. 194-7.

273. Griffith, M.E., et al., *C-antineutrophil cytoplasmic antibody positivity in vasculitis patients is associated with the Z allele of alpha-1-antitrypsin, and P-antineutrophil cytoplasmic antibody positivity with the S allele.* Nephrol Dial Transplant, 1996. 11(3): p. 438-43.

274. Esnault, V.L., et al., *Alpha 1-antitrypsin genetic polymorphism in ANCA-positive systemic vasculitis.* Kidney Int, 1993. 43(6): p. 1329-32.

275. Segelmark, M., et al., *The PiZ gene of alpha 1-antitrypsin as a determinant of outcome in PR3-ANCA-positive vasculitis.* Kidney Int, 1995. 48(3): p. 844-50.

276. Rooney, C.P., et al., *Anti-proteinase 3 antibody activation of neutrophils can be inhibited by alpha1-antitrypsin.* Am J Respir Cell Mol Biol, 2001. 24(6): p. 747-54.

277. **Shock, A. and H. Baum, *Inactivation of alpha-1-proteinase inhibitor in serum by stimulated human polymorphonuclear leucocytes. Evidence for a myeloperoxidase-dependent mechanism.* Cell Biochem Funct, 1988. 6(1): p. 13-23.**
278. **Taggart, C., et al., *Oxidation of either methionine 351 or methionine 358 in alpha 1-antitrypsin causes loss of anti-neutrophil elastase activity.* J Biol Chem, 2000. 275(35): p. 27258-65.**
279. **Brachemi, S., et al., *Increased membrane expression of proteinase 3 during neutrophil adhesion in the presence of anti proteinase 3 antibodies.* J Am Soc Nephrol, 2007. 18(8): p. 2330-9.**
280. **Mestas, J. and C.C. Hughes, *Of mice and not men: differences between mouse and human immunology.* J Immunol, 2004. 172(5): p. 2731-8.**
281. **Hunter, M.G. and B.R. Avalos, *Phosphatidylinositol 3'-kinase and SH2-containing inositol phosphatase (SHIP) are recruited by distinct positive and negative growth-regulatory domains in the granulocyte colony-stimulating factor receptor.* J Immunol, 1998. 160(10): p. 4979-87.**
282. **Dong, F. and A.C. Larner, *Activation of Akt kinase by granulocyte colony-stimulating factor (G-CSF): evidence for the role of a tyrosine kinase activity distinct from the Janus kinases.* Blood, 2000. 95(5): p. 1656-62.**
283. **Hellmich, B., et al., *Granulocyte-macrophage colony-stimulating factor (GM-CSF) but not granulocyte colony-stimulating factor (G-CSF) induces plasma membrane expression of proteinase 3 (PR3) on neutrophils in vitro.* Clin Exp Immunol, 2000. 120(2): p. 392-8.**
284. **Nakamae-Akahori, M., et al., *Enhanced neutrophil motility by granulocyte colony-stimulating factor: the role of extracellular signal-regulated kinase and phosphatidylinositol 3-kinase.* Immunology, 2006. 119(3): p. 393-403.**
285. **Loike, J.D., et al., *CD11c/CD18 on neutrophils recognizes a domain at the N terminus of the A alpha chain of fibrinogen.* Proc Natl Acad Sci U S A, 1991. 88(3): p. 1044-8.**
286. **Ley, K., et al., *Sequential contribution of L- and P-selectin to leukocyte rolling in vivo.* J Exp Med, 1995. 181(2): p. 669-75.**
287. **Kishimoto, T.K., et al., *Neutrophil Mac-1 and MEL-14 adhesion proteins inversely regulated by chemotactic factors.* Science, 1989. 245(4923): p. 1238-41.**
288. **Sly, L.M., et al., *SHIP prevents lipopolysaccharide from triggering an antiviral response in mice.* Blood, 2009. 113(13): p. 2945-54.**
289. **Chaussade, C., et al., *Evidence for functional redundancy of class IA PI3K isoforms in insulin signalling.* Biochem J, 2007. 404(3): p. 449-58.**
290. **Jackson, S.P., et al., *PI 3-kinase p110beta: a new target for antithrombotic therapy.* Nat Med, 2005. 11(5): p. 507-14.**
291. **Noort, W.A., et al., *Similar myeloid recovery despite superior overall engraftment in NOD/SCID mice after transplantation of human CD34(+) cells from umbilical cord blood as compared to adult sources.* Bone Marrow Transplant, 2001. 28(2): p. 163-71.**

292. **Ueda, T., et al., *Hematopoietic capability of CD34+ cord blood cells: a comparison with CD34+ adult bone marrow cells.* Int J Hematol, 2001. 73(4): p. 457-62.**
293. **Lang, J., et al., *Generation of hematopoietic humanized mice in the newborn BALB/c-Rag2null Il2rgammanull mouse model: a multivariable optimization approach.* Clin Immunol, 2011. 140(1): p. 102-16.**
294. **Suratt, B.T., et al., *Neutrophil maturation and activation determine anatomic site of clearance from circulation.* Am J Physiol Lung Cell Mol Physiol, 2001. 281(4): p. L913-21.**
295. **Furze, R.C. and S.M. Rankin, *The role of the bone marrow in neutrophil clearance under homeostatic conditions in the mouse.* FASEB J, 2008. 22(9): p. 3111-9.**
296. **Saverymuttu, S.H., et al., *The kinetics of 111indium distribution following injection of 111indium labelled autologous granulocytes in man.* Br J Haematol, 1985. 61(4): p. 675-85.**
297. **Nathan, C., *Neutrophils and immunity: challenges and opportunities.* Nat Rev Immunol, 2006. 6(3): p. 173-82.**
298. **Penack, O., et al., *Management of sepsis in neutropenic patients: guidelines from the infectious diseases working party of the German Society of Hematology and Oncology.* Ann Oncol, 2011. 22(5): p. 1019-29.**
299. **Hajjar, E., et al., *Structures of human proteinase 3 and neutrophil elastase--so similar yet so different.* FEBS J, 2010. 277(10): p. 2238-54.**
300. **Doshi, M., et al., *Identification of human neutrophils during experimentally induced inflammation in mice with transplanted CD34+ cells from human umbilical cord blood.* Int J Hematol, 2006. 84(3): p. 231-7.**
301. **Unsinger, J., et al., *Sepsis-induced human lymphocyte apoptosis and cytokine production in "humanized" mice.* J Leukoc Biol, 2009. 86(2): p. 219-27.**
302. **Rongvaux, A., et al., *Human thrombopoietin knockin mice efficiently support human hematopoiesis in vivo.* Proc Natl Acad Sci U S A, 2011. 108(6): p. 2378-83.**
303. **Barclay, A.N., et al., *The Leucocyte Antigen Facts-Book*. 2nd ed1997: Academic Press, San Diego.**
304. **Skubitz, K.M., K.D. Campbell, and A.P. Skubitz, *CD66a, CD66b, CD66c, and CD66d each independently stimulate neutrophils.* J Leukoc Biol, 1996. 60(1): p. 106-17.**
305. **Yoon, J., A. Terada, and H. Kita, *CD66b regulates adhesion and activation of human eosinophils.* J Immunol, 2007. 179(12): p. 8454-62.**
306. **Daeron, M., *Fc receptor biology.* Annu Rev Immunol, 1997. 15: p. 203-34.**
307. **Elghetany, M.T., *Surface antigen changes during normal neutrophilic development: a critical review.* Blood Cells Mol Dis, 2002. 28(2): p. 260-74.**

308. Laviolette, M., et al., *Comparison of two modified techniques for purifying blood eosinophils.* J Immunol Methods, 1993. 165(2): p. 253-61.

309. Gibbs, B.F., et al., *A three-step procedure for the purification of human basophils from buffy coat blood.* Inflamm Res, 1997. 46(4): p. 137-42.

310. Zarco, M.A., et al., *Phenotypic changes in neutrophil granulocytes after G-CSF administration in patients with acute lymphoblastic leukemia under chemotherapy.* Haematologica, 1998. 83(6): p. 573-5.

311. Tsuchiya, M., et al., *Isolation and characterization of the cDNA for murine granulocyte colony-stimulating factor.* Proc Natl Acad Sci U S A, 1986. 83(20): p. 7633-7.

312. Souza, L.M., et al., *Recombinant human granulocyte colony-stimulating factor: effects on normal and leukemic myeloid cells.* Science, 1986. 232(4746): p. 61-5.

313. Fukunaga, R., et al., *Three different mRNAs encoding human granulocyte colony-stimulating factor receptor.* Proc Natl Acad Sci U S A, 1990. 87(22): p. 8702-6.

314. Kuijpers, T.W., et al., *Membrane surface antigen expression on neutrophils: a reappraisal of the use of surface markers for neutrophil activation.* Blood, 1991. 78(4): p. 1105-11.

315. Sengelov, H., et al., *Subcellular localization and dynamics of Mac-1 (alpha m beta 2) in human neutrophils.* J Clin Invest, 1993. 92(3): p. 1467-76.

316. de Haas, M., et al., *Granulocyte colony-stimulating factor administration to healthy volunteers: analysis of the immediate activating effects on circulating neutrophils.* Blood, 1994. 84(11): p. 3885-94.

317. Karadogan, C., et al., *rHuG-CSF increases the platelet-neutrophil complex formation and neutrophil adhesion molecule expression in volunteer granulocyte and stem cell apheresis donors.* Ther Apher Dial, 2006. 10(2): p. 180-6.

318. Orr, Y., et al., *Conformational activation of CD11b without shedding of L-selectin on circulating human neutrophils.* J Leukoc Biol, 2007. 82(5): p. 1115-25.

319. Bone, R.C., *The pathogenesis of sepsis.* Ann Intern Med, 1991. 115(6): p. 457-69.

320. Andonegui, G., et al., *Endothelium-derived Toll-like receptor-4 is the key molecule in LPS-induced neutrophil sequestration into lungs.* J Clin Invest, 2003. 111(7): p. 1011-20.

321. Mizgerd, J.P., et al., *Neutrophil emigration in the skin, lungs, and peritoneum: different requirements for CD11/CD18 revealed by CD18-deficient mice.* J Exp Med, 1997. 186(8): p. 1357-64.

322. Hashiguchi, N., et al., *Whole-Blood Assay to Measure Oxidative Burst and Degranulation of Neutrophils for Monitoring Trauma Patients.* European Journal of Trauma, 2005. 31(4): p. 379-388.

323. Lacy, P., *Mechanisms of degranulation in neutrophils.* Allergy Asthma Clin Immunol, 2006. 2(3): p. 98-108.

324. Lock, R.J., *ACP Broadsheet No 143: January 1994. Detection of autoantibodies to neutrophil cytoplasmic antigens.* J Clin Pathol, 1994. 47(1): p. 4-8.

325. Savige, J.A., et al., *A review of immunofluorescent patterns associated with antineutrophil cytoplasmic antibodies (ANCA) and their differentiation from other antibodies.* J Clin Pathol, 1998. 51(8): p. 568-75.

326. Little, M.A., et al., *Anti-proteinase 3 anti-neutrophil cytoplasm autoantibodies recapitulate systemic vasculitis in mice with a humanized immune system.* PLoS One, 2012. 7(1): p. e28626.

327. Zhang, Y.H., et al., *In vivo induction of apoptosis (programmed cell death) in mouse thymus by administration of lipopolysaccharide.* Infect Immun, 1993. 61(12): p. 5044-8.

328. Norimatsu, M., et al., *Lipopolysaccharide-induced apoptosis in swine lymphocytes in vivo.* Infect Immun, 1995. 63(3): p. 1122-6.

329. Terstappen, L.W., M. Safford, and M.R. Loken, *Flow cytometric analysis of human bone marrow. III. Neutrophil maturation.* Leukemia, 1990. 4(9): p. 657-63.

330. Dransfield, I., et al., *Neutrophil apoptosis is associated with a reduction in CD16 (Fc gamma RIII) expression.* J Immunol, 1994. 153(3): p. 1254-63.

331. Cros, J., et al., *Human CD14dim monocytes patrol and sense nucleic acids and viruses via TLR7 and TLR8 receptors.* Immunity, 2010. 33(3): p. 375-86.

332. Auffray, C., M.H. Sieweke, and F. Geissmann, *Blood monocytes: development, heterogeneity, and relationship with dendritic cells.* Annu Rev Immunol, 2009. 27: p. 669-92.

333. Tadema, H., et al., *Increased expression of Toll-like receptors by monocytes and natural killer cells in ANCA-associated vasculitis.* PLoS One, 2011. 6(9): p. e24315.

334. Williams, O., et al., *Discovery of dual inhibitors of the immune cell PI3Ks p110delta and p110gamma: a prototype for new anti-inflammatory drugs.* Chem Biol, 2010. 17(2): p. 123-34.

335. Day, R.B. and D.C. Link, *Regulation of neutrophil trafficking from the bone marrow.* Cell Mol Life Sci, 2012. 69(9): p. 1415-23.

336. Uchida, N., et al., *Optimal conditions for lentiviral transduction of engrafting human CD34+ cells.* Gene Ther, 2011. 18(11): p. 1078-86.